

VOLUME 122

N. 1

RIVISTA ITALIANA

DI

PALEONTOLOGIA

E

STRATIGRAFIA

ISSN: 0035-6883

MILANO

DIPARTIMENTO DI SCIENZE DELLA TERRA

VIA MANGIAGALLI, 34

MARCH 2016

FIRST RECORD OF DUGONGIDAE (MAMMALIA: SIRENIA) FROM THE FLORESTA CALCARENITES FORMATION (LATE BURDIGALIAN–EARLY LANGHIAN, REGGIO CALABRIA, SOUTHERN ITALY)

GIUSEPPE CARONE¹, ANTONELLA CINZIA MARRA² & CATERINA MESIANO³

¹Museo Civico di Ricadi (MURI), via Roma, 89861 Santa Domenica di Ricadi (VV), Italy. E-mail: p.carone@libero.it

²Dipartimento di Scienze Matematiche e Informatiche, Scienze Fisiche e Scienze della Terra, Università degli Studi di Messina, Viale F. Stagno D'Alcontres 31, 98166 Messina, Italy. E-mail: antonella.marra@unime.it

³Museo di Paleontologia e Scienze Naturali del Parco dell'Aspromonte, Bova, Reggio Calabria, Italy.

To cite this article: Carone G., Marra A.C. & Mesiano C. (2016) - First record of Dugongidae (Mammalia: Sirenia) from the Floresta Calcarenes Formation (late Burdigalian-early Langhian, Reggio Calabria, Southern Italy). *Riv. It. Paleont. Strat.* 122(1): 1-6

Key words: Mammalia, Sirenia, Systematics, Early-Middle Miocene, Southern Italy.

Abstract. A sirenian rib has been recovered at Motta San Giovanni (Reggio Calabria) in the “Floresta Calcarenes”, a formation cropping out in Sicily and Calabria and dated late Burdigalian-Langhian. Although the rib is not a diagnostic bone for taxonomy, its presence in southern Calabria extends the knowledge about the paleobiogeography of the Family Dugongidae in the Mediterranean basin. The find is hitherto the only record of sirenians in the Floresta Calcarenes. Moreover, the specimen extends back to the Early-Middle Miocene (late Burdigalian-Langhian) the occurrence of sirenians in Calabria, previously determined based on substantial material from the Late Miocene (Tortonian) of the Monte Poro area (Vibo Valentia). The paleoenvironment of the Floresta Calcarenes was a warm and shallow sea, consistent with the paleoecology of Dugongidae.

INTRODUCTION

A rib referable to the Family Dugongidae has been recorded in the “Floresta Calcarenes” Formation cropping out at Motta San Giovanni, near Reggio Calabria (southern Italy; Fig.1). Calcarenes are locally named “Pietra di Lazzaro” and used as decorative stones.

The specimen was recovered during the cut of a block from a quarry located at “Contrada Salto”, near Motta San Giovanni (Reggio Calabria), 650-670m a.s.l., 38° 0' 1.035" N, 15° 42' 59.923" E.

Although the rib is not a diagnostic bone for taxonomy, its discovery is relevant to the distribution of Dugongidae in the Mediterranean Basin during the late Burdigalian-Langhian (late Early to Middle Miocene) and dates back the Sirenians' record of Calabria.

GEOLOGICAL SETTING

The “Floresta Calcarenes” Formation crops out in the Calabria-Peloritani Terrane (CPT), loca-

ted at the intersection between the NW/SE-trending southern Apennines and the SE-trending Sicilian Maghrebides. During the Early Oligocene, the CPT resulted from the emplacement of a fragment of the European margin onto the African paleomargin. The CPT lies on a Serravallian substratum and two superimposed tectonic units are present: “Sicilide” Unit, lower sequence of flyschoid deposits, variegated sandstones and andesitic tuffites; “Calabride” Unit, upper sequence of igneous and metamorphic nappes thrust onto the lower unit, with remnants of Meso-Cenozoic covers (Carbone et al. 1983, 2008; Carmisciano et al. 1981; Lentini et al. 1990). The tectonic units are unconformably covered by the “Capo d'Orlando” Flysch, late Oligocene-early Burdigalian in age (according to Carbone et al. 2008, 2011; Giunta et al. 2013). The “Antisicilide”, made up of varicoloured clays, overthrust the “Capo d'Orlando” Flysch during the mid-late Burdigalian (Carbone et al. 1993, 2008). The “Floresta Calcarenes” Formation (FC) lies on the Antisicilide clays, excluding some localities of eastern Peloritani, where it lies directly on the “Capo d'Orlando” Flysch or the crystalline basement (Carbone et al. 1993, 2008, 2011; Giunta et al. 2013). The FC Fm. is locally overlain by the “Motta” Flysch, a siliciclastic succession cropping out in Calabria and attributed



Fig. 1 - Geographical location of Motta San Giovanni and geological sketch map of the area.

to the Middle Miocene (Barrier et al. 1987).

The FC Fm. occurs in small isolated outcrops in the Peloritani, more frequently, and in the Aspromonte Mountains, and it is made up of sandstones with abundant calcareous cement and rich in bioclasts and siliciclasts, which can locally be conglomeratic.

Carbone et al. (1993) consider the scattered outcrops of the FC Fm. as the result of an extremely active synsedimentary tectonic regime, which involved the south-verging thrusting.

The calcarenites present two main *facies* related to different marine depths (Carbone et al. 1993): 1) shallow water *facies*, rich in bryozoans and rho-

dolites; deep water *facies* with mixed siliciclastic elements, related to resedimentation events.

The shallow-water *facies* is made of pale grey carbonates with reworked bryozoans and coralline algae, interpreted as near *in situ* packstones deposited on shallow ramp (less than 50 meters under the sea level; Buxton and Pedley 1989; Carbone et al. 1993). It is often overlain by bioclastic carbonates, locally cross-stratified (Carbone et al. 1993). The deep-water *facies* is resedimentated, and may presents graded or massive strata. Carbonate and siliciclastic sediments were well washed before transportation, as indicated by the lack of fine grain matrix, and were deposited flowing down slopes (Carbone et al. 1993).

In the hypotheses sustained by Carbone et al. (1993), the most reliable source of siliciclastic materials is the subaerial erosion of small islands emerged for the strong tectonic activity. During late Burdigalian to early Langhian, these units developed diachronously as a consequence of the combined effects of marine eustatism and tectonism. Carbonate packstones rich in bioclasts were formed during a marine highstand in the shallow sea waters around the small islands (late Burdigalian); later the sea level fell and determined the end of carbonate deposition; shallower deposits were progressively dismantled and resedimentated in adjacent lows (Langhian). During the Serravallian, a marine highstand submerged the small islands and determined the extended deposition of clays in all areas (Carbone et al. 1993).

Lithostratigraphic correlations are very difficult, due to the short persistence of diachronic basins and the scattered distribution of outcrops.

Samples from the section of Monte Bammina (near Novara di Sicilia, Sicily) yielded a fauna of Foraminifera useful for dating. The basal levels have been attributed to the late Burdigalian due to the presence of *Globigerinoides trilobus*, *Globorotalia* [recte *Paragloborotalia*] *siakensis*, and *Globorotalia* [recte *Paragloborotalia*] *acrostoma*; the upper levels are attributed to the Langhian due to the presence of *Globigerinoides irregularis*, *Praeorbulina glomerosa glomerosa*, and *Praeorbulina glomerosa circularis* (Carbone et al. 1993).

At "Contrada Salto", the Floresta Calcarenites lie in concordance on the varicolored clays belonging to the Antisicilide complex. At the bottom, calcarenites lie slightly inclined, while at the top they may locally be cross-bedded. The Floresta Calcaren-

nites are overlain by Holocene deposits. In the quarry, the FC presents the *facies* of biolithites rich in bryozoans and rhodolites related to deposition in a warm shallow sea. Accordingly to the interpretation proposed by Carbone et al. (1993), the deposition of coralline algal packstones might be attributed to late Burdigalian.

SYSTEMATIC PALEONTOLOGY

Class **MAMMALIA** Linnaeus, 1758

Order **Sirenia** Illiger, 1811

Family **Dugongidae** Gray, 1821

Dugongidae indeterminate

Referred specimen: Left anterior rib (MPSNA unnumbered) embedded in matrix sectioned into a slab (Fig. 2).

Locality: Quarry at Contrada Salto, Motta San Giovanni (Reggio Calabria; 38° 0' 1.035" N, 15° 42' 59.923" E).

Formation: "Floresta Calcarenes" Formation.

Age: Early-Middle Miocene, late Burdigalian-Langhian.

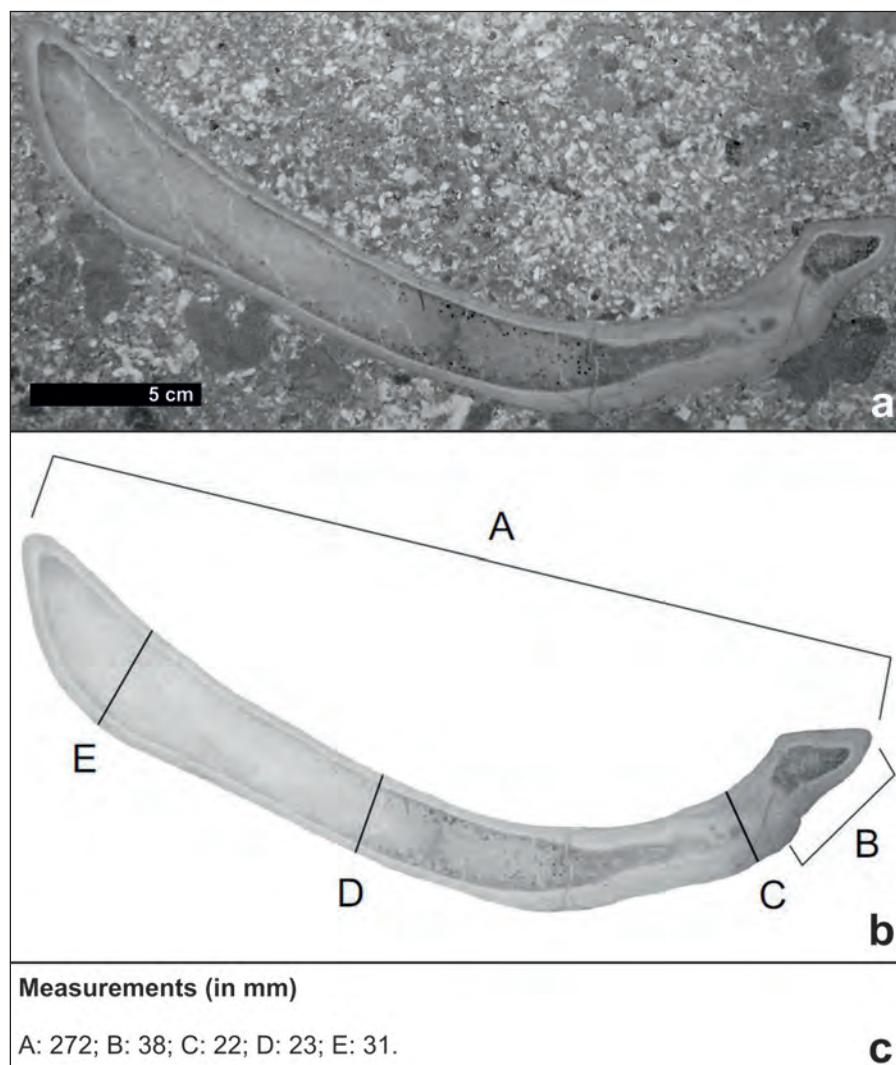
Repository: The specimen is kept in the collections of Museo di Paleontologia e Scienze Naturali del Parco dell'Aspromonte (Bova, Reggio Calabria)

Description. The anatomical terminology and measurements follow Domning (1978). The left rib is embedded in the carbonatic matrix and is preserved in a sectioned slab (Fig. 2a). Because of the commercial use of the calcarenites for floors, the rock and the embedded rib were sliced and polished to obtain a tile. The rib was not exposed, but it were noticed after the cut, as a dense (pachyosteosclerotic) bone showing a light brown outline and a dark interior. Descriptions and measurements are done on the bone included in the slab.

The proximal curvature (angle) is very slight; the capitulum is joined to the shaft by a thick neck. The tuberculum seems pronounced and extends up above the level of the neck. A ventral process is not present. The poorly developed articular processes suggest that the rib belonged to a young specimen.

Fig. 2 - Sirenian rib housed at MPSNA:

a) specimen in the slab; b) plan of measurements: A - total length; B - tip of capitulum to lateral edge of tuberculum; C - proximal thickness; D - mid-shaft thickness; E - distal thickness; c) measurements.



| Age | Locality | Formation | Collection and Catalogue Number | Skeletal Elements | Species | References |
|----------------------------------|---|---|---------------------------------|--|---|-------------------------------------|
| VIENNA BASIN (Paratethys) | | | | | | |
| Burdigalian | Mägenwil, Argovia Canton (Switzerland) | ? | NHMBe unnum. | Maxilla with teeth | <i>Metaxytherium stuederi</i> = <i>M. krahuletzii</i> | Pilleri, 1987 |
| Lower Burdigalian | Schindergraben, Eggenburg (Austria) | Burgschleinitz Form. | KME GH 21/34 | Six isolate molars | <i>Metaxytherium krahuletzii</i> | Domning and Pervesler, 2001 |
| | Burgschleinitz (Austria) | | HMH 262 | Skull fragments, maxilla | | |
| IONIAN BASIN (Tethys) | | | | | | |
| Langhian | Rdum tax-Xagħra, Gozo (Malta) | Upper Globigerina Limestone Member | NMNH-TF-01225 | Rib fragment | Dugongidae indet. | Bianucci et al., 2011 |
| Burdigalian-Langhian | Jabal Zaitan (Libya) | Garat Jahanam Member, Marada Formation | BMNH M45674 | Skull, vertebrae and ribs | <i>Rytiodus heali</i> | Domning and Sorbi, 2011 |
| | Apulia (Italy) | "Pietra Leccese" | ? | ? | <i>Metaxytherium</i> sp. | Bianucci et al., 2003 |
| | Motta San Giovanni, Calabria (Italy) | "Foresta Calcarene" | MPSNA unnum. | Rib | Dugongidae indet. | This paper |
| Late Burdigalian-Langhian | Qammieh, Mellieħa, (Malta) | Upper Main Phosphorite Conglomerate Bed | NMNH TF-01226 | Two incomplete ribs | Dugongidae indet. | Bianucci et al., 2011 |
| Burdigalian | Mgarr ix-Xini, Gozo (Malta) | Lower Main Phosphorite Conglomerate Bed | NMNH TF-01227 | Rib | Dugongidae indet. | Bianucci et al., 2011 |
| Lower Miocene | Ragusa, Sicily (Italy) | Ragusa Form. Iminio Mm | BMNH M12607 | Postcranial skeleton | <i>Metaxytherium</i> sp. | Hopwood, 1927 |
| BALEARIC BASIN (Tethys) | | | | | | |
| Burdigalian-Langhian | Son Morelló, Majorca (Spain)* | ? | ? | ? | <i>Metaxytherium</i> sp. | Cañigüeral, 1952 |
| | Olèrdola, Mas Romeu vell, Catalonia (Spain) | Cambrils Alcanar Groups | MV 1210 | Skull, mandible, vertebrae, ribs. | <i>Metaxytherium catalanicum</i> = <i>M. krahuletzii</i> | Piller et al., 1989 |
| Late Burdigalian | Manosque, Provence (France) | "Molasse calcare et sablo-marneuse" | MPNRL-MAN2000 | Skull, vertebrae, ribs. | <i>Metaxytherium</i> cf. <i>krahuletzii</i> | Sorbi, 2008 |
| Burdigalian | Beaucaire, Languedoc (France) | ? | ? | Skeleton (lost) | <i>Metaxytherium beaumonti</i> = <i>M. krahuletzii</i> | Depéret and Roman, 1920 |
| TYRRENIAN BASIN (Tethys) | | | | | | |
| Burdigalian-Langhian | Pianu di Bosa, Sardinia (Italy) | Modolo Formation | MDLCA unnumber. | Axis, three fragmentary vertebrae and ribs | <i>Metaxytherium curvieri</i> = <i>M. cf. krahuletzii</i> | Comaschi-Caria, 1957 |
| | Monte Alvu, Bosa, Sardinia (Italy) | Modolo Formation | MAC. PL.1228 | Zygomatic process of squamosal, teeth, incomplete mandible and ribs. | <i>Metaxytherium</i> cf. <i>krahuletzii</i> | Carone and Rizzo (Work in progress) |
| | Rosignano and Vignale, Piedmont (Italy) | Pietra da Cantoni Group | PU 13923/33,34 | Two rib fragments | Sirenia indet. | Sorbi, 2007 |

Tab. 1 - Representative sirenian records from the western Mediterranean Basin during Burdigalian-Langhian time. Institutional abbreviations: BMNH = Natural History Museum, London, England; MAC = Museo di Storia Naturale Aquilegia, Cagliari, Italy; MDLCA = Museo Sardo di Geologia e Paleontologia Domenico Lovisato, Università di Cagliari, Cagliari, Italy; MPNRL = Maison du Parc Naturel Régional du Luberon, France; MPSNA = Museo di Paleontologia e Scienze Naturali del Parco dell'Aspromonte, Bova, Reggio Calabria, Italy; MV = Museo di Vilafranca, Vilafranca del Penedès, Spain; KME = Krahuletz-Museum, Eggenburg, Austria; NHM-Be = Naturhistorisches Museum, Bern, Switzerland; NMNH = National Museum of Natural History, Mdina, Malta; PU = Museo di Geologia e Paleontologia dell'Università di Torino, Torino, Italy.

The bulge in the distal portion of the shaft, and the thick neck, suggest that it is an anterior rib. The distal end tapers slightly to an oval termination, probably rugose, for cartilage attachment.

The rib from Motta San Giovanni does not represent a diagnostic skeletal element that can be taxonomically assigned below the level of Family. Its morphology is consistent with that of the Dugongidae, which is the only sirenian Family known from the Mediterranean Miocene. Measurements are within the variability of the Family Dugongidae (Fig. 2b and c).

DISCUSSION AND CONCLUSIONS

Dugongidae is a Family of extinct and living sirenians with a wide geographical and biostrati-

graphical distribution (Tab. 1, Fig. 3).

Fossils of Dugongidae have been collected in several Miocene localities of the Mediterranean region. During the latest Burdigalian-early Langhian, two sirenians, belonging to two distinct Subfamilies, were present in the Mediterranean Basin (Tab. 1, Fig. 3): *Rytiodus heali* (Dugongidae, Dugonginae), characterized by broad, mediolaterally-compressed, blade-like tusks with enamel mainly on the medial side, probably specialized as seagrass feeders that used their tusks in excavation of seagrass rhizomes; and *Metaxytherium* (Dugongidae, Halitheriinae) whose early and middle Miocene members (*M. krahuletzii* and *M. medium*, respectively) were characterized by small tusks and were probably adapted to a generalized seagrass diet.

Sirenian remains have been found in the Lo-

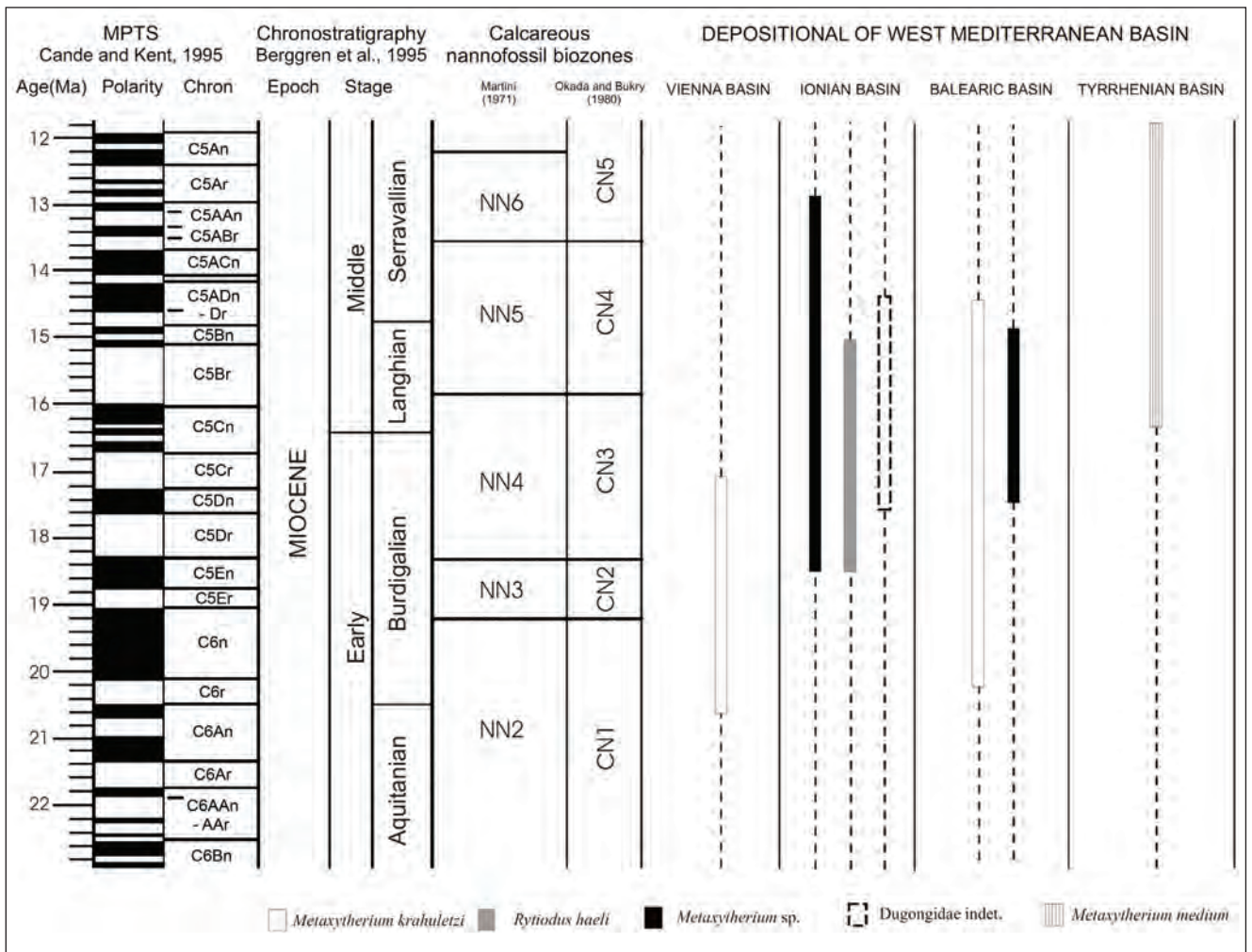


Fig. 3 - Stratigraphic distribution of Dugongidae spp. occurrences in the western Mediterranean basins. Abbreviations: VB, Vienna Basin; IB, Ionian Basin; BB, Balearic Basin; TB, Tyrrhenian Basin.

wer Miocene Marada Formation (Jabal Zaltan, Libya); most of these were described as *Rytiodus heali*, but some represent *Metaxytherium* sp. as well (Domning & Sorbi 2011). Some fragmentary remains referable to *Metaxytherium* come also from Malta, Gozo, Apulia and Sicily. Therefore in this area dugongines and halitheriines seem to have lived sympatrically.

Due to its morphology and taxonomic significance, the rib reported here could represent both sirenian taxa.

Nevertheless, the presence of a sirenian rib in the FC Fm. at Motta San Giovanni marks a new occurrence in the geographical distribution of Dugongidae in the Mediterranean area during the Early-Middle Miocene, often represented by scant materials roughly attributable to Dugongidae (Tab. 1).

Furthermore, the specimen represents the first record of sirenians in the Floresta Calcareni-

tes Formation, cropping out in southern Calabria and northeastern Sicily. The FC Fm. is represented by scattered and diachronical outcrops, whose different *facies* are interpreted as different phases of development through time (Carbone et al. 1993). Outcrops referable to pale grey carbonates with reworked bryozoans and coralline algae, like Motta San Giovanni ones, are representative of the first phase of deposition (late Burdigalian) and occur along the modern Tyrrhenian coast of NE Sicily and in the southern margin of Aspromonte in Calabria (Carbone et al. 1993). These packstones were formed on a ramp in shallow waters, deep less than 50 meters, as indicated by algal and foraminiferal associations, around the small islands emerged for tectonism (Carbone et al. 1993). This environment was favourable to sirenians.

Moreover, it is possible to infer a precise dating for the rib, if is accepted the development of

the FC Fm. *facies* sustained by Carbone et al. (1993), which consider the carbonatic packstones formed in a first depositional phase, attributable to late Burdigalian.

This find represents the earliest occurrence of sirenians in Calabria, previously represented only by abundant remains from the Late Miocene (Tortonian) of the Monte Poro area, near Vibo Valentia (Carone and Domning 2007).

Acknowledgements. The Authors are deeply indebted to Daryl P. Domning (Howard University, USA) and an anonymous reviewer for improving the paper with their suggestions, and to prof. Lorenzo Rook (University of Florence) for critical reading. Prof. Renato Crucitti, Director of the “Museo di Paleontologia e Scienze Naturali del Parco dell’Aspromonte” is acknowledged for his constant activity of fossil’s preservation and for allowing this study. A final mention to Mr. Carmelo Ambrogio (Cea costruzioni srl) for recovering the fossil and depositing it to the Parco dell’Aspromonte Paleontological Museum.

REFERENCES

- Adams L.A. (1866) - On the Discovery of Remains of *Hali-therium* in the Miocene Deposits of Malta. *Quarterly J. Geol. Soc.*, 22: 595-596.
- Barrier P. (1987) - Stratigraphie des dépôt pliocène et pleistocène du Détroit de Messine (Italie). *Doc. Trav. Inst. géol. Albert de Lapparent (IGAL)*, 11: 59-81.
- Berggren W.A., Kent D.V., Swisher C.C. & Aubry M. (1995) - A revised Cenozoic geochronology and chronostratigraphy. In: Berggren W.A. et al. (Eds) - Geochronology, Time Scales and Global Stratigraphic Correlation. *SEPM Sp. Pub.*, 54: 129-212.
- Bianucci G., Gatt M., Catanzariti R., Sorbi S., Bonavia C.G., Curmi R. & Varola A. (2011) - Systematics, biostratigraphy and evolutionary pattern of the Oligo-Miocene marine mammals from the Maltese Islands. *Geobios*, 44: 549-585.
- Bianucci G., Landini W.E. & Varola A. (2003) - New records of *Metaxytherium* (Mammalia: Sirenia) from the late Miocene of Cisterna quarry (Apulia, Southern Italy). *Boll. Soc. Paleontol. It.*, 42(1-2): 59-63.
- Bonardi G., Cavazza W., Perrone V. & Rossi S. (2001) - Calabria-Peloritani terrane and northern Ionian Sea. In: Vai G.B. & Martini I.P. (Eds) - Anatomy of an Orogen: The Apennines and Adjacent Mediterranean Basins: 287-306. Kluwer Academic Publishers, Dordrecht.
- Cande S.C. & Kent D.V. (1995) - Revised calibration of the geomagnetic polarity timescale for the Late Cretaceous and Cenozoic. *J. Geoph. Res.*, 100: 6093-6095.
- Cañigüeral J. (1952) - Un notable sirénido en Mallorca. *Ibérica*, (2)16(245): 387-390.
- Carbone S., Messina A. & Lentini F. (2008) - Note Illustrative della Carta geologica d’Italia alla Scala 1:50.000 Foglio 601 Messina Reggio di Calabria. Servizio Geologico d’Italia, APAT, S.E.L.C.A., Firenze, 179 pp.
- Carbone S., Messina A. & Lentini F. (2011) - Note Illustrative della Carta geologica d’Italia alla Scala 1:50.000 Fogli 587 e 600 Milazzo-Barcellona. Servizio Geologico d’Italia, APAT, S.E.L.C.A., Firenze, 262 pp.
- Carbone S., Pedley H.M., Grasso M. & Lentini F. (1993) - Origin of the “Calcareni di Floresta” of NE Sicily: late orogenic sedimentation associated with a middle Miocene sea-level high stand. *Giornate di Geologia*, 55(2)(3): 105-116, Bologna.
- Carone G. & Rizzo R. (In progress) - Miocene sirenian fossils from Sardinia (Italy).
- Carone G. & Domning D.P. (2007) - *Metaxytherium serresii* (Mammalia: Sirenia): new pre-Pliocene record, and implications for Mediterranean paleoecology before and after the Messinian Salinity Crisis. *Boll. Soc. Paleontol. It.*, 46(1): 55-92.
- Domning P.D. & Sorbi S. (2011) - *Rytiodus heali*, sp. nov., a new sirenian (Mammalia, Dugonginae) from the Miocene of Libya. *J. Vert. Paleontol.*, 31(6):1338-1355.
- Domning D.P. (1978) - Sirenian evolution in the North Pacific Ocean. *Univ. California Pub. Geol. Sci.*, 118: 1-176.
- Giunta G., Carbone S., Catalano R., Di Maio D. & A. Sulli A. (2013) - Note Illustrative della Carta geologica d’Italia alla Scala 1:50.000 Foglio 599 Patti. Servizio Geologico d’Italia, APAT, S.E.L.C.A., Firenze, 222 pp.
- Grasso M., Pedley M., Distefano R. & Cormaci C. (1996) - Upper Miocene reefs in southern Calabria: new records from the Palmi and Vibo Valentia areas and their palaeogeographic and neotectonic importance. *Boll. Soc. Geol. It.*, 115: 29-38.
- Gray J.E. (1821) - On the natural arrangement of vertebrate animals. *London Medical Repository*, 15: 296-310.
- Illiger C. (1811) - Prodomus Systematis Mammalium et Avium: Additis Terminis Zoographicis Utriusque Classis, Eorumque Versione Germanica. Sumptibus C. Salfeld, Berlin, 302 pp.
- Linnaeus C. (1758) - Systema Naturae per Regna Tria Naturae, Secundum Classes, Ordines, Genera, Species, cum Characteribus, Differentiis, Synonymis, Locis. Tomus I, Editio decima, reformata. Laurentii Salvii, Stockholm, 823 pp.
- Martini E. (1971) - Standard Tertiary and Quaternary calcareous nannoplankton zonation. In: Farinacci A. (Eds) - Proceedings 2nd International Conference Planktonic Microfossils, (Ed. Tecnosci.) 2: 739-785, Roma.
- Okada H. & Bukry D. (1980) - Supplementary modification and introduction of code numbers to low latitude coccoliths biostratigraphic zonation. *Mar. Micropalaeontol.* 5(2): 321-325.
- Pillari G., Biosca J. & Via L. (1989) - The Tertiary Sirenia of Catalonia. *Brain Anat. Ist.*: 1-98.
- Sorbi S. (2008) - New record of *Metaxytherium* (Mammalia, Sirenia) from the lower Miocene of Manosque (Provence, France). *Geodiversitas*, 30(2): 433-444.

A FOSSIL WHIP-SCORPION (ARACHNIDA: THELYPHONIDA) FROM THE UPPER CARBONIFEROUS OF THE CARNIC ALPS (FRIULI, NE ITALY)

PAUL A. SELDEN¹, JASON A. DUNLOP² & LUCA SIMONETTO³

¹Paleontological Institute and Department of Geology, University of Kansas, 1475 Jayhawk Boulevard, Lawrence, Kansas 66045, USA and Natural History Museum, London SW7 5BD, UK. E-mail: selden@ku.edu

²Museum für Naturkunde, Leibniz Institute for Evolution and Biodiversity Science, Invalidenstraße 43, D-10115 Berlin, Germany. E-mail: Jason.Dunlop@mfn-berlin.de

³Museo Friulano di Storia Naturale, via Marangoni 39-41, 33100 Udine, Italia. E-mail: luca.simonetto@comune.udine.it

To cite this article: Selden P. A., Dunlop J. A. & Simonetto L. (2016) - A fossil whip-scorpion (Arachnida: Thelyphonida) from the Upper Carboniferous of the Carnic Alps (Friuli, NE Italy). *Riv. It. Paleont. Strat.* 122(1): 7-12

Key words: Chelicerata, Gzhelian, Kasimovian, Pennsylvanian, Uropygi.

Abstract. A new and well-preserved fossil whip scorpion (Arachnida: Uropygi: Thelyphonida) is described from the Late Carboniferous of the Carnic Alps, Friuli, Italy. It is referred to *Parageralinura marsiglioi* n. sp. The new specimen is the first Carboniferous arachnid to be described from mainland Italy and is possibly the youngest Palaeozoic thelyphonid.

INTRODUCTION

Whip scorpions (Uropygi: Thelyphonida) are a distinctive group of arachnids which superficially resemble scorpions, but differ in having robust, subchelate pedipalps, a slender first pair of legs used as tactile appendages, and a long, thin flagellum (whip) forming the tail at the end of the opisthosoma which gives the group one of its common names. They are also sometimes referred to as vinegaroons, because another of their specialities is the ability to defend themselves by spraying a noxious compound, which includes acetic acid, from glands near the base of the tail. This behaviour is often associated with aggressive posturing, in which the opisthosoma is raised almost at right angles to the prosoma, further enhancing their scorpion-like appearance. For a summary of thelyphonid biology see Haupt (2000). The catalogue of Harvey (2003) recorded 103 living species in sixteen genera, all within a single family. Prendini (2011) updated this to 110 species. Extant whip scorpions can be found throughout the tropics in Africa, Asia (Fig. 1) and the Americas. Most are found in humid rainforest-type habitats, although some members of the American genus *Mastigoproctus* Pocock, 1894 inhabit more arid environments. Fossil whip scorpions are extremely

rare and only seven species are currently recognized in the literature. A putative Cenozoic example from California described by Pierce (1945) proved to be an unidentifiable organic fragment (Dunlop & Tetlie 2008). The Cretaceous Crato formation of north-eastern Brazil (~115 Ma) has yielded *Mesoproctus rowlandi* Dunlop, 1998, identifiable to the extant family Thelyphonidae. Incomplete material assigned to the same genus implies that these were very large whip scorpions, perhaps related to *Mastigoproctus* (see also Dunlop & Martill 2002). The six remaining species all come from the Late Carboniferous Coal Measures and span a time interval of ~306-319 Ma. They were last revised by Tetlie & Dunlop (2008) who recognized four Carboniferous genera, and proposed that all of them should be treated as plesion taxa with respect to the living family. The principal reason for this was that the pedipalps in the Palaeozoic whip scorpions are not fully subchelate and lack a projection (apophysis) which opposes the terminal podomere to form a claw. Subchelate pedipalps thus become a putative apomorphy of the Cretaceous-Recent Thelyphonidae.

Coal Measures whip scorpions include an unnamed carapace belonging to a modern-looking animal found in the Late Carboniferous (Kasimovian) of the Lugansk Province in the Donets Basin of Ukraine (Selden et al. 2014). Named species comprise *Proschizomus petrunkevitchi* Dunlop & Horrocks, 1996 from the British Middle Coal Measures



Fig. 1 - Recent thelyphonid, *Thelyphonus doriae* Thorell, 1888, Bukit Panjang, Singapore (1°21'23.38"N 103°48'46.48"E); photo P. A. Selden.

which lacks median eyes and has pedipalps orientated vertically rather than horizontally. It was thus speculated as being on the lineage which leads to another, closely related, arachnid order Schizomida. *Parageralinura neerlandicus* Laurentiaux-Viera & Laurentiaux, 1961, from the Netherlands, and *Parageralinura naufraga* (Brauckmann & Koch, 1983), from Germany, were placed in a genus together based on features such as noticeably robust leg femora. *Geralinura carbonaria* Scudder, 1884, from Mazon Creek in the USA, and *Geralinura britannica* Pocock, 1911, from the British Middle Coal Measures, were redefined by Tetlie & Dunlop (2008) as belonging to a genus characterized by a fairly elongate pygidium (the last three ring-like opisthosomal segments). Finally, *Prothelyphonus bohemicus* (Kušta, 1884) is noticeably larger (body length up to ~30 mm, excluding tail) and more gracile than the other penecontemporaneous fossil whip scorpions. *Prothelyphonus bohemicus* is currently known from a series of mostly rather spectacular fossils (Kušta 1884, 1888; Frič 1904; Petrunkevitch 1953; Dunlop & Penney 2012) from Rakovník and Chomle in the Bohemian Coal Mea-

sures of the Czech Republic. Here, we report *Parageralinura marsiglioi* n. sp. from the Upper Carboniferous of the Carnic Alps, Italy.

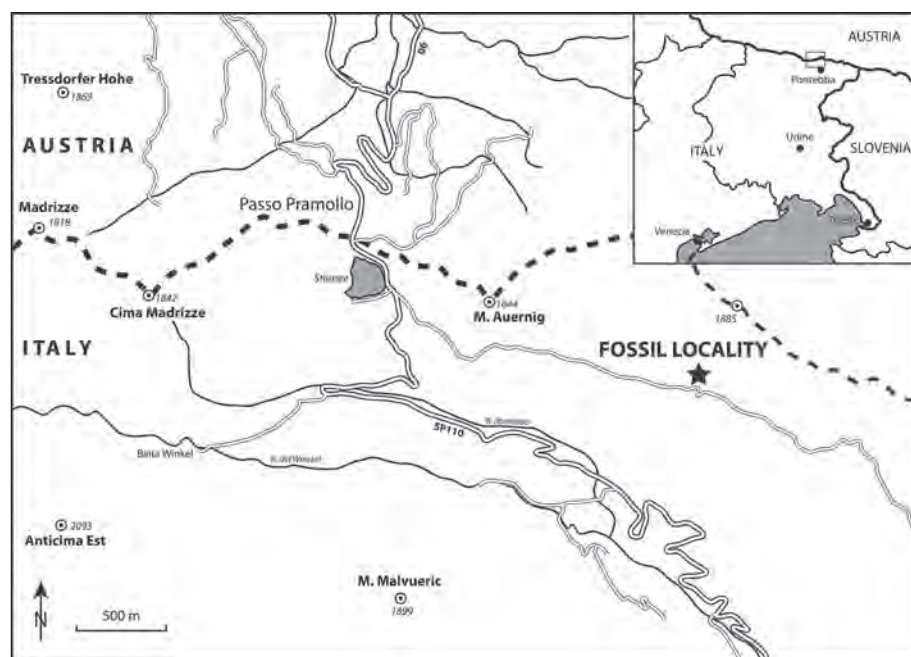
GEOLOGICAL SETTING

The single specimen (part only) comes from the southern side of Mt Auernig, east of Passo Pramollo-Naßfeld, and north of the village of Pontebba (Udine), near the Italian-Austrian border (Fig. 2). This is not far from the locality which yielded *Adelophthalmus* in the underlying Meledis Formation (Lamsdell et al. 2013). The thelyphonid locality, informally known as “Frana Vecchia” (Old Landslide), is on the mountain road leading to Casera For and Casera Cerchio from Passo Pramollo, approximately one kilometre from Casera Auernig. Here, at 46°33'09.6"N 013°18'03.0"E, the road crosses the base of a landslide fan. The specimen was found in debris on a small terrace at the base of the landslide scar, where a few metres of Upper Carboniferous pelites and arenites are exposed. The fossil is on a small slab of dark, thin sandstone. The rocks that crop out just above the terrace are attributed to the Pizzul Formation (Venturini 1990, 2006) and it is most likely that the slab came from this unit. The Pizzul Formation (Kasimovian-Gzhelian A-E) is the second unit from the base of the Pramollo Group (Upper Moscovian-Gzhelian E, Upper Carboniferous) (Selli 1963; Venturini 1990). The whole group is characterized by alternation of transgressive-regressive cycles related to glacio-eustatic control and tectonic activity (Vai & Venturini 1997). The result is a thick sequence of conglomerates and sandstones with high quartz content, preserved in a fluvio-deltaic environment and interbedded with marine shallow-water pelites and carbonates.

MATERIAL AND METHODS

The fossil consists of a relatively complete thelyphonid preserved in dorsal view. The chelicerae and first legs are not preserved; pedipalps and legs II–IV are preserved mainly as proximal podomeres; right leg III preserves the distal podomeres, which include a short basitarsus. Median and/or lateral eyes cannot be seen; folds on the carapace suggest muscle attachment sites. The opisthosoma is preserved in dorsal view, with a tergite count of 12, including a short anterior one, and three narrow ones posteriorly, forming the pygidium. A patch of cuticle at the left posterolateral corner, which shows faint tergite segmentation continuing across it (Fig. 3B, v?), is interpreted as part of the ventral surface.

Fig. 2 - Position of the fossil locality (star) at Frana Vecchia, just north of the ridge track leading east from the road SP110 from Pontebba to Passo Pramollo, which is situated on the Italy-Austria border; spot heights in metres. Inset: location map of the Passo Pramollo area near Pontebba in the north of Friuli.



The specimen is held in the Museo Archeologico e Naturalistico (via G. Pascoli 25, 33017 Tarcento, Udine, Italy), inventory number MPT 39217. It was studied under a Leica Wild MZ8 stereomicroscope, drawn using a camera lucida attachment, and photographed using a Canon EOS 5D MkIII camera attached to the microscope, both dry and under ethanol in cross-polarized light. To enhance depth of field, several photographs were taken of each part of the specimen and then stacked using Adobe Photoshop CS6; finally, a mosaic of these photographs was created to produce a final, high-resolution picture of the whole specimen for study. Final drawings were made based on the camera lucida drawings and the photographs using iDraw (www.ideeo.com). Abbreviations: 1-12 opisthosomal tergite numbers, II-IV leg numbers, bt basitarsus, car carapace, fe femur, L length, pa patella, pd pedipalp, tt telotarsus, ti tibia, v ventral, W width.

SYSTEMATIC PALEONTOLOGY

Order **Thelyphonida** Latreille, 1804

Genus *Parageralinura* Tetlie & Dunlop, 2008

Remarks. Of the four known Coal Measures genera, we can rule out affinities with *Proschizomus* since the pedipalps in the new fossil clearly articulate in a more horizontal plane, as in living species, rather than up and down in a vertical plane. We can also exclude *Geralinura*, which was re-diagnosed by Tetlie & Dunlop (2008) on the presence of an elongate pygidium at the posterior end of the opisthosoma in which the terminal (12th) segment is particularly long. The pygidium in the new fossil is squatter (Fig. 3). *Protheblyphonus* is represented by a single species of large (~3 cm long) and quite gracile fossils in which the pedipalps are particularly

massive; specifically they are noticeably longer than the carapace. The pedipalps in the new fossil appear to be shorter than the carapace (Fig. 3).

This leaves *Parageralinura*, a genus proposed by Tetlie & Dunlop (2008) to accommodate two species (see below) from Germany and the Netherlands. Characters proposed in the original diagnosis of this genus are a bluntly rounded pygidium and somewhat inflated femora of legs II-IV compared to other Coal Measures species. Both these features can be seen in the new fossil (Fig. 3). Tetlie & Dunlop (2008) also mentioned a somewhat broad opisthosoma in their diagnosis, which fits less well to the new fossil. However, this character may be less reliable as it was partly based on the original holotype of the German species *Parageralinura naufraga* in Brauckmann & Koch's (1993) description. A probably conspecific specimen discovered later from the same (type) locality of Hagen-Vorhalle (Brauckmann et al 2003: pl. 10, fig. 2) shows more typical body proportions for a whip scorpion and implies that the holotype may be compressed and slightly distorted. On balance we feel that the pedipalp proportions, terminal end of the opisthosoma and the inflated leg femora are most consistent with *Parageralinura*.

Parageralinura marsiglioi n. sp.

Fig. 3

Material: Holotype (part only) and only known specimen,

MPT 39217 in the Museo Archeologico e Naturalistico, via G. Pascoli 25, 33017 Tarcento, Udine, Italy.

Horizon and locality: Kasimovian–Gzhelian (Upper Carboniferous); from “Frana Vecchia”, southern side of Mt Auernig, Passo Pramollo, Pontebba, Udine, Italy.

Etymology: The species is named after the finder of the specimen, Giordano Marsiglio, director of the Museo Archeologico e Naturalistico, Tarcento, Udine, Italy.

Diagnosis: *Parageralinura marsiglioi* differs from the two other species in the genus by its larger size (~25 mm, cf. ~11 and ~16 mm), more slender opisthosoma (L/W ratio 2.60, cf. 1.72 and 1.90), and shorter, broader telson articles.

Description. Cuticle pustulate, especially on carapace. Total body L (excluding telson) 24.70 mm. Carapace elongate; L 8.88, W 6.81 (L/W ratio 1.30); posterior margin straight, posterolateral margins straight and diverging forwards, anterolateral margins then curve slightly forwards from about mid-length, becoming straight to anterior tip of carapace; posterior half with median groove, posterior procurved semicircular groove abuts posterior margin, other grooves radiate from median to lateral margins (Fig. 3). Pedipalps subraptorial, with tumid podomeres; fe L 3.78 mm, pa L 3.08 mm. Legs II–IV with notably inflated femora; podomere lengths: leg II fe 5.83 mm (W 2.06 mm, L/W ratio 2.83); pa 3.42 mm; ti 4.44 mm; leg III fe 6.78 mm (W 2.27 mm, L/W ratio 2.99), pa 3.50 mm, ti 4.24 mm, bt 1.32 mm, tt 2.19 mm (with 3 tarsomeres); leg IV fe 9.40 mm (W 2.59 mm, L/W ratio 3.62), pa 4.00 mm, ti 5.48 mm. Opisthosoma elongate suboval, L 16.31 mm, W 6.27 mm (L/W ratio 2.60), with 12 tergites, last three form a squat pygidium (L 3.23 mm, anterior W 4.16 mm, posterior W 2.08 mm). Telson flagelliform, L \geq 11.37 mm; W 1.12 mm; at least 11 rather broad articles (ratio W tergite 12/W telson 1.86), each about as wide as long (Fig. 3C).

DISCUSSION

The two known species of *Parageralinura* are not easy to distinguish from one another and lack explicit diagnostic apomorphies. Instead, differences are largely in body proportions: *P. naufraga* is larger (~16 mm long), and the pygidium is slightly smaller compared to the rest of the opisthosoma; whereas *P. neerlandica* is smaller (~11 mm), with possibly a slightly more inflated opisthosoma and a proportionally larger pygidium. They are geographically and stratigraphically close to one another and we cannot completely rule out the possibility that

they are different stages of the same morphospecies. The new fossil differs from the German and Netherlands material in being larger than both (almost 25 mm) and in having a more slender opisthosoma. Comparative opisthosoma L/W ratios are as follows: *P. marsiglioi* n. sp. 2.60, *P. neerlandica* 1.72, *P. naufraga* 1.90. Furthermore, the telson articles of the new species are rather shorter and broader than in other thelyphonids, and certainly than in the other *Parageralinura* species (see, e.g. Brauckmann et al. 2003, fig. 22; Laurentiaux-Viera & Laurentiaux 1961, fig. 2). For these reasons, we consider the fossil a new species of *Parageralinura*.

The new thelyphonid is the first Coal Measures arachnid to be described from the Italian mainland; the only other Italian find is a representative of the extinct arachnid order Trigonotarbida from the San Giorgio Basin (Westphalian D) of Sardinia described by Selden & Pillola (2009). As noted above, fossil whip scorpions are extremely uncommon and any new record is of note.

Parageralinura marsiglioi is stratigraphically younger than the other species in the genus. *P. naufraga* is the oldest known thelyphonid, from the Vorhalle-Schichten of Hagen-Vorhalle, Germany, which belong to the R2c goniatite subzone, Namurian B (middle Bashkirian). *Parageralinura neerlandica* from Limburg, Netherlands, is of Langsettian, Westphalian A age (uppermost Bashkirian). Whilst a precise age cannot be determined for the new species, it dates to Kasimovian–Gzhelian, and is therefore younger than either of its congeners. Indeed, it may be the youngest Palaeozoic thelyphonid, since the Lower Kasimovian age of the carapace described by Selden et al. (2014) from Ukraine, the hitherto youngest Palaeozoic thelyphonid, is at the older end of the possible stratigraphic range of the new *P. marsiglioi*.

Acknowledgments. We thank Giordano Marsiglio, director of the Museo Archeologico e Naturalistico, Tarcento (Udine), for kindly providing the specimen for study, Corrado Venturini (Dipartimento di Scienze Biologiche, Geologiche e Ambientali, Bologna University) for helpful information on the stratigraphical position of the sample, and Lorenzo Prendini and Derek Siveter for their valuable reviews of the manuscript. The visits by PAS to Berlin and Udine were funded by the Alexander von Humboldt Foundation and the University of Kansas.

REFERENCES

- Dunlop J.A. (1998) - A fossil whipscorpion from the Lower Cretaceous of Brazil. *J. Arachnol.*, 26: 291–295.

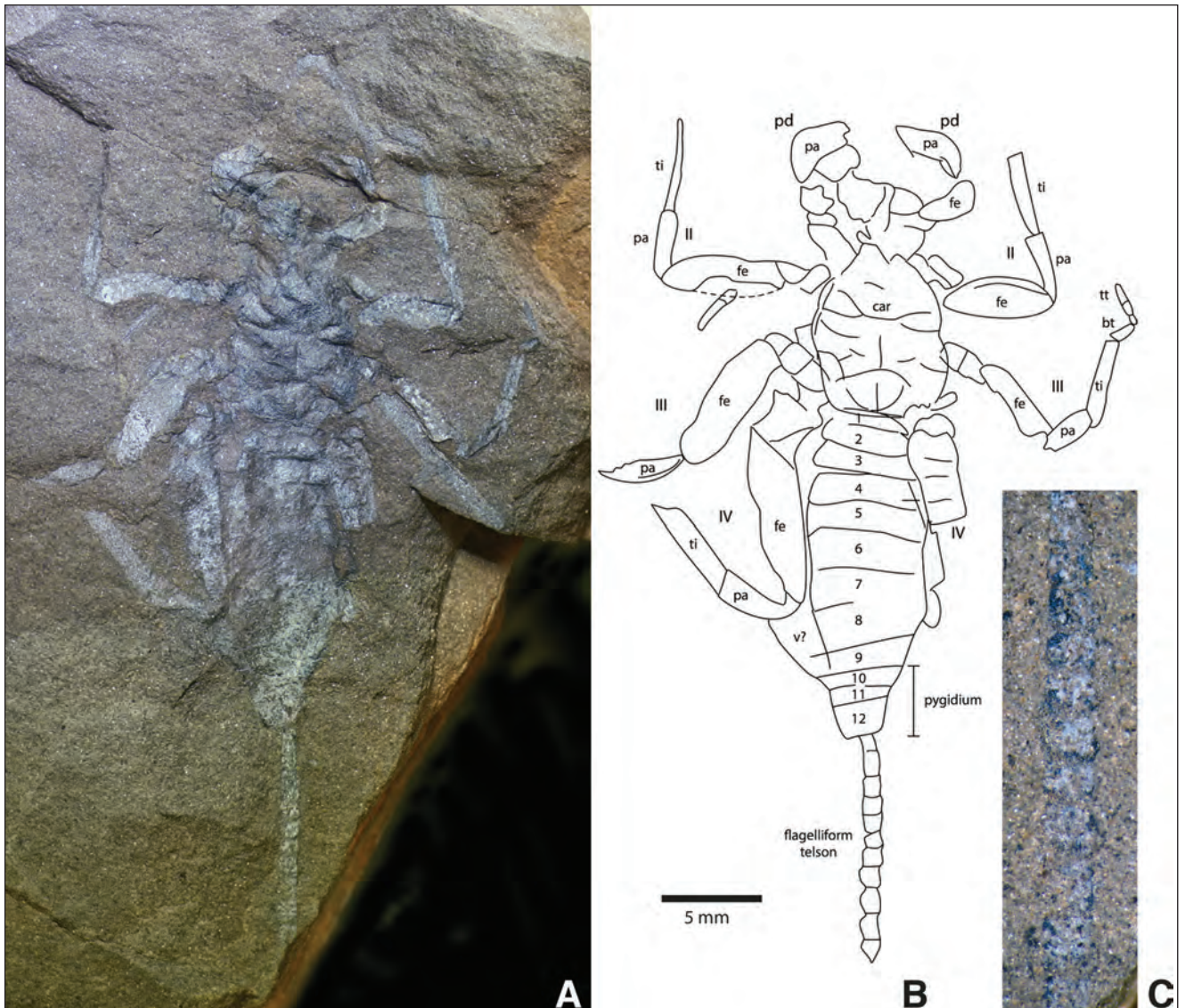


Fig. 3 - *Parageralinura marsiglioi* n. sp. from the Upper Carboniferous (Kasimovian–Gzhelian) Pizzul Formation, Friuli, specimen MPT 39217. A) Photograph of holotype and only known specimen, under alcohol and cross-polarized light. B) Interpretative drawing of the specimen in A. C) Detail of flagelliform telson.

- Dunlop J.A. & Horrocks C.A. (1996) - A new Upper Carboniferous whip scorpion (Arachnida: Uropygi: Thelyphonida) with a revision of the British Carboniferous Uropygi. *Zool. Anz.*, 234: 293-306.
- Dunlop J.A. & Martill D.M. (2002) - The first whipspider (Arachnida: Amblypygi) and three new whipscorpions (Arachnida: Thelyphonida) from the Lower Cretaceous Crato Formation of Brazil. *Trans. R. Soc. Edinb., Earth Sci.*, 92: 325-334.
- Dunlop J.A. & Penney D. (2012) - Fossil arachnids. Siri Sci. Press, Manchester, 192 pp.
- Dunlop J.A. & Tetlie O.E. (2008) - The Miocene whipscorpion *Thelyphonus hadleyi* is an unidentifiable organic remain. *J. Arachnol.*, 35: 551-553.
- Frič A. (1904) - Palaeozoische Arachniden. A. Frič, Prague, 85 pp.
- Harvey M.S. (2003) - Catalogue of the smaller arachnid orders of the world. CSIRO Pubs, Collingwood, xi + 385 pp.
- Haupt J. (2000) - Biologie der Geißelskorpione (Uropygi Thelyphonida). *Mem. Soc. Ent. It.*, 78: 305-319.
- Kušta J. (1884) - *Thelyphonus bohemicus* n. sp., ein fossiler Geißelscorpion aus der Steinkohlenformation von Rakonitz. *Sber. K. Böhm. Ges. Wiss., Mat.-Nat. Kl.*, 1884: 186-191.
- Kušta J. (1888) - O nových arachnidech z karbonu Rakovnického. (Neue Arachniden aus der Steinkohlenformation bei Rakonitz). *Sber. K. Böhm. Ges. Wiss., Mat.-Nat. Kl.*, 1888: 194-208.
- Lamsdell J.C., Simonetto L. & Selden P.A. (2013) - First eurypterid from Italy: a new species of *Adelophthalmus* (Chelicerata: Eurypterida) from the Upper Carboniferous of the Carnic Alps (Friuli, NE Italy). *Riv. It. Paleont. Strat.*, 119: 147-151.
- Latreille P.A. (1804) - Histoire naturelle, generale et particuliere, des Crustacés et des Insectes, 7: 144-305. F. Dufart, Paris.
- Laurentiaux-Viera F. & Laurentiaux D. (1961) - *Prothelyphonus*

- neerlandicus*, nov. sp., Uropyge du Westphalien du Limbourg Hollandais. *Med. Geol. Sticht.*, N.S., 13: 29-34.
- Petrunkovitch A.I. (1953) - Palaeozoic and Mesozoic Arachnida of Europe. *Mem. Geol. Soc. Am.*, 53: 1-128.
- Pierce W.D. (1945) - A fossil whiptail scorpion from Cabrillo Beach. *Bull. S. Cal. Acad. Sci.*, 44: 7-8.
- Pocock R.I. (1911) - A monograph of the terrestrial Carboniferous Arachnida of Great Britain. *Monogr. Pal. Soc.*, 64: 1-84.
- Prendini L. (2011) - Order Thelyphonida Latreille, 1804. In: Zhang Z.-Q. (Ed.) - Animal biodiversity: An outline of higher-level classification and survey of taxonomic richness. *Zootaxa*, 3148: 155.
- Scudder S.H. (1884) - A contribution to our knowledge of Paleozoic Arachnida. *Proc. Am. Acad. Arts Sci.*, 20: 13-22.
- Selden P.A. & Pillola G.L. (2009) - A trigonotarbid arachnid from the Upper Carboniferous of the San Giorgio Basin, Sardinia. *Rev. It. Paleont. Strat.*, 115: 269-274.
- Selden P.A., Shcherbakov D.E., Dunlop J.A. & Eskov K.Yu. (2014) - Arachnids from the Carboniferous of Russia and Ukraine, and the Permian of Kazakhstan. *Pal. Zeit.* 88: 297-307.
- Selli R. (1963) - Schema geologico delle Alpi Carniche e Giulie Occidentali. *Giornale di Geologia*, ser. 2, 30: 1-121.
- Tetlie O.E. & Dunlop J.A. (2008) - *Geralinura carbonaria* (Arachnida; Uropygi) from Mazon Creek, Illinois, USA, and the origin of subchelate pedipalps in whip scorpions. *J. Paleontol.*, 82: 299-312.
- Thorell T. (1888) - Pedipalpi e Scorpioni dell'Arcipelago Malese conservati nel Museo Civico di Storia Naturale di Genova. *Ann. Mus. Civ. Stor. Nat. Genova*, Ser. 2, 6: 327-428.
- Vai G.B. & Venturini C. (1997) - Moskovian and Artinskian rocks in the frame of the cyclic Permo-Carboniferous of the Carnic Alps and related areas. *Geodiversitas*, 19: 173-186.
- Venturini C. (1990) - Geologia delle Alpi Carniche centro orientali. *Museo Friulano di Storia Naturale*, 36: 1-222.
- Venturini C. (2006) - Evoluzione geologica delle Alpi Carniche. *Museo Friulano di Storia Naturale*, 48: 1-207.

SIRENIA FOSSILS FROM QOM FORMATION (BURDIGALIAN) OF THE KABUDAR AHANG AREA, NORTHWEST IRAN

NASROLLAH ABBASSI^{1,*}, DARYL P. DOMNING², NAVID NAVIDI IZAD³ & SAFOORA SHAKERI⁴

¹Department of Geology, Faculty of Science, University of Zanjan, Zanjan 38791-45371, Iran. E-mail: abbasi@znu.ac.ir *Corresponding Author.

²Department of Anatomy, Howard University, Washington, DC 20059, U.S.A.

³Department of Geology, Faculty of Earth Sciences, Kharazmi University, Tehran 15719-14911, Iran.

⁴Research affairs office, Faculty of Engineering, University of Zanjan, Zanjan 38791-45371, Iran.

To cite this article: Abbasi N., Domning D. P., Navidi Izad N. & Shakeri S. (2016) - Sirenia fossils from Qom Formation (Burdigalian) of the Kabudar Ahang area, Northwest Iran. *Riv. It. Paleont. Strat.* 122(1): 13-24

Keywords: Marine mammal fossils, Sirenia, Burdigalian, Qom Formation, Iran.

Abstract. Fossil remains of sirenians (Mammalia; Dugongidae) are reported from the late early Miocene (Burdigalian) Qom Formation near the town of Shirin Su, northwest Kabudar Ahang region, west of Tehran, Iran. The fossils consist of partial postcranial skeletons preserved mostly as natural molds in limestone. In the absence of skulls or other diagnostic elements, it is not evident which dugongid subfamily these specimens represent: Halitheriinae or Dugonginae. Both subfamilies were present in contemporaneous Western Tethys (Mediterranean) deposits, but so far only dugongines have been found in Neogene rocks of Eastern Tethys. Since the Iranian deposits are located between these two parts of the former Tethys seaway, it will be interesting to see which group(s) the Iranian sirenians prove to represent, once their taxonomic identity has been determined through future discoveries.

INTRODUCTION

Reconnaissance and discovery of mammal fossils from unknown areas is important for paleontologists, because new data are useful to reconstruct and/or improve our knowledge about the paleobiogeographic ranges of organisms. The Iranian plateau was located in the central part of Tethys, which acted as a seaway and/or bridge for the migration of either marine or terrestrial mammals during the Cenozoic Era. Thus collecting of mammal fossils from Iran and adjacent areas will improve knowledge of mammal distributions before and after the Eurasian-Afroarabian closure. The Late Miocene Maragheh bone beds are a famous site for vertebrate paleontology in Iran, which has been investigated for 150 years (Khanikoff 1858; Rodler & Weithofer 1890; Mecquenem 1925; Campbell et al. 1980). There are, however, few reports about mammal fossils from other parts of Iran (e.g. Najafi & Bazarghani Gilani 2006). Initially, Reuter et al. (2007) reported Miocene marine mammals (Sirenia) from the Qom Formation of the Zefreh area, Central Iran. Recently, sirenian fossils have also been collected and

preliminarily studied from the Asmari Formation of the Zagros Mountains (Dezful and Bastak areas) and the Qom Formation of Central Iran (Zefreh-Chahriseh, Malayer and Kabudar Ahang areas; Mirzaie Ataabadi et al. 2014). Additional occurrences of mammal fossils have been reported from the abandoned decorative-stone quarry of Shirin Su in northwest Kabudar Ahang, Central Iran. Based on local reports, the Iranian authors visited and studied marine mammal fossils of Shirin Su in March and September 2014. The main purpose of this paper is to add to data on mammal paleontology from the Iranian plateau.

GEOLOGICAL SETTING

The Qom Formation is the main Oligo-Miocene lithostratigraphic unit in Central Iran. It crops out from east of Semnan and north of Nain to Mount Ararat in eastern Turkey (Fig. 1). Lithostratigraphic units equivalent to the Qom Formation are known as the Asmari Formation (Oligo-Miocene) and Guri Member (lower Miocene) of the Mishan Formation in the Zagros Mountains. Oligo-Miocene limestone of the Esfahan-Sirjan basin with local

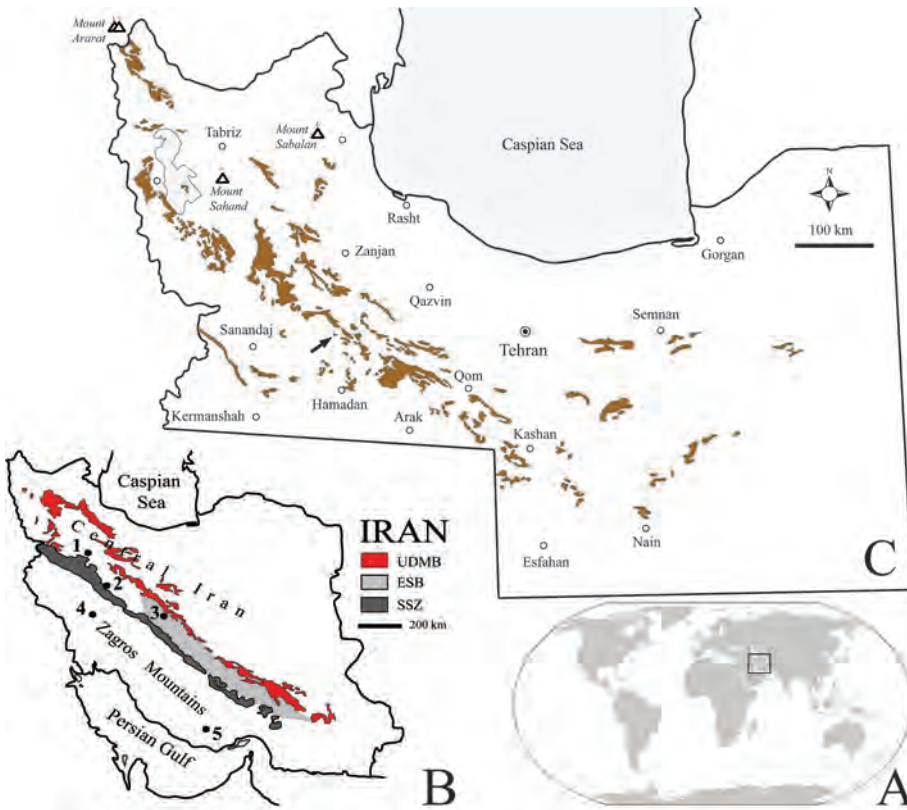


Fig 1 - Outcrops of the Qom Formation in Central Iran. A) Location of Iran on the world map. B) Location of Central Iran, Esfahan-Sirjan basin and Zagros Mountains in Iran; areas where sirenians found include: 1 - Kabudar Ahang, 2 - Malayer, 3 - Zefreh-Chahrisch, 4 - Dezful, 5 - Bastak. Abbreviations: UDMB, Urumieh-Dokhtar Magmatic Belt; ESB, Esfahan-Sirjan basin; SSZ, Sanandaj-Sirjan Zone (base map modified by Nogole Sadat & Almasian 1993). C) Outcrops of the Qom Formation in Central Iran (modified from Rahimzadeh 1994); arrow indicates the Shirin Su section.

units (e.g. the Chahar Gonbad Formation) are correlative with the Qom Formation.

The Qom Formation has extensive outcrops in the Kabudar Ahang area, in Hamadan Province (Fig. 2). The Qom Formation was deposited in a fault-controlled marine basin with different lithofacies in the Ab-e garm, Avaj, Razan, and Sanandaj-Sirjan zones (Bolourchi 1979). The major faults of this area, all of them with NW-SE strike, include the Hassan Abad, Ahmad Abad-Avaj, and Aznove-Morgh Abad faults (Fig. 2).

The northern part of the Ab-e garm zone

includes the southeastern parts of the Soltanieh Mountains. The Soltanieh zone was uplifted in a horst after the Eocene. Thus, the Qom Formation has exposures on the southern flanks of the Soltanieh Mountains.

The Ab-e garm zone is located in the southern range of the Hassan Abad fault. The Qom Formation in this zone includes light-colored limestone with green marlstone and detrital beds of sandy limestone intercalations. The formation is 440 m thick, with Burdigalian foraminifers (Bolourchi 1979).

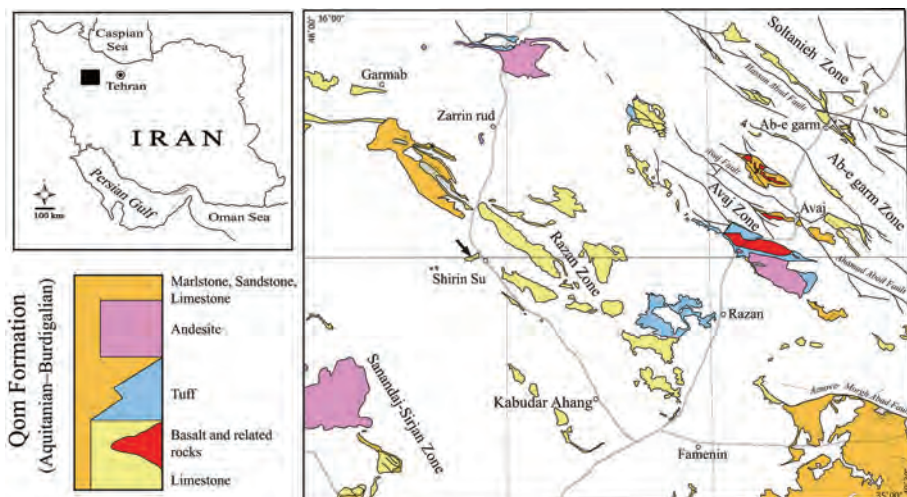


Fig 2 - Qom Formation lithofacies in the Kabudar Ahang area with main local geological zones. The studied section (arrow) is located west of Shirin Su.

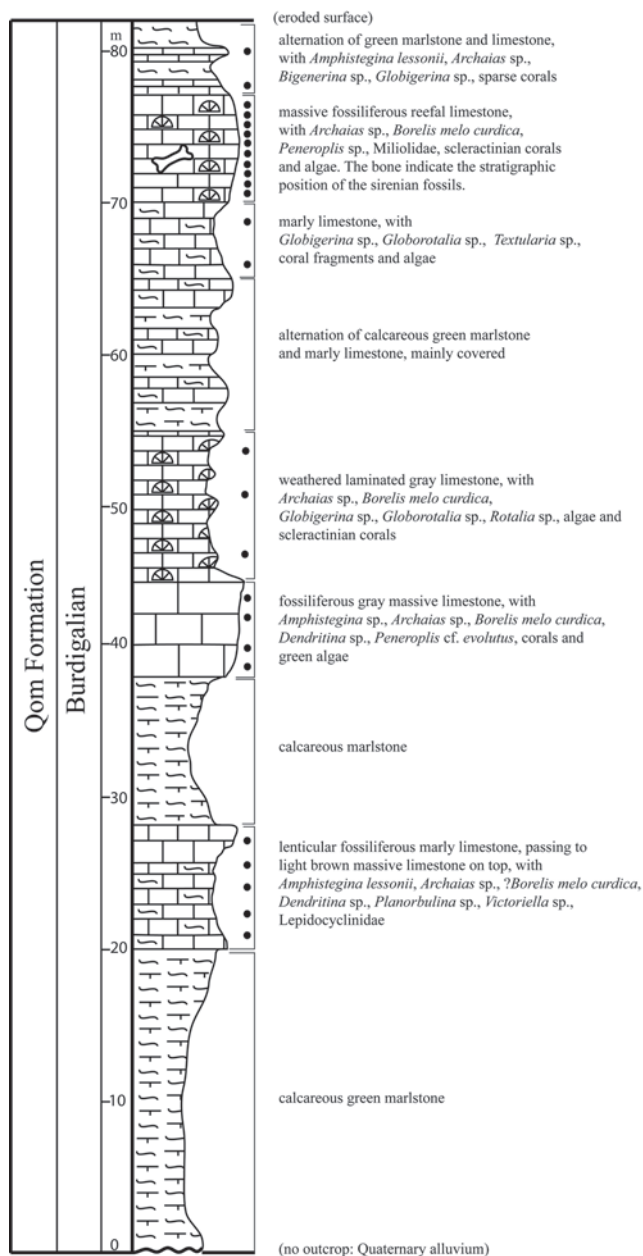


Fig. 3 - Stratigraphical column of surveyed section of the Qom Formation west of Shirin Su. Mammal fossils have been found in the upper massive fossiliferous reefal limestone. Black points indicate the locations of collected micropaleontology samples.

The Avaj zone is located around the Avaj-Ahmad Abad faults. The Qom Formation in the north Avaj fault zone predominantly contains marly limestone with detrital limestone intercalations. It is locally interbedded with tuff beds and accompanied by basalt, olivine basalt, and basaltic andesite. The thickness of the formation here exceeds 1100 m. The microfauna collected from the lower part of the formation represents the Aquitanian Stage while fossils from the upper part include Burdigalian

microfauna (Bolourchi 1979).

In the southern part of the Avaj fault, the Qom Formation is 2400 m thick, and includes huge volcanic rocks and tuffaceous sediments reactivated with the Avaj fault. The formation is divided here into 6 units, including limestone, tuff, andesite, hornblende andesite, dacitic andesite, basaltic andesite, basalt, and diabase. The microfaunas indicate an Aquitanian age for the lower limestone and tuff, and Burdigalian for the upper tuff and limestone (Bolourchi 1979).

The Qom Formation is well developed in the Razan zone in southern parts of the Aznove-Morgh Abad fault zone. The formation consists of green-gray, well-stratified, marly limestone intercalated with sandstone and lenses of reefal limestone. The lower part of the formation (2700 m) is Aquitanian, and the upper part (700 m) is Burdigalian (Bolourchi 1979).

The Qom Formation cropping out in the most southwestern areas of the Kabudar Ahang is a part of the Sanandaj-Sirjan zone, where the formation includes andesite rock.

The studied section of the Qom Formation, where the sirenian fossils have been found, crops out in a hill west of the town of Shirin Su, northwest Kabudar Ahang. The Qom Formation is 82 m thick in this outcrop, and includes alternating marlstone, bioclastic reefal limestone, marly limestone, massive bioclastic (mainly coral) limestone, and calcareous marlstone (Fig. 3). The mammal fossils were found in the upper massive fossiliferous reefal limestone. Samples from limestone layers contain the following foraminifera: *Amphistegina lessonii*, *Amphistegina* sp., *Archaias* sp., *Bigenerina* sp., *Borelis melo curdica*, *Dendritina* sp., *Globigerina* sp., *Globorotalia* sp., *Peneroplis* cf. *evolutus*, *Peneroplis* sp., *Planorbulina* sp., *Rotalia* sp., *Textularia* sp., *Triloculina* sp., *Victoriella* sp., Lepidocyclinidae, Miliolidae.

This assemblage is equivalent to the *Borelis melo curdica* assemblage zone of Wynd (1965), the *Borelis melo* group-*Meandropsina iranica* assemblage zone of Adams and Bourgeois (1967) and Daneshian and Ramezani Dana (2007), and the *Borelis melo curdica*-*Borelis melo melo* assemblage zone (Laursen et al. 2009) of the Asmari Formation in the Zagros Mountains, indicating a Burdigalian age for this section.

Neither the lower nor the upper boundaries of the exposed section are known (Fig. 3), but ba-

sed on paleontological data these sediments belong to upper parts of the Qom Formation in the Kabudar Ahang area and are equivalent to the (f) member of the Qom Formation at the type locality, east of Qom (Furrer & Soder 1955; Bozorgnia 1966).

MATERIALS AND METHODS

The sirenian fossils from Shirin Su comprise postcranial remains of at least three individuals. Specimen 1 (ICHTO 12) is an articulated partial skeleton preserved in two loose blocks. Block 1 (ICHTO 12/1, 1.6 x 1.2 x 1m) and block 2 (ICHTO 12/2, 3 x 2.5 x 1.2m) contain relatively complete natural molds of the articulated vertebrae and ribs, displaying the dorsal and ventral sides, respectively, of one individual. Impressions of vertebrae and ribs in these blocks are numbered in the figures according to their estimated anatomical positions. These blocks have been transported to the municipal office of Shirin Su town for preservation and geo-tourism. Specimen 2 (1 x 0.5 x 0.3 m) is also a loose block, containing natural molds of ribs, which remains in the quarry. Specimen 3 is a group of exposed ribs that remain in situ.

The stratigraphical position of the mammal fossils was determined by sampling and surveying bed by bed. Twenty-eight thin sections were prepared for micropaleontology. Dr. Abdoreza Moghadasi, a micropaleontology specialist in the paleontology laboratories of the National Iranian Oil Company, studied these thin sections and determined its foraminifera and the age of the studied section.

SYSTEMATIC PALEONTOLOGY

Class **MAMMALIA** Linnaeus, 1758

Order **Sirenia** Illiger, 1811

Family **Dugongidae** Gray, 1821

Dugongidae indeterminate

Figs 4-5

Referred specimens: Three sets of associated postcranial bones (ribs and, in two cases, vertebrae), preserved as natural molds in part. The most complete specimen is presently housed in the municipal office of Shirin Su town, bearing the numbers 12/1 and 12/2 in the catalog of the Iranian Cultural, Handicraft and Tourism Organization (ICHTO) of Kabudar Ahang Township, Hamadan Province; the other two specimens remain in the quarry.

Locality: Abandoned decorative-stone quarry near the town of Shirin Su, northwest Kabudar Ahang region, Central Iran. GPS coordinates are 35° 29' 50.4" N and 48° 25' 23.6" E.

Formation: Qom Formation.

Age: Late early Miocene (Burdigalian).

Description. The two specimens in loose blocks are preserved mainly as natural molds with some bone fragments, and include thoracic, lumbar, sacral, and caudal vertebrae and ribs. The third specimen comprises some ribs exposed in situ. Detailed descriptions of these specimens are as follows:

ICHTO 12/1 (block 1): This block contains molds of the dorsal sides of thoracic, lumbar, sacral, and parts of caudal vertebrae (neural arches) and ribs (Fig. 4A). Sixteen thoracic vertebrae are visible; these are numbered T3-T18 based on the conservative assumption that this animal had 18 thoracics and 18 pairs of ribs, which is the minimum number observed in other dugongids. Only molds of pleurapophyses of the lumbar and sacral vertebrae and partial transverse processes of caudal vertebrae are preserved. The spinous processes of the vertebrae are preserved as deep hollows (5 cm in depth) that are heart-shaped in cross section (Fig. 4C). Prezygapophyses form elongate hollows in T7 to T9, and postzygapophyses form round hollows with mild curvature. Seventeen casts of thoracic vertebrae are distinguishable. Only molds of the pleurapophyses of the right side of the lumbar and sacral vertebrae are visible. Similarly, only one transverse process of the first caudal vertebra remains. A mold of a small piece of bone is visible that may be a chevron bone. Some parts of articular areas of ribs and vertebrae are distinguishable, including tubercula on flattened parts of ribs. Other parts are shown in detail in Fig. 4C.

ICHTO 12/2 (block 2): This block preserves natural molds of ventral parts of thoracic and lumbar vertebrae and ribs; 14 thoracic (numbered 5 to 18), 3 lumbar, 1 sacral, and 1 caudal vertebrae are visible (Fig. 4B). Ventral processes and epiphyses of the vertebral bodies are distinguishable (Fig. 4D). Thickness of epiphyses varies from 0.5 to 1 cm, decreasing toward the rear. The vertebrae after vertebra number 15 are partly covered by sediments (Fig. 4E). Each thoracic vertebra contacts its ribs with flat facets. The details of neural arches are visible on the posterior vertebrae (Fig. 4E), where the canal is elliptical, and 3 cm in diameter. What appears to be a foramen 1 cm in diameter is visible on the anterodorsal part of T15, but this may not be a part of this vertebra. There are molds of canals that may be related to neural canals (?IVF in Fig. 4E). Prezygapophyses and postzygapophyses are distinct as anterior and posterior impressions in the rock. Most of the lumbar, sacral, and caudal vertebrae are covered by sediment and only their left transverse processes are visible. Molds of other bones are also present; some of them are V-shaped, possibly attributable to chevron bones. A triangular flat mold may represent a blade-shaped bone (?B in Fig. 4B).

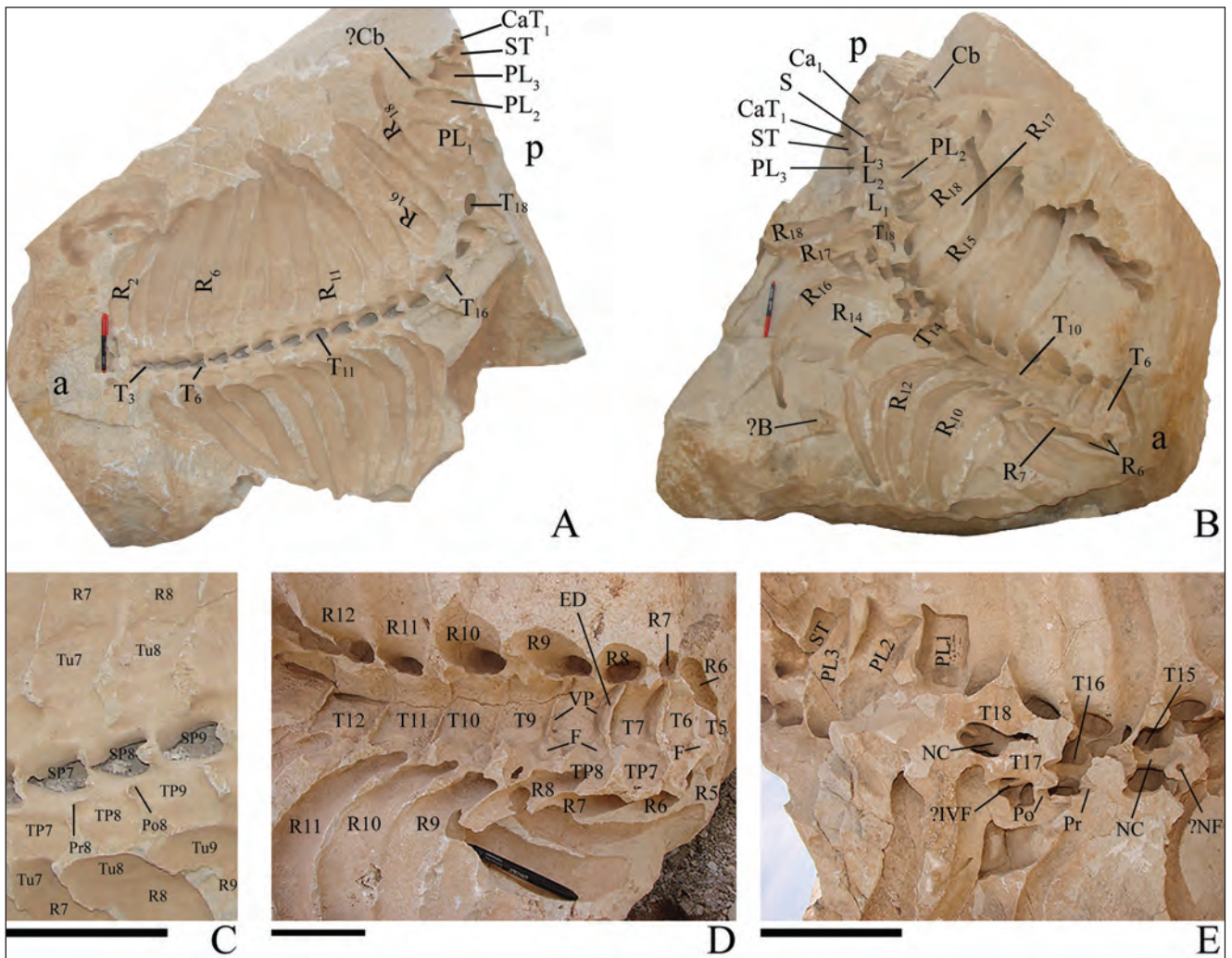


Fig. 4 - Specimen ICHTO 12 of *Sirenia* fossils from Kabudar Ahang. A) Block 1 (ICHTO12/1) with molds of dorsal sides of thoracic, lumbar, sacral, and caudal vertebrae and ribs. Dark-colored tips of spinous processes and other fragments of the vertebrae are still present in the cavities of the mold. B) Block 2 (ICHTO 12/2) with molds of ventral sides of thoracic, lumbar, sacral, and caudal vertebrae and ribs. C) Close-up of vertebrae no. 7 to 9 and details of mold preservation in block 1. D) Close-up of anterior vertebrae and adjacent ribs in block 2. E) Details of posterior vertebrae and adjacent ribs of block 2. Abbreviations: a, anterior; ?B, unidentified blade like bone; Ca, caudal vertebra; CaT, caudal transverse process; Cb, chevron bone; F, articular facet; ED, epiphysis of body; ?IVF, unidentified intervertebral foramen; L, lumbar vertebra; NC, neural canal; ?NF, presumably neural foramina; p, posterior; PL, pleurapophysis; Po, postzygapophysis; Pr, prezygapophysis; R, rib; S, sacral vertebra; SP, spinous process; ST, sacral vertebra transverse processes; T, thoracic vertebra; TP, transverse process; Tu, tubercle of rib; VP, ventral process of vertebra. Numbers show estimated anatomical positions. Pen for scale in A and B is 14 cm long, scale bars equal 10 cm.

Specimens 2 and 3: These fossils include only ribs. Specimen 2 is a mold of five wide and close-set ribs (Fig. 5A). Specimen 3 comprises thick and round sections of ribs (Fig. 5B).

Discussion. Ancestors of sea cows (*Sirenia*; manatees and dugongs) and whales (Cetacea), the first marine mammals, appeared about 50 million years ago in the early Eocene (Berta et al. 2006). These mammals today are exclusively aquatic throughout their lives. However, the sirenian Family Prorastomidae (early-middle Eocene), the earliest sea cows, had both fore and hind legs, and some were able to walk on land, like the earliest cetaceans (Domning

2000, 2001; Springer et al. 2015).

The Protosirenidae, also known only from the Eocene, were the next sirenian family to appear after the prorastomids (Domning 1994). They still had four legs, but probably spent little if any time on land (Domning and Gingerich 1994; Domning 2000). They were followed in turn by the fully-aquatic families Dugongidae (which first appeared in the middle Eocene, and are represented today only by the dugong, *Dugong dugon*) and the Trichechidae (which first appeared in the late Oligocene, and include the modern manatees, *Trichechus* spp.) (Domning 2009).

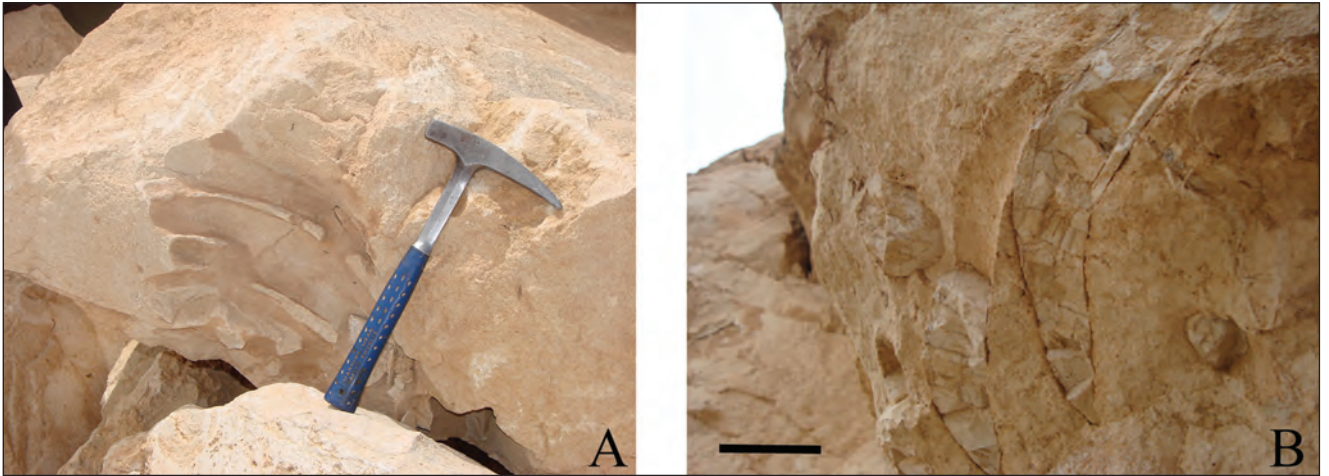


Fig. 5 - Specimens 3 and 4 of *Sirenia* fossils from Kabudar Ahang. A) Specimen 3 includes external molds of five ribs. Length of hammer 30 cm. B) Specimen 4 includes fragmentary ribs. Scale bar 5 cm.

The sirenians known to have been present in Western Tethys during the Aquitanian and Burdigalian include members of two subfamilies of Dugongidae, the Halitheriinae (represented by the common genus *Metaxytherium*; e.g. Domning & Pervesler 2001), and the Dugonginae (represented by the rare genus *Rytiodus*; e.g. Domning & Sorbi 2011). Still rarer are members of the trichechid subfamily Miosireninae, known only from western and northwestern Europe (e.g. *Miosiren*).



Fig. 6 - Late Oligocene-Early Miocene basins with carbonate deposition in Iran as straits between Western and Eastern Tethys (modified from Harzhauser & Piller 2007). Reported localities of *Sirenia* fossils include: 1 - Kabudar Ahang, 2 - Malayer, 3 - Zefreh-Chahriseh, 4 - Dezful, 5 - Bastak. Abbreviations: UDMB: Urumich-Dokhtar Magmatic Belt bridge; ESB: Esfahan-Sirjan Basin; SSZ: Sanandaj-Sirjan Zone bridge.

In Eastern Tethys, much less collecting of fossil sirenians has been done, but three species are already known from the Aquitanian of India: *Bharatisiren kachchhensis*, *Kutchisiren cylindrica*, and *Domningia sodbae* (Bajpai et al. 1987; Bajpai & Domning 1997; Bajpai et al. 2010; Thewissen & Bajpai 2009). Interestingly, all three of these are dugongines (Vélez-Juarbe et al. 2012). The halitheriines, which are so common in Miocene Europe (*Metaxytherium* spp.), have not been detected in the Indian Ocean, although halitheriines were represented there in the Eocene (Bajpai et al. 2006). A fourth Miocene specimen from the Indian Ocean (Madagascar), incorrectly identified by Collignon & Cottreau (1927) as “*Halitherium* sp.”, is probably also a dugongine. So the fossils from Iran are of special interest, as they represent a sample from the very seaway that connected Eastern and Western Tethys: are they dugongines, as the Indian Ocean record leads us to expect; or halitheriines, the most common sirenians in Europe; or both, or even something else?

Unfortunately, the specimens so far found in Iran are not diagnostic beyond the family level; identification to the subfamily level or below must await more complete specimens, ideally skulls. However, their morphology is consistent with that of the Dugongidae – specifically the heart-shaped cross sections of the thoracic neural spines, which have a pronounced median concavity on the posterior side (Fig. 4A, C). This morphology occurs in some Miocene dugongids (e.g., Simpson 1932: figs. 6, 7), but is not observed in the Miocene trichechid *Miosiren kocki* (Sickenberg 1934:315, pl. 11), which is

| | Eocene | Oligocene | Miocene | Pliocene |
|------------|----------------|-----------|------------|----------|
| Austria | - | - | 1, 2 | - |
| Croatia | - | - | 3 | - |
| Egypt | 4, 5, 6, 7 | 8 | - | - |
| France | 9 | 10, 11 | 12, 13 | 14, 15 |
| Hungary | 16, 17, 18, 19 | 16, 19 | 16, 19, 20 | - |
| India | 21, 22 | 22 | 23, 24, 25 | - |
| Iran | - | - | 26, 27, 28 | - |
| Israel | 29 | - | - | - |
| Italy | 30 | 31 | 32, 33, 34 | 35,36 |
| Libya | 37, 38, 39 | 40 | 41 | 15 |
| Madagascar | 42, 43 | - | 44 | - |
| Malta | - | 45 | 46 | - |
| Morocco | 47 | - | - | 48 |
| Pakistan | 49, 50 | - | 51 | - |
| Portugal | - | - | 52 | 52 |
| Romania | 53 | 54 | - | - |
| Spain | 55 | - | 56 | - |
| Tunis | 57 | - | 58 | - |
| Turkey | - | - | 59 | - |
| Yemen | 60 | - | - | - |

Tab. 1 - Distribution of Tethyan Sirenian fossils, including representative localities and literature citations. 1 (Pervesler et al. 2000), 2 (Domning & Pervesler 2013), 3 (Šuklje 1938), 4 (Zalmout & Gingerich 2012), 5 (Domning & Gingerich 1994), 6 (Gingerich et al. 1994), 7 (Gingerich 1992), 8 (Domning et al. 1994), 9 (Sagne 2001), 10 (Bizzarini 1994), 11 (Patte 1963), 12 (Ginsburg et al. 1979), 13 (Sorbi 2008), 14 (Canocchi 1987), 15 (Domning & Thomas 1987), 16 (Kretzoi 1953), 17 (Kordos 1977), 18 (Kordos 1983), 19 (Kordos 1985), 20 (Kretzoi 1951), 21 (Bajpai et al. 2009), 22 (Bajpai et al. 2006), 23 (Thewissen & Bajpai 2009), 24 (Bajpai et al. 2010), 25 (Bajpai & Domning 1997), 26 (Reuter et al. 2007), 27 (Mirzaie Ataabadi et al. 2014), 28 (this report), 29 (Goodwin et al. 1998), 30 (Sickenberg 1934), 31 (Lydekker 1892), 32 (Guido et al. 2011), 33 (Carone & Domning 2007), 34 (Bianucci et al. 2003), 35 (Sorbi & Vaiani 2007), 36 (Tinelli et al. 2012), 37 (Savage & White 1965), 38 (Savage 1971), 39 (Savage 1975), 40 (Coster et al. 2015), 41 (Domning & Sorbi 2011), 42 (Samonds et al. 2009), 43 (Andrianavalona et al. 2015), 44 (Collignon & Cottreau 1927), 45 (Zammit-Maempel 1982), 46 (Adams 1866), 47 (Zouhri et al. 2014), 48 (Ennouchi 1954), 49 (Zalmout et al. 2003), 50 (Gingerich et al. 1998), 51 (Reza et al. 1984), 52 (Estevens 1998), 53 (Fuchs 1990), 54 (Fuchs 1971), 55 (Pilleri et al. 1989), 56 (Pilleri 1989), 57 (Benoit et al. 2013), 58 (Geraads 1989), 59 (Inan et al. 2008), 60 (As-Saruri et al. 1999).

the only non-dugongid sirenian known in the world that is contemporary with the Iranian fossils.

Most parts of Central Iran and the Zagros zones were occupied by early Miocene basins with carbonate deposition, which formed straits between

Eastern and Western Tethys. Migrations of marine organisms occurred by way of these passages (Harzhauser et al. 2007; Harzhauser & Piller 2007).

The Urumieh-Dokhtar and Sanandaj-Sirjan ridges divided this connection into three straits: the Qom basin in the north, the Esfahan-Sirjan basin in the middle part, and the Asmari basin in the south (Fig. 6).

The cool climate around the Oligocene-Miocene boundary was replaced by warmer conditions in the Miocene (Zachos et al. 2001). This was favorable for marine mammals of the Mediterranean-Iranian basins. The Iranian Miocene marine mammals so far discovered are found in the southern parts of the Urumieh-Dokhtar magmatic belt. The northern parts of the Miocene basin belonged to the Paratethyan realm, where so far we have no reports of marine mammal fossils from Iran. Miocene mammal biodiversity, however, shows essential changes after the Middle Miocene in the Paratethys (Rögl 1999). Uniformity between Eastern and Western Tethys marine mammal faunas could have been maintained by migration through the Iranian straits (Qom, Esfahan-Sirjan and Asmari basins), but this connection was terminated by the collision of the Arabian and Iranian plates. Thereafter, evolution of marine mammals in both parts of Tethys was independent and autonomous (Vélez-Juarbe 2014). On the other hand, new terrestrial passages were created, and migrations and connections of Eurasian-Arabian-African land mammals occurred by way of the *Gomphotherium* land bridge (Rögl 1999).

A high biodiversity of gastropods, bivalves and corals was found in the western parts of Tethys (Mediterranean area) prior to the formation of this land bridge. This high diversity became displaced towards the southeastern part of Tethys (Indian Ocean-Arabian Sea-eastern Africa [IAA]) after the Burdigalian and formation of the *Gomphotherium* land bridge. It seems that this disparity also involved marine mammals, so that sirenians are now absent from the Mediterranean although *Dugong dugon* is found in the IAA (Jefferson et al. 1994). Table 1 shows distribution of sea cow fossils around the Mediterranean and IAA. Certainly, our understanding of Tethyan sirenian paleobiogeography will improve through addition of Iranian data. The distribution of sirenian fossil records in Iran is considerable, but the lack of more diagnostic material

prevents their determination to species or genus.

Apart from biogeographic considerations, the occurrence of sirenians in marine deposits is one of the best indicators of the presence of seagrasses (marine angiosperms), on which sirenians in marine waters have fed throughout their history, but which are rarely fossilized themselves (Domning 1981; Vélez-Juarbe 2014; Reich et al. 2015). The carbonates and other early Miocene marine deposits of Iran surely represent depositional environments that supported diverse seagrasses along with the sirenians reported here. Consideration of this implication of sirenian presence, along with sedimentological, invertebrate, and other indications of seagrass presence, can add a further dimension to paleoecological reconstructions of this region of Tethys.

CONCLUSIONS

The Miocene marine sediments of the Qom Formation are good candidates for marine mammal investigations. Vertebrate fossils discovered in the Qom Formation of Shirin Su belong to the Sirenia, and probably represent the Family Dugongidae. Their identification to genus or species requires the discovery of skulls, which unfortunately have not yet been found in the studied section. The early Miocene basins with carbonate deposition of Iran developed as straits between western and eastern parts of Tethys and were channels of connection and migration for marine mammals.

Acknowledgements. We thank Mahdi Gholami, manager of ICHTO of Kabudar Ahang Township, for her help. Dr. Abdoreza Moghadasi of the National Iranian Oil Company helped us with identification of microfauna. Dr. Marco Cherin (University of Perugia, Italy) and Dr. Jorge Vélez-Juarbe (Natural History Museum of Los Angeles County, California, USA) helped us to improve the original manuscript.

REFERENCES

Adams A.L. (1866) - On the discovery of remains of *Halitherium* in the Miocene deposits of Malta. *Quart. J. Geol. Soc. London*, 22: 595-596.

Adams T.D. & Bourgeois F. (1967) - Asmari biostratigraphy. Iranian Oil Operating Companies, Geological and Exploration Division, Report 1074 (unpublished): 1-37.

Andrianavalona T.H., Ramihangihajason T.N., Rasoamiaramana A., Ward D.J., Ali J.R. & Samonds K.E. (2015) -

Miocene shark and batoid fauna from Nosy Makamby (Mahajanga Basin, northwestern Madagascar). *PLoS ONE*, 10(6). DOI: 10.1371/journal.pone.0129444.

As-Saruri M.L., Whybrow P.J. & Collinson M.E. (1999) - Geology, fruits, seeds, and vertebrates (?Sirenia) from the Kaninah Formation (Middle Eocene), Republic of Yemen. In: Whybrow P.J. & Hill A.P. (Eds) - Fossil vertebrates of Arabia: with emphasis on the Late Miocene Fauna, Geology and Palaeoenvironments of the Emirate of Abu Dhabi: 443-453. Yale Univ. Press, New Haven & London.

Bajpai S., Singh M.P. & Singh P. (1987) - A new sirenian from the Miocene of Kachchh, western India. *J. Palaeontol. Soc. India*, 32: 20-25.

Bajpai S. & Domning D.P. (1997) - A new dugongine sirenian from the early Miocene of India. *J. Vert. Paleontol.*, 17: 219-228.

Bajpai S., Domning D.P., Das D.P. & Mishra V.P. (2009) - A new middle Eocene sirenian (Mammalia, Protosireniidae) from India. *Neues Jahrb. Geol. P.-A.*, 252: 257-267.

Bajpai S., Domning D.P., Das D.P., Vélez-Juarbe J. & Mishra V.P. (2010) - A new fossil sirenian (Mammalia, Dugonginae) from the Miocene of India. *Neues Jahrb. Geol. P.-A.*, 258(1): 39-50.

Bajpai S., Thewissen J.G.M., Kapur V.V., Tiwari B.N. & Sahni A. (2006) - Eocene and Oligocene sirenians (Mammalia) from Kachchh, India. *J. Vert. Paleontol.*, 26: 400-410.

Benoit J., Adnet S., El Mabrouk E., Khayati H., Ben Haj Ali M., Marivaux L., Merzeraud G., Merigeaud S., Vianey-Liaud M. & Tabuce R. (2013) - Cranial remain from Tunisia provides new clues for the origin and evolution of Sirenia (Mammalia, Afrotheria) in Africa. *PLoS ONE*, 8: e54307. doi:10.1371/journal.pone.0054307.

Berta A., Sumich J., Kovacs, K. (2006) - Marine Mammals: Evolutionary Biology. Academic Press, San Diego, CA, 547 pp.

Bianucci, G., Landini W. & Varola A. (2003) - New records of *Metaxytherium* (Mammalia: Sirenia) from the late Miocene of Cisterna quarry (Apulia, southern Italy). *Boll. Soc. Paleontol. Ital.*, 42(1-2): 59-63.

Bizzarini F. (1994) - Osservazioni sull'*Halittherium schinzii* Kaup, 1838 (Sirenia, Mammalia) conservato presso il Museo Civico di Storia Naturale di Venezia. *Boll. Mus. Civ. St. Nat. Venezia*, 43: 163-171.

Bolourchi M.H. (1979) - Explanatory text of Kabudar Ahang Quadrangle Map, 1:250000. Geol. Survey of Iran. Geol. Quadrangle D5: 107 pp.

Bozorgnia F. (1966) - Qum Formation stratigraphy of the central basin of Iran and its intercontinental position. *Iran. Petrol. Inst. Bull.*, 24: 69-75.

Campbell B.G., Amini M.H., Bernor R.L., Dickinson W., Drake R., Morris R., Van Couvering J.A. & Van Couvering J.A.H. (1980) - Maragheh: a classical late Miocene vertebrate locality in northwestern Iran. *Nature*, 287: 837-841.

Canocchi D. (1987) - On a skull of a sirenian from the Early Pliocene of Siena, Tuscany. *Riv. It. Paleont. Strat.*, 92(4): 497-513.

- Carone G. & Domning D.P. (2007) - *Metaxytherium serresii* (Mammalia: Sirenia): new pre-Pliocene record, and implications for Mediterranean paleoecology before and after the Messinian Salinity Crisis. *Boll. Soc. Paleontol. Ital.*, 46: 55-92.
- Collignon M. & Cottreau J. (1927) - Paléontologie de Madagascar. XIV. Fossiles du Miocène marin. *Ann. Paléontol.*, 16: 135-171.
- Coster P.M.C., Beard K.C., Salem M.J., Chaimanee Y., Brunet M. & Jaeger J.J. (2015) - A new early Oligocene mammal fauna from the Sirt Basin, central Libya: biostratigraphic and paleobiogeographic implications. *J. Afr. Earth Sci.*, 104: 43-55.
- Daneshian J. & Ramezani Dana L. (2007) - Early Miocene benthic foraminifera and biostratigraphy of the Qom Formation, Deh Namak, Central Iran. *J. Asian Earth Sci.* 29: 844-858.
- Domning D.P. (1981) - Sea cows and sea grasses. *Paleobiol.*, 7: 417-420.
- Domning D.P. (1994) - A phylogenetic analysis of the Sirenia. In: Berta A. & Deméré T.A. (Eds) - Contributions in Marine Mammal Paleontology Honoring Frank C. Whitmore, Jr., *Proc. San Diego Soc. Nat. Hist.*, 29: 177-189.
- Domning D.P. (2000) - The readaptation of Eocene sirenians to life in water. *Hist. Biol.*, 14: 115-119.
- Domning D.P. (2001) - The earliest known fully quadrupedal sirenian. *Nature*, 413: 625-627.
- Domning D.P. (2009) - Sirenian evolution. In: Perrin W.F., Würsig B. & Thewissen J.G.M. (Eds) - Encyclopedia of Marine Mammals, ed. 2: 1016-1019. Acad. Press, San Diego.
- Domning D.P. & Gingerich P.D. (1994) - *Protosiren smithae*, new species (Mammalia, Sirenia), from the late Middle Eocene of Wadi Hitan, Egypt. *Contr. Mus. Paleontol., Univ. Michigan*, 29: 69-87.
- Domning D.P. & Pervesler P. (2001) - The osteology and relationships of *Metaxytherium krabuletzki* Depéret, 1895 (Mammalia: Sirenia). *Abh. Senckenberg. Naturf. Ges.*, 553: 1-89.
- Domning D.P. & Pervesler P. (2013) - The sirenian *Metaxytherium* (Mammalia: Dugongidae) in the Badenian (Middle Miocene) of Central Europe. *Austrian J. Earth Sci.*, 105: 125-160.
- Domning D.P. & Thomas H. (1987) - *Metaxytherium serresii* (Mammalia: Sirenia) from the Lower Pliocene of Libya and France: a reevaluation of its morphology, phyletic position, and biostratigraphic and paleoecological significance. In: Boaz N., El-Arnauti A., Gaziry A.W., Heinzelin J. de & Boaz D.D. (Eds) - Neogene Paleontology and Geology of Sahabi: 205-232. Alan R. Liss, New York.
- Domning D.P. & Sorbi S. (2011) - *Rytiodus beali*, sp. nov., a new sirenian (Mammalia, Dugonginae) from the Miocene of Libya. *J. Vert. Paleontol.*, 31: 1338-1355.
- Domning D.P., Gingerich P.D., Simons E.L. & Ankel-Simons F.A. (1994) - A new early Oligocene dugongid (Mammalia, Sirenia) from Fayum Province, Egypt. *Contr. Mus. Paleontol., Univ. Michigan*, 29: 89-108.
- Domning D.P. & Gingerich P.D. (1994) - *Protosiren smithae*, new species (Mammalia, Sirenia), from the late middle Eocene of Wadi Hitan, Egypt. *Contr. Mus. Paleontol., Univ. Michigan*, 29: 69-87.
- Ennouchi E. (1954) - Un sirénien, *Felsinotherium* cf. *serresi*, à Dar bel Hamri. *Serv. Géol. Maroc, Notes et Mém.*, 121: 77-82.
- Estevens M. (1998) - Mamíferos marinhos do Neogénico de Portugal. Distribuição geográfica e estratigráfica. *Comunicações. Actas do V Congresso Nacional de Geologia*, 84: A161-A164.
- Fuchs H. (1971) - Contribuțiia cunoașterea răspîndirii stratigrafice și geografice a sirenelor în Bazinul Transilvaniei. *Bul. Soc. Ști. Geol. R. S. România*, 13: 195-200.
- Fuchs H.B. (1990) - Adatok az Erdélyi-medence ásatag szirénjeinek ismeretéhez (VII): Szirénfogak Kolozsvár (Cluj, România) környékéről. (Einige Angaben zur Kenntnis von fossilen Sirenen (VII). Sirenenzähne aus der Umgebung von Cluj (Klausenburg, Rumänien). *Földtani Közlöny*, 120: 89-92.
- Furrer M.A. & Soder P.A. (1955) - The Oligo-Miocene marine formation in the Qum region (Central Iran) (with discussion). *4th World Petrol. Cong., Rome, sec.*, 1: 267-277.
- Geraads D. (1989) - Vertébrés fossiles du miocène supérieur du Djebel Krechem el Artsouma (Tunisie centrale). Comparaisons biostratigraphiques. *Geobios*, 22: 777-801.
- Gingerich P.D. (1992) - Marine mammals (Cetacea and Sirenia) from the Eocene of Gebel Mokattam and Fayum, Egypt: stratigraphy, age, and paleoenvironments. *Univ. Michigan Pap. Paleontol.*, 30: 1-84 pp.
- Gingerich P.D., Domning D.P., Blane C.E. & Uhen M.D. (1994) - Cranial morphology of *Protosiren fraasi* (Mammalia, Sirenia) from the middle Eocene of Egypt: A new study using computed tomography. *Contrib. Mus. Paleontol. Univ. Michigan*, 29: 41-67.
- Gingerich P.D., Arif M., Bhatti M.A. & Clyde W.C. (1998) - Middle Eocene stratigraphy and marine mammals (Mammalia: Cetacea and Sirenia) of the Sulaiman Range, Pakistan. In: Beard K.C. & Dawson M.R. (Eds) - Dawn of the Age of Mammals in Asia. *Bull. Carnegie Mus. Nat. Hist.*, 34: 239-259.
- Ginsburg L., Janvier P., Mornand J. & Pouit D. (1979) - Découverte d'une faune de mammifères terrestres d'âge vallésien dans le falun miocène de Doué-la-Fontaine (Maine-et-Loire). *C.R. Somm. Séances Soc. Géol. France*, 5-6: 223-227.
- Goodwin M.B., Domning D.P., Lipps J.H. & Benjamini C. (1998) - The first record of an Eocene (Lutetian) marine mammal from Israel. *J. Vert. Paleontol.*, 18: 813-815.
- Gray J.E. (1821) - On the natural arrangement of vertebrate animals. *London Med. Repos.*, 15: 296-310.
- Guido A., Marra A.C., Mastandrea A., Tosti F. & Russo F. (2011) - Micromorphological, geochemical, and diagenetic characterization of sirenian ribs preserved in the Late Miocene paleontological site of Cessaniti (southern Calabria, Italy). *Facies*, 58: 179-190.
- Harzhauser M. & Piller W.E. (2007) - Benchmark data of a changing sea - paleogeography and paleobiogeography and events in the Central Paratethys during the Miocene.

- Palaeogeogr., Palaeoclimatol., Palaeoecol.*, 253: 8-31.
- Harzhauser M., Kroh A., Mandic O., Piller W.E., Göhlich U., Reuter M. & Berning B. (2007) - Biogeographic responses to geodynamics: a key study all around the Oligo-Miocene Tethyan Seaway. *Zool. Anz.*, 246: 241-256.
- Illiger C. (1811) - Prodomus Systematis Mammalium et Avium: Additis Terminis Zoographicis Utriusque Classis, Eorumque Versione Germanica. Sumptibus C. Salzfild, Berlin, 302 pp.
- Inan S., Tasli K., Eren M., Inan N., Koç H., Zorlu K., Taga H., Zorlu K., Arslanbaş O. & Demircan F. (2008) - First finding of *Metaxytherium* (sea cow) in the Miocene limestones of the Erdemli (Mersin) area (S Turkey). *Türk. Jeol. Kurul. Bild.*, 61: 1-7.
- Jefferson T.J., Leatherwood S. & Webber M.A. (1994) - Marine Mammals of the World. FAO Species Identification Guide, FAO and UNEP Publications, Rome, 320 pp.
- Khanikoff M. (1858; in Abich H.1858) - Tremblement de terre observé à Tabriz en Septembre 1856, Notice physiques et géographiques de M. Khanykof sur l'Azerbeïdjan, communiquées par H. Abich (lu le 17 Janvier, 1857). *Bull. Class. Physico-Math. Acad. Imp. Sci. Saint-Petersbourg*, 16: 337-352.
- Kretzoi M. (1951) - Új sziréna-típus a Magyar Miocénből. (Neuer Sirenen-Typus aus dem ungarischen Miozän.) *Földt. Közlöny (Bull. Hung. Geol. Soc.)*, 81: 438-441.
- Kretzoi M. (1953) - A legidősebb Magyar ősemős-lelet. (Le plus ancien vestige fossile de mammifère en Hongrie). *Földt. Közlöny (Bull. Hung. Geol. Soc.)*, 83: 273-277.
- Kordos L. (1977) - Új Felsőéocén sziréna (*Paralitherium tarkanyense* n.g. n.sp.) Felsőtárkányból. *Magyar Állami Földtani Intézet Évi Jelentése*, 1975: 349-367.
- Kordos L. (1983) - *Sirenavus* or *Eotheroides* species (Mammalia, Sirenia) from the Eocene of the Tatabánya Basin (Hungary). *Fragm. Min. Pal.*, 11: 41-42.
- Kordos L. (1985) - The evolution of the Cenozoic sirenian on the basis of Hungarian fossil remains. *Abstrs. VIIIth Congr., Regional Comm. Mediterranean Neogene Stratig., Symposium on European Late Cenozoic Mineral Resources* (Budapest, Sept. 15-22, 1985): 314.
- Laursen G.V., Monibi S., Allan T.L., Pickard N.A.H., Hosseiny A., Vincent B., Hamon Y., van Buchem F.S.P., Moallemi A. & Druillion G. (2009) - The Asmari Formation Revisited: Changed Stratigraphic Allocation and New Biozonation. First International Petroleum Conference and Exhibition Shiraz, Iran, B29.
- Lydekker R. (1892) - On a remarkable sirenian jaw from the Oligocene of Italy, and its bearing on the evolution of the Sirenia. *Proc. Zool. Soc. London*, 1892(1): 77-83.
- Linnaeus C. (1758) - Systema Naturae per Regna Tria Naturae, Secundum Classes, Ordines, Genera, Species, cum Characteribus, Differentiis, Synonymis, Locis. Tomus I, Editio decima, reformata. Laurentii Salvii, Stockholm, 823 pp.
- Mecquenem R. de (1925) - Contribution à l'étude des fossiles de Maragha. *Ann. Paléontol.*, 13: 135-160.
- Mirzaie Ataabadi M., Orak Z., Paknia M., Alizadeh J.M., Gholamalian H., Mojiabadi I., Mirzaie J. & Yazdi M. (2014) - First report of marine mammal remains from the Oligo-Miocene deposits of Central Iran and Zagros basins. In: Abbassi N. (Ed.) - Proceedings of the Eighth Symposium of the Iranian Paleontological Society. *Iran. Paleontol. Soc. Univ. Zanjan*: 124-129, Zanjan.
- Najafi A. & Bazargani Gilani K. (2006) - Ivory fossil from Mianeh area, Northwest Iran. *J. Sci. Univ. Tebran*, 32: 275-281.
- Nogole Sadat M.A.A. & Almasian M. (1993) - Tectonic map of Iran 1:1000000. Treatise on the Geology of Iran Publications. Geol. Surv. Iran, Tehran.
- Patte E. (1963) - Présence de l'*Halitherium* dans l'Oligocene du Poitou. *Bull. Soc. Géol. France*, 7: 536-537.
- Pervesler P., Roetzel R. & Domning D.P. (2000) - Lower Miocene Seacows from Austria. In: Piller W.E., Daxner-Höck, G., Domning D.P., Forke H.C., Harzhauser M., Hubmann B., Kollmann H.A., Kovar-Eder J., Krystyn L., Nagel D., Pervesler P., Rabeder G., Roetzel R., Sanders D. & Summesberger H. (Eds) - Palaeontological highlights of Austria. *Mitt. Österr. Geol. Ges.*, 92: 213-215.
- Pilleri G. (1989) - Endocranial cast of *Metaxytherium* (Mammalia: Sirenia) from the Miocene of Cerro Gordo, Almería, Spain. In: G. Pilleri (Ed.) - Contributions to the paleontology of some Tethyan Cetacea and Sirenia (Mammalia) II. *Brain Anat. Inst.*: 103-113, Ostermundigen (Switzerland).
- Pilleri G., Biosca Muntis, J. & Via Boada L. (1989) - The Tertiary Sirenia of Catalonia. *Brain Anat. Inst.*: 1-98, Ostermundigen (Switzerland).
- Rahimzadeh F. (1994) - Treatise on the geology of Iran, Oligocene, Miocene, Pliocene. *Geol. Surv. Iran Publ.*, 12: 1-311 (in Persian).
- Reich S., Martino E.D., Todd J.A., Wesselingh F.P. & Renema W. (2015) - Indirect paleo-seagrass indicators (IPSIs): a review. *Earth-Sciences Reviews* 143: 161-186.
- Reuter M., Piller W.E., Harzhauser M., Mandic O., Berning B., Rögl F., Kroh A., Aubry M.-P., Wielandt-Schuster U. & Hamedani A. (2007) - The Oligo-Miocene Qom Formation (Iran): evidence for an early Burdigalian restriction of the Tethyan Seaway and closure of its Iranian gateways. *Int. J. Earth Sci.*, 98: 627-650.
- Reza S.M., Barry J.C., Meyer G.E. & Martin L. (1984) - Preliminary report on the geology and vertebrate fauna of the Miocene Manchar Formation, Sind, Pakistan. *J. Vert. Paleontol.*, 4: 584-599.
- Rodler A. & Weithofer K.A. (1890) - Die Wiederkauer der Fauna von Maragha. *Denkschr. k. Ak. Wiss. Mat. Nat. Kl. Bd. LVII, Abt. II*, Vienne: 753-772.
- Rögl F. (1999) - Mediterranean and Paratethys. Facts and hypotheses of an Oligocene to Miocene paleogeography (short overview). *Geol. Carpathica*, 50: 339-349.
- Sagne C. (2001) - *Halitherium taulannense*, nouveau sirénien (Sirenia, Mammalia) de l'Éocène supérieur provenant du domaine Nord-Téthysien (Alpes-de-Haute-Provence, France). *C. R. Acad. Sci. Paris, Serie 2: Sciences de la Terre et des Planètes*, 333: 471-476.
- Samonds K.E., Zalmout I.S., Irwin M.T.D., Krause W., Rogers

- R.R. & Raharivony L.L. (2009) - *Eotheroides lambondrano*, new middle Eocene seacow (Mammalia, Sirenia) from the Mahajanga Basin, northwestern Madagascar. *J. Vert. Paleontol.*, 29: 1233-1243.
- Savage R.J.G. (1971) - Review of the fossil mammals of Libya. In: Gray C. (Ed) - Symposium on the geology of Libya. University of Libya: 215-225.
- Savage R.J.G. (1975) - *Prorastomus* and new early Tertiary sirenians from North Africa. [Abstr.] *Amer. Zool.*, 15(3): 824.
- Savage R.J.G. & White M.E. (1965) - Two mammal faunas from the early Tertiary of central Libya. *Proc. Geol. Soc. London*, 1623: 89-91.
- Sickenberg O. (1934) - Beiträge zur Kenntnis tertiärer Sirenen. *Mém. Mus. Royal. Hist. Nat. Belgique*, 63: 1-352.
- Simpson G.G. (1932) - Fossil Sirenia of Florida and the evolution of the Sirenia. *Bull. Am. Mus. Nat. Hist.*, 49: 419-503.
- Sorbi S. (2008) - New record of *Metaxytherium* (Mammalia, Sirenia) from the lower Miocene of Manosque (Provence, France). *Geodiversitas*, 30: 433-444.
- Sorbi S. & Vaiani S.C. (2007) - New sirenian record from Lower Pliocene sediments of Tuscany (Italy). *Riv. It. Paleontol. Strat.*, 113: 299-304.
- Springer M.S., Signore A.V., Paijmans J.L.A., Vélez-Juarbe J., Domning D.P., Bauer C.E., He K., Crerar L., Campos P.F., Murphy W.J., Meredith R.W., Gatesy J., Willerslev E., MacPhee R.D.E., Hofreiter M. & Campbell K.L. (2015) - Interordinal gene capture, the phylogenetic position of Steller's sea cow based on molecular and morphological data, and the macroevolutionary history of Sirenia. *Mol. Phylogen. Evol.*, 91: 178-193.
- Šuklje F. (1938) - Mediteranska sirena iz Vrapča kod Zagreba i Otruševca kod Samobora. *Glasnik Hrvatskoga Prirodoslovnoga Društva Zagreb*, 49-50: 87-93.
- Thewissen J.G.M. & Bajpai S. (2009) - A new Miocene sirenian from Kutch, India. *Acta Palaeontol. Pol.*, 54: 7-13.
- Tinelli C., Ribolini A., Bianucci G., Bini M. & Landini W. (2012) - Ground penetrating radar and palaeontology: The detection of sirenian fossil bones under a sunflower field in Tuscany (Italy). *Comptes Rendus Palevol*, 11: 445-454.
- Vélez-Juarbe J. (2014) - Ghost of seagrasses past: using sirenians as a proxy for historical distribution of seagrasses. *Palaeogeogr., Palaeoclimatol., Palaeoecol.*, 400: 41-49.
- Vélez-Juarbe J., Domning D.P. & Pyenson N.D. (2012) - Iterative evolution of sympatric seacow (Dugongidae, Sirenia) assemblages during the past ~26 million years. *PLoS ONE*, 7(2): e31294.
- Wynd J.G. (1965) - Biofacies of Iranian oil consortium agreement area. Iranian Oil Operating Companies, Geological and Exploration Division, Report 1082 (unpublished): 1-212.
- Zachos J., Pagani M., Sloan L., Thomas E. & Billups K. (2001) - Trends, rhythms, and aberrations in global climate 65 Ma to present. *Science*, 292: 686-693.
- Zalmout I.S. & Gingerich P.D. (2012) - Late Eocene sea cows (Mammalia, Sirenia) from Wadi Al Hitán in the Western Desert of Fayum, Egypt. *Univ. Michigan Pap. Paleontol.*, 37: 1-158.
- Zalmout I.S., Ul-Haq M. & Gingerich P.D. (2003) - New species of *Protosiren* (Mammalia, Sirenia) from the early middle Eocene of Balochistan (Pakistan). *Contrib. Mus. Paleontol., Univ. Michigan*, 31: 79-87.
- Zammit-Maempel G. (1982) - The folklore of Maltese fossils. *Papers in Mediterranean Social Studies*, 1: 1-29.
- Zouhri S., Gingerich P.D., Elboudali N., Sebti S., Noubhani A., Rahali M. & Meslou S. (2014) - New marine mammal faunas (Cetacea and Sirenia) and sea level change in the Samlat Formation, Upper Eocene, near Ad-Dakhla in southwestern Morocco. *Comptes Rendus Palevol*, 13: 599-610.

COMPARING THE BODY MASS VARIATIONS IN ENDEMIC INSULAR SPECIES OF THE GENUS *PROLAGUS* (OCHOTONIDAE, LAGOMORPHA) IN THE PLEISTOCENE OF SARDINIA (ITALY)

BLANCA MONCUNILL-SOLÉ¹, CATERINELLA TUVERI², MARISA ARCA² & CHIARA ANGELONE^{1*}

¹Institut Català de Paleontologia Miquel Crusafont, Edifici Z ICTA-ICP, Carrer de les Columnes s/n, Campus de la Universitat Autònoma de Barcelona, 08193 Cerdanyola del Vallès, Barcelona, Spain. E-mail: blanca.moncunill@icp.cat, chiara.angelone@icp.cat. *Corresponding author.

²Soprintendenza Archeologia della Sardegna, via G. Asproni 33, 08100 Nuoro, Italy. E-mail: caterinella.tuveri@beniculturali.it, marisa.arca@beniculturali.it.

To cite this article: Moncunill-Solé B., Tuveri C., Arca M. & Angelone C. (2016) - Comparing the body mass variations in endemic insular species of the genus *Prolagus* (Ochotonidae, Lagomorpha) in the Pleistocene of Sardinia (Italy). *Riv. It. Paleont. Strat.* 122(1): 25-36

Keywords: Body mass, regression models, postcranial bones, Island Rule, Mediterranean islands, *Prolagus figaro*, *P. sardus*.

Abstract. *Prolagus figaro* and *P. sardus* are part of an endemic insular anagenetic lineage that populated Sardinia since the earliest Late Pliocene to Holocene. BM of some populations of these two species was calculated using regression models. The best BM proxies for *Prolagus* are: femur length, zeugopod measurements and distal humerus diameter. The anagenetic lineage shows a BM increase of ca 20% from the populations of *P. figaro* (398-436 g) to *P. sardus* (504-525 g). The trend shown by the size of lower third premolar, even if not directly comparable with BM, is opposite (ca -30% at the transition *P. figaro*-*P. sardus*). Compared to *P. cf. calpensis*, a continental species of similar age, BM of *P. figaro* is ca +25%. The comparison with the insular endemic *P. aprivencius* evidenced differences in BM range and timespan required to attain it, due to the different size and palaeogeographical situation of the islands. Insular endemic *Prolagus* follow the small mammal pattern of Island Rule. Mein's (1983) biphasic model seems applicable to the evolution of *P. figaro*. A tachytelic phase followed by a bradytelic one seems to characterize also the appearance of *P. sardus*, at least for dental traits, a process probably triggered by important variations of abiotic and biotic traits of the environment, as indicated by the turnover that marks the onset of the Dragonara subcomplex. The prediction of life history traits and other biological attributes of Sardinian *Prolagus* using BM should be considered with caution due to the complexity of ecological selective regimes of Sardinia.

INTRODUCTION

Body size is a fundamental trait in the biology and ecology of species as it shows tight correlation with several physiological, behavioral, morphological, ecological and life history attributes (Peters 1983; Calder 1984). The best proxy for quantifying the BS of individuals is their body mass or weight (Gingerich et al. 1982). Thus, predicting the BM of fossil species is of critical significance for knowing their biology as well as for understanding and quantifying their adaptations to habitats (Palombo 2009a). For most of mammalian taxa, the allometric relationships among BM and bone/dental measurements of extant relative species allow the development of regression models to estimate the average weight of extinct ones (Damuth & MacFadden 1990; see Palombo 2009a: tab. 1 for a synopsis).

In spite of the abundance, diversity and ubiquity of fossil lagomorphs (leporids and ochotonids), models for estimating the BMs of species belonging to this order were developed very recently. Quintana Cardona (2005) and Quintana et al. (2011) provided the first models for leporids. Subsequently, expanding the database of Quintana Cardona (2005) and adding measurements of extant ochotonids, Moncunill-Solé et al. (2015) developed general and specific equations for estimating the BM of lagomorphs based on a multiproxy approach (teeth, cranial and postcranial measurements). BM estimation models for lagomorphs are going to enhance data about palaeocommunity structures and their palaeoenvironmental interpretations.

In view of the potential of this field, we decided to study the BM of the insular endemic ochotonids of the Pleistocene of Sardinia (Italy): *Prolagus figaro* and *Prolagus sardus*. *Prolagus figaro* is known from the latest Pliocene/earliest Pleistocene to the late Early Pleistocene of Sardinia (Capo Figari/

| Species | Fissure filling | Femora | Tibiae | Humeri |
|------------------------|-----------------|-------------------|-------------------|-------------------|
| | | N (coding) | N (coding) | N (coding) |
| <i>Prolagus figaro</i> | X3 | 10 | 6 | 14 |
| | | (SSN/X3/fe/1-10) | (SSN/X3/ti/1-6) | (SSN/X3/hu/1-14) |
| | IVm | 5 | — | — |
| | | (SSN/IVm/fe/1-5) | | |
| <i>Prolagus sardus</i> | X4 | 13 | 11 | — |
| | | (SSN/X4/fe/1-13) | (SSN/X4/ti/1-11) | |
| | XIr | 74 | 42 | 60 |
| | | (SSN/XIr/fe/1-74) | (SSN/XIr/ti/1-42) | (SSN/XIr/hu/1-60) |
| | VI6 | 20 | 9 | 49 |
| | | (SSN/VI6/fe/1-20) | (SSN/VI6/ti/1-9) | (SSN/VI6/hu/1-49) |

Tab. 1 - Fossil material used for performing the study.

Orosei 1 subcomplex of the *Nesogoral* FC- Orosei 2 subcomplex of the *Microtus* (*Tyrrhenicola*) FC; Palombo 2009b). *Prolagus sardus* is reported since the Middle Pleistocene (Dragonara subcomplex of the *Microtus* (*Tyrrhenicola*) FC; Palombo 2009b) until historical epoch in Sardinia and also in Corsica (Vigne & Valladas 1996; Wilkens 2004). We aim to:

1) Evaluate the BM trend of *Prolagus* in an insular habitat from an evolutionary point of view, as the two species of *Prolagus* from Sardinia are part of an anagenetic evolutionary lineage (Angelone et al. 2015).

2) Assess the response of fossil ochotonid species to insular regimes (Island Rule) (see Palombo 2009a and references therein for an update of the debate about this subject) as there are not extant relatives living on islands.

3) Provide data to increase the scarce biological knowledge of Sardinian *Prolagus*.

ABBREVIATIONS

BM: body mass; BS: body size; CMD1: Capo Mannu D1; IC: interval of confidence; FC: faunal complex; FL: femur length; FTDd: distal femoral transversal diameter; FTDp: proximal femoral transversal diameter; HAPDd: distal humeral anteroposterior diameter;

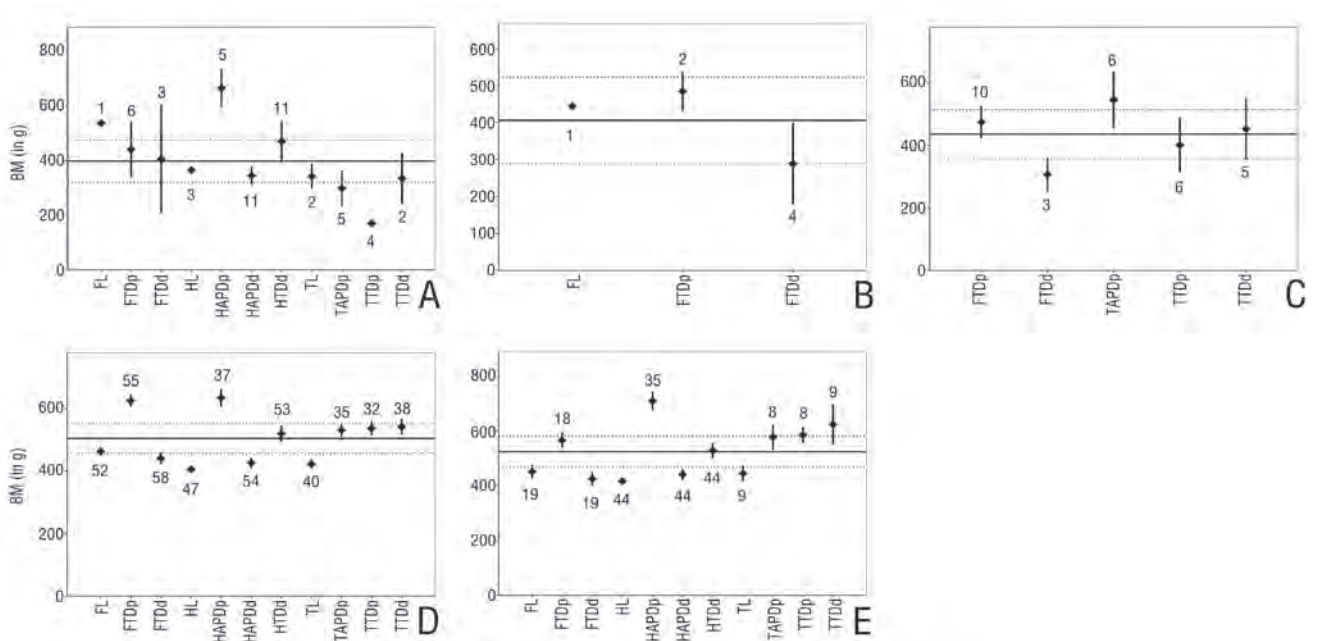


Fig. 1 - BM predictions (Y axis, in g) for *Prolagus figaro* and *P. sardus* calculated on the basis of different postcranial measurements (X axis). BM average (black line), confidence interval (dotted lines) and number of individuals are shown. A) *Prolagus figaro*, fissure infilling X3; B) *P. figaro*, fissure infilling IVm; C) *P. figaro*, fissure infilling X4; D) *Prolagus sardus*, fissure infilling XIr and E) *P. sardus*, fissure infilling VI6.

| Measurement | Equation | BM <i>Prolagus figaro</i> | | | | | | BM <i>Prolagus sardus</i> | | | |
|-------------------------|--------------------------------------|---------------------------|----|-------------------|---|-------------------|----|---------------------------|----|-------------------|----|
| | | X3 | | IVm | | X4 | | XIr | | VI6 | |
| | | \bar{x} (IC) | N | \bar{x} (IC) | N | \bar{x} (IC) | N | \bar{x} (IC) | N | \bar{x} (IC) | N |
| FL | $\log BM = -1.11 + 2.229 \log FL$ | 537.57 | 1 | 444.74 | 1 | – | – | 463.09 | 52 | 452.12 | 19 |
| | | | | | | | | (448.98-477.20) | | (426.38-477.85) | |
| FTDp | $\log BM = 0.498 + 2.217 \log FTDp$ | 441.19 | 6 | 484.96 | 4 | 474.51 | 10 | 624.91 | 55 | 566.28 | 18 |
| | | (337.88-544.51) | | (432.23-537.69) | | (423.18-525.84) | | (605.96-643.86) | | (538.47-594.08) | |
| FTDd | $\log BM = 0.318 + 2.481 \log FTDd$ | 406.21 | 3 | 289.40 | 2 | 306.13 | 3 | 440.50 | 58 | 424.84 | 19 |
| | | (207.12-605.30) | | (178.91-399.90) | | (251.76-360.51) | | (421.79-459.21) | | (398.98-450.70) | |
| HL | $\log BM = -1.221 + 2.418 \log HL$ | 364.47 | 3 | – | – | – | – | 633.99 | 47 | 416.71 | 44 |
| | | (360.73-368.22) | | | | | | (605.66-662.33) | | (403.42-430.00) | |
| HAPDp | $\log BM = 0.916 + 1.769 \log HAPDp$ | 665.15 | 5 | – | – | – | – | 633.99 | 37 | 709.82 | 35 |
| | | (593.75-736.56) | | | | | | (605.66-662.33) | | (675.19-744.15) | |
| HAPDd | $\log BM = 1.354 + 1.769 \log HAPDd$ | 345.03 | 11 | – | – | – | – | 425.75 | 54 | 441.69 | 44 |
| | | (311.26-378.80) | | | | | | (409.64-441.87) | | (421.16-462.25) | |
| HTDd | $\log BM = 1.053 + 1.513 \log HTDd$ | 470.57 | 11 | – | – | – | – | 519.21 | 53 | 528.79 | 44 |
| | | (393.39-547.74) | | | | | | (493.6-544.77) | | (501.34-556.24) | |
| TL | $\log BM = -1.271 + 2.254 \log TL$ | 342.28 | 2 | – | – | – | – | 422.18 | 40 | 445.57 | 9 |
| | | (296.52-388.03) | | | | | | (407.09-437.27) | | (415.82-475.32) | |
| TAPDp | $\log BM = 0.599 + 2.265 \log TAPDp$ | 298.77 | 5 | – | – | 545.27 | 6 | 530.28 | 35 | 578.26 | 8 |
| | | (233.38-364.16) | | | | (454.86-635.69) | | (509.28-551.47) | | (530.81-625.71) | |
| TTDp | $\log BM = 0.219 + 2.577 \log TTDp$ | 170.50 | 4 | – | – | 400.62 | 6 | 536.58 | 32 | 586.70 | 8 |
| | | (155.93-185.06) | | | | (312.36-488.68) | | (513.18-559.98) | | (558.05-615.35) | |
| TTDd | $\log BM = 0.461 + 2.584 \log TTDd$ | 334.94 | 2 | – | – | 452.19 | 5 | 540.94 | 38 | 624.73 | 9 |
| | | (241.77-428.12) | | | | (353.44-550.93) | | (516.22-565.66) | | (551.11-698.36) | |
| Arithmetic Mean | | 397.88 | | 406.37 | | 435.74 | | 503.86 | | 525.05 | |
| | | (320.68-475.08) | | (289.50-523.23) | | (357.59-513.90) | | (456.89-550.83) | | (468.12-581.97) | |
| Weighted Average | | 402.34 | | 423.34 | | 453.326 | | 520.83 | | 512.40 | |

Tab. 2 - BM predictions (in g) for the populations of *Prolagus figaro* and *P. sardus* analyzed in this paper. Last two rows, highlighted in gray, show the arithmetic mean of BM calculated for each site, and their weighted average.

HAPDp: proximal humeral anteroposterior diameter; HL: humerus length; HTDd: distal humeral transversal diameter; Lp3: length of the third premolar; N: sample size; SSN: Soprintendenza dei Beni Archeologici per le Province di Sassari e Nuoro, sede di Nuoro; TAPDp: proximal tibia anteroposterior diameter; TL: tibia length; TTDd: distal tibia transversal diameter; TTDp: proximal tibia transversal diameter; \bar{x} : arithmetic mean; \bar{x}_w : weighted mean.

MATERIAL

The samples of *P. figaro* and *P. sardus* come from the Monte Tuttavista karstic complex (E Sardinia; Abbazzi et al. 2004) (Tab. 1). Remains of *P. figaro* come from infillings X3, IVm and X4, pertaining to the Capo Figari/Orosei 1 subcomplex of the *Nesogoral* FC-Orosei 2 subcomplex of the *Microtus (Tyrrhenicola)* FC (latest Pliocene/earliest Pleistocene to the late Early Pleistocene; Palombo 2009b). In this context, notice that Palombo (2009b) gave a different relative temporal arrangement of the aforementioned infillings (IVm-X4-X3). Remains of *P. sardus* have been sampled from infillings XIr and VI6, included in the Dragonara subcomplex of the *Microtus (Tyrrhenicola)* FC (Middle and Late Pleistocene; Palombo 2009b). Infillings XIr and VI6 were accumulated in a quite short time and their palaeontological contents are taxonomically homogeneous (see Angelone et al. 2008 for discussion). Preliminary analysis of *Prolagus* remains and literature data based on other taxa (Angelone et al. 2009; Palombo 2009b and references therein) pointed out that X3, IVm and X4

also are taxonomically homogeneous infillings. The fossil material is curated at the SSN.

METHODS

The skeletal maturation indicates the complete cessation of longitudinal growth and, consequently, the moment when animals achieve the final BS which is maintained until their death (Peters 1983). Thus, BM estimations of *Prolagus* species were only carried out on individuals that have already attained skeletal maturity (fused epiphyses). Specimens with unfused or broken epiphyses were not considered. *Ochotona*, the extant relative of *Prolagus*, shows a minimal sexual dimorphism (Smith 1988; Nowak 1999). For this reason, we did not assume BM differences between sexes in our fossil sample.

For undertaking the BM estimations, we followed the methodology described and illustrated by Moncunill-Solé et al. (2015: fig. 1). The following measurements were taken on postcranial remains: 1) FL, FTDd and FTDp on femora; 2) HL, HAPDp, HAPDd and HTDd on humeri; and 3) TL, TAPDp, TTDp and TTDd on tibiae. Moncunill-Solé et al. (2015) observed that burrower species of *Ochotona* and leporids show significant differences in the allometric models of the humerus, but not in other skeletal elements (femur and tibia). Although *Ochotona* is the closest relative of *Prolagus*, we preferred to use a general regression model for humeri (i.e. models that include data of leporids and *Ochotona*) because the locomotion of the species of *Prolagus* is not well known. The equations are shown

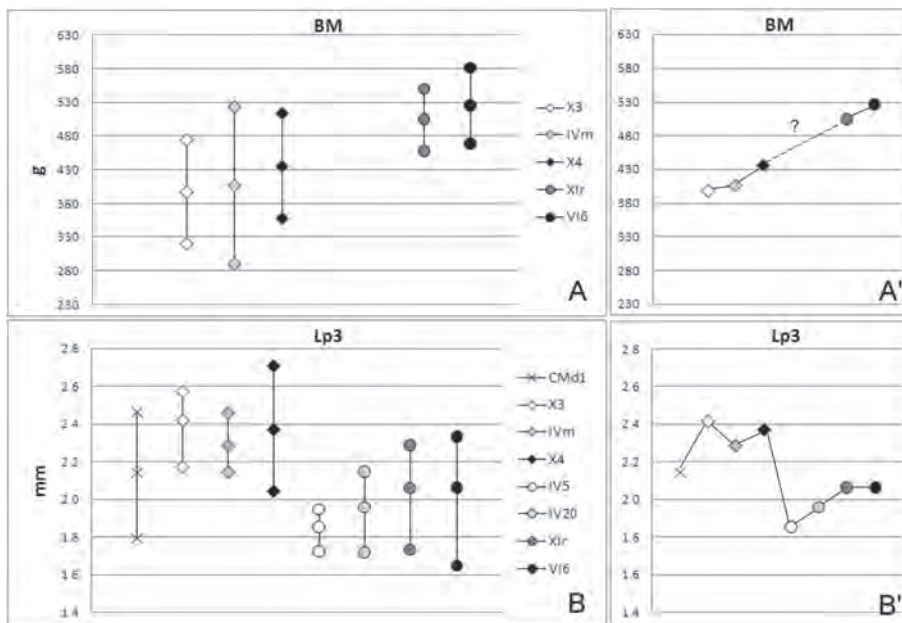


Fig. 2 - BM range A) and Lp3 range B) showing max, average and min values of *Prolagus* aff. *figaro* (cross, CMd1), *P. figaro* (diamonds, X3, IVm, X4) and *P. sardus* (circles, IV5, IV20, XIr, VI6), with detail of average values and trends of BM (A') and Lp3 (B').

in Tab. 2. Once the regression models were applied, we eliminated outliers due to their potential for skewing the distributions. We followed the criterion of Tukey (1977): outliers (Y) were considered when $Y < (Q1 - 1.5IQR)$ or $Y > (Q3 + 1.5IQR)$ (where Q1 is the 25th percentile, Q3 is the 75th percentile, and IQR the interquartile range $(Q3 - Q1)$) (Quinn & Keough 2002). For each specific measurement, it was calculated an arithmetic mean (\bar{x}) and a confidence interval (IC) $[\bar{x} \pm ((\sigma/\sqrt{N})Z_{\alpha}/2)]$. Based on the BM of each measurement, we performed an arithmetic average (\bar{x}) and a weighted average (\bar{x}_w) $[(X_1W_1 + X_2W_2 + \dots + X_NW_N)/(W_1 + W_2 + \dots + W_N)]$.

In order to compare the different populations of *Prolagus* and analyze the BM variation, we performed ANOVA analyses and post hoc tests (Tukey HSD) ($\alpha = 0.05$) using the IBM SPSS Statistics 19 software.

RESULTS

The results of BM estimations (means, IC, N) are shown in Tab. 2 and are represented in Fig. 1.

For *P. figaro*, we estimate a weight of 397.88 g (320.68-475.08) in fissure filling X3, of 406.37 g (289.50-523.23) in IVm and of 435.74 g (357.59-513.90) in X4. For *P. sardus* the results are greater, 503.86 g (456.89-550.83) in fissure filling XIr and 525.05 g (468.12-581.97) in VI6. We do not observe significant differences between \bar{x} and \bar{x}_w (their difference is ca 10-20 g) and the latter falls perfectly in the IC of the former (Tab. 2). Statistically, there are only significant differences ($p < 0.05$) between the oldest population of *P. figaro* (X3) and the youngest of *P. sardus* (VI6).

When the BM estimations of each measurement are assessed, a similar pattern could be observed comparing the populations with the lar-

gest N (VI6 and XIr) (Fig. 1). The variables FTDp and HAPDp estimate a BM far above the arithmetic mean (between 100-200 g greater), especially in VI6 population. The other variables fall next or inside the IC of the arithmetic mean (specially FL, TAPDp, TTDp, TTDd and HTDd). Analyzing the results of the other populations (X3, IVm and X4), we observe more heterogeneous patterns. This may be consequence of: 1) few measurements taken in postcranial bones (3 in IVm and 5 in X4) and 2) small N (ranging from 1 to 11 individuals in X3). However, in this latter population (X3), it is already evident a large value of BM when HAPDp measurement is used, but not in FTDp.

DISCUSSION

BM of Sardinian *Prolagus*: trends and best estimators. Based on dental morphology, a relative temporal arrangement of the studied fissure has been attempted. Preliminary results suggested the relative chronological arrangement X3-IVm-X4 (from older to younger) of populations of *P. figaro* (Angelone et al. 2009). In the case of populations of *P. sardus*, infilling XIr is older than VI6 on the basis of a morphological cline (Angelone et al. 2008). In view of this and the BM results, the three selected populations of *P. figaro* show a total weight increase of ca 10% from the oldest fissure filling (X3) to the youngest (X4) (see Tab. 2, Fig. 1 and 2A). The BM of the oldest population of *P.*

sardus here analyzed (XIr) is ca 15% greater than the youngest of *P. figaro* (X4). The average BMs of the two populations of *P. sardus* selected for this study show a very slight difference (average BM of VI6 is about 4% larger). Finally, the total increase among the oldest (X3) to the youngest populations (VI6) of Sardinian *Prolagus* is of 32% (statistically significant, $p < 0.05$). Thus, we can affirm that Sardinian *Prolagus* increased its BM (average) throughout the Pleistocene.

The best BM estimator for an extinct species not only depends on the accuracy of the model (statistical values), but also on a subjective judgment of the results of predictions (Reynolds 2002). According to the fissure infilling with highest sample (XIr) (Fig. 1d), hindlimb bones seem to be the better BM estimators for *Prolagus* species (as shown also in Moncunill-Solé et al. 2015), particularly FL, TAPDp, TTDp and TTDd. However, HTDd also gives adjusted estimations. All these measurements predicted BM that fall inside the IC of the arithmetic mean and, consequently, we can consider them good proxies for the estimation of BM in the genus *Prolagus*. However, N must be taken into due account. For example, the BM predicted by FL (N=1) in X3 population is far above the arithmetic mean. It is recommendable to work with the largest sample possible in order to better represent the biological variability of the species and, thus, obtain more realistic values. The measurements regarded as the best BM estimators are surprising for two facts. Firstly, zeugopods (tibiae), which are involved in the locomotion and lifestyle of the animal, normally predict worse the BM of mammals (Scott 1990). Secondly, the lengths of long bones are also considered as less accurate than diameters or perimeters (Scott 1990). However, in the case of lagomorphs, the models that use length or zeugopodial measurements are as reliable (coefficient of determination or average absolute per cent prediction) as those that use other postcranial elements, in contrast to other mammalian orders (see also Moncunill-Solé et al. 2015).

Taking into consideration quantitative results, HAPDp measurement overestimates in all populations the BM in *Prolagus* and could not be considered a reliable proxy. FTDp does not show a clear pattern, being far above in the case of XIr population (those with the largest N), but not in others (X3, IVm, X4, VI6). The BM overestimation observed when HAPDp is used for prediction is indicative

that this measurement does not only represent the BM of the species but also other biological attributes, such as locomotion or phylogeny. Samuels & Valkenburgh (2008) described some skeletal specializations of rodents depending on their locomotion style. For example, a broad and robust distal humerus is indicative of fossorial or semifossorial habits. We encourage the scientific community to perform new studies that analyze the locomotion, biomechanics and skeletal proportions of *Prolagus* species in comparison with its extant relatives (*Ochotona* spp.). This will increase the biological knowledge of *Prolagus* and might help us to discard those measures that are correlated with their locomotion or phylogeny for predicting BM.

BM and teeth size: the case of Sardinian *Prolagus*. It is interesting to compare the trends of BM vs Lp3 in the *P. figaro* – *P. sardus* lineage. We take into consideration p3 because it is the most reliable tooth position for specific identification in lagomorphs. As shown in Fig. 2b, average Lp3 increases (ca 13%) when the oldest population of *P. figaro* (X3) is compared to *P. aff. figaro* from CMD1 site, the “founder” of the Sardinian lineage. Lp3 of *P. figaro* shows a maximum oscillation of 6% in the considered populations. A drastic drop of Lp3 (almost 30%) is recorded between *P. figaro* (X4) and the oldest studied population of *P. sardus* (IV5). After IV5, Lp3 values of *P. sardus* increase slightly through time (total increase of ca 11% in the studied populations) following an asymptotic pattern (see also Angelone et al. 2008). When we analyzed the BM variation, the first thing that we observe is that its record is more incomplete than for teeth: BM estimations are not available for *P. aff. figaro* and older populations of *P. sardus* (Fig. 2a). Moreover, we have to take into due account that BM values have been obtained after complex data treatment, whereas Lp3 are raw data. Nevertheless, it is evident that BM and Lp3 of Sardinian *Prolagus* follow quite different trends. The differences are not so evident among populations of *P. figaro*: average BM increases of ca 10%, whereas average Lp3 fluctuates of ca 6%. Evident discrepancies can be noticed with the appearance of *P. sardus*. Average Lp3 drops of ca 30% between youngest *P. figaro* (X4) and oldest *P. sardus* (IV5). Then, Lp3 average increases through time in *P. sardus* attesting to a value of 2.06 mm (VI6) which is ca 15% smaller than in X4. Lacking

data relative to older infillings (IV5 and IV20), we can only state that younger ones (XIr and VI6) show a higher BM average (ca 15-20%) than *P. figaro* (X4). Hypothesizing a dramatic BM decrease between *P. figaro* and *P. sardus* followed by an explosive increase to exceed *P. figaro* BM values is not realistic. The most parsimonious hypothesis is that BM followed a general increase trend through the transition *P. figaro*-*P. sardus* and throughout the evolution of *P. sardus*, countertrending Lp3 drastic drop observed at the transition *P. figaro* – *P. sardus*.

The fact that p3 dimensional trend shows evident discrepancies with BM pattern inferred through postcranial elements casts doubts about the usage of p3 as a proxy for BM estimation in insular endemic *Prolagus*. Compared to continental species of *Prolagus*, insular endemic species show a noticeable enlargement of the size of p3 vs the size of molariform elements of the lower tooth row (see Angelone 2005: fig. 6 for a qualitative comparison) probably due to a reassessment in jaw mechanics. At any rate, the reliability of teeth as BM proxies has been questioned also in studies that took into consideration a continental species of *Prolagus* as well as a wider selection of fossil lagomorphs case studies (Moncunill-Solé et al. 2015). They prefer models based on postcranial bones, as directly related to weight bearing.

Timing and patterns of BM variations in Sardinian *Prolagus*. Mein (1983) illustrated a biphasic pattern of evolution on islands consisting in a first tachytelic step in which the immigrant species undergoes sudden morpho-dimensional changes corresponding to its entrance to insular selective regimes and a second step in which the taxon undergoes a relatively long bradytelic phase. Millien (2006) further corroborated and “quantified” Mein’s rule. According to some authors (Sondaar 1977; Alcover et al. 1981; Lister 1989, 1996), the tachytelic stage is a change in the “evolutionary direction” (sensu Sondaar 1977; e.g. BS shift or low gear locomotion) whereas the bradytelic one is a further continuation of the existing “direction of the change” (ib., e.g. harvesting saving by increase of hypsodonty, changes in dentognathic feeding apparatus, or developing traits for searching fallback resources). Evans et al. (2012) estimated a minimum of 4000 years for small mammals to become giants (ca 16000 generations).

If we apply Mein’s model to Sardinian *Prolagus* lineage, the first phase should have taken place during or short after the Early/Late Pliocene boundary (age of the CMD1 fossil assemblage). Indeed, *P. aff. figaro* from CMD1 shows very slight morphological modifications due to endemism, evidence of its very recent arrival from mainland (Angelone et al. 2015). The Lp3 of *P. aff. figaro* is comparable to the values of populations of continental Italy from MN16 (absence record for MN15; Angelone et al. 2015) and is between 7-13% smaller than *P. figaro*. There is no record of the possible changes of BM occurred in the 1 Ma that separate CMD1 and the oldest populations of *P. figaro* from Monte Tuttavista. We have not enough data to clearly recognize the tachytelic stage of Mein’s model in *P. aff. figaro*-*P. figaro* and to verify/quantify the dimensional changes and the time span needed to produce them. The populations of *P. figaro* here analyzed should cover a time span of ca 0.3-0.4 Ma (inferred from Palombo 2009b: fig 2). In this time span, slight weight fluctuations have been observed, which may correspond to the bradytelic phase of Mein’s model.

The appearance of *P. sardus* (closely related to *P. figaro* and not an immigrant from mainland; Angelone et al. 2015) occurred during the transition from the Orosei 2 subcomplex to the Dragonara subcomplex (ca 0.8-0.7 Ma; inferred from Palombo 2009b: fig 2). This transition is characterized by the highest species turnover recorded in the Quaternary of Sardinia (Palombo 2009b). Leaving aside the reason of this dramatic change (see next section), it seems to have triggered a new biphasic evolutionary phenomenon which follows Mein’s model too. In general the phyletic lineages of Sardinian small mammals underwent outright (geologically speaking), an abrupt and noticeable increase in dental size (Abbazzi et al. 2004). Contrarily *Prolagus*, as stated above, experienced a drastic Lp3 decrease. The absence of data from IV5 and IV20 fissure fillings does not allow us to quantify changes in BM. Teeth size and morphology in early populations of *P. sardus* underwent an evolution comparable to Mein’s model first phase. The slight, asymptotic growth of *P. sardus* Lp3 and postcranial measurements (Angelone et al. 2008), that in our data covers the interval between ca 0.6-0.4 Ma (inferred from Palombo 2009b: fig. 2), parallelizes Mein’s model second phase. Indeed, Mein’s rule focuses on the first stages of colonization of the island, making reference to the

biological adaptation of the species to the new selective regimes. However later on, changes can also take place consequence of the variation in the environment. Abiotic changes (climatic, topographic, among others) and variations of biotic traits (e.g. levels of predation, intra- and interspecific competition), both have a significant role to drive evolution (Alcover et al. 1981; Brockhurst et al. 2014). Our data seem to indicate that Mein's model can be applied several times to a taxon during its evolution of an island, if significant ecological changes occur (e.g. climatic changes or variation in levels of selective regimes). The study of other mammalian lineages of the Pleistocene of Sardinia or other islands may provide more case studies to support this hypothesis.

Driving factors in the evolution of Sardinian *Prolagus*: some hypotheses. The sea level low stand at the Early/Late Pliocene transition allowed the migration of *P. sorbini* from Italian mainland towards Sardinia (Angelone & Kotsakis 2001; Angelone et al. 2015). Insular selective regimes triggered the morpho-dimensional changes in the immigrant that led to *P. figaro*. *Prolagus figaro* survived until the end of the Orosei 2 subcomplex. The appearance of *Prolagus sardus* marks the onset of the Dragonara subcomplex, characterized by a complete turnover in the small mammals' component of Sardinian fauna (except for *Talpa*): the leporid and the glirid *Tyrrhenoglis* did not survive the transition; the insectivore *Nesiotites* and the rodents *Tyrrhenicola* and *Rbagamys*, descendants of taxa already present in the Orosei 2 subcomplex, underwent evident modifications of teeth morphology and a noticeable increase of teeth size probably coupled with a BS increase (Abbazzi et al. 2004); the ochotonid *Prolagus* underwent a decrease of Lp3 but an increase of BM.

The ancestors of the small mammal genera which survived into the Dragonara subcomplex were present and already showed endemic traits since the Orosei 2 subcomplex (i.e. *Tyrrhenicola*) or at least since the Capo Figari/Orosei 1 subcomplex. The competition among small mammal species as driving factor of the turnover between the Orosei 2/Dragonara subcomplexes can be ruled out and the extinction of glirids and of the leporid is not likely to have triggered a competition to occupy its niche in taxa with such a wide range of ecological

requirements, and the arrival of *Tyrrhenicola* already occurred earlier. The arrival of the canid *Cynotherium* (once regarded as a specialized *Prolagus* hunter, and recently considered a small-prey hunter, possibly also birds, without evident specialization in *Prolagus* hunting; Malatesta 1970; Lyras et al. 2006, 2010) occurred at the onset of the Orosei 2 subcomplex without triggering any sudden, evident change in small mammals, least of all in *Prolagus*, which increases its BM throughout Pleistocene. This fact apparently contradicts van der Geer et al. (2013) who noticed that the BS increase in insular small mammals that occurs following colonization or first appearance, ceases or is reversed after the arrival of mammalian predators or competitors. Probably the impact of a new predator was not so catastrophic because, contrarily to other islands, several carnivores were already present in Sardinia prior to *Cynotherium* (i.e. *Chasmaporthetes*, *Mustela* and *Pannonictis*; the latter also coexisted with *Cynotherium* for a while). In fact, due to its large area, Sardinia had selective regimes more similar to mainland than other Mediterranean islands. It could support the presence of terrestrial predators and had not a strong resource limitation as small islands (Heaney 1978, 1984). Thus, we can not affirm that the arrival of *Cynotherium sardoum* increased the extrinsic mortality of Sardinian pikas.

The most important cause of the turnover at the onset of the Dragonara subcomplex, and thus the trigger of the transition *P. figaro*-*P. sardus* is likely to be climate change, in particular those related to the mid-Pleistocene Transition. Even after Middle Pleistocene, the evolution of *P. sardus* seem related to climate changes and to consequent specific modifications of the environment. Preliminary data by Boldrini & Palombo (2010) suggested a correlation between limb length and temperature in *P. sardus*. Effects of climate on BS have been highlighted in insular endemic fossil vertebrates of the Mediterranean by van der Geer et al. (2013), according to whom BS fluctuates over time linked to climatic oscillation. Also Millien & Damuth (2004) noticed the influence of geographical climatic gradients and climatic change through time on fossil endemic insular species.

Regarding the extinction of Sardinian *Prolagus*, it probably occurred less than 2000 years ago, in the Roman period, between the arrival of *Rattus rattus* and the present time (Vigne 1982). Authors

do not agree on the importance of men's influence (directly by predation and indirectly by introduction of alien predators, competitors, parasites, infectious diseases, modification of the landscape by agricultural activities, among others) to the extinction of *Prolagus*.

Insular endemic lagomorphs and the Island Rule. Radical morpho-dimensional adaptations are observed in insular endemic organisms. In mammals, apart from modifications in dental, cranial and limbs morphology and relative proportions, it is observed a BS trend coined as Island Rule (Foster 1964; Van Valen 1973): in general small-sized mammals considerably increase their size, whereas large-sized mammals show an opposite trend. This ecogeographic rule is also observed in insular endemic fossil mammals. In the Neogene-Quaternary of Mediterranean islands and palaeoislands, insular gigantism and dwarfism have been the subject of several studies and debates (from the pioneer general studies, e.g. Vaufreij 1929; Thaler 1973; Sondaar 1977; Azzaroli 1982; to the most recent reviews, e.g. van der Geer et al. 2010; Lomolino et al. 2013 and references therein).

Lagomorphs are usually considered as small mammals together with rodents and insectivores. Although they have a larger size than the average of the small mammals, this order is far from reaching the size of the great majority of large mammals (e.g. elephants, rhinos, etc.). Their medium or intermediate BM undertakes a key position in ecosystems (Valverde 1964) and compromises their response (adaptation) to island environments (Island Rule). Actually in extant endemic insular leporids the BM trend reported in literature is variable, but mostly directed towards a reduction of the size (Foster 1963, 1964; Lawlor 1982; Palacios & Fernández 1992; Tomida & Otsuka 1993). In the case of ochotonids, no extant species are present on islands and their trend is unknown.

When we deal with insular endemic fossil lagomorphs, it is not easy to determine their actual BM and its relative variation compared to the continental ancestor. This is consequence of two facts: 1) mainly most remains consist in teeth, whose size, at least in lagomorphs, does not directly reflect BM (see above and Moncunill-Solé et al. 2015); and 2) the supposed ancestor is often unknown or wrongly identified (e.g. *P. sardus* from *P. michauxi* and *Gymne-*

sicolagus gelaberti from *P. crusafonti* in Lomolino et al. 2013 and van der Geer et al. 2013). A reliable BS estimation is available for an insular endemic fossil leporid, *Nuralagus rex* (Pliocene of Menorca, Spain), which BM has been calculated in 8 kg (Moncunill-Solé et al. 2015, who reconsidered the BM estimation of 12 kg by Quintana et al. 2011). Even if not quantifiable, the size increase with respect to its supposed continental ancestor, the relatively small-sized genus *Alilepus*, should have been quite remarkable.

For *Prolagus* species it is not possible to quantify exactly the relative BM increase of insular endemic vs their mainland ancestors. In the case of Sardinian *Prolagus*, this is due to the lack of studies of postcranial remains of *P. sorbinii*, whereas in the case of Apulian *Prolagus*, their continental ancestor is not known yet (Angelone 2007; Angelone & Čermák 2015; Angelone et al. 2015). Nevertheless, we can have a gauge of the BM difference between endemic insular *Prolagus* and continental species taking into consideration the only available BM datum of a continental *Prolagus*, i.e. the BM of *P. cf. calpensis* from the Late Pliocene of Spain, estimated in ca 320 g (based on average of femurs and tibiae; Moncunill-Solé et al. 2015). Thus, *P. figaro* from Monte Tuttavista X3 had a noticeably larger BM (ca 25%) than an almost coeval western European mainland *Prolagus*. One among the oldest known populations of *P. apricenicus* (Cava Fina F1; BM = ca 282 g; Moncunill-Solé et al. in press) had a BM ca 13% smaller than *P. cf. calpensis*, not because it decreased its size in an insular domain, but probably because the continental ancestor of Apulian *Prolagus* was a pre-Messinian, medium-sized species (see Angelone 2007; Angelone & Čermák 2015). Later populations of *P. apricenicus*, weighing ca 601 g (Moncunill-Solé et al. 2015), almost doubled the BM of *P. cf. calpensis*.

The known average BM range of both Sardinian species of *Prolagus* (397.88-525.05 g; a BM of 800 g for Mesolithic *P. sardus* inferred by Sondaar & van der Geer (2000) on a qualitative basis has to be verified) is smaller than the populations of *P. apricenicus*, whose BM range is ca 280-600 g (Moncunill-Solé et al. 2015, in press). The other Apulian species, *P. imperialis*, is traditionally considered gigantic, because it has the largest p3. However, our analyses and results make clear that dental remains do not directly reflect actual BM, and sometimes even counter-trend postcranial-based results. Pending a study

of postcranial remains of *P. imperialis*, we refrain to make inferences about its BM.

Millien (2011) argued that in smaller islands the evolutionary rate is higher. This possibly explains the explosive BM increase of *P. aprivicnicus*, confined to a very limited, fragmented area, in contrast to the *P. figaro*-*P. sardus* trend, which lived in a larger island.

In general, the scanty available quantitative data indicate that both fossil leporids and ochotonids follow the small mammal Island Rule pattern. They underwent a BM increase which extent is highly variable, though. This trend is not in line with the variable response observed in extant insular endemic leporids (see above).

BM and life history of insular endemic *Prolagus*. In the last twenty years, several researches have been focused on the life history of insular fossil species, principally addressed to dwarfism (Bromage et al. 2002; Raia et al. 2003; Raia & Meiri 2006; Köhler 2010; Kubo et al. 2011; Marín-Moratalla et al. 2011; Jordana et al. 2012, 2013; van der Geer et al. 2014) although, newly, investigations regarding gigantism have been performed (Moncunill-Solé et al. in press; Orlandi-Oliveras et al. in press). BM scales with several traits of the life history of species such as life span, fecundity, age at maturity, among others (Blueweiss et al. 1978; Peters 1983; Calder 1984). For this reason, at first sight, we could think in predicting some of these life history traits for *P. figaro* and *P. sardus* using the BM results of our analysis. However, Moncunill-Solé et al. (in press) analyzed the histology and BM of one of the Apulian insular endemic species of *Prolagus* (*P. aprivicnicus*) and suggested that it had a slower life history than expected from its BS. Histologically, the longevity is estimated of at least 7 years for *P. aprivicnicus* from F1 fissure filling contrasting with the 4.5 years expected from its BS (around 300 g). The selective regimes of insular habitats (low levels of extrinsic mortality and resource limitation) are the most probable triggers of this shift (Palkovacs 2003). This is also observed in extant ochotonids (*Ochotona* spp.) that dwell in rocky habitats which are subjected to a low average yearly mortality. They show a slower life history (later age at maturity and longer longevity) than the species of *Ochotona* that live in meadows, although both groups do not have steep differences in BM (Smith 1988).

Taking in consideration of the aforementioned, extant and extinct relative species that dwell in habitats with low levels of extrinsic mortality show a slower life history than expected from their BS. In the case of *P. figaro* and *P. sardus* the levels of extrinsic mortality may not be as low as in the case of *P. aprivicnicus* from Gargano consequence of the presence of predators. However, the ecological selective regimes of Sardinia would not be like the mainland's one. For this reason, the prediction of life history traits and other biological attributes using the estimated BM should be considered with caution. Probably, we would underestimate the values of these traits. The absence of histological data of extant and extinct ochotonids encourages the studies focused on this field in order to improve the biological knowledge of insular and mainland lagomorphs.

CONCLUSIONS

BMs were estimated for *P. figaro* from X3 (397.88 g), IVm (406.37 g) and X4 (435.74 g); and for *P. sardus* from XIr (503.86) and VI6 (525.05 g). These results allow us to state a significant increase of BM of the species *Prolagus* from Sardinia throughout the Pleistocene. The best measurements for determining the BM of *Prolagus* are FL, TAPDp, TTDp, TTDd and HTDd. In contrast, HAPDp and FTDp appear to be unreliable proxies. The BM increase opposes to the pattern of the Lp3, which shows a drastic drop at the transition between *P. figaro* and *P. sardus*. This is due to the fact that teeth are not weight-bearing elements, and thus, their use as BM proxies is not recommended. However, when the teeth dimensions are taken into account, the biphasic Mein's model (tachytelelic and bradytelelic stages) may be observed twice. This cannot be confirmed with BM estimations due to the absence of postcranial elements in some key sites as CMd1 (*P. aff. figaro*) and IV5 (oldest known population of *P. sardus*). The entrance of *Cynotherium* and the presence of other species of carnivores during the Pleistocene seem to not have influence on the pattern of adaption to insular ecological regimes of *Prolagus*.

Currently, the absence of ochotonids on islands does not allow us to know the adaptations of this group to insular ecological regimes (Island Rule). In

the fossil record, the two species of *Prolagus* studied in our research and one of the two endemic insular Apulian species (*P. apricenicus*) suggest a gigantism pattern for ochotonids. However, this latter species shows a more explosive increase of BM perhaps as a result that it dwelled in a smaller, fragmented area. It is observed in extant and extinct species that the environments with a lower extrinsic mortality can promote a lower life history (e.g. greater longevity than that expected for its BM). Thus, the estimations of life history traits taking into account the BM results of our research should be considered with caution.

Acknowledgements. We are grateful to the firms that perform quarrying activities at Monte Tuttavista for their kind collaboration; to M. Asole, P. Catte, A. Fancello, G. Mercuriu, G. Puligheddu, A. Useli for the careful work of preparation of the analyzed fossils; to M.A. Fadda and the Superintendents F. Lo Schiavo and F. Nicosia of the Soprintendenza Archeologica della Sardegna who allowed the study of the material analyzed in this paper; to T. Kotsakis, M.R. Palombo and to the reviewers S. Čermák, X. Jordana, and J. Quintana, and to the editor L. Rook for their useful remarks. This research was supported by the Spanish Ministry of Education, Culture and Sport (AP2010–2393, B.M.-S.).

REFERENCES

- Abbazzi L., Angelone C., Arca M., Barisone G., Bedetti C., Delfino M., Kotsakis T., Marcolini F., Palombo M.R., Pavia M., Piras P., Rook L., Torre D., Tuveri N., Valli A. & Wilkens B. (2004) - Plio-Pleistocene fossil vertebrates of Monte Tuttavista (Orosei, E. Sardinia, Italy): an overview. *Riv. It. Paleont. Strat.*, 110: 681-706.
- Alcover J.A., Moyà-Solà S. & Pons-Moyà J. (1981) - Les quimeres del passat: els vertebrats fòssils del Plio-Quaternari de les Balears i Pitiüses. Editorial Moll, Ciutat de Mallorca, 260 pp.
- Angelone C. (2005) - Evolutionary trends in dental morphology of the genus *Prolagus* (Ochotonidae, Lagomorpha) in the Mediterranean Islands. In: Alcover J.A. & Bover P. (Eds) - Proceedings of the International Symposium Insular Vertebrate Evolution: the Paleontological Approach. *Mon. Soc. Hist. Nat. Balears*: 17-26, Mallorca.
- Angelone C. (2007) - Messinian *Prolagus* (Ochotonidae, Lagomorpha, Mammalia) of Italy. *Geobios*, 40: 407-421.
- Angelone C. & Čermák S. (2015) - Two new species of *Prolagus* (Lagomorpha, Mammalia) from the Late Miocene of Hungary: taxonomy, biochronology and palaeobiogeography. *Paläontol. Z.*, 89(4): 1023-1038.
- Angelone C., Čermák S. & Kotsakis T. (2015) - The most ancient lagomorphs of Sardinia: an overview. *Geobios*, 48: 287-296.
- Angelone C. & Kotsakis T. (2001) - *Rhagapodemus azzarolii* n. sp. (Muridae, Rodentia) from the Pliocene of Mandriola (Western Sardinia, Italy). *Boll. Soc. Paleont. It.*, 40: 127-32.
- Angelone C., Tuveri C. & Arca M. (2009) - Biocronologia del Plio-Pleistocene sardo: il contributo degli ochotonidi (Lagomorpha, Mammalia). *Abstr. "IX Giornate di Paleontologia"*, 5, Apricena.
- Angelone C., Tuveri C., Arca C., López Martínez N. & Kotsakis T. (2008) - Evolution of *Prolagus sardus* (Ochotonidae, Lagomorpha) in the Quaternary of Sardinia island (Italy). *Quat. Int.*, 182: 109-115.
- Azzaroli A. (1982) - Insularity and its effects on terrestrial vertebrates: evolutionary and biogeographic aspects. In: Montanaro Gallitelli E. (Ed.) - Palaeontology, Essential of Historical Geology: 193-213. Edizioni S.T.E.M. Mucchi, Modena.
- Blueweiss L., Fox H., Hudzma V., Nakashima D., Peters R. & Sams S. (1978) - Relationships between body size and some life history parameters. *Oecol.*, 37: 257-272.
- Boldrini R. & Palombo M.R. (2010) - Did temperature regulate limb length in the Sardinian endemic ochotonid *Prolagus sardus*? *Abstr. "Convegno in memoria di Alberto Malatesta (1915-2007), geologo e paleontologo"*: 12-13, Roma.
- Bromage T.G., Dirks W., Erdjument-Bromage H., Huck M., Kulmer O., Öner R., Sandrock O. & Schrenk F. (2002) - A life history and climate change solution to the evolution and extinction of insular dwarfs: acypriot experience. In: Waldren W.H. & Ensenyat J.A. (Eds) - World Islands in Prehistory. International Insular Investigations, V Deia International Conference of Prehistory: 420-427. Archaeopress, Oxford.
- Brockhurst M.A., Chapman T., King K.C., Mank J.E., Paterson S. & Hurst D.H.H. (2014) - Running with the Red Queen: the role of the biotic conflicts in evolution. *Proc. Roy. Soc. B*, 281: 20141382.
- Calder W.A. III (1984) - Size, function, and life history. Dover Publications Inc., New York, 431 pp.
- Damuth J. & MacFadden B.J. (1990) - Body size in mammalian paleobiology. Estimations and biological implications. Cambridge University Press, Cambridge, 397 pp.
- Evans A.R., Jones D., Boyer A.G., Brown J.H., Costa D.P., Ernest S.K.M., Fitzgerald E.M.G., Fortelius M., Gittleman J.L., Hamilton M.J., Harding L.E., Lintulaakso K., Lyons S.K., Okie J.G., Saarinen J.J., Sibly R.M., Smith F.A., Stephens P.R., Theodor J.M. & Uhen M.D. (2012) - The maximum rate of mammal evolution. *Proc. Natl. Acad. Sciences USA*, 109: 4187-4190.
- Foster J.B. (1963) - The evolution of native land mammals of the Queen Charlotte Islands and the problem of insularity. PhD Thesis, University of Columbia, Vancouver.
- Foster J.B. (1964) - Evolution of mammals on islands. *Nature*, 202: 234-235.
- Gingerich P.D., Smith B.H. & Rosenberg K. (1982) - Allometric scaling in the dentition of primates and prediction of body weight from tooth size in fossils. *Am. J. Phys. Anthropol.*, 58: 81-100.
- Heaney L.R. (1978) - Island area and body size of insular mammals: evidence from the tri-colored squirrel (*Callosciurus prevostii*) of Southeast Asia. *Evolution*, 32: 29-44.

- Heaney L.R. (1984) - Mammalian species richness on islands on the Sunda Shelf, Southeast Asia. *Oecol.*, 61: 11-17.
- Jordana X., Marín-Moratalla N., De Miguel D., Kaiser T.M. & Köhler M. (2012) - Evidence of correlated evolution of hypsodonty and exceptional longevity in endemic insular mammals. *Proc. R. Soc. Biol. Sci.*, Ser. B, 279: 3339-3346.
- Jordana X., Marín-Moratalla N., Moncunill-Solé B., Bover P., Alcover J.A. & Köhler M. (2013) - First fossil evidence for the advance of replacement teeth coupled with life history evolution along an anagenetic mammalian lineage. *PLoS ONE*, 8: e70743.
- Köhler M. (2010) - Fast or slow? The evolution of life history traits associated with insular dwarfing. In: Pérez-Mellado V. & Ramon C. (Eds) - Islands and Evolution: 261-280. Institut Menorquí d'Estudis, Maó, Menorca.
- Kubo M.O., Fujita M., Matsu'ura S., Kondo M. & Suwa G. (2011) - Mortality profiles of Late Pleistocene deer remains of Okinawa Island: evidence from the Hanandagama cave and Yamashita-cho cave I sites. *Anthropol. Sci.*, 119: 183-201.
- Lawlor T.E. (1982) - The evolution of body size in mammals: evidence from insular populations in Mexico. *Am. Nat.*, 119: 54-72.
- Lister A.M. (1989) - Rapid dwarfing of red deer on Jersey in the Last Interglacial. *Nature*, 342: 539-542.
- Lister A.M. (1996) - Dwarfing in island elephants and deer: processes in relation to time of isolation. *Symp. Zool. Soc. London*, 69: 277-292.
- Lomolino M.V., van der Geer A.A.E., Lyras G.A., Palombo M.R., Sax D.F. & Rozzi R. (2013) - Of mice and mammoths: generality and antiquity of the island rule. *J. Biogeogr.*, 40: 1427-1439.
- Lyras G., Van der Geer A.A.E., Dermitzakis M.D. & De Vos J. (2006) - *Cynotherium sardous*, an insular canid (Mammalia: Carnivora) from the Pleistocene of Sardinia, and its origin. *J. Vert. Paleont.*, 26: 735-745.
- Lyras G., Van der Geer A.A.E. & Rook L. (2010) - Body size of insular carnivores: evidence from the fossil record. *J. Biogeogr.*, 37: 1007-1021.
- Marín-Moratalla N., Jordana X., García-Martínez R. & Köhler M. (2011) - Tracing the evolution of fitness components in fossil bovids under different selective regimes. *C. R. Palevol*, 10: 469-478.
- Masini F., Petruso D., Bonfiglio L. & Mangano G. (2008) - Origination and extinction patterns of mammals in three central Western Mediterranean island form the Late Miocene to Quaternary. *Quat. Int.*, 182: 63-79.
- Mein P. (1983) - Particularités de l'évolution insulaire chez les petits Mammifères. *Coll. Int. C.N.R.S.*, 330: 189-193.
- Millien V. (2006) - Morphological evolution is accelerated among island mammals. *PLoS Biol.*, 4(10): e321.
- Millien V. (2011) - Mammals evolve faster in smaller areas. *Evolution*, 65(7): 1935-1944.
- Millien V. & Damuth J. (2004) - Climate change and size evolution in an island rodent species: new perspectives on the Island Rule. *Evolution*, 58(6): 1353-1360.
- Millien V. & Jaeger J.-J. (2001) - Size evolution of the lower incisor of *Microtia*, a genus of endemic murine rodents from the late Neogene of Gargano, southern Italy. *Paleobiology*, 27: 379-391.
- Moncunill-Solé B., Orlandi-Oliveras G., Jordana X., Rook L. & Köhler M. (in press) - First approach of the life history of *Prolagus aprivencus* (*Ochotonidae*, *Lagomorpha*) from Terre Rosse sites (Gargano, Italy) using body mass estimation and paleohistological analysis. *C. R. Palevol.*, <http://dx.doi.org/10.1016/j.crpv.2015.04.004>.
- Moncunill-Solé B., Quintana J., Jordana X., Engelbrektsson P. & Köhler M. (2015) - The weight of fossil leporids and ochotonids: body mass estimation models for the order Lagomorpha. *J. Zool.*, 295: 269-278.
- Nowak R.M. (1999) - Walker's Mammals of the World Volume II. Johns Hopkins University Press, Baltimore, 2015 pp.
- Orlandi-Oliveras G., Jordana X., Moncunill-Solé B. & Köhler M. (in press) - Bone histology of the giant fossil dormouse *Hypnomys onicensis* (Gliridae, Rodentia) from Balearic Islands. *C. R. Palevol.* <http://dx.doi.org/10.1016/j.crpv.2015.05.001>.
- Palacios F. & Fernández J. (1992) - A new subspecies of hare from Majorca (Balearic Islands). *Mammalia*, 56: 71-85.
- Palombo M.R. (2009a) - Body size structure of Pleistocene mammalian communities: what support is there for the "island rule"? *Integr. Zool.*, 4: 341-356.
- Palombo M.R. (2009b) - Biochronology, palaeobiogeography and faunal turnover in western Mediterranean Cenozoic mammals. *Integr. Zool.*, 4: 367-386.
- Peters R.H. (1983) - The ecological implications of body size. Cambridge University Press, Cambridge, 329 pp.
- Quinn G.P. & Keough M.J. (2002) - Experimental design and data analysis for biologists. Cambridge University Press, New York, 537 pp.
- Quintana Cardona J. (2005) - Estudio morfológico y funcional de *Nuralagus rex* (Mammalia, Lagomorpha, Leporidae). Unpublished PhD thesis, Universitat Autònoma de Barcelona.
- Quintana J., Köhler M. & Moyà-Solà S. (2011) - *Nuralagus rex*, gen. et sp. nov., an endemic insular giant rabbit from the Neogene of Minorca (Balearic Islands, Spain). *J. Vert. Paleontol.*, 31: 231-240.
- Raia P., Barbera C. & Conte M. (2003) - The fast life of a dwarfed giant. *Evol. Ecol.*, 17: 293-312.
- Raia P. & Meiri S. (2006) - The island rule in large mammals: paleontology meets ecology. *Evolution*, 60: 1731-1742.
- Reynolds P.S. (2002) - How big is a giant? The importance of method in estimating body size of extinct mammals. *J. Mammal.*, 83: 321-332.
- Samuels J.X. & Valkenburgh B.V. (2008) - Skeletal indicators of locomotor adaptations in living and extinct rodents. *J. Morphol.*, 269: 1387-1411.
- Scott K.M. (1990) - Postcranial dimensions of ungulates as predictors of body mass. In: Damuth J. & MacFadden B.J. (Eds) - Body size in mammalian paleobiology: estimation and biological implications: 301-305. Cambridge University Press, Cambridge.
- Smith A.T. (1988) - Patterns of pika (genus *Ochotona*) life history variation. In: Boyce M.S. (Ed.) - Evolution of Life

- Histories: Theory and Patterns from Mammals: 233-256. Yale University Press, New Haven.
- Sondaar P.Y. (1977) - Insularity and its effect on mammal evolution. In: Hecht M.K., Goody P.C. & Hecht B.M. (Eds) - Major patterns in vertebrate evolution: 671-707. Plenum Publishing Corporation, New York.
- Sondaar P.Y. & van der Geer A.A.E. (2000) - Mesolithic environment and animal exploitation on Cyprus and Sardinia/Corsica. In: Mashkour M., Choyke A.M., Buitenhuis H. & Poplin F. (Eds) - Archaeozoology of the Near East IVA: 67-73. ARC Publications 32, Groningen.
- Thaler L. (1973) - Nanisme et gigantisme insulaires. *La Recherche*, 37: 741-750.
- Tomida Y. & Otsuka H. (1993) - First Discovery of Fossil Amami Rabbit (*Pentalagus furnessi*) from Tokunoshima, Southwestern Japan. *Bull. Nat. Sci. Mus. Tokyo*, Ser. C, 19: 73-79.
- Tukey J.W. (1977) - Exploratory Data Analysis. Addison-Wesley, Boston, 688 pp.
- Valverde J.A. (1964) - Estructura de una comunidad de vertebrados terrestres. *Mon. Est. Biol. Doñana*, 1: 1-129.
- van der Geer A.A.E., de Vos J., Dermitzakis M. & Lyras G. (2010) - Evolution of Island Mammals: Adaptation and Extinction of Placental Mammals on Islands. Wiley-Blackwell, Oxford, 496 pp.
- van der Geer A.A.E., Lyras G.A., Lomolino M.V., Palombo M.R. & Sax D.F. (2013) - Body size evolution of palaeo-insular mammals: temporal variations and interspecific interactions. *J. Biogeogr.*, 40: 1440-1450.
- van der Geer A.A.E., Lyras G., MacPhee R.D.E., Lomolino M. & Drinia H. (2014) - Mortality in a predator-free insular environment: the dwarf deer of Crete. *Am. Mus. Novit.*, 3807: 1-26.
- Van Valen L. (1973) - Pattern and the balance of nature. *Evol. Theory*, 1: 31-49.
- Vaufrey R. (1929) - Les éléphants nains des îles méditerranéennes et la question des isthmes pléistocènes. *Arch. Inst. Pal. Hum.*, 6: 1-220.
- Vigne J.-D. (1982) - Zooarchaeology and the biogeographical history of the mammals of Corsica and Sardinia since the last ice age. *Mammal Rev.*, 22: 87-96.
- Vigne J.D. & Valladas H. (1996) - Small mammal fossil assemblages as indicators of environmental change in northern Corsica during the last 2500 Years. *J. Archaeol. Sci.*, 23: 199-215.
- Wilkens B. (2004) - La fauna sarda durante l'Olocene: le conoscenze attuali. *Sard. Cors. Bal. Antiquae*, 1: 181-197.

CORAL ASSEMBLAGES AND BIOCONSTRUCTIONS ADAPTED TO THE DEPOSITIONAL DYNAMICS OF A MIXED CARBONATE-SILICICLASTIC SETTING: THE CASE STUDY OF THE BURDIGALIAN BONIFACIO BASIN (SOUTH CORSICA)

MARCO BRANDANO¹, FRANCESCA R. BOSELLINI², ANDREA MAZZUCCHI¹ & LAURA TOMASSETTI¹

¹Dipartimento di Scienze della Terra, La Sapienza Università di Roma, P. Aldo Moro 5 Roma, I-00185. E-mail: marco.brandano@uniroma1.it, andrea.mazzucchi@uniroma1.it, laura.tomassetti@uniroma1.it

²Dipartimento di Scienze Chimiche e Geologiche, Università di Modena e Reggio Emilia, via Campi 103, 41125 Modena, Italy. E-mail: francesca.bosellini@unimore.it

To cite this article: Brandano M., Bosellini F. R., Mazzucchi A. & Tomassetti L. (2016) - Coral assemblages and bioconstructions adapted to the depositional dynamics of a mixed carbonate-siliciclastic setting: the case study of the Burdigalian Bonifacio Basin (South Corsica). *Riv. It. Paleont. Strat.* 122(1): 37-52.

Key words: Coral bioconstruction, Miocene, Burdigalian, Corsica, mixed carbonate-siliciclastic, coastal environments.

Abstract. Coral bioconstructions associated with mixed carbonate-siliciclastic settings are known to be strongly controlled by coastal morphology and paleotopography. A striking example is represented by the different types of coral bioconstructions and coral-rich deposits of the Cala di Labra Formation deposited in the coastal environment of the Bonifacio Basin (Corsica, France) during the Early Miocene. Detailed mapping on photomosaics allowed accurate documentation of the internal organization of coral deposits as well as lateral and vertical facies relationships. Four types of coral bioconstructions (CB) and one reworked coral deposits (RCD) have been recognized. The CB are represented by sigmoidal cluster reefs, coral carpets and skeletal conglomerates rich in corals. The RCD occurs in lens-shaped bodies intercalated within clinofolds composed of bioclastic floatstones and coarse packstones. The investigated bioconstructions can be contextualised in a coastal environment. In the upper shoreface corals developed in association with the oyster *Hyothisa*, above bioclastic conglomerates sourced by ephemeral streams and erosion of the granitic coastline. In the lower shoreface corals formed sigmoidal bioconstructions interpreted as cluster reefs, whereas coral carpets developed during a relative sea-level rise related to the middle Burdigalian transgressive phase. The reworked coral deposits can be interpreted as lobe-shaped deposits of coarse-grained bioclastic submarine fans formed at the base of the depositional slope of an infralittoral prograding wedge system.

INTRODUCTION

In the Mediterranean region, during the Miocene time, a series of well-exposed carbonate platforms as well as shallow-water mixed carbonate-siliciclastic systems were commonly characterized by the occurrence of different types of coral bioconstructions, ranging from barrier reefs, fringing reefs, patch reefs and coral carpets (Santisteban & Taberner 1988; Braga et al. 1990; Pomar 1991; Esteban 1996; Pedley 1996; Bosellini 2006; Reuter et al. 2006; Brandano et al. 2010; Vigorito et al. 2010; Perrin & Bosellini 2012; Vescogni et al. 2014).

In particular, the development of coral bioconstructions in shallow water mixed carbonate-siliciclastic systems is no longer thought to be an exceptional phenomenon in the fossil record, and increasing attention to these alternative/marginal and turbid-water coral ecosystems in modern seas

makes their fossil analogs a challenging topic to explore. Studies on ancient coral communities living in marginal conditions including for example low light, high turbidity and high siliciclastic input, or high nutrients are important to understand the current structure of reefs and how they could potentially respond to global changes. Quite recently most studies investigated the response of coral assemblages to siliclastic inputs within the so-called turbid-water environments (Wilson & Lokier 2002; Sanders & Baron-Szabo 2005; Silvestri et al. 2011; Wilson 2012; Novak et al. 2013), while less common is research dedicated to understand the depositional processes, and influence of coarse terrigenous sediments and rocky substrate on the development of coral bioconstructions and biota thriving in these habitats (e.g Santisteban & Taberner 1988; Braga et al. 1990).

The Cala di Labra Fm., deposited in the small but articulated Bonifacio embayment during the Burdigalian, is characterized by a high variability

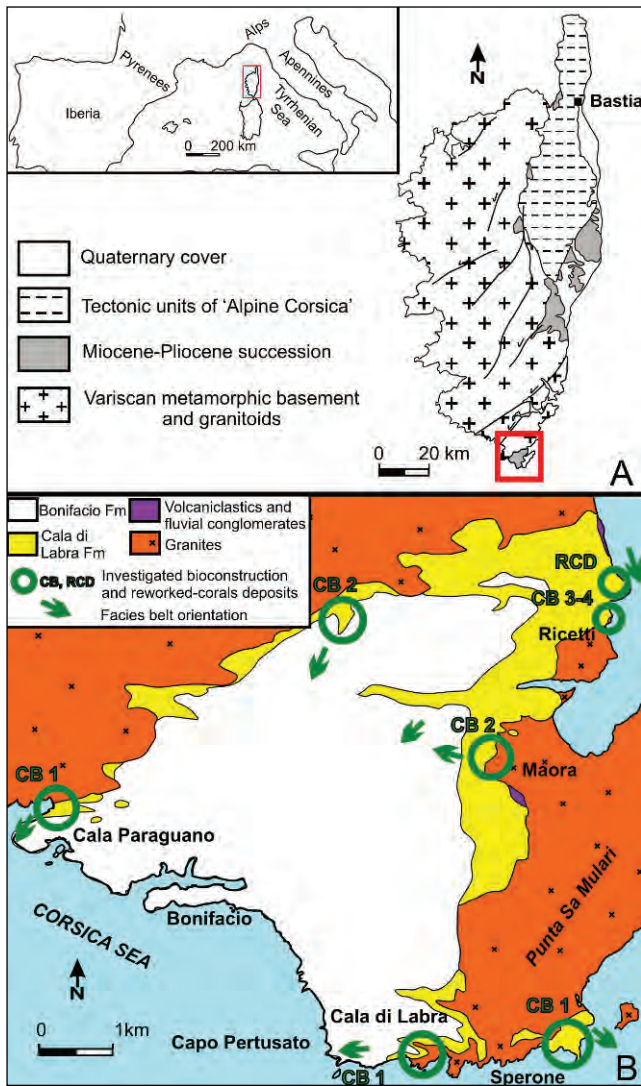


Fig. 1 - A) Schematic geological map of Corsica (Carmignani et al. 2004). B) Geological map of Bonifacio Basin and location of investigated outcrops and coral bioconstructions (modified from Reynaud et al. 2013).

of coral-rich deposits and bioconstructions. Excellent exposures provided the possibility to analyse their geometry, internal structure and facies associations in different depositional subenvironments (Reynaud et al. 2013; Tomassetti et al. 2013; Galloni et al. 2014).

In this study, we document the different types of coral bioconstructions and we aim to evaluate the control that factors such as coastal morphology, paleotopography and siliciclastic input exerted on their growth and depositional dynamics.

GEOLOGICAL SETTING

Corsica Island (France), located in the We-

| Lithostratigraphy | Ferrandini et al. 2002, 2003 | Brandano et al. 2009 | Reynaud et al. 2013 | Galloni et al. 2014 |
|-------------------------|------------------------------|-------------------------|---------------------------------------|---|
| Bonifacio Formation | Early Langhian | Late Burdigalian | Serravallian to Tortonian Langhian | |
| Cala di Labra Formation | Late Burdigalian | Late/Middle Burdigalian | Burdigalian | R3 Late R2 Middle R1 Early Burdigalian |
| Balistra Formation | Aquitanian Oligocene | | Aquitanian Oligocene | |

Fig. 2 - Lithostratigraphic scheme of Oligocene-Miocene deposits of Bonifacio Basin.

stern Mediterranean, is divided in two different geological domains: “Hercynian Corsica” and “Alpine Corsica” (Fig. 1a). The “Hercynian Corsica” consists of Precambrian-middle Paleozoic metamorphic rocks and scattered Paleozoic sedimentary rocks cut by Carboniferous-Permian granitoid and volcanic rocks related to calc-alkaline and alkaline magmatism (Durand-Delga 1984; Ferré & Leake 2001). The “Alpine Corsica” consists of a complex tectonic stack including metamorphic oceanic- and continental-derived thrust sheets related to the Alpine orogeny (Durand-Delga 1984).

Up to the late Eocene, the Corsica and Sardinia micro-plate experienced a NE-SW oriented rifting followed by an Early Miocene continental drifting related to the opening of the Ligurian-Provençal Basin (Carminati & Doglioni 2005; Carminati et al. 2010). During the Aquitanian-Burdigalian, the Sardinia-Corsica block recorded the fastest counter-clockwise angular rotation and extensive pyroclastic deposits covered the central-northern part of the Sardinia Trough (Carminati et al. 2012 and reference therein). The Oligocene-Miocene sedimentary cover of Corsica consists of continental clastic deposits exposed near Ajaccio and marine mixed carbonate-siliciclastic successions cropping out in the southern (Bonifacio), eastern (Aleria) and in the northern sectors (Saint Florent, Francardo) (Ferrandini et al. 2003).

The sedimentary succession of the Bonifacio Basin is represented by three formations: the Balistra Fm., The Cala di Labra Fm. and the Bonifacio Fm. (Ferrandini et al. 2003) (Fig. 1b). The Balistra Formation (Oligocene-Aquitanian) consists of conglomerates and volcanoclastic deposits, whereas the overlying Cala di Labra Formation records the Miocene marine transgression. Based on biostra-

Tab 1 - Description of textural and compositional characteristics of the facies.

| Facies | Texture, bedding and sedimentary structure | Composition |
|------------------------------------|--|---|
| Conglomerate | Matrix-supported conglomerates. | Granitoids pebbles and cobbles. |
| Fine conglomerate to sandstone | Massive fine-conglomerates, crudely stratified and bioturbated (<i>Thalassinoides</i>) sandstone with skeletal elements. | Granitoids pebble, quartz and feldspars, bivalves, echinoids, gastropods, LBF, red algae and rare and reworked corals. |
| Hybrid sandstone | Nodular- to cross-stratified hybrid sandstones. | Quartz, feldspars, red algae and LBF (<i>Amphistegina</i>) |
| Skeletal conglomerate with corals | Massive to crudely stratified conglomerates. | Granitoids pebbles, isolated massive corals in growth position, oysters, gastropods, echinoids and red algae. |
| Coral domestone | Coral domestone with packstone to hybrid sandstone matrix. | Massive and subordinate platy corals (<i>Porites</i> , subordinate <i>Tarbellastrea</i> , rare <i>Montastrea</i> and <i>Thegioastrea</i>) in growth position. Matrix: red algae followed by LBF (<i>Miogypsina</i> and <i>Amphistegina</i>), bivalves, echinoids, small benthic foraminifera, gastropods and bryozoans. |
| Coral platestone | Coral platestone with hybrid sandstone matrix | Platy and subordinate massive corals (<i>Porites</i> and <i>Tarbellastrea</i>) in growth position. Matrix: predominant red algae debris and LBF (<i>Amphistegina</i> and <i>Miogypsina</i>). |
| Coral mixstone | Coral mixstone with packstone matrix | Massive, platy and encrusting corals (<i>Porites</i> and subordinate favoids) in growth position. Matrix: Red algae, bivalves, echinoids and benthic foraminifera. |
| Coral rudstone to floatstone | Coral rudstone to floatstone in a quartz-rich packstone matrix | Reworked coral colonies followed by oysters, gastropods and echinoids. Matrix: bivalve, red algae, benthic foraminifera (<i>Heterostegina</i> , cibicides and rare miliolids) and mineral grains (quartz and feldspars). |
| Red algae branches floatstone | Nodular-bedded and bioturbated floatstones | Red algae (free-living branches and small size rhodoliths) subordinate bryozoans, pectinids, LBF and echinoids. |
| Bioclastic floatstone to packstone | Poorly sorted floatstone to moderate sorted packstone with cross-bedding. | Red algae debris, small benthic and planktonic foraminifera, LBF (<i>Heterostegina</i> and <i>Operculina</i>), gastropods, bryozoans and coral fragments. |

tigraphic data, Brandano et al. (2009) proposed a late-middle Burdigalian age for this formation (Fig. 2). The Bonifacio Formation (late Burdigalian-early Langhian) consists of sandstones, fine-conglomerates to cross-bedded coralline algae-rich calcarenites (Brandano et al. 2009), which are interpreted by Reynaud et al. (2013) as tidal deposits (Fig. 2).

The Cala di Labra Formation is 50 metres thick and consists, from bottom to top, of five superimposed lithofacies (Ferrandini et al. 2003; Brandano et al. 2009; Tomassetti & Brandano 2013; Galloni et al. 2014): a coral rich unit resting on boulders of a Variscan granite, a conglomeratic unit, a sandy to silty unit, and two bioclastic units showing prograding geometries. The siliciclastic facies represents deposition in the coastal environments from shoreface to upper offshore environment (Ferrandini et al. 2002; Reynaud et al. 2013; Tomassetti & Brandano 2013). Galloni et al. (2001, 2014) suggested that the coral-rich deposits actually represent three distinct superimposed, reef-building episodes: the first (R1) overlies the granitic palaeohighs; the second (R2) is coeval with the sandy deposits of shoreface environments; whereas the third (R3) episode is coeval with the prograding bioclastic unit (Fig. 2). In this work we investigate the coral-rich deposits corresponding to the R2 episode of Galloni et al. (2001, 2014), with the exception of the Rocchi Bianchi outcrop (the reworked coral deposits) that are referred to episode R3.

The limited thickness of coral bioconstructions of the Bonifacio embayment, and their relation and proximity with the granitic substrate, led Galloni et al. (2014) to interpret the coral deposits of Cala di Labra Fm. as fringing reefs and coral reefs.

MATERIAL AND METHODS

Bioconstructions and coral-rich deposits have been investigated along sea-cliffs and road cuts in six localities (Fig. 1b). Facies analysis has been carried out and four stratigraphic logs have been measured. Detailed mapping on photomosaics allowed documentation of the internal organization of coral deposits as well as lateral and vertical facies relationships. Detailed coral mapping allowed determination of coral cover (i.e. the total surface occupied by corals compared with the amount of sediment). Mapping was generally oriented with respect to the depositional dip as the paleogeography and physiography of the Bonifacio Basin has been recently reconstructed by Reynaud et al. (2013). These observations were complemented by examination of 120 thin sections.

Coral genera, growth forms and inter-coral associated fauna and sediment were characterized based on field observation and thin section analysis; coral growth fabric is defined following the nomenclature of Insalaco (1998).

RESULTS

Four types of coral bioconstructions, with associated sediments, and a reworked-coral deposit have been recognized (Tab. 1).

Coral bioconstruction 1. The first type of



Fig. 3 - Coral Bioconstruction 1: A) the coral domestone constitutes the bioconstruction core and grades landward to a platestone facies. B) Massive and subordinate platy colonies are essentially in place, close but rarely in contact.

coral bioconstruction (CB1) consists of a coral domestone, which is laterally associated with four other facies: coral platestone, hybrid sandstone, sandstone and a red algal floatstone.

The coral domestone is characterized by massive and subordinate platy colonies, which are basically in growth position, commonly close to each other but rarely in contact (Fig. 3a, b). Massive corals show domal and globular shape and generally range in size from 25 to 60 cm in diameter and from 15 to 50 cm in height. Occasionally they can show meter-size dimensions even reaching 3.5 m in length and 1 m in height. Platy corals usually range from 15 to 20 cm in diameter and 2 to 5 cm in height, although colonies up to 60 x 10 cm in size are also present. *Porites* is the dominant genus and exhibits both massive and platy growth forms (Fig. 4a). Colonies of *Tarbellastrea* (*T. chevaleri*, *T. reussiana*, *T. abditaxis*) (Fig. 4b, c, d), *Montastrea* (Fig. 4e, f), *Thegioastrea* (Fig. 4g, h) and rare *Favites* are subordinate but all characterized by a massive growth form. Bioerosion traces (*Gastrochaenolites*, *Caulostrepsis* and *Entobia*), can be common within coral colonies whereas encrustation is quite rare and represented by balanids and bryozoans.

The coral cover reaches values up to 66%, showing a moderate predominance of corals compared to the packstone matrix (Fig. 3b). Along the depositional dip more spaced colonies are separated by abundant matrix and some reworked corals occur. The matrix is a bioclastic packstone with a

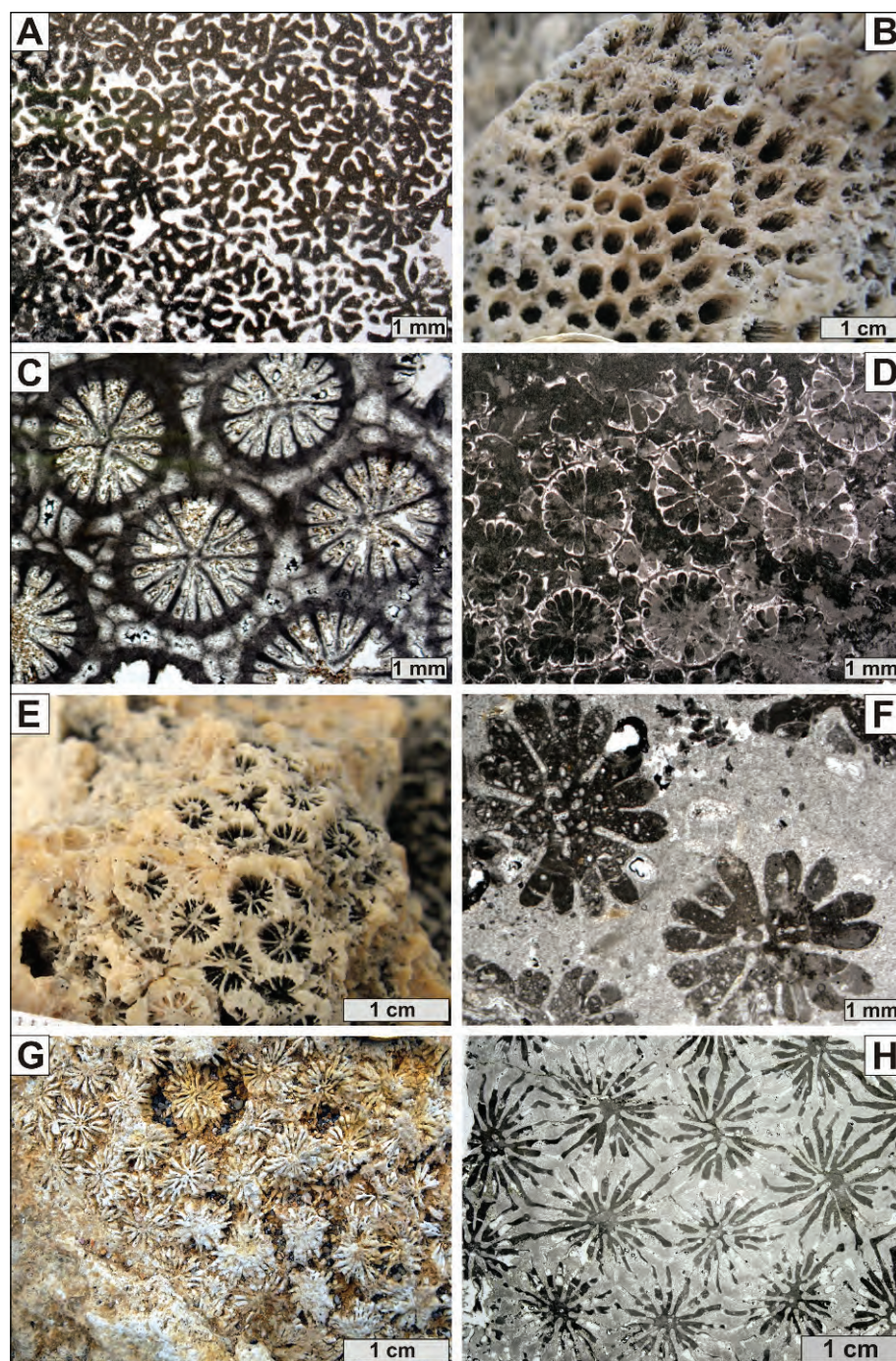
low siliciclastic fraction (Fig. 5a). Red algae are the dominant components and occur as branch fragments, small nodules and crusts together with large benthic foraminifera (LBF) such as *Miogypsina* and *Amphistegina* (Fig. 5a). Bivalves, echinoids spines and plates, small benthic foraminifera (rotaliids, textulariids and rare cibicids), bryozoans and gastropods represent other biotic components. The downdip coral arrangement and variation of the coral/matrix ratio characterize the coral domestone beds with sigmoidal geometry up to 2-3 m thick and about 15-20 m in length. These bioconstructions extend over an area of 700 x 400 m and achieve about 12 m in thickness.

Lateral facies relationships are well exposed at the Sperone outcrop (Fig. 6). Landward, the coral domestone passes into a coral platestone, interfingering with hybrid sandstones that finally pass into sandstones.

The coral platestone is mainly composed of platy corals that occasionally constitute the substrate for the attachment of massive colonies.

Corals are in growth position, locally in contact to each other and embedded into a sandstone matrix with red algae debris and LBF (*Amphistegina* and *Miogypsina*). The coral platestone interfingers with nodular to locally cross-bedded hybrid sandstones. Sub-rounded to sub-angular mineral grains (quartz and subordinate feldspars) represent the terrigenous fraction, whereas red algae debris, *Amphistegina*, bivalve and echinoid fragments constitu-

Fig. 4 - A) *Porites* in thin section. B) Outcrop view of massive *Tarbellastrea*. C) *Tarbellastrea chevalieri* in thin section. D) *Tarbellastrea reussiana* in thin section. E) Outcrop view of massive *Montastrea*. F) *Montastrea* in thin section. G) Outcrop view of massive *Thegioastrea*. H) *Thegioastrea* in thin section.



te the allochems (Fig. 5b). The hybrid sandstones grade into coarse- to fine-grained sandstones with skeletal elements (Fig. 5c, d). The sandstones occur as massive to crudely stratified deposits with diffuse to pervasive bioturbation (*Thalassinoides*). The poor biotic assemblage is mainly represented by fragmented bivalve shells, echinoid plates and LBF (*Amphistegina* and subordinate *Heterostegina*). Flat clypeasteroids, balanids and rare reworked coral colonies also occur.

At Cala Paraguanu, the more distal facies (red algal branches floatstones) crop out. Red algae

(*Spongites*, *Sporolithon* and melobesioids) dominate the biotic assemblage (Fig. 5e), and form free-living branches and small size rhodoliths frequently with boring traces (*Entobia*). Other constituents are bryozoans, pectinids, LBF and echinoids.

In the outcrop of Cala di Labra, Tomassetti et al. (2013) described a coral bioconstruction that colonized a granitic substrate characterized by an irregular and articulated surface. This coral buildup can be referred to the CB1. It appears as an organized lens-shaped structure, and its core consists of a relatively dense coral domestone with a moderate

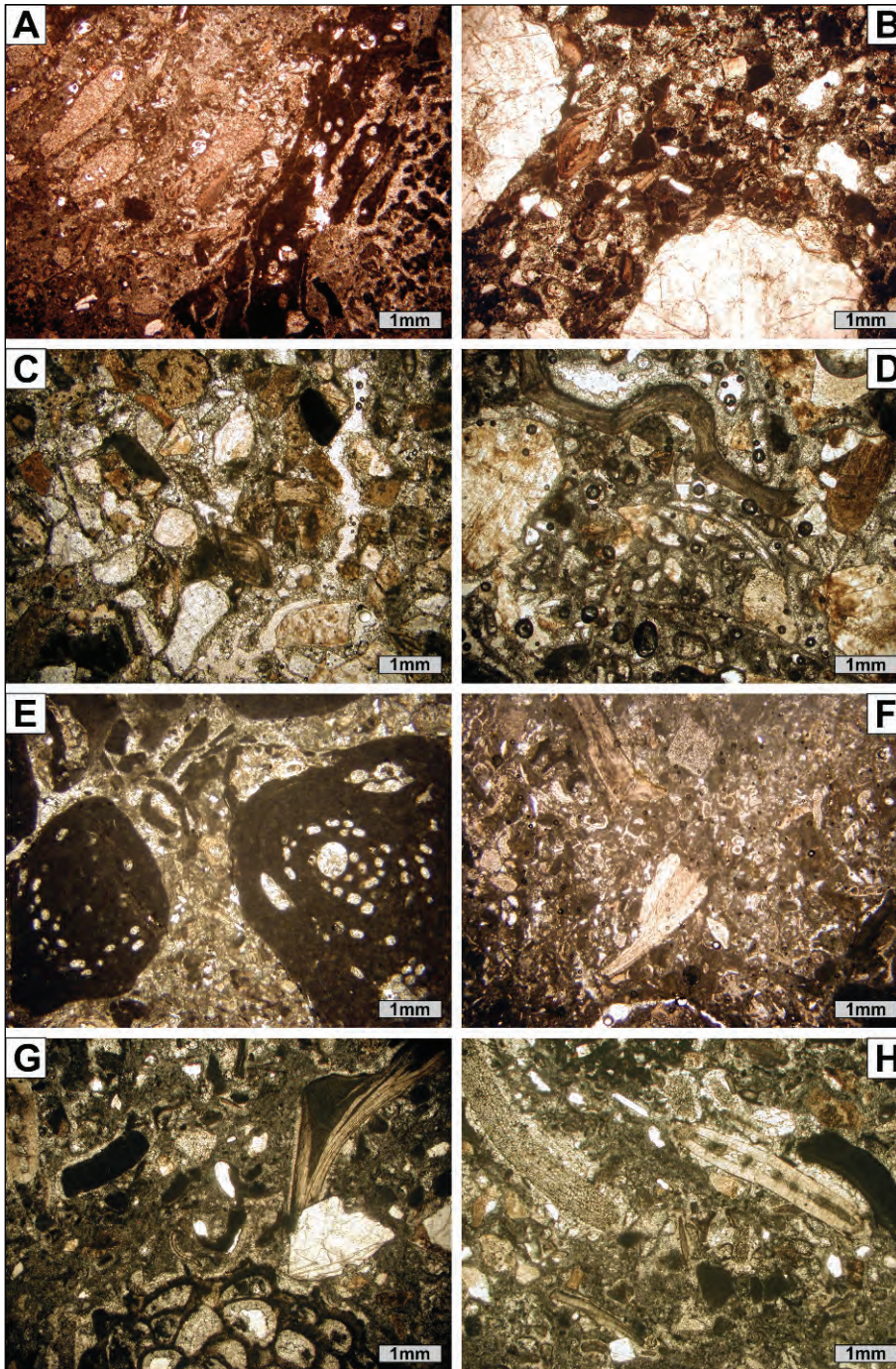


Fig. 5. - Photomicrographs of the facies. A) The main components of the coral domestone matrix are large benthic foraminifera such as *Miogypsina* and red algae. B) Terrigenous grains (quartz and feldspars) characterize the hybrid sandstones together with red algae debris and LBF (*Amphistegina*). C, D) Sandstones are composed of mineral grains (quartz, feldspars) and granitoids fragments with subordinate bioclastic fraction (bivalves, gastropods, *Amphistegina* and rare red algae). E) Red algae dominate the skeletal assemblage of the skeletal assemblage of the red algae branches floatstones. F) Packstone representing the matrix of the coral mixstone facies. Skeletal assemblage is characterized by red algae, bivalves, echinoids and benthic foraminifera. G) Red algae debris, bivalves, large benthic foraminifera (*Heterostegina*) and bryozoans together with subordinate mineral grains (quartz) constituting the coral rudstone matrix. H) *Heterostegina*, red algae, echinoids and bivalve fragments are the main components of the bioclastic floatstone.

increase of platy corals in the upper part. A coral rubble associated with granitic cobbles and pebbles is locally present at the base.

Interpretation. The coral domestone forms a close cluster reef (*sensu* Riding 2002) considering the arrangement of coral colonies. Coral morphology, together with sediment texture and composition, suggest well illuminated waters and relatively high hydrodynamic conditions. Recent studies in the Bonifacio Basin underlined that red algae and LBF (*Miogypsina* and *Amphistegina*), which dominate the packstone matrix, commonly characterize the

sediments of the coral bioconstructions developed within a deep part of the euphotic zone (Brandano et al. 2010; Tomassetti et al. 2013).

The coral platestone forms thin veneers following the substrate morphology. Platy corals in fact can colonize mobile loose substrates (Braga et al. 1990; Novak et al. 2013) and, locally, provide the substrate for massive corals (Reuter et al. 2012).

Facies characters of the hybrid sandstones and sandstones suggest deposition in the lower shoreface to offshore-transition, where the sediment was wave-worked but often homogenized by

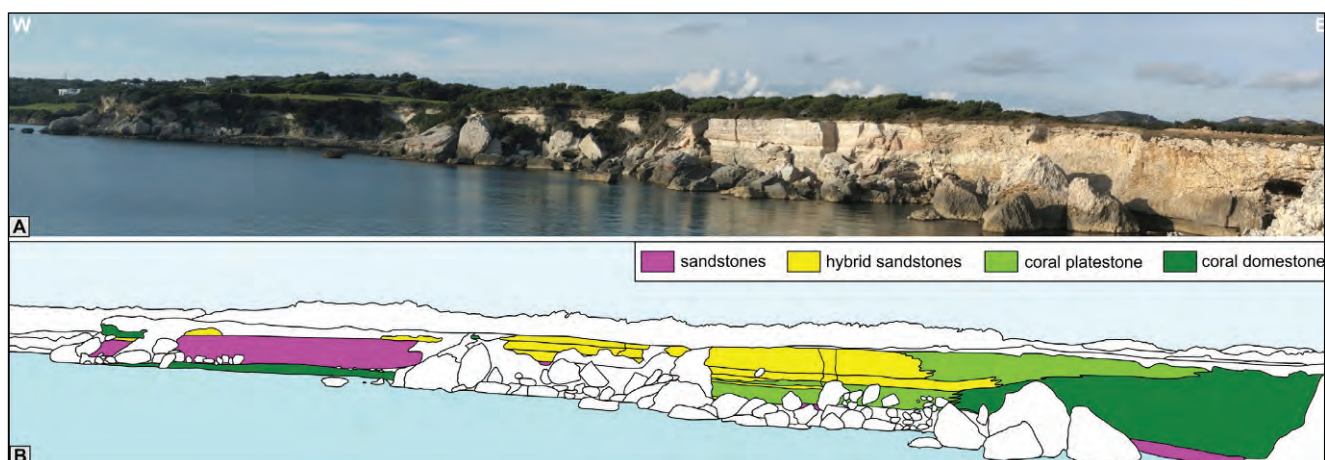


Fig. 6 - A) Photomosaic of Sperone outcrop. B) The line-drawing of this outcrop highlights facies lateral transition. Note the sandstones interfingering basinward into hybrid sandstones that pass into the coral platestone grading finally to the coral domestone.

bioturbation (Reading & Collinson 1996; Andreucci et al. 2009; Nalin et al. 2010). The presence of balanids, coralline algae nodules and fragments, thick *Amphistegina* specimens, coupled with the coarse sandsized textures, support such shallow depositional conditions. The terrigenous fraction derived from the granitic substrate is generally well sorted suggesting a high-energy environment and a proximal basement source.

Large benthic foraminifera, such as *Amphistegina*, inhabit these siliciclastic-rich sandy bottoms together with red algae according to their tolerance to the high siliciclastic input (Lokier et al. 2009). Flat clypeasteroids are shallow-burrowing endobenthic echinoids that thrived within this sandy substrate (Kroh & Nebelsick 2003).

Basinwards, the coral domestone passes into the branching red algal floatstone. This facies was deposited in the oligophotic zone as indicated by the prevalence of red algae and LBF (*Miogypsina*, *Amphistegina* and *Heterostegina*) and by the absence of coral colonies in growth position (Brandano et al. 2010).

Coral bioconstruction 2. The second type of bioconstruction (CB2) is characterized by a coral domestone fabric and is associated with fine conglomerates to sandstones and quartz-rich red algal floatstone to rudstone (Fig. 7).

Massive and subordinate platy colonies of *Porites*, *Tarbellastrea*, *Thegioastrea* and *Montastrea* constitute the coral domestone. Corals occur basically in growth position close to each other forming a small dense bioconstruction core (generally 1-2 m in

length). Moving downdip the coral coverage rapidly decreases from an average value of 50% to 40% and corals occur more spaced and embedded within the abundant matrix. Corals range in size from 10 to 90 cm in length and from 5 to 40 cm in height. Boring traces (*Caulostrepsis* and *Gastrochaenolites*) are commonly present on coral colonies. The inter-coral sediment consists of a coarse hybrid sandstone. Red algae dominate the biotic assemblage, followed by benthic foraminifera (*Miogypsina*, *Amphistegina*, cibicides and textularids), bivalves, echinoids, bryozoans and serpulids. The bioconstruction forms clinobeds with thickness ranging from 0.6 to 1.5 m with oblique-sigmoidal geometry and a few tens of meters in length. These clinobeds are characterized by a basinwards decrease in coral abundance (Fig. 7).

These types of bioconstructions develop closer to the granitic basement overlying fine conglomerates to coarse sandstones, which occur in fining upward beds (1 to 2 m thick) with crude stratification. Abraded and commonly bored fragments of bivalves represent the main bioclastic component of the siliciclastic deposits together with echinoid plates, gastropods shells, and rare red algae.

Landward, the bioconstruction interfingers with bioclastic sandy conglomerates, and sandstone. The skeletal fraction is represented by molluscs, echinoid remains, red algae and subordinate LBF (*Miogypsina* and *Amphistegina*) and bryozoans. Massive and platy coral colonies occur both in growth position and reworked. The siliciclastic fraction is represented by granitic lithoclasts, abundant quartz and feldspar grains. Traces of bioturbation (*Thalassinoides*) may occur.

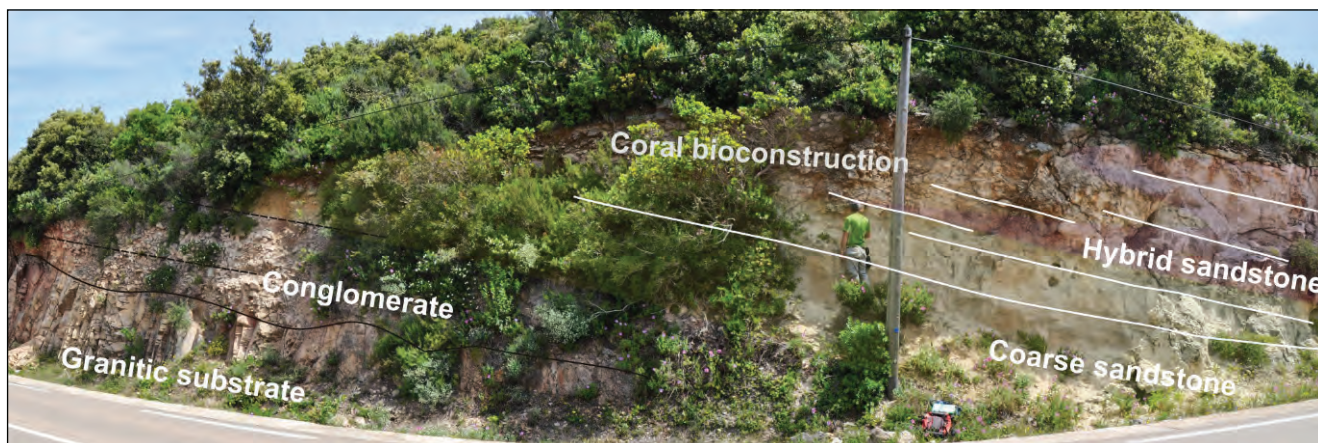


Fig. 7 - Coral Bioconstruction 2: close to the granitic basement, small coral bioconstructions developed on fine conglomerates. These are domestones consisting of massive and rare platy colonies. Basinward, coral growth is reduced, finally passing into coarse hybrid sandstones with isolated corals.

Interpretation. The coral domestone is characterized by corals close to each other in the bioconstruction core and downdip by more spaced colonies in abundant matrix. This structure is consistent with a cluster reef (*sensu* Riding 2002), which shows a close cluster in the bioconstruction core grading downdip to a more spaced structure. As suggested by the coral growth forms and the inter-coral sediment, this facies developed in a relatively high energy environment of the euphotic zone. Massive *Porites*, *Tarbellastrea* and other faviids corals formed buildups with a similar bioclastic matrix (red algae, echinoids, molluscs and benthic foraminifera) from the top down to 20 m depth in the Middle Miocene Ermenek Platform of Turkey (Janson et al. 2010).

The sandy conglomerate and sandstone deposited in a shoreface setting dominated by a high siliciclastic input derived from the proximal granitic basement source.

Molluscs and clypeasteroids, together with red algae debris predominate among the highly abraded skeletal grains of the shoreface deposits (Nalin & Massari 2009; Brandano et al. 2010). The bioerosion traces on coral colonies, with occurrence of *Gaestrochaenolites* and *Caulostrepsis*, are in agreement with the proposed environments.

Coral bioconstruction 3. The coral bioconstruction 3 (CB3) is characterized by a coral mixstone fabric associated with bioclastic packstone and hybrid sandstones.

The coral mixstone consists of massive, platy and encrusting colonies that are close to each other but mostly not in contact (Fig. 8a) *Porites* represents

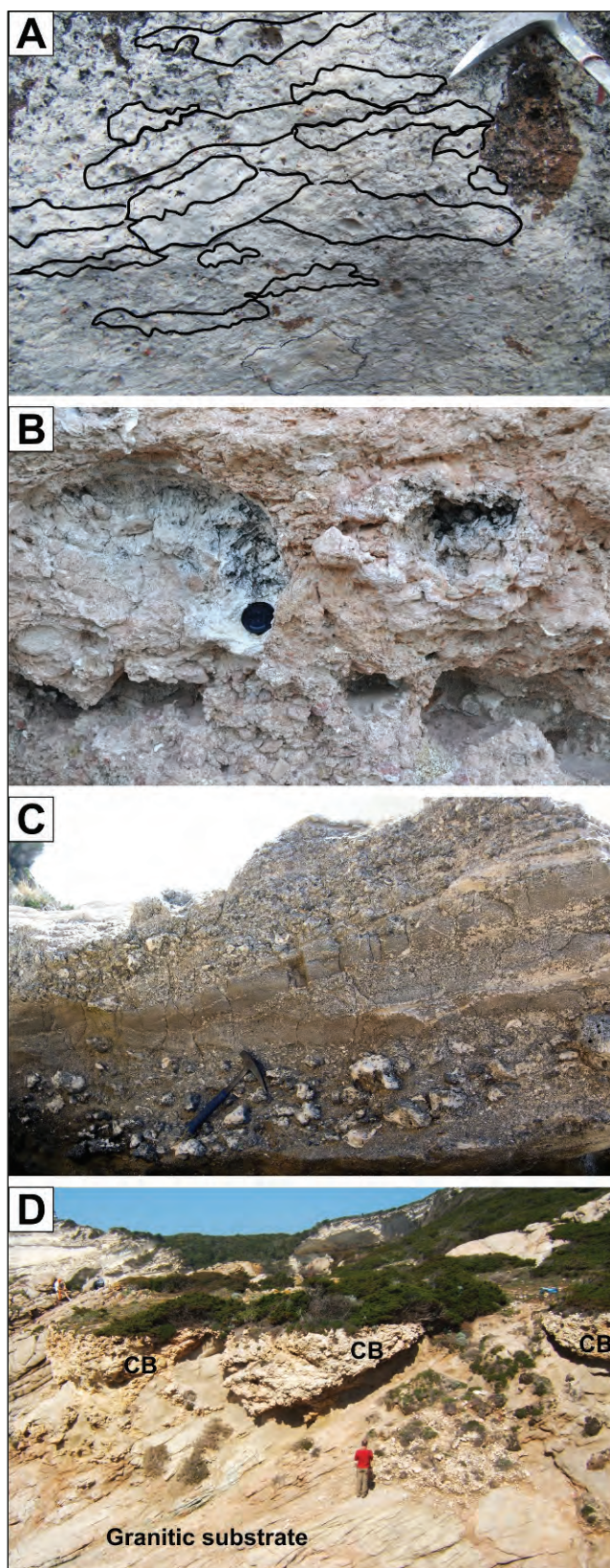
the dominant genus followed by less common faviids. The sediment between the colonies is abundant and consists of a moderately/poorly sorted packstone with abundant red algae (Fig. 5e). Other bioclastic components are bivalves, echinoids and benthic foraminifera (rotaliids, textularids, rare miliolids and *Amphistegina*). Serpulids, bryozoans, balanids, encrusting and planktonic foraminifera complete the assemblage. This bioconstruction shows a lateral extension of about 20 m and a total thickness of 2 m (with beds 30 to 60 cm thick), and interfingers laterally with the skeletal sandstones.

The skeletal sandstones are thinly nodular-bedded with undulate lamination and commonly bioturbated. The bioclastic fraction is represented by the large benthic foraminifera *Heterostegina* and *Operculina*, bivalves, echinoids, corals, gastropods, subordinate small benthic foraminifera and red algae debris.

Interpretation. Corals of the mixstone facies thrived within moderate hydrodynamic conditions of the mesophotic zone, as suggested by the coral morphologies, the inter-coral sediment texture and composition. This bioconstruction, extending more laterally than in height following the siliciclastic substrate, is here interpreted as a coral carpet (*sensu* Riegl & Piller 1999). Modern faviid coral carpets representing a rigid non-uniform mixstone characterize the northern Red Sea (Riegl & Piller 1999, 2000). There, platy, massive and branching corals produce a framework up to 1 m thick at depths from 10 m down to 30-45 m.

In the Bonifacio Basin, these small bioconstructions displayed a patchy distribution within

Fig. 8 - A) Coral Bioconstruction 3: biostromal beds of coral mixstone are 30 to 60 cm thick and achieve a lateral extent of about 20 m; domal, platy and encrusting coral colonies are the main growth forms; hammer for scale. B) Coral Bioconstruction 4: corals and oysters constitute a bioconstruction that develops above a layer of conglomerates. Scattered domal colonies of *Porites* and *Thegioastrea* occur in growth position, within a conglomerate with sub-rounded to sub-angular granitoid pebbles and abraded bioclasts, lens cap for scale (5 cm). C) Lenticular bodies of cross-bedded coral rudstone to floatstone are intercalated within cross-bedded bioclastic floatstone to packstone. Reworked and broken corals are associated with oyster fragments. D) In Cala di Labra outcrop lens-shaped coral bioconstructions colonized the granitic substrate. The coral fabric is represented by a coral domestone with a moderate increase of platy corals in the upper part.



coarse sandy areas represented by the skeletal sandstones. The skeletal sandstones characterized by common bioturbation were deposited in the lower shoreface environment (Nalin et al. 2010). Nummulitids inhabited the loose sandy bottom together with bivalves and clypeasteroids. Present-day *Operculina* and *Heterostegina* live from the shallow-water and high-energy environment to more quiet and deeper habitats, with major abundance between 30 and 40 m (Hohenegger et al. 1999; BouDagher-Fadel 2008).

Coral bioconstruction 4. The fourth type of bioconstruction is strictly associated with a skeletal conglomerate (Fig. 8b).

The skeletal fraction is represented by the abundant disarticulated oyster *Hyotissa hyotis* (Linnaeus, 1758) and by massive corals that are surrounded by disarticulated and intensively bored unidentified oyster shells. *Porites* and faviid (common *Thegioastrea*) colonies occur in growth position usually unbound and dispersed, commonly with *Gastrochaenolites* boring traces. Other bioclasts are represented by bivalves, serpulids, echinoids, less common red algae and small benthic foraminifera. Gastropod fragments also occur mostly as cortoids. The conglomerate consists of sub-angular to sub-rounded granitoid pebbles, mostly ranging in size between 3 and 5 cm and rarely up to 15 cm.

These deposits show an irregular lens-shaped geometry up to 1 m in thickness and about 5 m in length with a convex top and flat base. This bioconstruction lies on a fining upward matrix-supported conglomerate bed, made up of sub-rounded pebbles and cobbles of granitoids and lacking marine skeletal elements.

Interpretation. The CB4 is interpreted as a colonization of massive corals associated with oysters that developed in a high energy environment as suggested by the coral morphologies, the reworked oyster shells and the conglomerate matrix with highly

abraded bioclastic fragments. *Hyotissa* is a marine and estuarine suspension feeder usually cemented to hard subtidal substrata (Zuschin & Piller 1997; Wiedl et al. 2013) and commonly associated with corals. It is strictly stenohaline and also stenotherm (Stenzel 1971). Dense populations of *Hyotissa*, however, may also occur free-living on the substrate or attached to dead and degraded coral colonies (Slack-Smith 1998; Zuschin & Baal 2007) at water depths less of 10 m (e.g. Titschack et al. 2010). The conglomerate with sub-angular to sub-rounded pebbles and cobbles and lacking bioclasts is interpreted as a gravelly shore deposit. A double provenance for pebbles and cobbles could be assumed. They were eroded or collapsed from the near granitic cliffs and deposited by ephemeral streams.

Reworked-coral deposit (RCD). The RCD is represented by a coral rudstone to floatstone, that occurs in lens-shaped bodies intercalated within bioclastic floatstones and coarse packstones.

The coral rudstone to floatstone is characterized by corals that are not in growth position, but only occur as reworked massive colonies and fragments, commonly aligned and occasionally imbricated (Fig. 8c).

In addition to corals, oysters, gastropods (turritellids) and echinoids fragments commonly occur. Larger foraminifera (*Heterostegina*, *Operculina* and *Miogyopsina*), red algae debris and small benthic foraminifera (cibicids, textularids and rare miliolids) complete the biotic assemblage. The siliciclastic fraction is abundant and represented by quartz and feldspars grains and subordinate granitic lithoclasts.

Bioclastic floatstones and coarse packstones are commonly organized in cross-bedded sets (first order) that are 30 to 60 cm thick with bedding-plane discordant laminations and stack in 2 to 3 m thick co-sets (Fig. 8c). Coarse packstones are well to moderately sorted and composed predominantly of red algae debris, small benthic and planktonic foraminifera, bivalves and echinoids fragments (Fig. 5h). Sub-spherical rhodoliths, flat clypeasteroids and deep-burrower echinoids are also present. Floatstones are poorly sorted with an abundant siliciclastic component. Bioclasts are represented by red algae, larger foraminifera such as *Heterostegina* and *Operculina* (Fig. 5g), turritellids, bivalves, bryozoans, coral fragments and small benthic foraminifera (rotaliids, textularids and rare miliolids).

Interpretation. The RCD represents a transported and resedimented deposit as suggested by the presence of reworked and broken coral colonies within lens-shaped bodies that are embedded in a bioclastic facies. This facies is interpreted as bioclastic and calciclastic submarine fan deposits (*sensu* Payros & Pujalte 2008). Coarse-grained bioclastic and calciclastic submarine fan systems are characterized by an abundance of coarse-grained rudstones and the almost complete lack of muddy sediments. In these systems, small radial lobes develop at the base of the slope and are represented by frequently cross-bedded coarse-grained rudstones (Payros & Pujalte 2008). Payros & Pujalte (2008) underlined how the outer portion of heterozoan distally steepened ramps may supply a calciclastic sediment stock close to the slope break. In particular, part of the sediment accumulated between the middle ramp and the slope break can be transported to the slope and involved in sediment gravity flows, thus forming calciclastic sedimentary accumulations at the toe of the slope in the outer ramp. Clearly, sediment transport from the middle ramp to the ramp slope was facilitated during storm periods and downwelling high-energy currents (rip currents), with large amounts of loose bioclastic sediment transported and shed off the ramp to the slope. Paleoenvironmental and paleoclimatic conditions favoring the development of heterozoan skeletal assemblage are of course necessary to promote the development of these bioclastic fans. The bioclastic floatstones and coarse packstones in the Bonifacio Basin result from combined accumulation in the oligophotic zone of in situ-produced red algal debris and material (such as mineral grains, coral fragments and some small benthic foraminifera) swept from shallower environments and transported by wind-driven and storm currents into a depositional slope below the storm wave base level (Hernandez-Molina et al. 2000; Tomassetti & Brandano 2013). According to Tomassetti & Brandano (2013), this depositional slope can be attributed to a coastal prograding wedge system (*sensu* Hernandez-Molina et al. 2000).

DISCUSSION

Basin morphology and coral bioconstructions. A paleogeographic reconstruction of the investigated area during the Aquitanian to Burdigalian

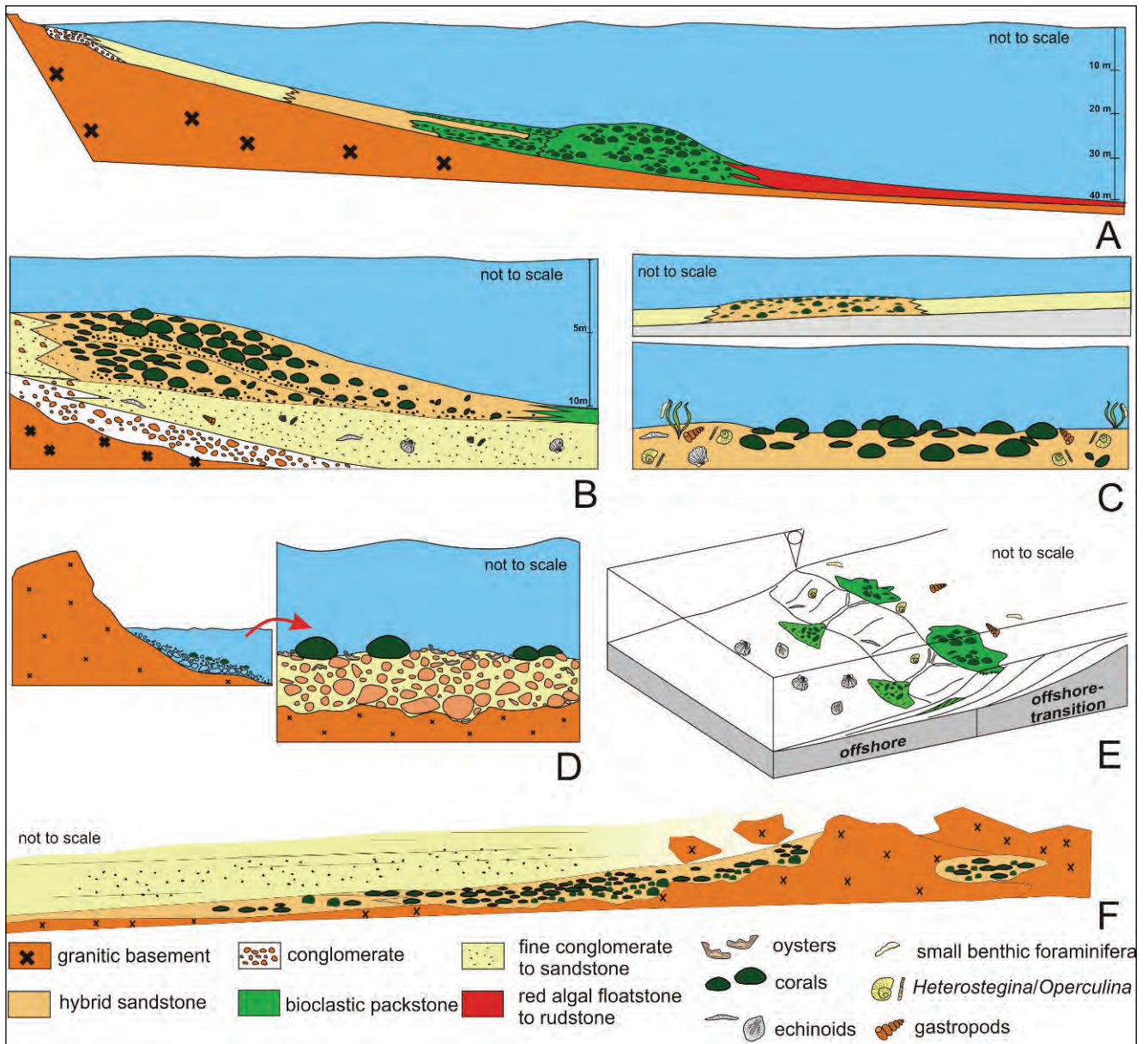


Fig. 9 - The Coral Bioconstruction 1 A) represents buildups of moderate relief that occurred in the deep euphotic zone; the Coral Bioconstruction 2 B) developed in a shallower environment, closer to the granitic basement on coastal conglomerate and was more influenced by the terrigenous input; the Coral Bioconstruction 3 C) consists of thin veneers of coral mixstone representing coral carpets that are patchily distributed within coarse skeletal sands; on the gravelly substrate of a pocket beach delimited by rocky sea cliff developed the Coral bioconstruction 4 D) characterized by sparse coral colonies associated with oysters; the cross-bedded coral rudstone to floatstone E) represents deposits of coarse-grained calciclastic submarine fans at the base of a depositional slope; in the Cala di Labra outcrop F) the coral bioconstruction settled directly on the offshore granitic substrate forming lens (after Tomassetti et al. 2013).

interval has been recently proposed by Reynaud et al. (2013) on the basis of thickness and facies distributions of the two formations: Cala di Labra and Bonifacio Fms. According to this reconstruction, the Bonifacio Basin evolved from an embayment during the Aquitanian and early Burdigalian to a complex strait in the Late Burdigalian. This strait developed between two main islands, Corsica and Sardina, and two basins: the East Corsica Basin and the West Corsica Basin that passed westwards to the

Castel Sardo Basin (Cherchi et al. 2008; Reynaud et al. 2013). The Cala di Labra Fm. embayment was characterised by a gradual increase of water depth to the southwest and limited at southeast by a granitic ridge (Punta Sa Mulari) (Fig. 1b).

The coral bioconstructions of the first type (CB1) are located in the distal portion of the embayment, in particular in the western side of the bay, at Cala Paraguano, and in the southeast of Punta Sa Mulari ridge (Fig. 1b). The coral bioconstructions

of the distal part of the bay include also the coral buildups documented by Tomassetti et al. (2013) at the Cala di Labra locality (Fig. 8 d, 9a).

The CB2 are located at both sides of the proximal portion of the Bonifacio embayment with corals settled on sandy to conglomerate substrate close to the crystalline basement (Fig. 9b). The CB4 developed in the gravelly shoreface of the internal portion of the bay, characterized by granitic cliffs whose collapse likely supplied the gravel for the shoreface (Fig. 9d). The coral carpet CB3 overlies the CB4 and the CB1 in the Cala di Labra outcrop. The CB3 represents the gradual deepening of the shoreface environment following the progressive transgression that characterized the initial stage of the Burdigalian (Tomassetti & Brandano 2013) (Fig. 9c). However, the development of coral carpets is also controlled by bottom topography. As underlined by Riegl & Piller (2000), coral carpets prefer areas with little topographic differentiation. Consequently, in the Bonifacio Basin the CB3 may be considered also to represent the colonization by corals of flat mobile substrates when they developed in the mesophotic zone.

Depositional model. The different coral bioconstructions and coral assemblages of the Bonifacio Basin show a suite of facies associations that reflects their different position in the articulated Bonifacio embayment and consequently their connection with different depositional processes (Fig. 9a-f). However, with the exception of the CB4 that formed in a coarse clastic-dominated near-shore environment, the other bioconstructions (CB1 and 2) show a common depositional architecture that produced a sigmoidal geometry. It is represented in fact by a flat portion with platy and encrusting corals evolving to the core of the bioconstruction (i.e. cluster reef) usually dominated by corals with domal growth-forms, and by a bioclastic-dominated slope with scattered corals followed basinward by rudstone to floatstone rich in free living red algal branches (Fig. 5e, 9a,b).

Bioconstructions similar to CB 1 have been observed also in Northern Sardinia (Capo Testa), where an analogous mixed carbonate-siliciclastic system occurs (Brandano et al. 2010). The sigmoidal profile along the depositional dip direction resulted from the important nearshore siliciclastic supply, probably stabilized by seagrass meadows. The sigmoid front was stabilized by massive corals, limiting

bioclastic sedimentation along the slope and toe of the slope by the oligophotic biota.

On the basis of the bioclastic components, sediment texture and coral growth forms, a bathymetric interval between the storm-wave base (swb) and fair-weather-wave base (fwwb) may be inferred for CB1, with massive corals growing under good light conditions and relatively high hydrodynamic energy. The CB2 differs from CB1 in having increased of coarse terrigenous supply and smaller sigmoids, most likely related to their development in the more proximal and shallow shoreface environment of the Bonifacio embayment.

The coral carpet bioconstruction (CB3) is found only in the Ricetti outcrop and it overlies the CB4 following the middle Burdigalian transgressive phase (Tomassetti & Brandano 2013). Generally, coral carpets preferentially form in areas with low topographic differentiation, and in environments characterized by low sedimentation and accumulation (Riegl & Piller 2000). Considering the stratigraphic position of the CB 3 and its location in the embayment, we suggest that a small relative sea level rise and flat mobile substrates promoted the development of coral carpet bioconstructions.

The RCD form lens-shaped bodies that are embedded in the upper prograding bioclastic unit of Cala di Labra Fm. This unit has been interpreted as an infralittoral prograding wedge characterized by substantial nearshore siliciclastic supply, whereas the carbonate production is usually limited in nearshore environments, but increases with depth in the transition zone and offshore (Tomassetti & Brandano 2013). Infralittoral prograding wedge was introduced by Hernández-Molina et al. (2000) to describe Holocene seaward-prograding sedimentary bodies observed at water depth of 20-30 m in the Mediterranean Sea, and deposited below storm-wave base during stillstand of sea level. Their first outcrop counterparts have been described by Pomar & Tropeano (2001) and by Pomar et al. (2015) and interpreted as representing deposition below storm-wave base of sediment transported basinward by storm-generated currents (downwelling currents). The RCD facies represents the lobe deposits of coarse-grained bioclastic submarine fans (c.f. Payros & Pujalte 2008) occurring at the base of the depositional slope of an infralittoral prograding wedge system (Fig. 9e). Original coral bioconstructions, source of the RCD bioclastic fraction, were

probably present near the offshore-transition and topographic break into the slope (Fig. 9e). These bioconstructions may have been represented by small coral patches with a cluster reef structure (*sensu* Riding 2002). Indeed, the absence of a dense coral framework and early cementation, together with the abundance of matrix (Riding 2002), may have promoted the mobilization of corals and sediment as individual grains by storms or rip currents, which commonly affect the prograding wedge (Hernandez-Molina et al. 2000). These sediments may have been transported downslope by high-density turbidity currents, which can transport coarse sediment (coarse sand to cobble) supported by the fluid turbulence and dispersive pressure resulting from grain collision (Lowe 1982; Tucker 1992). Small bioherms placed at the platform top are recorded also in the coeval prograding flat-topped platform of Sardinia (Benisek et al. 2009).

Carbonate-siliciclastic mixing. In the geological record there are many examples where coral reef deposits are closely associated with siliciclastic sedimentary rocks (Dabrio et al. 1981; Santisteban & Taberner 1988; Braga et al. 1990; Sanders & Baron-Szabo 2005; Silvestri et al. 2011; Morsilli et al. 2012; Novak et al. 2013). In many of these examples the siliciclastic input is represented by the fine fractions of the sediments (clay or silt). Examples with coral bioconstructions also associated with coarse terrigenous sediments are documented only from fan deltas depositional settings (Santisteban & Taberner 1988; Braga et al. 1990; Wilson & Lokier 2002; Karabiyikoglu et al. 2005). In the Bonifacio Basin, the lower Burdigalian siliciclastic deposits of Cala di Labra Fm. are represented by fluvial conglomerates, marine conglomerates and sandstones, whereas hemipelagic marls were deposited later, during the middle to late Burdigalian (Brandano et al. 2009; Reynaud et al. 2013). According to this picture, corals were most likely not affected by high turbidity levels (which results in rapid light attenuation) and by periodic smothering and burial associated with a mobile and fine siliciclastic-dominated sediment substrate (Perry 2005). On the contrary, they thrived under coarse terrigenous input derived mainly by erosional processes along the rocky shoreline and subordinately by ephemeral fluvial systems.

As in many modern coastal examples, we also observed a basinward decrease in terrigenous input associated with a simultaneous increase of

skeletal carbonate production (Mount 1984; James et al. 1992; Halfar et al. 2004). In the nearshore environments of the Bonifacio embayment, the coral colonies (CB4) are dispersed in the conglomerates of the shoreface (c.f Dorsey 1997). In the CB2, the terrigenous fraction is still conspicuous and the bioconstruction developed above fine conglomerates to sandstones with the matrix between corals represented by hybrid sandstone. A decrease of terrigenous input and grain-size is clear in the CB1 that developed in the distal part of the embayment in more open conditions that favoured a skeletal carbonate production dominated by red algae and subordinately by benthic foraminifera and molluscs in the meso and oligophotic zones.

CONCLUSIONS

In this paper we document the occurrence of different coral bioconstructions and coral-rich deposits in the Bonifacio Basin, which was a complex and articulated embayment during the Early Miocene. Sigmoidal cluster reefs (CB1 and CB2), coral carpets (CB3) and skeletal conglomerates rich in corals (CB4) have been recognized.

These coral deposits developed within a mixed carbonate-siliciclastic setting and their depositional architecture and growth fabrics were strongly controlled by coastal morphology, paleotopography and sedimentary processes affecting the different areas of the basin.

In the upper shoreface corals, together with the oyster *Hyotissa*, represent the main component of bioclastic conglomerates alimented by ephemeral streams and erosion of the granitic coastline. Reef-building capacity took place in the lower shoreface, where corals formed small sigmoidal bioconstructions interpreted as cluster reefs. A coral carpet deposited above the CB4 following the middle Burdigalian transgressive phase and colonizing a flat mobile substrate.

The impact of siliciclastic sediments on the coral assemblages clearly reflected their position within the Bonifacio embayment. However, corals were not affected by high turbidity levels as the siliciclastic input resulted mainly from erosional processes affecting the rocky shoreline and subordinately from ephemeral fluvial systems that delivered only coarse sediments.

The suite of coral deposits of the Cala di Labra Fm. also includes the reworked coral deposits of Rocchi Bianchi (RCD), herein interpreted as lobe deposits of coarse-grained bioclastic submarine fans formed at the base of the depositional slope of an infralittoral prograding wedge system.

Acknowledgments. Financial support has been provided by Italian PRIN 2010-11 (M.B and F.B) and by La Sapienza Ateneo project (L.T) and by 'Avvio alla Ricerca' Sapienza Project (A.M). Criticisms and comments by reviewers James Klaus, Michele Morsilli and Editors Fabrizio Berra and Lucia Angiolini are much appreciated.

REFERENCES

- Andreucci S., Pascucci V., Murray A.S. & Clemmensen L.B. (2009) - Late Pleistocene coastal evolution of San Giovanni di Sinis, west Sardinia (Western Mediterranean). *Sediment. Geol.*, 216: 104-116.
- Benisek M.F., Betzler C., Marcano G. & Mutti M. (2009) - Coralline-algal assemblages of a Burdigalian platform slope: Implications for carbonate platform reconstruction (northern Sardinia, western Mediterranean Sea). *Facies*, 55: 375-386.
- Bosellini F.R. (2006) - Biotic changes and their control on Oligocene-Miocene reefs: a case study from the Apulia Platform margin (southern Italy). *Palaeogeogr., Palaeoclimatol., Palaeoecol.*, 241: 393-409.
- Boudagher-Fadel M.K. (2008) - Evolution and geological significance of larger benthic foraminifera. *Dev. Palaeontol. Stratigr.*, 21, 544 pp.
- Braga J.C., Martin J.M. & Alcalá B. (1990) - Coral reefs in coarse-terrigenous sedimentary environments (upper Tortonian, Granada Basin, Southern Spain). *Sediment. Geol.*, 66: 135-150.
- Brandano M., Jadoul F., Lanfranchi A., Tomassetti L., Berra F., Ferrandini M. & Ferrandini J. (2009) - Stratigraphic architecture of mixed carbonate-siliciclastic system in the Bonifacio Basin (Early-Middle Miocene, South Corsica). Excursion Guidebook, 27th IAS Meeting of Sedimentology, Alghero: 299-313.
- Brandano M., Tomassetti L., Bosellini F. & Mazzucchi A. (2010) - Depositional model and paleodepth reconstruction of a coral-rich, mixed siliciclastic-carbonate system: The Burdigalian of Capo Testa (northern Sardinia, Italy). *Facies*, 56: 433-444.
- Carmignani L., Conti P., Cornamusini G. & Meccheri M. (2004) - The Internal Northern Apennines, the Northern Tyrrhenian Sea and the Sardinia-Corsica Block: 59-77. Special Volume of the Italian Geological Society for the IGC Florence (2004).
- Carminati E. & Doglioni C. (2005) - Mediterranean geodynamics. In: Selley R.C., Cocks L.R.M. & Plimer I.R. (Eds) - Encyclopedia of Geology: 135-146, Elsevier Amsterdam.
- Carminati E., Lustrino M., Cuffaro M. & Doglioni C. (2010) - Tectonics, magmatism and geodynamics of Italy: what we know and what we imagine. In: Beltrando M., Peccerillo A., Mattei M., Conticelli S. & Doglioni C. (Eds) - The Geology of Italy: tectonics and Life Along Plate Margins, Electronic Edition. Journal of the Virtual Explorer, v 36 (ISSN 1441-8142, paper 9).
- Carminati E., Lustrino M. & Doglioni C. (2012) - Geodynamic evolution of the central and western Mediterranean: Tectonics vs. igneous petrology constraints. *Tectonophysics*, 579: 173-192.
- Cherchi A., Mancin N., Montadert L., Murru M., Terasa-Putzu M., Schiavinotto F. & Verrubbi V. (2008) - Les conséquences stratigraphiques de l'extension oligo-miocène en Méditerranée occidentale à partir d'observations dans le système de grabens de Sardaigne (Italie). *Bull. Soc. Geol. Fr.*, 3: 267-287.
- Dabrio C.J., Esteban M. & Martin J.M. (1981) - The coral reef of Njar, Messinian (uppermost Miocene), Almería Province, SE Spain. *J. Sedim. Petrol.*, 51: 521-539.
- Dorsey R.J. (1997) - Origin and significance of rhodolith-rich strata in the Punta El Bajo section, southeastern Pliocene Loreto basin. In: Johnson M.E. & Ledesma-Vazquez J. (Eds) - Pliocene Carbonates and Related Facies Flanking the Gulf of California, Baja California, Mexico. *Geol. Soc. America Spec. Paper*, 318: 83-109.
- Durand-Delga M. (1984) - Principaux traits de la Corse Alpine et corrélations avec les Alpes ligures. *Mem. Soc. Geol. It.*, 28: 285-329.
- Esteban M. (1996) - An overview of Miocene reefs from Mediterranean areas: general trends and facies models. In: Franseen E.K., Esteban M., Ward W.C. & Rouchy J.-M. (Eds) - Models for Carbonate Stratigraphy from Miocene Reef Complexes of Mediterranean Regions. *Soc. Econ. Paleontol. Mineral., Concepts Sedimentol. Paleontol.*, 5: 3-54.
- Ferrandini J., Gattacceca J.R.M., Ferrandini M., Deino A. & Janin M.C. (2003) - Chronostratigraphy and paleomagnetism of oligo-miocene deposits of Corsica (France): geodynamic implications for the liguro-provençal basin spreading. *B. Soc. Geol. Fr.*, 174: 357-371.
- Ferrandini M., Galloni F., Babinot J.F. & Margerel J.P. (2002) - La plate-forme burdigalienne de Bonifacio (Corse du Sud): microfaune (foraminifères, ostracodes) et paléoenvironnements. *Rev. micropaleontol.*, 45: 57-68.
- Ferré E.C. & Leake B.E. (2001) - Geodynamic significance of early orogenic high-K crustal and mantle melts: example of the Corsica Batholith. *Lithos*, 59: 47-67.
- Galloni F., Cornee J.J., Rebelle M. & Ferrandini M. (2001) - Sedimentary anatomies of early Miocene coral reefs in South Corsica (France) and South Sardinia. *Géologie Méditerran.*, 28: 73-77.
- Galloni F., Chaix C. & Cornee J.J. (2014) - Architecture and composition of the Upper Burdigalian z-coral build-ups of southern Corsica (Mediterranean). *C. R. Geosci.*, 346: 45-51.
- Halfar J., Ingle J.C. Jr & Godinez-Orta L. (2004) - Modern non-tropical mixed carbonate-siliciclastic sediments and environments of the southwestern Gulf of Califor-

- nia, Mexico. *Sed. Geol.*, 165: 93–115.
- Hernández-Molina F.J., Fernández Salas L.M., Lobo F., Somoza L., Díaz Del Rio, V. & Alveirinho Dias J.M. (2000) - The infralittoral prograding wedge: a new large-scale progradational sedimentary body in shallow marine environments. *Geo-Mar. Lett.*, 20: 109-117.
- Hohenegger J., Yordanova E., Nakano Y. & Tatzreiter F. (1999) - Habitats of larger foraminifera on the reef slope of Sesoko Island, Okinawa, Japan. *Mar. Micropaleontol.*, 36: 109-168.
- Insalaco E. (1998) - The descriptive nomenclature and classification of growth fabrics in fossil scleractinian reefs. *Sediment. Geol.*, 118: 159-186.
- James N.P., Bone Y., van der Borch C.C. & Gostin V.A. (1992) - Modern carbonate and terrigenous clastic sediments on a cool water, high energy, mid-latitude shelf: Lape-dece, southern Australia. *Sedimentology*, 39: 877-903.
- Janson X., Van Buchem F.S.P., Dromart G., Eichenseer H.T., Dellamonica X., Boichard R., Bonnaffe F. & Eberli G. (2010). Architecture and facies differentiation within a Middle Miocene carbonate platform, Ermenek, Mut Basin, southern Turkey. In: Van Buchem F.S.P., Gerdes K.D. & Esteban M. (Eds) - Mesozoic and Cenozoic carbonate systems of the Mediterranean and the Middle East: stratigraphic and diagenetic reference models. *Geol. Soc. London, Spec. Publ.*, 329: 265-290.
- Karabiyikoğlu M., Tuzcu S., Çinerb A., Deynoux M., Örcend S. & Hakyemez A. (2005) - Facies and environmental setting of the Miocene coral reefs in the late-orogenic fill of the Antalya Basin, western Taurides, Turkey: implications for tectonic control and sea-level changes. *Sed. Geol.*, 173 (1-4): 345-371.
- Kroh A. & Nebelsick J.H. (2003) - Echinoid assemblages as a tool for palaeoenvironmental reconstruction - an example from the Early Miocene of Egypt. *Palaeogeogr., Palaeoclimatol., Palaeoecol.*, 201: 157-177.
- Lokier S.W., Wilson M.E.J. & Burton L.M. (2009) - Marine biota response to clastic sediment influx: a quantitative approach. *Palaeogeogr., Palaeoclimatol., Palaeoecol.*, 281: 25-42.
- Lowe D.R. (1982) - Sediment gravity flows: II. Depositional models with special reference to the deposits of high-density turbidity currents. *J. Sed. Petrol.*, 52: 279-297.
- Morsilli M., Bosellini F.R., Pomar L., Hallock P., Aurell M. & Papazzoni C.A. (2012) - Mesophotic coral buildups in a prodelta setting (Late Eocene, southern Pyrenees, Spain): a mixed carbonate-siliciclastic system. *Sedimentology*, 59: 766-794.
- Mount J.F. (1984) - Mixing of siliciclastic and carbonate sediments in shallow shelf environments. *Geology*, 112: 432-435.
- Nalin R. & Massari F. (2009) - Facies and stratigraphic anatomy of temperate carbonate sequence (Capo Colonna Terrace), Late Pleistocene southern Italy. *J. Sedim. Res.*, 69: 210-225.
- Nalin R., Ghinassi M. & Basso D. (2010) - Onset of temperate carbonate sedimentation during transgression in a low-energy siliciclastic embayment (Pliocene of the Val d'Orcia Basin, Tuscany, Italy). *Facies*, 56: 353-368.
- Novak V., Santodomingo N., Rösler A., Di Martino E., Braga J.C., Taylor P.D., Johnson K.G. & Renema W. (2013) - Environmental reconstruction of a late Burdigalian (Miocene) patch reef in deltaic deposits (East Kalimantan, Indonesia). *Palaeogeogr., Palaeoclimatol., Palaeoecol.*, 374: 110-122.
- Payros A. & Pujalte V. (2008) - Calciclastic submarine fans: an integrated overview. *Earth-Sci. Rev.*, 86: 203-246.
- Pedley H.M. (1996) - Miocene reef distributions and their associations in the central Mediterranean region: an overview. In: Franseen E.K., Esteban M., Ward W.C. & Rouchy J.-M. (Eds) - Models for Carbonate Stratigraphy from Miocene Reef Complexes of Mediterranean Regions. *Soc. Econ. Paleontol. Mineral., Concepts Sedimentol. Paleontol.*, 5: 73-87.
- Perrin C. & Bosellini F.R. (2012) - Paleobiogeography of scleractinian reef corals: changing patterns during the Oligocene-Miocene climatic transition in the Mediterranean. *Earth-Sci. Rev.*, 111: 1-24.
- Perry C.T. (2005) - Structure and development of detrital reef deposits in turbid nearshore environments, Inhaca Island, Mozambique. *Mar. Geol.*, 214: 143-161.
- Pomar L. (1991) - Reef geometries, erosion surfaces and high-frequency sea-level changes, Upper Miocene reef complex, Mallorca, Spain. *Sedimentology*, 38: 243-269.
- Pomar L. & Tropeano M. (2001) - The Calcarene di Gravina Formation in Matera (southern Italy): new insights for coarse-grained, large-scale, cross-bedded bodies encased in offshore deposits. *AAPG Bulletin*, 85: 661-690.
- Pomar L., Aurell M., Bádenas B., Morsilli M. & Al-Awwad S.F. (2015) - Depositional model for a prograding oolitic wedge, Upper Jurassic, Iberian basin. *Marine and Petroleum Geology*, 67, pp.556-582.
- Reading H.G. & Collinson J.D. (1996) - Clastic coasts. In: Reading H.G. (Ed.) - *Sedimentary Environments: Processes, Facies and Stratigraphy*: 154-231, Blackwell Science, Oxford.
- Reuter M., Brachert T.C. & Kroeger K.F. (2006) - Shallow-marine carbonates of the tropical-temperate transition zone: effects of hinterland climate and basin physiography (Late Miocene, Crete, Greece). *Geol. Soc. London Spec. Publ.*, 255: 159-180.
- Reuter M., Piller W.E. & Erhart C. (2012) - A Middle Miocene carbonate platform under silici-volcanoclastic sedimentation stress (Leitha Limestone, Styrian Basin, Austria) – Depositional environments, sedimentary evolution and palaeoecology. *Palaeogeogr., Palaeoclimatol., Palaeoecol.*, 350-352: 198-211.
- Reynaud J.Y., Ferrandini M., Ferrandin, J., Santiago M., Thionon I., André J.P., Barthet Y., Guennoc P.O.L. & Tessier B. (2013) - From non-tidal shelf to tide-dominated strait: The Miocene Bonifacio Basin, Southern Corsica. *Sedimentology*, 60: 599-623.
- Riding R. (2002) - Structure and composition of organic reefs and carbonate mud mounds: concepts and categories. *Earth-Sci. Rev.*, 58: 163-231.
- Riegl B. & Piller W. E. (1999) - Coral frameworks revisited-reefs and coral carpets in the northern Red Sea. *Coral*

- Reefs*, 18: 241-253.
- Riegl B. & Piller W.E. (2000) - Reefs and coral carpets in the northern Red Sea as models for organism-environment feedback in coral communities and its reflection in growth fabrics. *Geol. Soc., Lond., Spec. Publ.*, 178: 71-88.
- Sanders D. & Baron-Szabo R.C. (2005) - Scleractinian assemblages under sediment input: their characteristics and relation to the nutrient input concept. *Palaeogeogr., Palaeoclimatol., Palaeoecol.*, 216: 139-181.
- Santisteban C. & Taberner C. (1988) - Sedimentary models of siliciclastic deposits and coral reefs interrelation. In: Doyle L.J. & Roberts H.H. (Eds) - Carbonate-clastic transitions. *Dev. Sedimentol.*, 42: 35-76.
- Silvestri G., Bosellini F.R. & Nebelsick J.H. (2011) - Microtaphofacies analysis of Lower Oligocene turbid-water coral assemblages. *Palaios*, 26: 805-820.
- Slack-Smith S.M. (1998) - Order Ostreoida. In: Beesley P.L., Ross G.J.B. & Wells A. (Eds) - Mollusca: The Southern Synthesis. Fauna of Australia 5A: 268-282. CSIRO Melbourne.
- Stenzel H.B. (1971). Oysters. In: Moore R.C. (Ed) - Treatise on Invertebrate Paleontology, Part N Mollusca 6 (3): 953-1224, Geolog. Soc. America Inc., Colorado.
- Titschack J., Zuschin M., Spötl C. & Baal C. (2010) - The giant oyster *Hyotissa hyotis* from the northern Red Sea as a decadal-scale archive for seasonal environmental fluctuations in coral reef habitats. *Coral Reefs*, 29: 1061-1075.
- Tomassetti L. & Brandano M. (2013) - Sea level changes recorded in mixed siliciclastic-carbonate shallow-water deposits: the Cala di Labra Formation (Burdigalian, Corsica). *Sediment. Geol.*, 294: 58-67.
- Tomassetti L., Bosellini F. & Brandano M. (2013) - Growth and demise of a Burdigalian coral bioconstruction on a granite rocky substrate (Bonifacio Basin, southeastern Corsica). *Facies*, 59: 703-716.
- Tucker M.E. (1992) - Carbonate depositional systems II: deeper-water facies of pelagic and resedimented limestones. In: Tucker M.E. & Wright V.P. (Eds) - Carbonate Sedimentology: 228-283, Oxford.
- Vescogni A., Bosellini F.R., Cipriani A., Gürler G., Ilgar A. & Paganelli E. (2014) - The Dağpazarı carbonate platform (Mut Basin, Southern Turkey): Facies and environmental reconstruction of a coral reef system during the Middle Miocene Climatic Optimum. *Palaeogeogr., Palaeoclimatol., Palaeoecol.*, 410: 213-232.
- Vigorito M., Murru M. & Simone L. (2010) - Carbonate production in rift basins: models for platform inception, growth and dismantling, and for shelf to basin sediment transport, Miocene Sardinia Rift Basin, Italy. In: Mutti M., Piller W.E. & Betzler C. (Eds) - Carbonate systems during the oligocene-miocene climatic transition. *Int. Assoc. Sedim. Spec. Publ.*, 42: 257-282, Oxford.
- Wiedl T., Harzhauser M., Kroh A., Ćorić S. & Piller W.E. (2013) - Ecospace variability along a carbonate platform at the northern boundary of the Miocene reef belt (Upper Langhian, Austria). *Palaeogeogr., Palaeoclimatol., Palaeoecol.*, 370: 232-246.
- Wilson M.E.J. (2012) - Equatorial carbonates: an earth systems approach. *Sedimentology*, 59: 1-31.
- Wilson M.E.J. & Lokier S.W. (2002) - Siliciclastic and volcanoclastic influences on equatorial carbonates: insights from the Neogene of Indonesia. *Sedimentology*, 49: 583-601.
- Zuschin M. & Piller W.E. (1997) - Bivalve distribution on coral carpets in the northern bay of Safaga (Red Sea, Egypt) and its relation to environmental parameters. *Facies*, 37: 183-194.
- Zuschin M. & Baal C. (2007) - Large gryphaeid oysters as habitats for numerous sclerobionts: a case study from the northern Red Sea. *Facies*, 53: 319-327.

BULLDOZING AND RESTING TRACES OF FRESHWATER MUSSEL *ANODONTA WOODIANA* AND SUBSTRATE CHARACTERISTICS IN LAKE-MARGIN AND RIVER SETTINGS OF UMBRIA, ITALY

PAOLO MONACO^{1*}, FEDERICO FAMIANI² & FABIO LA IACONA³

¹Dipartimento di Fisica e Geologia, via Pascoli snc, 06123 Perugia, Italy. E-mail: paolo.monaco@unipg.it. *Corresponding author.

²School of Advanced Studies-Geology Division, University of Camerino, Via Gentile III da Varano, I-62032 Camerino, Italy. E-mail: federico.famiani@unicam.it

³Via Masaniello 50, 93016 Riesi, Caltanissetta, Italy. E-mail: laiaconaf@gmail.com

To cite this article: Monaco P, Famiani F. & La Iacona F. (2016) - Bulldozing and resting traces of freshwater mussel *Anodonta woodiana* and substrate characteristics in lake-margin and river settings of Umbria, Italy. *Riv. It. Paleont. Strat.*, 122(1): 53-62.

Key words: Ichnology, freshwater, *Anodonta* mussel, substrate, Umbria, Italy.

Abstract. The neoichnology of the freshwater mussel *Anodonta* (*Sinanodonta*) *woodiana* (Lea, 1834) is examined herein in some continental environments of Umbria (central Italy), such as lake-margin and river dam-margin settings. This study, based on analysis of about 200 traces, reveals that this mussel burrows employing two types of behaviours: bulldozing which produces horizontal meanders to straight bilobate traces, often filled with peloidal faecal pellets (pseudofaeces and backfill), and resting (vertical stationary into substrate) while filter feeding. A new type of very soft substrate, the 'cloudground' is proposed. It is placed at the water-sediment interface, above the soupground. After four years of observation, the cloudground was buried with shells and traces, preserving through the fossilization barrier about 20% of the *Anodonta* traces. This bivalve activity is a useful tool to recognize preservation of mud in quiet environments and parallels ichnological evidence of unknown epichnial trace fossils in the continental realm. Cloudground with resting traces must be investigated also in modern marine basin floor environments where cloud of mud dominates and considered also in geological record.

INTRODUCTION

Some substrate characteristics, such as firmness and water content, may influence the formation of traces (modern and fossils) and their preservation is fundamental to trespass the fossilization barrier in many types of marine and freshwater environments (Bromley 1990, 1996; Ekdale 1985; Goldring 1995; Hasiotis 2002; La Croix et al. 2015; Melchor et al. 2012; Miller 2007; Monaco 2002; Seilacher 1964, 1982). Among burrowing bivalves, mussels and clams can represent a very important category of burrowers in different types of marine, transitional and freshwater substrates (Bromley 1996; Frey & Seilacher 1980; Frey & Pemberton 1985; Ekdale 1985; Goldring 1995; Ekdale & Bromley 2001; Gingras et al. 2001; Buatois & Mángano 2011; Melchor et al. 2012; Scott et al. 2012; Gosling 2015; Knaust 2015). The most known are endobenthic siphon-bearing bivalves such as tellinids and nuculids, some of which include tracemakers of the recently named ichnofamily Siphonichnidae (*Siphonichnus* spp.), which includes equilibrichnia

with a predominantly deposit-feeding behaviour (Dashtgard & Gingras 2012; Zonneveld & Gingras 2013; Knaust 2015). Less known are studies in the freshwater substrates, such as lake margin settings (Buatois & Mángano 2007; Scott et al. 2012) or fluvial environments (Buatois & Mángano 2007; Melchor et al. 2012). Different ethologic behaviours, e.g. pascichnia, fodinichnia and repichnia, are preserved in different types of grounds, usually softground, hardground or woodground (Clarke 1981; Crampton 1990; Evans 1999; Hasiotis 2002; Monaco et al. 2011; Buatois & Mángano 2011; Melchor et al. 2012; Knaust & Bromley 2012; Scott et al. 2012; Seilacher 1990; Stárková et al. 2015). La Croix et al. (2015) indicate that there is a marked diminution in the sizes of traces and a corresponding decrease in their distribution (reduced abundance of burrowed versus unburrowed beds) with decreasing salinity. The salinity influence has been discussed also in Buatois & Mángano (2011). The soupground and soupground/softground boundary, in contrast to the case of soft-firm-hard and wood substrates, has been poorly exploited in the littoral zone of the freshwater realm (Hasiotis 2002; Buatois & Mángano 2011; Melchor et al. 2012; Scott et al. 2012).

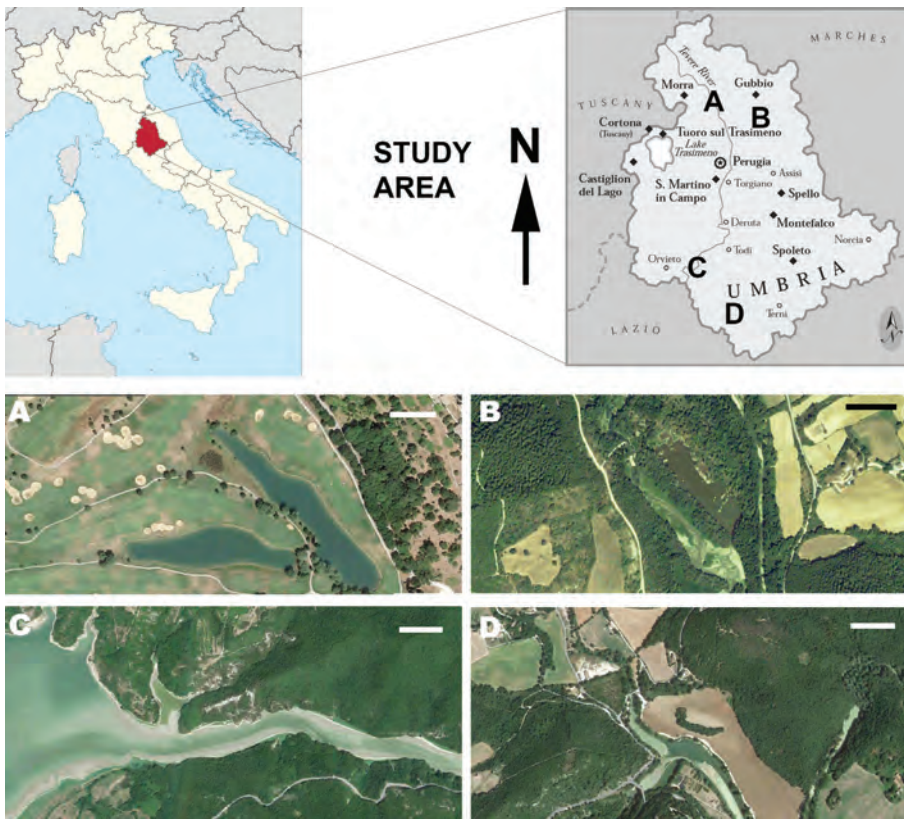


Fig. 1 - Study area with localization of *Anodonta* sites. A) Antognolla lakes. B) Chiascio river. C) Corbara dam - Tevere river; D) Rio Grande - Amelia dam. Umbria map is redrawn from IGM map 1:100.000. Bar = 500 m.

Anodonta is a genus of freshwater mussels in the family Unionidae, the river mussels, and can be found in many freshwater environments as lakes, rivers and continental ephemeral ponds but little is known about their burrowing activity (Taylor 1981). In North America, since the important studies of the great American conchologist Isaac Lea (1792-1886), many species have been described (Clarke 1981; Taylor 1981; Yen 1947), indicating that further phylogenetic analysis of the Anodontinae is required including both North American and Eurasian species (Douda et al. 2011). Since the time of Lea there has been much confusion regarding the taxonomic status of this and other *Anodonta* of western North America (Williams et al. 1993).

The aim of this paper is to show how the freshwater mussel of the species *Anodonta woodiana* can produce burrows in littoral lakes and river margins of Umbria (central Italy), reaching a few centimeters in thickness over softground, producing locomotion and resting traces.

STUDY AREA AND METHODS

In recent decades several species of freshwater mussels have a remarkable expansion, representing some of the most invasive species; they have considerably altered ecosystems worldwide (Kiss

1992; Paunovic et al. 2006; Douda et al. 2011). One of the most invasive aquatic species is the Chinese pond mussel *Anodonta (Sinanodonta) woodiana* (Lea 1834; Kiss 1992). *A. woodiana* is a species of East Asian unionid mussel that has a mandatory parasitic stage (*glochidium*) which encysts on fish. The high incidence of *A. woodiana* is due to introduction of allochthonous species of fishes at different sites in Europe (Kiss 1992; Douda et al. 2011). Their high invasion potential has been partially attributed to their free-living larvae, which have a high dispersal capability. The first documentation of *A. woodiana* in Italy was made in 1996 (Cianfanelli et al. 2007). The beginning of colonization in Umbria is not documented but in recent years a colonization by allochthonous aquatic species has increased among plants, vertebrates and invertebrates. *A. woodiana* is dispersed along lowland rivers, associated wetlands and manmade canals. Heavily modified and artificial aquatic habitats, with high silting rates, are especially suitable for population by *A. woodiana*. A mass occurrence of the Chinese pond mussel was observed among these habitats, particularly where bottom substrates were characterized by the domination of silt-clay where traces are preserved at the soupy/softground boundary.

A. woodiana lives almost entirely in mud and fine sand in lentic or weakly flowing waters (rivers, channels), filter feeding on suspended phytoplankton by filtering water through the oral siphon, which protrudes outside the shell in the back. Has a higher resistance to pollution than the native species, making it able to live in heavily populated areas.

The study sites are: A) the dam of Amelia, B) dams on the Tiber River (Valfabbrica and Corbara) and C) the Antognolla artificial lakes (two wide manmade basins in a golf course) (Fig. 1). The widespread distribution of *Anodonta* gives us reason to analyse the different sites where it was found or documented its presence.

A) Dam of Amelia. The basin of the Rio Grande is located northwest of Amelia. The reservoir 'Lago Vecchio' is an artificial lake with the Great Dam Bridge made at the bottleneck between Mount Cimino and the Colle of Amelia. The basin was used in the past for

the operation of mills downstream from the dam. Today the Lake is used for tourist and recreational purposes, though it has undergone considerable silting. The fill consists of silty/clay that has bridged a large part of the reservoir. During the summer of 2012, the severe drought almost completely dried up the basin and revealed a significant population of *A. woodiana*. Most of the specimens were in life position.

B) Dams on the Tiber River (Valfabbrica and Corbara). Northwest of Valfabbrica, a dam of reservoir is under construction. The basin, of considerable size (up 5 km long), is sited where outcrops sandy to marly rocks belonging to the Marnoso-arenacea Formation, crumble easily, producing mostly clay-rich sediments. A rather significant population of *A. woodiana* was observed in deposits that have accumulated in the submerged area. The Corbara dam (a very large dam basin of the Tiber River valley up to 15 km long during rainy periods) was built on various deep-water carbonate Mesozoic to Cainozoic sediments of the Umbro-Marchean succession to generate electricity in the 1960s. Abundant *Anodonta* has been observed along sides of lake and in the seasonal variations of the water level. The alteration of the equilibrium profile of the Tiber River and the abundant supply of terrigenous material due to the frequent floods of recent years has led to a significant accumulation of deposit in the upper part of the basin. It varies from pebbles, sand and silt to clay that accumulated during the rainy periods and emerged periodically, highlighting a considerable population of *A. woodiana* (hundreds of specimens in the freshwater margins). There are numerous examples disarticulated by heron predation (Fig. 2A). Most of the specimens are in life position of (Fig. 3A, B, C).

C) Two lakes in the Golf course of Antognolla (Fig. 2A-F, 3D) are located close to Pierantonio close to Umbertide, where artificially produced excavations were made at the beginning of 1990 to produce the Golf Course; these lakes are now populated by hundreds of *A. woodiana* that feed along every sides of two lakes together with tens of carp (up one meter long) and many other invertebrates (annelids, snails and small crustaceans). Methods of analysis consist of observation and measurement of size, depth and taphonomy of traces and shells that show results summarized in Fig. 4. Traces of *Anodonta woodiana* mussels, distributed along the banks of rivers and lakes, are analysed focusing on the soupy/soft boundary; the main tool to analyze the differences in the consistency of silt-clay deposits is a manual penetrometer or a telescopic ball boy for golf balls (Fig. 2D), measuring the time of settling the cloud of mud in suspension. Variables are the quiet condition of water during seasons and the distance of traces from the coast. Consistency has been evaluated up to one meter in water depth during spring, summer and autumn over a period of four consecutively years (2012 to 2015) and during water level rise. About 200 traces of *A. woodiana* are considered in this study.

ANODONTA LIFE HISTORY

Anodonta (with several species largely studied in the USA and Canada) occur in lakes, slow rivers (Taylor 1981) and some reservoirs (Nedeau et al. 2009) in mud or sand substrates (Clarke 1981) and are typically found at low elevations (Frest & Johannes 1995). The distribution of freshwater mussels within a water body is probably dependent on the size and geology of the water body and on the distribution of host fish during the mussel's repro-

ductive period (Watters 1992). *Anodonta* is a relatively sedentary filter feeder that consumes plankton and other particulate matter (e.g. organic material and polluting particles) that is suspended in the cloudy water column. As they feed, they filter large quantities of particulate matter and excrete those particles as 'pseudofaeces', which can be an important, nutrient-rich food source for benthic macro- and microinvertebrates (reviewed by Vaughn et al. 2008). In general, species of *Anodonta* grow quickly, reach sexual maturity in four to five years, and have a maximum life span probably of about 15 years (Dudgeon & Morton 1983; Heard 1975). Like other freshwater mussels, they rely on host fishes and other organisms to reproduce and disperse (Lefevre & Curtis 1910; Kiss 1992; Cianfanelli et al. 2007; Douda et al. 2011). Because freshwater mussels are usually unable to move far on their own, their association with fish allows them to colonize new areas, or repopulate areas from which mussels have been extirpated (Paunovic et al. 2006; Douda et al. 2011). Fertilization occurs when female mussels inhale sperm through their incurrent siphon during the appropriate reproductive period (Lefevre & Curtis 1910). Eggs incubate and hatch into larvae, or glochidia, which are released into the water, either individually or in packets (called conglutinates). Glochidia attach to fish, heron legs and encyst in host fish tissues from 2 to 36 hours after they attach. Once metamorphosed, juvenile mussels drop from their host fishes to the substrate (McMahon & Bogan 2001).

RESULTS

Substrate characteristics and burrows of *Anodonta woodiana*.

A) *Substrate characteristics*. Before feeding, *Anodonta woodiana*, moves through shallow substrates producing different traces (Fig. 2A-F). In previous literature the soupground represents the least cohesive category of ground (Bromley 1996; Ekdale 1985; Goldring 1995, among others). As indicated by Bromley (1996) "the aquatic soupground has fluid consistency; the grains are hardly in contact or are separated by mucoid substances, and animal may 'swim' through the substrate. Nevertheless, mucus- and other organic-walled tubes may be constructed by sedentary endobenthos" (Bromley 1996, p. 17). The upper part of the soupground is poorly

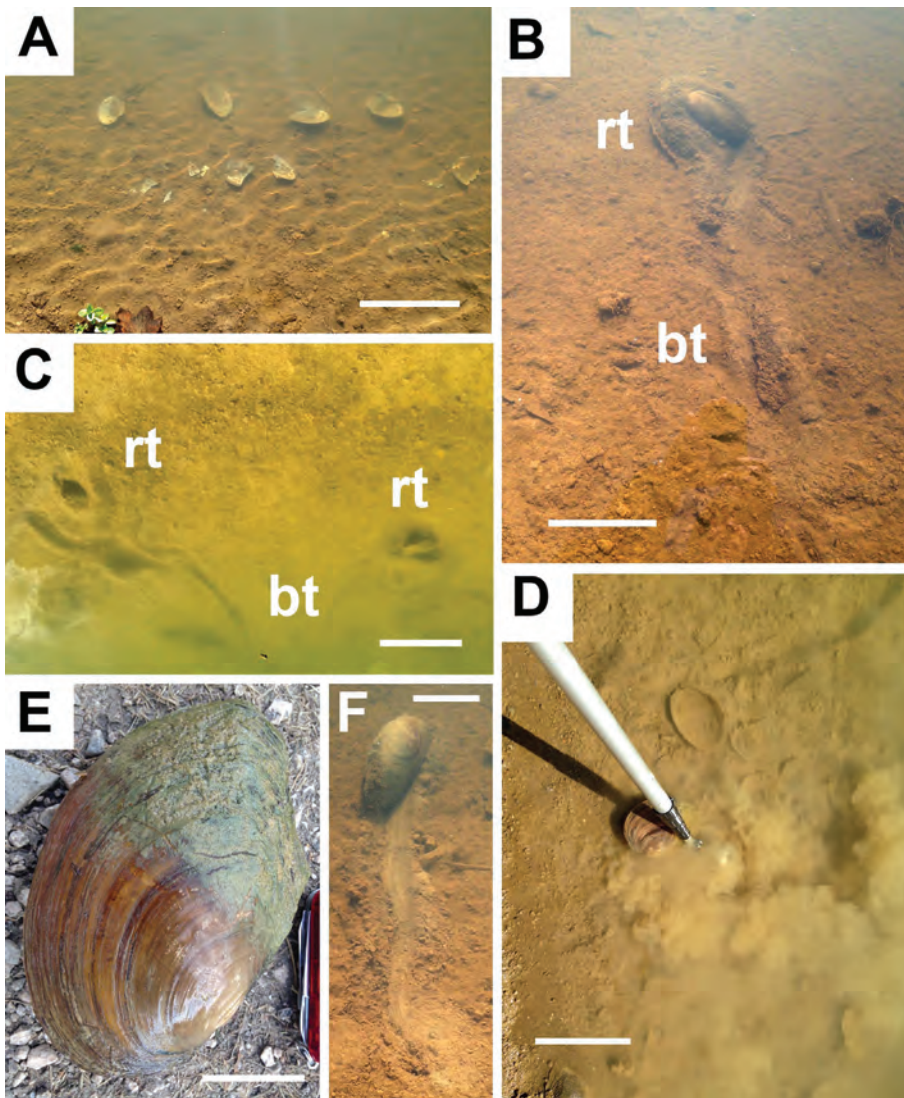


Fig. 2 - Burrows of *Anodonta* (*Sinanodonta*) *woodiana* (Lea, 1834) in Antognolla Golf course marginal lakes. A) Detached shells after the heron feeding activity (late summer), bar = 50 cm. B-C) Bulldozing trace (bt) and resting trace (rt) of *Anodonta woodiana*, bar = 20 cm. D) Cloudground disturbed by a telescopic ball boy for golf balls, depth 40 cm, bar = 25 cm. E) *Anodonta woodiana* complete shell (live specimen) with mud in resting trace, bar = 5 cm. F) Horizontal movement towards deepest part of lake, bar = 15 cm.

exploited by researchers because not preserved in the geological record (Lobza & Schieber 1999), although this substrate is the rule in modern aquatic realms (e.g. in continental lacustrine deposits, Hasiotis 2002; Buatois & Mángano 2011; Scott et al. 2012, or in abyssal basin plain, Rona 2004; Rona et al. 2003; see cloud of mud in the film ‘Volcanoes of the Deep Sea’). Usually, in polluted marginal lakes and dams of Umbria the mere touch of the upper part of a soupground creates a wide cloud of mud that suspended for long time (up two hours) in water (Fig. 2D). Single particles of clay/silt dispersed in the water remain for long time in suspension due to the presence in the water of many pollution particles. Polluting particles, probably formed by nitrates or sulfates (dispersed in the waters by human activity) or other fats pollutants, tend to produce a proliferation of algal mucilaginous film that adhere to the particles of sediment causing them to remain in suspension for a long time, much greater than

a sediment in unpolluted waters. Another type of clay/silt dispersion above the bottom are benthic nepheloid layers (BNL, Cindy Pilskaln, personal communication, 2010). Benthic nepheloid layers are permanent clays particle (2-5 μm) that form re-suspension of mud, in which their behaviour is different close the sediment-water interface in marine (and freshwater) realm and more complicate due the presence of salinity-induced currents and energetic flows (Cindy Pilskaln, personal communication, 2010). Due to this characteristic this upper, up to 2 cm thick level, can be considered as a new type of substrate which is named here as ‘cloudground’. Cloudground, if disturbed, produces a cloud of clay that can fluctuate within the water for a very long time, much greater than a soupground. Softground (mud or silty mud) and looseground (sand and gravels) conversely, include thixotropic sediment and soft dilatant sediments; Seilacher (2007) said: “the initial establishment of a permanent

burrow in softground requires some wall-support mechanisms either through compression alone or together with mucus impregnation". Excavation and backfill burrowing techniques become practicable in looseground and towards the firmer end of the softground range (Bromley 1996, p. 17).

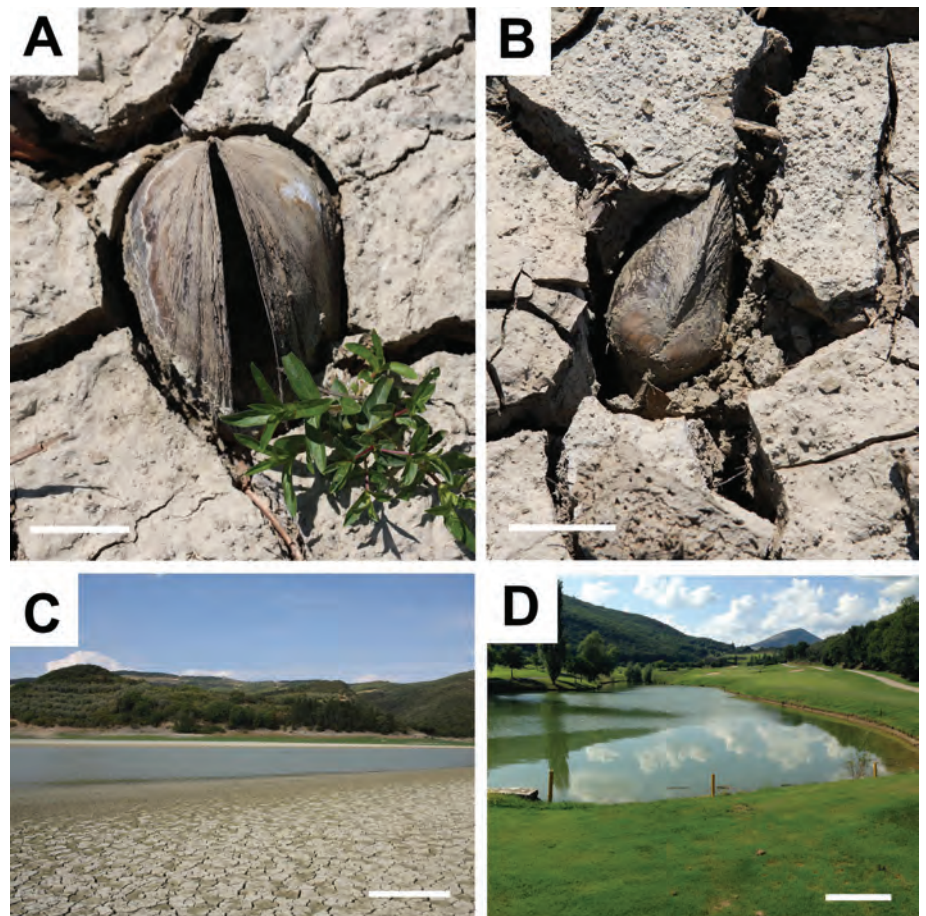
B) Anodonta (Sinanodonta) woodiana burrowing. In littoral grounds of lakes and rivers of Umbria, hundreds of *Anodonta* burrows reveal two different behaviours and traces of this mussel: the first consists of 'bulldozing' activity (Seilacher 2007, pp. 75 and 80); this occurs in the cloudground and soupground, where the mussel not only rolls over the ground, but forcefully accumulates quantities of green-yellow mud in front distributing laterally, producing two ridges separated by a central furrow (bt = bulldozing traces in Figs. 2B, C). This vagile locomotion produces unidirectional, meandering to straight traces, 4 to 8 cm wide and up to 250 cm long, with frequent loops and an irregular shape. The movement of the mussels using their foot is so slow as not to disturb the cloudground (if not in small part). Usually, each of outer marginal ridges are elevated, up to 3 cm high respect to central fur-

row (Fig. 2B, C). The base of the central furrow reaches the upper part of underlying softground and often is filled by pseudofaeces (see Fig. 2F). Locally, the central furrow appears more brown and with some backfill structures. The resting traces (rt = resting trace in Fig. 2B, C), conversely, are oval, round to elongate and are present when the mussel slips through the mud, reaching the softground (anchored to firmground) and placing their shell vertically or obliquely (see the grey half of the mud-filled test in Figs 2E, 3A-B), opening their valves in order to filter food. Abandoned resting traces leave circular structures at the end of the traces of movement, up to 20 cm wide (Fig. 2C).

CONSIDERATIONS

Some taphonomic characteristics, such as trail shape, ground type, ethology, articulated or disarticulated shells, destroyers of traces and their preservation are showed in Fig. 4. Other elements can be detected by observation of behaviours of *A. woodiana* in Umbrian dams and lakes.

Fig. 3 - A-B) Two in situ specimens of *Anodonta (Sinanodonta) woodiana* (open and attached valves) buried within the desiccated bank mud, Corbara Dam, bar = 5 cm. C) The Corbara dam during falling water (summer), bar = 1 m. D) Lake of Antognolla Golf course, bar = 1 m.



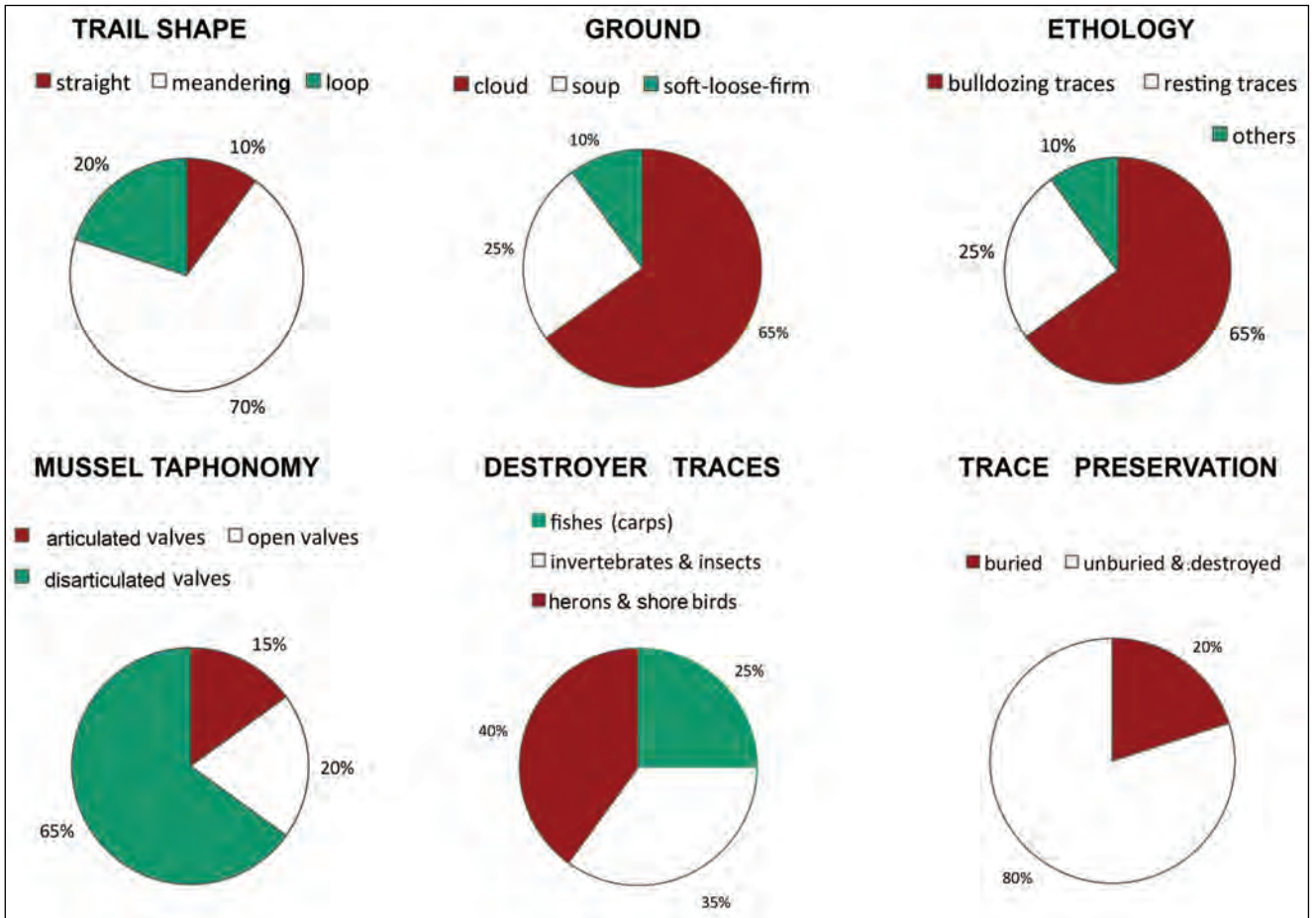


Fig. 4 - Taphonomic features of 200 traces of *Anodonta (Sinanodonta) woodiana* and substrate characteristics from Umbria dams, rivers and lakes.

a) *Continental ichnofacies and substrate characteristics.* The vertical organization of the substrate and their cohesiveness are fundamental to preserve traces of organisms (Ekdale 1985) in different ichnofacies (Hasiotis 2002; Buatois & Mángano 2011). In submerged continental sediments of the geological record bioturbation usually took place mainly in water-saturated sediments close below the water-sediment interface, in soft to firmer levels below, in which discrete trace fossils can be preserved as cubichnia and repichnia among many others (Ekdale et al. 1984; Uchman et al. 2013; Wetzel 2010; Buatois & Mángano 2011). In lacustrine deposits different types of structures can be observed, such as clastic dikes, ball and pillows, water escape structures, deformation by growth of carbonate and silica minerals and pervasive to surficial bioturbation (Buatois & Mángano 2011; Stárková et al. 2015). Many other structures are known in river environments and sub-environments (Buatois & Mángano 2011; Melchor et al. 2012). Continental ichnofacies thus are largely exploited and traces are largely differen-

tiated (see among others Bromley 1996; Hasiotis 2002; Melchor et al. 2012; Miller 2007; Buatois & Mángano 2011; Scott et al. 2012). *Scoyenia*, *Mermia*, *Coprinisphaera* and continental *Skolithos* ichnofacies are the main known ichnofacies and occur with hundreds of ichnotaxa (Hasiotis 2002; Zonneveld et al. 2006; Buatois & Mángano 2011; Melchor et al. 2012; Scott et al. 2012).

Exploiting the fluvio-lacustrine substrates of Umbria we can demonstrate that is not true that freshwater *Anodonta woodiana* burrowed only in soft/firmgrounds, contrary to the current consensus among ichnologists (e.g. Buatois & Mángano 2011; Stárková et al. 2015), but can also originate (100%) in polluted cloudground and upper part of soupground.

b) *Fossilization barrier.* Usually, geologists and ichnologists make little use of information derived from modern environments in their analysis of biogenic structure because biological information cannot be applied directly to trace fossils and the geological record of bioturbation (Bromley 1996,

chapter 6). A barrier separates the two realms, modern and fossil respectively, that Seilacher (1967) called 'the fossilization barrier' or 'modern to fossil transition'. This concept is valid not only for body fossils but also for trace fossils (see more explanation and examples of ichnological fossilization in Bromley 1996; Buatois & Mángano 2011). Neoichnological study of *Anodonta woodiana* in Umbria can help to understand how modern traces can cross the fossilization barrier; in fact, only 20% of the bulldozing/resting traces of *A. woodiana* are completely covered after four years by soft mud, with a sedimentation rate of 2 cm every year. The destruction of the other 80% of tracks is due to the very rapid escape of carp, or caused by rapid movement or feeding by the fishes, which produce *Undichna* or *Piscichnus* of the *Mermia* ichnofacies (Buatois & Mángano 2011; Scott et al. 2012). In Umbria the disturbance is due to large carp (often longer than 1 m), which remove the surface of the very soft mud. The traces preserved in the littoral zone from the destructive action by organisms such as fishes, herons, annelids, aquatic and semi-aquatic insects (dipterans, coleopterans), crustaceans and molluscs show crossing and a slight flattening (Bromley 1996; Dashtgard & Gingras 2012). When the water levels of lakes and rivers rise (the falling produces a subaerial exposure that can form polygonal desiccation cracks with destruction of traces, see Fig. 3A-B), they can be buried by sediment and cemented, crossing the fossilization barrier (Hasiotis 2002; Buatois & Mángano 2011; Melchor et al. 2012; Scott et al. 2012).

c) *Mass mortality and burial.* Hundreds of *Anodonta* are killed every year by herons and other shorebirds (Fig. 2A); their dead shells are found mostly disarticulated with valves scattered (Fig. 2A) or still attached but distant from their traces. A year later with rising water all open shells are covered with 2 cm of mud, and in four years are totally buried by mud or colonized by green algae.

d) *Potential for preservation in fossil record.* It is very difficult to calculate accurately the preservation potential of traces and shells of *Anodonta woodiana*; however, from observations made after four years, we have seen that the greatest potential for preservation occurs in buried traces far from shore, while those closer to the banks and shoreline tend to be fragmented or destroyed by birds and waves. It is estimated that a small percentage, about 20% of

the deepest traces are buried by mud and thus preserved. We must also consider changes in the water levels of all areas due to rainy periods and seasonal waves affecting the preservation of traces (Hasiotis 2002; Buatois & Mángano 2011; Scott et al. 2012).

In many studies of the geological record, it seems that the food for bioturbating organisms was concentrated near the water-sediment interface (mixed tier, see Bromley & Ekdale 1986; Svrda 2007; Scott et al. 2012; Uchman 2007) or distributed in the water column; therefore, few organisms exploit the deeper, more cohesive sediments in which preservation of discrete trace fossils would be possible (Buatois & Mángano 2011; Monaco et al. 2012; Uchman et al. 2013, among others). This issue has produced a number of misleading models that must be revised taking into account new neoichnologic observations about cloudground-soupground horizons for repichnia, cubichnia, pasichnia and foodinichnia. Therefore, this question remains open for paleoichnologists and only fresh neoichnologic studies, as the case of *Anodonta woodiana*, can be utilized to provide new data on the preservation of burrows in the substrate according to environmental characteristics.

FINAL REMARKS

The analysis of about 200 traces of *Anodonta woodiana* in reservoirs and lake margins in Umbria (central Italy) show a diffuse activity of this mussel in the very soft substrate (see diffusion trend in Wetzel 2008). The new category of this substrate, the cloudground, is proposed herein; it develops when pollution is very high and moved particles of mud/silt that remain in suspension for a long period time over the trace due to the presence of pollutant fats surrounding the particle of clay/silt. These chemical and biological conditions of polluted fresh water induce the bloom of foreign pioneer and invasive species such as *Anodonta woodiana*. Cloudground can be preserved above the soupground and colonized. Remains unexplored if it can be recovered also in the geological record, crossing the fossilization barrier and be compacted. The activity of *Anodonta woodiana* consists of two traces, the first due to the meandering to straight locomotion producing bulldozing structures of the mud (bulldozing redistribution with two ridges and a central fur-

row filled with pseudofaeces and backfill), and the second due to burial when the mussels place their shell vertically with open valves to filter nutrients in suspension (oval to round resting traces). The first resembles bulldozing trace fossil (e.g. *Nereites missouriensis* or sand dollar echinoids) preserved as epichnia in shallow or deep water marine deposits (other traces of infaunal bivalves are not considered here, because far from the aim of this work), while the second, resting traces or cubichnia (Buatois & Mángano 2011), can be compared to some resting trace fossils (e.g. *Lockeia* or *Cardioichnus*, among others, see Seilacher 2007).

Anodonta woodiana is subject to periods of mass mortality that are testified by a sudden increase of dead concave-upwards specimens and coquinas pavements of disarticulated shells on the lake-river floors; mass mortality is balanced by rapid repopulation in short periods (months?) with larvae attached to legs of herons and encysted to fishes in each lake and river of Umbria. Mass mortality occurs also in underwater conditions whose reasons require further analysis over a long period of time. This little-studied mussel provides new useful information about the behaviour of invasive populations of freshwater mussels and the substrate characteristics.

Acknowledgements. We thank to two reviewers (A. Baucon and an anonymous reviewer) and the associate Editor F. Feletti to improve the manuscript. Thanks to Gabriele Bigini, Monica Alunni Bernardini, Linda Berardi and Gaia Giuliacci for providing access for sampling and measurement of the cohesiveness of the substrate and sampling *Anodonta (Sinanodonta) woodiana* specimens in lakes of the Antognolla Golf course (Pierantonio, Umbertide). Funds Ric. Var. (2013-2014), University of Perugia, Physics and Geology Department (P. Monaco).

REFERENCES

- Bromley A. & Ekdale A.A. (1986) - Composite ichnofabrics and tiering of burrows. *Geol. Mag.*, 123(1): 59-65.
- Bromley R.G. (1990) - Trace fossils, biology and taphonomy. Special topics in paleontology. Unwin Hyman Ltd, London, 280 pp.
- Bromley R.G. (1996) - Trace fossils. Biology, taphonomy and application. Chapman & Hall, London, 361 pp.
- Buatois L., Mángano M.G. (2011) - Ichnology. Organism-Substrate Interactions in Space and Time. Cambridge University Press, Cambridge, 358 pp.
- Cianfanelli S., Lori E. & Bodon M. (2007) - Non-indigenous freshwater molluscs and their distribution in Italy. In: Gherardi F. (Ed.) - Biological invaders in inland waters: profile, distributions and threats: 103-123. Elsevier, Amsterdam.
- Clarke A.H. (1981) - The Freshwater Molluscs of Canada. *National Museum of Natural Sciences, National Museums of Canada, Ottawa*, 446 pp.
- Crampton J.S. (1990) - A new species of Late Cretaceous wood-boring bivalve from New Zealand. *Palaeontology*, 33(4): 981-992.
- Dashtgard S.E. & Gingras M.K. (2012) - Marine Invertebrate Neoichnology. In: D. Knaust & A. Bromley (Eds) - Trace Fossils as indicators of sedimentary environments: 273-295. Elsevier, Developments in Sedimentology.
- Douda K., Vrilek M., Slavik O. & Reichard M. (2011) - The role of host specificity in explaining the invasion success of the freshwater mussel *Anodonta woodiana* in Europe. *Biological Invasions*: 14, 127-137.
- Dudgeon D. & Morton B. (1983) - The population dynamics and sexual strategy of *Anodonta woodiana* (Bivalvia: Unionacea) in Plover Cove Reservoir, Hong Kong. *J. Zool. (London)*, 201(2): 161-183.
- Ekdale A.A. (1985) - Paleocology of the marine endobenthos. *Palaeogeogr., Palaeoclimatol., Palaeoecol.*, 50: 63-81.
- Ekdale A.A. & Bromley A. (2001) - A day and a night in the life of a cleft-foot clam: *Protovirgularia* - *Lockeia* - *Lophocentrum*. *J. Sedim. Petrol.*, 34: 119-124.
- Ekdale A.A., Bromley R.G. & Pemberton G.S. (1984) - Ichnology: the use of trace fossils in sedimentology and stratigraphy. *Society of Economic Geologists and Paleontologists, Short Course*, 15: 1-317.
- Evans S. (1999) - Wood-boring bivalves and boring linings. *Bull. of Geol. Soc. Denmark*, 45: 130-134.
- Frest T.J. & Johannes E.J. (1995) - Interior Columbia Basin mollusk species of special concern. Final report to the Interior Columbia Basin Ecosystem Management Project, Walla, WA. Contract #43-0E00-4-9112, 274 pp. plus appendices.
- Frey R.W. & Seilacher A. (1980) - Uniformity in marine invertebrate ichnology. *Lethaia*, 13: 183-207.
- Frey R.W. & Pemberton G.S. (1985) - Biogenic structures in outcrops and cores. *Bull. Canadian Petrol. Geol.*, 33: 72-115.
- Gingras M.K., Pemberton G.S. & Saunders T. (2001) - Bathymetry, sediment texture, and substrate cohesiveness; their impact on modern *Glossifungites* trace assemblages at Willapa Bay, Washington. *Palaeogeogr., Palaeoclimatol., Palaeoecol.*, 169: 1-21.
- Goldring R. (1995) - Organisms and the substrate: response and effect. In: D. W. J. Bosence & P. A. Allison (Eds) - Marine palaeoenvironmental analysis from fossils. *The Geological Society of London, Spec. Publ.*: 151-180.
- Gosling E. (2015) - Marine Bivalve Molluscs, Second Edition. John Wiley & Sons, Ltd, Wiley Blackwell, UK, 536 pp.
- Hasiotis S.T. (2002) - Continental trace fossils. *SEPM Short Course Notes 51*, Tulsa, 132 pp.
- Heard W.H. (1975) - Sexuality and other aspects of reproduction in *Anodonta* (Pelecypoda: Unionidae). *Malacologia*, 15(1): 81-103.
- Kiss A. (1992) - The propagation, growth and biomass of the

- Chinese huge mussel (*Anodonta woodiana woodiana* Lea, 1834). *University of Agricultural Sciences Godollo (Hungary). Internal work report*: 1-33.
- Knaust D. & Bromley R.G. (2012) (Eds)- Trace Fossils as Indicators of Sedimentary Environments, 1st Edition. Development in Sedimentology, 64. Elsevier, 960 pp.
- Knaust D. (2015) - Siphonichnidae (new ichnofamily) attributed to the burrowing activity of bivalves: Ichnotaxonomy, behaviour and palaeoenvironmental implications. *Earth-Sci. Rev.*, 150: 497-519.
- La Croix A.D., Dashtgard S.E., Gingras M.K., Hauck T.E. & MacEachern J.A. (2015) - Bioturbation trends across the freshwater to brackish-water transition in rivers. *Palaeogeogr., Palaeoclimatol., Palaeoecol.*, 440: 66-77.
- Lefevre G. & Curtis W.C. (1910) - Reproduction and parasitism in the Unionidae. *J. Expl. Zool.*, 9: 79-115.
- Lobza V. & Schieber J. (1999) - Biogenic sedimentary structures produced by worms in soupy, soft muds: Observations from the Chattanooga Shale (Upper Devonian) and experiments. *J. Sedim. Res.*, 69: 1041-1049.
- McMahon R.F. & Bogan A.E. (2001) - Mollusca: Bivalvia. In: J. H. Torp & A. P. Covich (Eds) - Ecology and Classification of North American Freshwater Invertebrates, 2nd Edition: 331-429. Academic Press.
- Melchor R.N., Genise J.F., Buatois L.A. & Umazano A.M. (2012) - Fluvial Environments. In: D. Knaust & R. Bromley (Eds) - Trace Fossils as Indicators of Sedimentary Environments: 329-378. Elsevier, Amsterdam.
- Miller W. (2007) - Trace Fossils, concepts, problems, prospects. Elsevier, 611 pp.
- Monaco P. (2002) - Tracce fossili di invertebrati marini e loro rapporti con il substrato: esempi dal mesozoico e dal terziario dell'Appennino Umbro e dell'area Vicentina. *Studi e Ricerche - Assoc. Amici del Museo - Museo Civico "G. Zannato" Montecchio Maggiore, VI, vol. Dic. 2002*, 15: 29-38.
- Monaco P., Famiani F., Bizzarri R. & Baldanza A. (2011) - First documentation of wood borings (*Teredolites* and insect larvae) in Early Pleistocene lower shoreface storm deposits (Orvieto area, central Italy). *Boll. Soc. Paleont. Ital.*, 50(1): 55-63.
- Monaco P., Trecci T. & Uchman A. (2012) - Taphonomy and ichnofabric of the trace fossil *Avetoichnus luisae* Uchman & Rattazzi, 2011 in Paleogene deep-sea fine-grained turbidites: examples from Italy, Poland and Spain. *Boll. Soc. Paleont. Ital.*, 51(1): 1-16.
- Nedeau E.J., Smith A.K., Stone J. & Jepsen S. (2009) - Freshwater Mussels of the Pacific Northwest, Second Edition. The Xerces Society for Invertebrate Conservation, 51 pp.
- Paunovic M., Csányi B., Simic V., Stojanovic B. & Cacic P. (2006) - Distribution of *Anodonta (Sinanodonta) woodiana* (Rea, 1834) in inland waters of Serbia. *Aquatic Invasions*: 1(3), 154-160.
- Rona P. (2004) - Secret survivor. *Nat. Hist.*, 113: 50-55.
- Rona P. et al. (2003) - *Paleodictyon*, a living fossil on the deepsea floor. *Eos Transactions AGU, Fall Meeting Supplement, Abstract OS32A-0241*: 84.
- Savrda C.E. (2007) - Trace Fossils and Marine Benthic Oxygenation. In: W. Miller III (Ed.) - Trace Fossils, Concepts, Problems, Prospects: 149-156. Elsevier, Amsterdam.
- Scott J.J., Buatois L.A. & Mángano G. (2012) - Lacustrine environments. In: D. Knaust & R. Bromley (Eds) - Trace Fossils as Indicators of Sedimentary Environments: 379-417. Elsevier, Amsterdam.
- Seilacher A. (1964) - Biogenic sedimentary structures. In: J. Imbrie & N. Newell (Eds) - Approaches to Paleocology: 296-316. Wiley, New York.
- Seilacher A. (1967) - Bathymetry of trace fossils. *Mar. Geol.*, 5: 413-428.
- Seilacher A. (1982) - General remarks about event beds. In: G. Einsele & A. Seilacher (Eds) - Cyclic and Event stratification: 161-174. Springer Verlag, Berlin, Heidelberg, New York.
- Seilacher A. (1990) - Aberration in bivalve evolution related to photo- and chemosymbiosis. *Hist. Biol.*, 3: 289-311.
- Seilacher A. (2007) - Trace Fossil Analysis. Springer Verlag, Berlin, 226 pp.
- Stárková M., Martínek K., Mikuláš R. & Rosenau N. (2015) - Types of soft-sediment deformation structures in a lacustrine Ploužnice member (Stephanian, Gzhelian, Pennsylvanian, Bohemian Massif), their timing, and possible trigger mechanism. *Int J. Earth Sci. (Geol. Rundsch.)*, online version, DOI 10.1007/s00531-015-1155-5.
- Taylor D.W. (1981) - Freshwater mollusks of California: a distributional checklist. *California Fish and Game*, 67: 140-163.
- Uchman A. (2007) - Deep-sea Ichnology: development of major concepts. In: W. Miller III (Ed.) - Trace Fossils, Concepts, Problems, Prospects: 248-263. Elsevier.
- Uchman A., Rodríguez-Tovar F.J., Machanic E. & Kędzierski M. (2013) - Ichnological characteristics of Late Cretaceous hemipelagic and pelagic sediments in a submarine high around the OAE-2 event: A case from the Rybie section, Polish Carpathians. *Palaeogeogr., Palaeoclimatol., Palaeoecol.*, 370: 222-231.
- Vaughn C.C., Nichols S.J. & Spooner D.E. (2008) - Community and foodweb ecology of freshwater mussels. *J. North Amer. Benthol. Soc.*, 27(2): 409-423.
- Watters G.T. (1992) - Unionids, fishes, and the species-area curve. *J. Biogeogr.*, 19(5): 481-490.
- Wetzel A. (2008) - Recent bioturbation in the deep South China sea: a uniformitarian ichnologic approach. *Palaios*, 23: 601-615.
- Wetzel A. (2010) - Deep-sea ichnology: observations in modern sediments to interpret fossil counterparts. *Acta Geol. Pol.*, 60(1): 125-138.
- Williams J.D., Warren M.L.J., Cummings K.S., Harris J.L. & Neves R.J. (1993) - Conservation Status of freshwater Mussels of the United States and Canada. *Fisheries*, 18(9): 6-22.
- Yen T. C. (1947) - Pliocene fresh-water mollusks from northern Utah. *J. Paleontol.*, 21: 268-277.
- Zonneveld J.P., Lavigne J., Bartels W. & Gunnel G. (2006) - *Lunulichnus tuberosus* Ichnogen. and Ichnosp. Nov. from the Early Eocene Wasatch Formation, Fossil Butte Na-

tional Monument, Wyoming: an arthropod-constructed trace fossil associated with alluvial firmgrounds. *Ichnos*, 13: 87-94.

Zonneveld J.P. & Gingras M.K. (2013) - The ichnotaxonomy of vertically oriented, bivalve-generated equilibrichnia. *J. Paleontol.*, 87: 243-253.

A NEW RECORD OF *MESSAPICETUS* FROM THE PIETRA LECCESE (LATE MIOCENE, SOUTHERN ITALY): ANTITROPICAL DISTRIBUTION IN A FOSSIL BEAKED WHALE (CETACEA, ZIPHIIDAE)

GIOVANNI BIANUCCI^{1*}, ALBERTO COLLARETA^{1,2}, KLAAS POST³, ANGELO VAROLA¹
& OLIVIER LAMBERT⁴

¹Dipartimento di Scienze della Terra, Università di Pisa, Via Santa Maria, 53, 56126, Pisa, Italy. E-mail: bianucci@dst.unipi.it, alberto.collareta@for.unipi.it. *Corresponding author.

²Dottorato Regionale in Scienze della Terra Pegaso, Via Santa Maria, 53, 56126, Pisa, Italy.

³Natuurhistorisch Museum Rotterdam, P.O. Box 23452, 30001, Rotterdam, The Netherlands. E-mail: klaaspost@fishcon.nl

⁴Institut Royal des Sciences Naturelles de Belgique, D.O. Terre et Histoire de la Vie, 29, rue Vautier, 1000 Brussels, Belgium. E-mail: olivier.lambert@naturalsciences.be

To cite this article: Bianucci G., Collareta A., Post K., Varola A. & Lambert O. (2016) - A new record of *Messapicetus* from the Pietra leccese (Late Miocene, Southern Italy): antitropical distribution in a fossil beaked whale (Cetacea, Ziphiidae). *Rin. It. Paleont. Strat.* 122(1): 63-74.

Key words: Odontoceti, Ziphiidae, *Messapicetus longirostris*, *Messapicetus gregarius*, late Miocene, Italy, Peru, palaeoecology, palaeobiogeography, antitropical distribution.

Abstract. A new partial fossil skeleton of *Messapicetus longirostris* (Cetacea: Odontoceti: Ziphiidae) collected in Cisterna quarry (Lecce) from Tortonian (upper Miocene) sediments of the “Pietra leccese” is described. It comprises the fragmentary skull (including most of the rostrum), parts of the mandibles, five teeth, the fragmentary right scapula, and one vertebral centrum. This new record, here referred to a juvenile individual, expands our knowledge about the skeletal anatomy of *M. longirostris*; this species was until now only known by the holotype, an almost complete skull from the same Cisterna quarry. Moreover, the new specimen confirms the distinction between *M. longirostris* and *M. gregarius* (late Miocene, Pisco Formation, Peru) based on several osteological characters (e.g., the presence of a distinct maxillary tubercle and prominent notch in the latter species). New dating of layers in Cerro Colorado, the type locality of *M. gregarius*, suggests that *M. longirostris* and *M. gregarius* were contemporaneous sister-species with an antitropical distribution (a biogeographical pattern currently shown by two extant ziphiid genera). Unlike extant ziphiids, feeding predominantly on squid and benthopelagic fish in deep waters, the stem ziphiid *M. gregarius* was recently proposed to have been a raptorial piscivore who may have fed mainly on schools of epipelagic fish. Similarities at the level of the morphology and proportions of the oral apparatus suggest that the two species of *Messapicetus* may have occupied roughly identical ecological and trophic niches, a hypothesis supported by the characterization of the Pietra leccese environment as neritic.

INTRODUCTION

The fossil record of marine vertebrates from the Pietra leccese. Fossil marine vertebrates from the Pietra leccese, a Miocene calcarenite limestone outcropping in Salento (southern Italy), are known since the nineteenth century thanks to the contributions of the famous naturalists Oronzo Gabriele Costa and Giovanni Capellini (Costa 1853, 1856, 1864; Capellini 1878). After these early publications, other important descriptions specifically devoted to cetaceans were produced by Bassani & Misuri (1912), Moncharmont Zei (1950, 1956) and Menesini & Tavani (1968).

Since the end of the 1980's, one of the authors (A.V.), in collaboration with the University of Pisa, started an intensive monitoring of some

quarries and sawmills of Pietra leccese, which led to the discovery and recovery of a large number of fossil marine vertebrates (cetaceans, sirenians, turtles, and fishes). Many of these finds were initially collected by the “Gruppo Naturalisti Salentini” and then became the first nucleus of the fossil vertebrate collection of the Museo dell’Ambiente of the University of Salento. Other specimens are kept in the Museo di Storia Naturale of the University of Pisa. Related to this activity, several publications appeared (Bianucci et al. 1992, 1994a, 1994b, 2003; Bianucci 2001; Bisconti & Varola 2000, 2006; Carnevale et al. 2002; Bianucci & Landini 2006). The most significant result of these studies is the detailed survey of the Cisterna quarry, located ca 2 km southeast of the town of Lecce and north of the village of Cavallino (Fig. 1). From the Tortonian strata outcropping in this quarry, an impressive marine vertebrate fossil assemblage referred to cetaceans

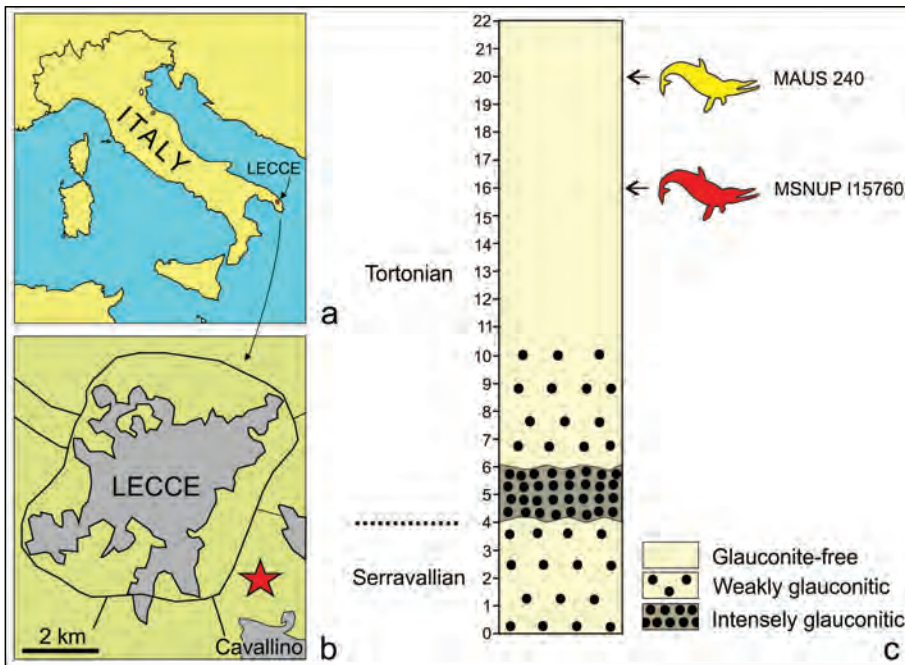


Fig. 1 - Location and stratigraphic section of Cisterna quarry near Lecce, southern Italy, where the holotype (MAUS 240) of *Messapicetus longirostris* and the referred specimen (MSNUP I15760) here described were found. a) Map of Italy with Lecce town. b) Map of Lecce and surrounding area with Cisterna quarry (star). c) Section of Cisterna quarry (from Mazzei et al. 2009) with the stratigraphical position of the two *M. longirostris* specimens.

(mysticetes and odontocetes), sirenians, fishes (teleosts and elasmobranchs), and turtles was collected. Part of this material has been already the object of publications, and three significant specimens were described as holotypes of three new genera and three new species: *Archaeoschrichtius ruggieroi* Bisconti & Varola, 2006, the currently oldest known grey whale (Eschrichtiidae), *Zygophyseter varolai* Bianucci & Landini, 2006, a stem raptorial sperm whale (stem Physeteroidea), and *Messapicetus longirostris* Bianucci et al., 1992, an archaic long-snouted beaked whale (stem Ziphiidae). Although other remains from Cisterna quarry are still under preparation, another interesting ziphiid specimen was recently freed from the hard limestone matrix and fully prepared. It is here described in detail, compared to other fossil ziphiids, and referred to the species *Messapicetus longirostris*.

Beaked whales and their fossil record.

Among extant cetaceans, beaked whales are one of the most mysterious families, due to their deep-sea habitat, elusive habits, and apparent low abundance. Despite their relatively large size (4-12 m in length) and high diversity (at least 22 extant species), these toothed whales are one of the least known groups of mammals. Their skull and teeth exhibit specialized morphological features linked to suction feeding (e.g. reduction of the functional dentition) and to sexual dimorphism (e.g. mandibular tusks, rostral pachyosteosclerosis in the genus *Mesoplodon*,

and great development of rostral maxillary crest in *Hyperoodon*) (Mead 2008).

Scarce until recently, their fossil record is now one of the best documented among cetaceans. Recent research on specimens from phosphorite layers outcropping on the bottom of deep oceanic areas and from inland deposits resulted in the description of 17 new genera and 22 new species.

Several new genera and species recovered by trawling and long-line fishing from phosphorite deposits along the Indian and Atlantic oceanic floor off the coasts of South Africa, Portugal, and Spain were described (Bianucci et al. 2007, 2008, 2013). Two main features distinguish the fossil ziphiid assemblages recovered from the ocean floor: an unexpectedly high diversity (10 new genera and 14 new species), and the occasional presence of unusual, aberrant traits (for example the enormous spherical rostral premaxillary protuberance of *Globicetus hibernus* Bianucci et al., 2013).

Inland deposits yielded the oldest ziphiid records, from early and middle Miocene of Ecuador (Bianucci et al. 2004) and Belgium (Lambert & Louwye 2006), as well as many other specimens from the Neogene of Belgium (Bianucci and Post 2004; Lambert 2005), Italy (Bianucci 1997), the eastern coast of U.S.A. (Post et al. 2008; Lambert et al. 2010), Argentina (Buono & Cozzuol 2013), and Peru (Muizon 1984; Lambert et al. 2009, 2010; Bianucci et al. 2010). Another putative fossil beaked whale, *Squaloziphius emlongi* Muizon, 1991 from

the early Miocene of Washington state, was recently considered either in a more basal position within Odontoceti (e.g. Geisler et al. 2011; Lambert et al. 2013) or as sister group of all ziphiids (Lambert et al. 2015b).

All the Peruvian ziphiids come from late Miocene levels of the Pisco Formation, where the best preserved ziphiid remains, referred to the species *Messapicetus gregarius* Bianucci et al., 2010, *Nazcacetus urbinai* Lambert et al., 2009, and *Ninoxiphius platyrostis* Muizon, 1983 (Muizon 1984; Lambert et al. 2013) were found. The record of *M. gregarius* is especially interesting, as eight cranial specimens from a few layers of a single locality were described, providing a unique opportunity to describe intraspecific variation (Bianucci et al. 2010). More recently, new investigations in Cerro Colorado, the type locality of *M. gregarius*, evidenced an even higher concentration of fossils attributed to this species: on the whole, 12 specimens, some including postcranial remains, were reported in a geological map and positioned along a stratigraphical section, together with all other vertebrates outcropping in this highly fossiliferous area (Bianucci et al. in press). Interestingly, one of these fossils was found associated with numerous skeletons of a clupeiform fish (*Sardinops* sp. cf. *S. sagax*); this association is tentatively interpreted as representing the last meal of the beaked whale (Lambert et al. 2015a). Thanks to these recent discoveries from Peru, *Messapicetus* represents the best-known fossil beaked whale to date.

INSTITUTIONAL ABBREVIATIONS

MAUS, Museo dell'Ambiente, Università del Salento, Lecce, Italy; MSNUP, Museo di Storia Naturale, Università di Pisa, Italy; MUSM, Museo de Historia Natural, Universidad Nacional Mayor de San Marco, Lima, Peru; USNM, National Museum of Natural History, Smithsonian Institution, Washington D.C., USA.

SYSTEMATIC PALEONTOLOGY

Order **Cetacea** Brisson, 1762

Suborder **Odontoceti** Flower, 1867

Family Ziphiidae Gray, 1850

Genus *Messapicetus*

Bianucci, Landini & Varola, 1992

Type species: *Messapicetus longirostris* Bianucci, Landini & Varola, 1992, from the Tortonian beds of Pietra leccese (southern Italy).

Referred species: *Messapicetus gregarius* Bianucci, Lambert & Post, 2010, from the Tortonian beds of the Pisco Formation (Peru).

Messapicetus longirostris

Bianucci, Landini & Varola, 1992

Figs 2-5, Tab. 1

1992 *Messapicetus longirostris* Bianucci, Landini & Varola, p. 261, fig 1-2.

1994 *Messapicetus longirostris* - Bianucci, Landini & Varola, p. 232, fig 1-7.

Holotype: MAUS 240, nearly complete skull lacking small portions (antorbital process, premaxillary crest and part of nasal) of the left side of cranium, collected in 1987 by one of the authors (A.V.) from the Tortonian beds of Cisterna quarry, near Lecce (southern Italy).

Emended diagnosis: *Messapicetus longirostris* differs from *M. gregarius* in the lesser posterior extension of the dorsomedial closure of the mesorostral groove by the premaxillae; lacking a distinct maxillary tubercle and prominent notch; the more slender premaxillary crest; the more gradual posteroventral descent of the medial margin of the maxilla from the vertex; and the presence of two or three dorsal infraorbital foramina on the right maxilla (contra only one foramen in *M. gregarius*).

The new record from Cisterna quarry

Referred specimen: MSNUP I15760, fragmented skull consisting of most of the rostrum, fragmentary portions of basioccipital and of exoccipitals (including incomplete occipital condyles), a portion of the postalveolar part of the left mandible, a fragment of the symphyseal portion of the mandibles, five teeth, one deformed centrum of a ?caudal vertebra, and a fragment of scapula, all from the same individual.

Horizon and locality: The specimen was found in 1987 by one of the authors (A.V.) during stone mining activities in the Cisterna quarry, ca 2 km southeast to the town of Lecce and north to the village of Cavallino (Salento, southern Italy, Fig. 1a, b), in the informally named "Pietra leccese" formation. This unit consists of generally massive, uniformly fine-grained planktonic foraminiferal biomicrites (Mazzei et al. 2009). At the Cisterna quarry, a stratigraphical section ca 22 m thick was measured and dated to the Langhian (lower portion) and Tortonian (middle and upper portions) ("Section 20" in Mazzei et al. 2009). MSNUP I15760 was collected ca 6 m below the top of the section. The holotype of *Messapicetus longirostris* (MAUS 240) was found in the same quarry at a horizontal distance of about 50 meters from MSNUP I15760 and 4 m higher in the section (Fig 1c). The 12 m upper portion of this section, including MSNUP I15760 and MAUS 240, consists of a yellowish glauconite-free biomicrite showing a planktonic foraminiferal association referable to the *Neoglobobadrina aostaensis* zone of Iaccarino & Salvatorini (1982), sensu Foresi et al. (2002), ranging between about 10.5 and 8.14 Ma (middle Tortonian).

Description and comparison

Skull. Typical for *Messapicetus* spp., the rostrum appears extremely elongated; in dorsal view, it tapers progressively from the proximal to the distal portion (Fig. 2).

Similar to the holotype of *M. longirostris*, the

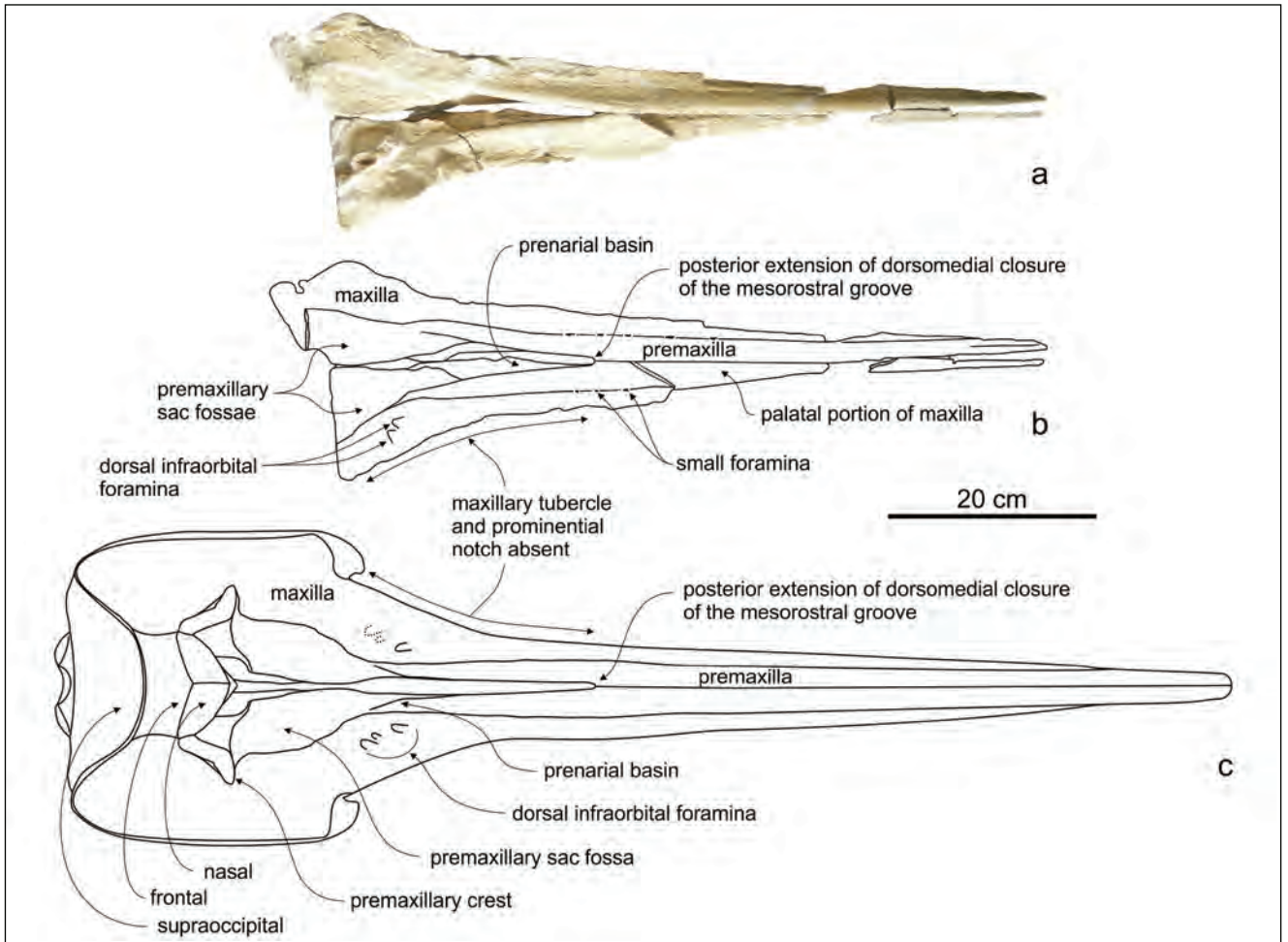


Fig. 2 - *Messapicetus longirostris* from Cisterna quarry (Lecce, southern Italy). a) Incomplete rostrum of the referred specimen MSNUP I15760 in dorsal view. b) Corresponding line drawing. c) Reconstruction of the skull in dorsal view, based on the holotype MAUS 240.

posterior portion of the lateral margin of the rostrum is rectilinear, without the distinct maxillary tubercle and prominent notch observed in the holotype and all the referred specimens of *M. gregarius* (Bianucci et al. 2010). This is the most distinctive feature separating *M. longirostris* from the Peruvian species. The preserved dorsal anterior portion of the rostrum is formed only by the premaxillae. The surface is marked by a longitudinal sulcus also observed in the holotype of *M. longirostris* and in *M. gregarius*. The premaxilla-maxilla suture is marked by a shallow sulcus along the distal half of the rostrum; the sulcus becomes almost invisible in the proximal half of the rostrum, where the suture is marked by several small foramina followed anteromedially by short sulci (a feature not observed in other specimens of *Messapicetus* spp.). The cross section of the premaxilla on the rostrum seems less dorsally convex than in the holotype and in *M. gregarius*, al-

though this character is difficult to assess due to the incompleteness and breakage of the specimen. In the closely related *Ziphirostrum marginatum* du Bus, 1868, intraspecific variation at the level of the elevation of the premaxillae on the rostrum was similarly noted (Lambert 2005). The medial margins of the premaxillae contact each other with a suture extending from 505 mm to 230 mm from the rostrum base. Consequently the medial closure of the mesorostral groove extends for 41% of the rostrum length, less than in *M. gregarius* (> 50%). Due to the diagenetic lateral compression of the skull of the holotype of *M. longirostris*, artificially closing the mesorostral groove both anteriorly and posteriorly to the portion with a medial sutural contact, it was originally not easy to estimate the actual extension of this sutural contact in the latter; nevertheless, thanks to further preparation of the fossil, the posterior end of the sutural contact is now clearly visible at ca 206

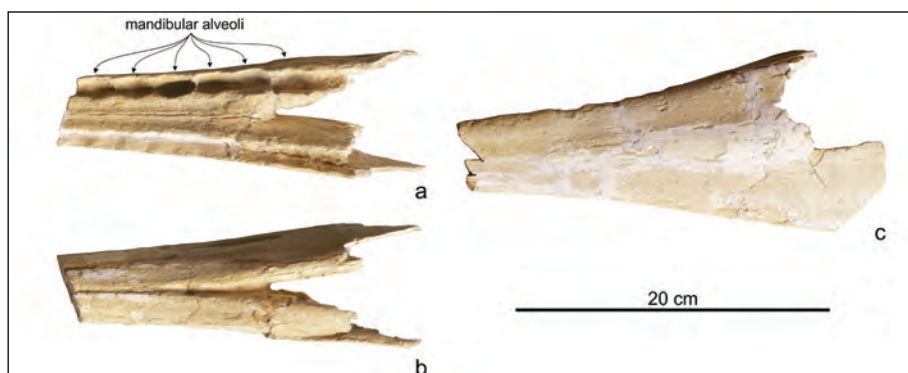


Fig. 3 - *Messapicetus longirostris* from Cisterna quarry (Lecce, southern Italy), incomplete mandibles of the referred specimen MSNUP I15760. a) Fragment of ankylosed symphyseal portion of mandibles in dorsal view. b) the same in ventral view. c) Posterior portion of left mandible in lateral view.

mm from the rostrum base (contra 120 mm as erroneously reported by Bianucci et al. 1994b). Consequently, the dorsally open posterior portion of the mesorostral groove represents ca 30% of the rostral length in the holotype, a value similar to that of the referred specimen MSNUP I15760 (32%) and proportionally longer than in the holotype of *M. gregarius* (25%) and the referred specimen MUSM 1481 (ca 23%). Therefore, the lesser extension of the dorsomedial closure of the mesorostral groove may be an additional character distinguishing *M. longirostris* from *M. gregarius*, although this character was observed as variable in *Ziphirostrum marginatum*. This open posterior portion of the mesorostral groove is anteriorly delimited by a clear U-shaped medial notch in the referred specimen MSNUP I15760, with the posteriorly diverging medial margins of the premaxillae forming an angle of ca 14 degrees. The medial margins of the premaxillae are not optimally preserved on the posteriormost portion of the rostrum. Nevertheless, in this area the premaxillae are clearly excavated, forming the typical prenarial basin of *Messapicetus* and other related genera (e.g. *Beneziphius*, *Ziphirostrum*). The incomplete premaxillary sac fossae are slightly transversely concave. Two dorsal infraorbital foramina pierce the right maxilla near the rostrum base: in the same position, the holotype of *M. longirostris* exhibits three foramina, contrasting with the single foramen present in the holotype and referred specimen of *M. gregarius*. This is apparently another minor difference between *M. longirostris* and *M. gregarius*. Only the posterior portion of the maxillary alveolar groove is preserved: it is transversely narrow, without distinct alveoli.

Mandibles: The two mandibles are ankylosed (Fig. 3a, b) and the posterior part of the symphyseal portion is half-circled in cross section. The total width at the posterior end of the symphyseal portion is 60 mm, narrower than in the holotype of *M.*

gregarius (69 mm) and the referred specimen MUSM 1038 (72 mm). The alveoli on this symphyseal portion are large and conspicuous; seven alveoli are counted on the right side, with an anteroposterior diameter of 21–25 mm and a transverse diameter of 12–13 mm. Three mental foramina are visible on the left ventrolateral surface. The posterior portion of the left mandible (Fig. 3c) is too fragmentary for significant observations (mandibular condyle and most of the coronoid process are missing). Judging by these fragments, the mandibles do not exhibit significant differences with those, well known, of *M. gregarius*.

Teeth: The largest tooth (Fig. 4a) is similar to several detached teeth associated to the holotype of *M. gregarius* (Bianucci et al. 2010: fig. 10f-k), with the transversely flattened root and the maximum anteroposterior width located at its proximal end. The crown is conical, slightly transversely flattened with a ratio between minimum and maximum diameters at the crown base equal to 0.9 (0.6 to 0.8 in *M. gregarius*), and medially curved. The enamel is smooth, without longitudinal striations and keels. Apart from the larger size, this tooth does not differ significantly from part of the teeth of *Ziphirostrum marginatum* (Lambert 2005: fig. 9). Unlike the holotype of *M. gregarius*, no apical wear and no indication of occlusal wear on the mesial and distal surfaces could be detected. The four other detached teeth (Figs 4b–e) are significantly smaller and have a proximal widening of the root lower than in the largest tooth. Moreover their root exhibits a swelling at about two thirds of their length from the proximal end. Their crowns are pointed and similarly lack apical and occlusal wear. These smaller teeth share similarities with teeth of members of several non-ziphiid odontocete families, for example eurhino-delphinids. Considering the narrow alveolar row on the proximal portion of the rostrum and the large

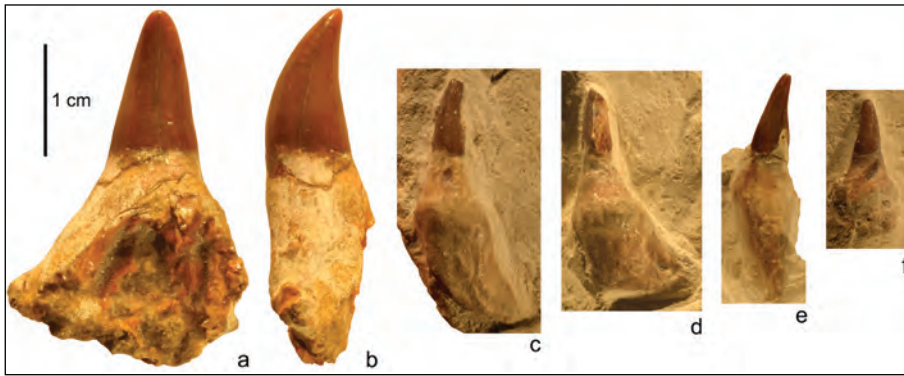


Fig. 4 - *Messapicetus longirostris* from Cisterna quarry (Lecce, southern Italy), five detached teeth of the referred specimen MSNUP I15760. a) Largest tooth in medial view. b) The same in distal view. c-f) Small teeth still partially enclosed in sediment.

| | a-b | c | d | e | f |
|--------------------------------------|------|------|------|------|-------|
| Total length | 31.9 | 21.8 | 20.3 | 18.3 | +12.2 |
| Root length | 18.8 | 15.3 | 12.9 | 12.6 | |
| Crown length | 14.7 | 6.5 | 7.4 | 5.7 | 5.3 |
| Maximum mesiodistal diameter of root | 21.6 | 5.7 | 5.3 | 9.5 | - |
| Mesiodistal diameter at crown base | 8.5 | 3.7 | 3.7 | 3.5 | 2.9 |
| Transverse diameter at crown base | 7.4 | - | - | - | - |

Tab. 1 - Measurements (in mm) of the detached teeth of the referred *Messapicetus longirostris* specimen (MSNUP I15760) from Cisterna quarry (Lecce, southern Italy). Letters a-f refer to the elements of Fig. 4. +, incomplete; -, no data.

and distinct alveoli in the symphyseal portion of the mandible, it is possible that this marked difference in size for the preserved teeth (also observed in the detached teeth of the holotype of *M. gregarius*) is linked to their origin in different regions of the tooth row. In *Tasmacetus shepherdii*, the only extant ziphiid with a complete series of functional post-apical upper and lower teeth, the size of the crown and the extent of the root vary markedly along the tooth row, with the smaller teeth positioned anteriorly (Oliver 1937: pl. 4; Mead & Payne 1975: fig.

1c; USNM 484878).

Scapula: While the lateral surface of the fragmentary right scapula has been prepared, the medial surface of the delicate blade remains embedded in the hardened micritic matrix. The general outline of the flat and thin blade cannot be reconstructed due to the erosion of its anterior, posterior, and suprascapular (dorsal) borders; however, the ventral-most portion of the posterior border is preserved and draws a rectilinear line posterodorsally (Fig. 5a). Only the proximal portions of the acromion and coracoid process are preserved. With respect to the acromion, which projects anteriorly and upwards, the coracoid process is more downward-oriented, starting from the anterior end of the glenoid fossa. The glenoid fossa is well preserved and roughly oval-shaped; its medial border is less convex than the lateral border. As observed in many odontocetes (e.g. Ichishima & Kimura 2000; Sanchez & Bertta 2010), the wide fossa for the attachment of the infraspinatus muscle is posteriorly bordered by a ridge-like, poorly salient crest whose height decreases towards the dorsal edge of the scapula. The teres major muscle presumably originated posterior to this crest. Due to the fragmentary state of this bone, it was not possible to make detailed comparisons with the scapula of other ziphiids.

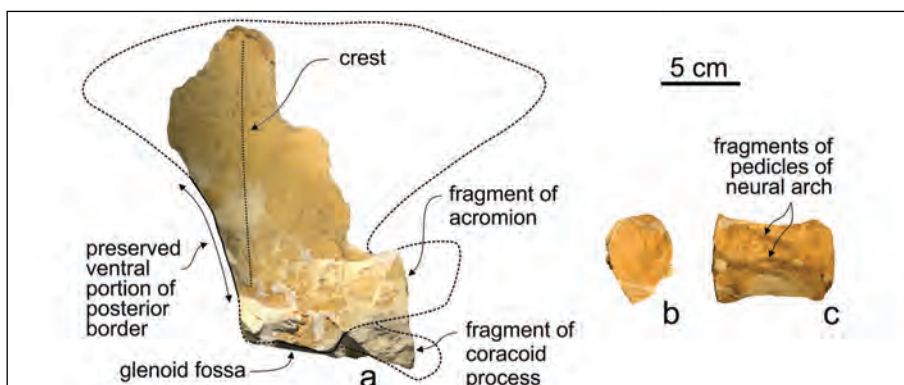


Fig. 5 - *Messapicetus longirostris* from Cisterna quarry (Lecce, southern Italy), fragmentary remains of the postcranial skeleton of the referred specimen MSNUP I15760. a) Right incomplete scapula in lateral view (dotted lines indicate a speculative reconstruction of the outline of the scapula). b) Deformed centrum of ?caudal vertebra in anterior view. c) The same in dorsal view.

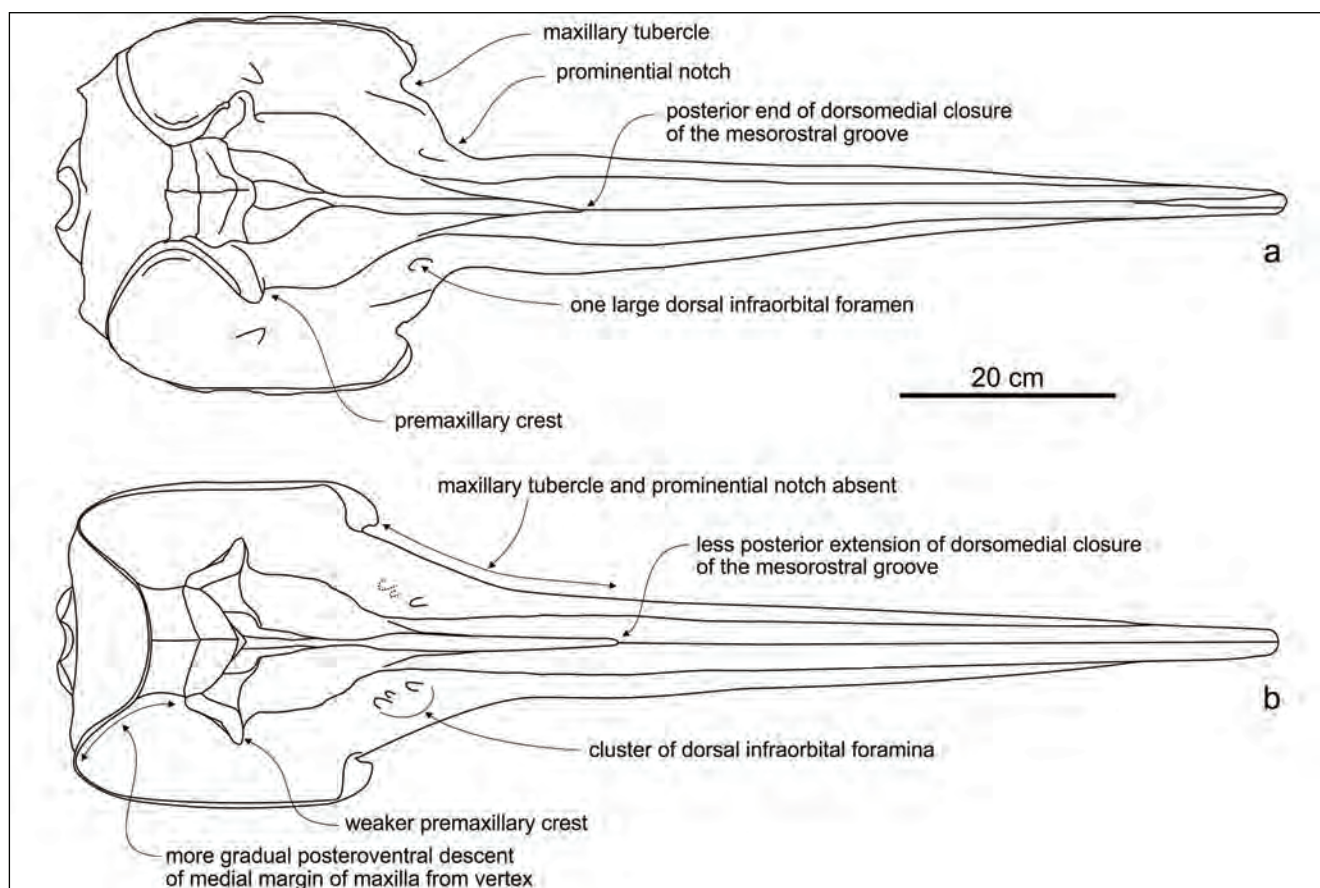


Fig. 6 - Comparison between the reconstructions of the skulls in dorsal view of: a) *Messapicetus gregarius* from Cerro Colorado (southern Peru); b) *Messapicetus longirostris* from Cisterna quarry (Lecce, southern Italy). Characters distinguishing the two species are indicated.

Vertebra: Only a partial vertebra, consisting of a 78 mm long centrum, is preserved (Fig. 5b-c). This vertebral centrum appears to have been heavily deformed by diagenetic compression and consequently its transverse section is ellipsoidal. In the dorsal surface a short proximal portion of the two pedicles are still preserved evidencing that originally the neural arch was transversely narrow. The small size, the anteroposterior elongation of the centrum, and the narrow neural arch suggest that this centrum belongs to a caudal vertebra.

DISCUSSION

Morphological characters separating *M. longirostris* and *M. gregarius*. Three characters observed in this specimen further support the specific separation between *M. longirostris* (known until now from a single specimen) and *M. gregarius* (with a larger sample of eight specimens described): 1) the absence of a distinct maxillary tubercle and of a prominent notch, as already pointed out by Bia-

nucci et al. (2010); 2) the lesser extension of the dorsomedial closure of the mesorostral groove, clearly visible in MSNUP I15760 and partly obscured due to lateral diagenetic compression in the holotype of *M. longirostris*; 3) the presence of a cluster of two-three dorsal infraorbital foramina on the right maxilla, contra only one foramen in *M. gregarius*. Two other differences between *M. longirostris* and *M. gregarius* underlined by Bianucci et al. (2010) concern portions of the skull unfortunately lacking in MSNUP I15760: the more slender premaxillary crest and the more gradual descent of the medial margin of the maxilla from the vertex (Fig. 6).

Age of the animal. Several observations support the attribution of the remains MSNUP I15760 to an immature individual:

The size is smaller than in the holotypes of *M. longirostris* and *M. gregarius*, both considered as adult animals. In fact the nearly complete rostrum of MSNUP I15760 is 660 mm in length vs. 775 and 844 mm respectively in the holotypes of *M. longiro-*

stris and *M. gregarius*. An even shorter rostrum (ca 540 mm) was observed in the skull of *M. gregarius* MUSM 1394, interpreted as a calf (Bianucci et al. 2010). Differences in the length of the rostrum much likely relate to an allometric rostral elongation during ontogeny, as observed in extant ziphiid species (references in Bianucci et al. 2010): in fact, the ratio between the width of the rostrum at base and the length of the rostrum is 0.26 in the holotype of *M. gregarius*, ca 0.30 in MSNUP I15760, and ca 0.39 in the calf MUSM 1394. Moreover, judging by the width at the posterior end of the symphyseal portion (see above), the mandibles appear narrower in MSNUP I15760 than in the holotype of *M. gregarius* and in the referred adult specimen MUSM 1038 (mandibles unknown in the holotype of *M. longirostris*).

Compared with the holotype of *M. longirostris*, the bones of the rostrum of MSNUP I15760 appear thinner, a feature also observed in the calf of *M. gregarius* MUSM 1394.

The preserved proximal portion of the maxillary alveolar row is narrower than in the holotype of *M. longirostris*.

The five teeth preserved do not display any apical or occlusal wear, whereas both wear types are observed in the teeth of the holotype of *M. gregarius* (teeth unknown in the holotype of *M. longirostris*).

Palaeobiogeography and palaeoecology.

As previously outlined (Bianucci et al. 2010), the fossil record suggests a wide geographic distribution for *Messapicetus*, with fossils from Italy (*M. longirostris*), Peru (*M. gregarius*), and possibly Maryland (cf. *Messapicetus* sp., Fuller & Godfrey 2007). Open during the late Miocene (Jacobs et al. 2004), the Central American Seaway allowed a direct communication between the Pacific and Atlantic oceans. Among other fossil ziphiids the genus *Ninoziphius* was also reported from both the southern coast of Peru (in younger deposits of the Pisco Formation) and the east coast of USA, similarly supporting a faunal link between south-eastern Pacific and North Atlantic (Muizon 1984). The assignation to *Ninoziphius* of the presumably early Pliocene North American fragmentary specimens was nevertheless recently questioned (Lambert et al. 2013).

Similar skull size and similar morphology of the oral apparatus suggest that the two species of *Messapicetus* may have occupied roughly identical

ecological niches. Based on this hypothesis, allopatric speciation may better explain the separation of the two species than sympatric speciation. Even if in different oceans, *M. gregarius* and *M. longirostris* might be considered as sister-species with an antitropical distribution, as for species of the extant ziphiids *Berardius* and *Hyperoodon* (see Davies 1963; Hare et al. 2002). Interestingly, the fossiliferous beds from Peru containing the holotype and most of the referred specimens of *M. gregarius* were recently reassigned, based on diatom biostratigraphy, to an age ranging between 9.9 and 8.9 Ma (Tortonian) (Di Celma et al. in press; Lambert et al. 2015a), younger than in previous works (13–11 Ma; Bianucci et al. 2010; Lambert et al. 2010). As a consequence, this new dating suggests that *M. longirostris* (10.5–8.14 Ma) and *M. gregarius* (9.9–8.9 Ma) were contemporaneous species with distinct geographical distributions.

Based on a high number of bony fish skeletons found associated with a partial skeleton of *M. gregarius* in the type Peruvian locality, Lambert et al. (2015a) suggested that unlike the extant ziphiids this stem beaked whale fed on clupeid fish in neritic and/or epipelagic environments. A similar feeding behaviour could be proposed for *M. longirostris*, a hypothesis that is supported by 1) the external neritic depositional environment of the Pietra leccese (Bossio et al. 2006); 2) the discovery in the same quarry and approximately the same stratigraphic horizon as the two known specimens of *M. longirostris* of four well preserved skull remains of Atlantic blue marlin *Makaira* sp. cf. *M. nigricans* (see Carnevale et al. 2002), a large fish whose extant relatives capture epipelagic prey in a similar way to that hypothesized for *M. gregarius*.

CONCLUSIONS

The fragmentary fossil described here provides new data about the stem beaked whale species *Messapicetus longirostris*, previously only known on the basis of the holotype, a nearly complete skull. In particular the mandibles and the teeth are described for the first time in this species; these parts do not differ significantly from the corresponding bones in the sister species *M. gregarius*. The fragment of scapula and the vertebral centrum represent the only described postcranial elements of *Messapicetus* and contribute to the very scarce record

of fossil postcranial remains of ziphiids worldwide. The relatively well-preserved rostrum of MSNUP I15760 confirms that the most significant character allowing the distinction between *M. longirostris* and *M. gregarius* is the absence of a distinct maxillary tubercle and of a prominent notch in the former. Moreover, two other potentially distinctive features are observed in *M. longirostris*: 1) the lesser extension of the dorsomedial closure of the mesorostral groove and 2) the presence of a cluster of two-three dorsal infraorbital foramina (contra only one foramen in *M. gregarius*). The small size, the relatively short rostrum, thin skull bones, small posterior maxillary alveoli, and the absence of apical or occlusal wear on teeth all together support the identification of MSNUP I15760 as an immature individual. Finally, this record confirms that *M. longirostris* and *M. gregarius* were probably contemporaneous species, living in distinct geographical area, but occupying a similar ecological niche.

Acknowledgements: We wish to thank R. Salas Gismondi (MUSM), J. G. Mead (USNM), C. Potter (USNM), C. Sorbini (MSNUP), and R. Malca Varas (MUSM) for allowing access to the specimens under their care. We also thank A. Berta and C. de Muizon for helpful reviews of the manuscript. This research was supported by a grant of the Italian Ministero dell'Istruzione, dell'Università e della Ricerca (PRIN Project 2012YJSBMK to G.B.).

REFERENCES

- Bassani F. & Misuri A. (1912) - Sopra un delfinoideo del calcare miocenico di Lecce (*Ziphiodelphis abeli* Dal Piaz). *Mem. R. Acc. Naz. Lincei, Cl. Sci. Fis. Mat. Nat.*, 9: 23-38.
- Bianucci G. (1997) - The Odontoceti (Mammalia Cetacea) from Italian Pliocene. The Ziphiidae. *Palaeontographia italica*, 84: 163-192.
- Bianucci G. (2001) - A new genus of kentriodontid (Cetacea: Odontoceti) from the Miocene of South Italy. *J. Vert. Paleontol.*, 21(3): 573-577.
- Bianucci G., Celma C., Landini W., Post K., Tinelli C., de Muizon C., Gariboldi K., Malinverno E., Cantalamessa G., Gioncada A., Collareta A., Salas-Gismondi R., Varas-Malca R., Urbina M. & Lambert O. (in press) - Mapping and vertical distribution of fossil marine vertebrates in Cerro Colorado, the type locality of the giant raptorial sperm whale *Livyatan melvillei* (Miocene, Pisco Formation, Peru). *J. Maps.*, doi:10.1080/17445647.2015.1048315.
- Bianucci G., Lambert O. & Post K. (2007) - A high diversity in fossil beaked whales (Mammalia, Odontoceti, Ziphiidae) recovered by trawling from the sea floor off South Africa. *Geodiversitas*, 29(4): 561-618.
- Bianucci G., Lambert O. & Post K. (2008) - Beaked whale mysteries revealed by seafloor fossils trawled off South Africa. *S. Afr. J. Sci.*, 104(3-4): 140-142.
- Bianucci G., Lambert O. & Post K. (2010) - High concentration of long-snouted beaked whales (genus *Messapicetus*) from the Miocene of Peru. *Palaeontology*, 53(5): 1077-1098.
- Bianucci G., Miján I., Lambert O., Post K. & Mateus O. (2013) - Bizarre fossil beaked whales (Odontoceti, Ziphiidae) fished from the Atlantic Ocean floor off the Iberian Peninsula. *Geodiversitas*, 35(1): 105-153.
- Bianucci G. & Landini W. (2006) - Killer sperm whale: a new basal physeteroid (Mammalia, Cetacea) from the Late Miocene of Italy. *Zool. J. Linn. Soc. Lond.*, 148(1): 103-131.
- Bianucci G., Landini W., Valleri G., Ragaini L. & Varola A. (2005) - First cetacean fossil records from Ecuador, collected from the Miocene of Esmeraldas Province. *Riv. Ital. Paleont. Strat.*, 111(2): 345-350.
- Bianucci G., Landini W. & Varola A. (1992) - *Messapicetus longirostris*, a new genus and species of Ziphiidae (Cetacea) from the late Miocene of "Pietra leccese" (Apulia, Italy). *Boll. Soc. Paleontol. Ital.*, 31(2): 261-264.
- Bianucci G., Landini W. & Varola A. (1994) - New remains of Cetacea Odontoceti from the "Pietra leccese" (Apulia, Italy). *Boll. Soc. Paleontol. Ital.*, 33(2): 215-230.
- Bianucci G., Landini W. & Varola A. (1994) - Relationships of *Messapicetus longirostris* (Cetacea, Ziphiidae) from the Miocene of South Italy. *Boll. Soc. Paleontol. Ital.*, 33(2): 231-241.
- Bianucci G., Landini W. & Varola A. (2003) - New records of *Metaxytherium* (Mammalia: Sirenia) from the late Miocene of Cisterna quarry (Apulia, southern Italy). *Boll. Soc. Paleontol. Ital.*, 42(1/2): 59-64.
- Bianucci G. & Post K. (2005) - *Caviziphius altirostris*, a new beaked whale from the Miocene southern North Sea basin. *Deinsea*, 11: 1-6.
- Bisconti M. & Varola A. (2000) - Functional hypothesis on an unusual mysticete dentary with double coronoid process from the Miocene of Apulia and its systematic and behavioural implications. *Palaeontographia Italica*, 87: 19-35.
- Bisconti M. & Varola A. (2006) - The oldest eschrichtiid mysticete and a new morphological diagnosis of Eschrichtiidae (gray whales). *Riv. Ital. Paleont. Strat.*, 112(3): 447-457.
- Bossio A., Foresi L.M., Margiotta S., Mazzei R., Salvatorini G. & Donia F. (2006) - Stratigrafia neogenico-quadernaria del settore nord-orientale della provincia di Lecce (con rilevamento geologico alla scala 1: 25.000). *Geologica Romana*, 39: 63-87.
- Brisson A.D. (1762) - Regnum Animale in Classes IX distributum sive synopsis methodica. Editio altero auctior. Theodorum Haak, Leiden, 294 pp.
- Buono M.R. & Cozzuol M.A. (2013) - A new beaked whale (Cetacea, Odontoceti) from the Late Miocene of Patagonia, Argentina. *J. Vert. Paleontol.*, 33 (4): 986-997.
- Capellini G. (1878) - Della Pietra leccese e di alcuni suoi fossili. *Mem. R. Accad. Sci. Ist. Bologna*, 9 (3): 227-258.
- Carnevale G., Sorbini C., Landini W. & Varola A. (2002) - *Ma-*

- kaira* cf. *M. nigricans* Lacépède, 1802 (Teleostei: Perciformes: Istiophoridae) from the Pietra leccese, Late Miocene, Apulia, Southern Italy. *Palaeontographia Italica*, 88: 63-75.
- Costa O.G. (1853) - Paleontologia del Regno di Napoli. Parte I. *Atti Accad. Pontan.*, 5: 233-433, 15 pls.
- Costa O.G. (1856) - Paleontologia del Regno di Napoli. Parte II. *Atti Accad. Pontan.*, 7(1): 1-378, 28 pls.
- Costa O.G. (1865) - Sul genere *Rythosodon*. *Rend. Accad. Sci. Fis. Mat.*, 4: 163-164.
- Davies J.L. (1963) - The antitropical factor in cetacean speciation. *Evolution*, 17: 107-116.
- Di Celma C., Malinverno E., Gariboldi K., Gioncada A., Rustichelli A., Pierantoni P., Landini W., Bosio G., Tinnelli C. & Bianucci G. (in press) - Stratigraphic framework of the late Miocene to Pliocene Pisco Formation at Cerro Colorado (Ica Desert, Peru). *J. Maps.*, doi: 10.1080/17445647.2015.1047906
- du Bus B.A.L. (1868) - Sur différents Ziphiides nouveaux du Crag d'Anvers. *B. Cl. Sci. Ac. Roy. Belg.*, 25: 621-630.
- Flower W.H. (1867) - Description of the skeleton of *Inia geoffrensis* and of the skull of *Pontoporia blainvillii*, with remarks on the systematic position of these animals in the order Cetacea. *Trans. Zool. Soc. London*, 6(3): 87-116.
- Foresi L.M., Margiotta S. & Salvatorini G. (2002) - Bio-cronostratigrafia a foraminiferi planctonici della Pietra leccese (Miocene) nell'area tipo di Cursi-Melpignano (Lecce, Puglia). *Boll. Soc. Paleontol. Ital.*, 41(2/3): 175-186.
- Fuller A.J. & Godfrey S. J. (2007) - A late Miocene ziphiid (*Messapicetus* sp.: Odontoceti: Cetacea) from the St. Marys Formation of Calvert Cliffs, Maryland. *J. Vert. Paleontol.*, 27 (2): 535-540.
- Geisler J.H., MCGowen M.R., Yang G. & Gatesy J. (2011) - A supermatrix analysis of genomic, morphological, and paleontological data for crown Cetacea. *BMC Evol. Biol.*, 11: 1-22.
- Gray J.E. (1850) - Catalogue of the specimens of Mammalia in the collections of the British Museum. Part I - Cetacea. Richard & John E. Taylor, London, 153 pp.
- Hare M.P., Cipriano F. & Palumbi S.R. (2002) - Genetic evidence on the demography of speciation in allopatric dolphin species. *Evolution*, 56: 804-816.
- Iaccarino S. & Salvatorini G. (1982) - A framework of planktonic foraminiferal biostratigraphy for Early Miocene to Late Pliocene Mediterranean area. *Paleontol. Stratigr. Evol.*, 2: 115-125.
- Ichishima H. & Kimura M. (2000) - A new fossil porpoise (Cetacea; Delphinoidea; Phocoenidae) from the early Pliocene Horokaoshirika Formation, Hokkaido, Japan. *J. Vert. Paleontol.*, 20: 561-576.
- Jacobs D.K., Hanev T.A. & Louie K.D. (2004) - Genes, diversity, and geological process on the Pacific coast. *Ann. Rev. Earth Plan. Sci.*, 32: 601-652.
- Lambert O. (2005) - Systematics and phylogeny of the fossil beaked whales *Ziphirostrum* du Bus, 1868 and *Choneziphius* Duvernoy, 1851 (Cetacea, Odontoceti), from the Neogene of Antwerp (North of Belgium). *Geodiversitas*, 27: 443-497.
- Lambert O., Bianucci G. & Post K. (2009) - A new beaked whale (Odontoceti, Ziphiidae) from the middle Miocene of Peru. *J. Vert. Paleontol.*, 29 (3): 910-922.
- Lambert O., Bianucci G. & Post K. (2010) - Tusk-bearing beaked whales from the Miocene of Peru: sexual dimorphism in fossil ziphiids? *J. Mammal.*, 91 (1): 19-26.
- Lambert O., Collareta A., Landini W., Post K., Ramassamy B., Di Celma C., Urbina M. & Bianucci G. (2015a) - No deep diving: evidence of predation on epipelagic fish for a stem beaked whale from the late Miocene of Peru. *P. Roy. Soc. Lond. B. Bio.*, 282: 20151530.
- Lambert O., Muizon C. de, & Bianucci G. (2013) - The most basal beaked whale *Ninoziphius platyrostris* Muizon, 1983: clues on the evolutionary history of the family Ziphiidae (Cetacea: Odontoceti). *Zool. J. Linn. Soc. Lond.*, 167(4): 569-598.
- Lambert O., Muizon C. de & Bianucci G. (2015b) - A new archaic homodont toothed whale (Mammalia, Cetacea, Odontoceti) from the early Miocene of Peru. *Geodiversitas*, 37: 79-108.
- Lambert O. & Louwe S. (2006) - *Archaeoziphius microglenoides*, a new primitive beaked whale (Mammalia, Cetacea, Odontoceti) from the Middle Miocene of Belgium. *J. Vert. Paleontol.*, 26(1): 182-191.
- Mazzei R., Margiotta S., Foresi L.M., Riforgiato F. & Salvatorini G. (2009) - Biostratigraphy and chronostratigraphy of the Miocene Pietra Leccese in the type area of Lecce (Apulia, southern Italy). *Boll. Soc. Paleontol. Ital.*, 48: 129-145.
- Mead J.G. (2008) - Beaked whales, overview. In: Perrin W.F., Würsig B.G. & Thewissen F.G.M. (Eds) - Encyclopedia of marine mammals, 2nd Ed: 94-97. Academic Press, San Diego.
- Mead J.G. & Payne R.S. (1975) - A specimen of the Tasman beaked whale *Tasmacetus shepherdi*, from Argentina. *J. Mammal.*, 56: 213-218.
- Menesinini E. & Tavani G. (1968) - Resti di *Scaldicetus* (Cetacea) nel Miocene della Puglia. *Boll. Soc. Paleontol. Ital.*, 7(2): 87-93.
- Moncharmont Zei M. (1950) - Sopra una nuova specie di *Eurhinodelphis* della Pietra leccese. *Rend. Accad. Sci. Fis. Mat.*, 4(17): 1-11, 1 pl.
- Moncharmont Zei M. (1956) - *Hesperoina dalpiazi* n. gen. et n. sp., Platanistidae, Cetacea, della Pietra leccese. *Mem. Ist. Geol. Mineral. Univ. Padova*, 19: 1-10, 2 pls.
- Muizon C. de (1983) - Un Ziphiidae (Cetacea) nouveau du Pliocène inférieur du Pérou. *C. R. Acad. Sci., Série 2*, 297(1): 85-88.
- Muizon C. de (1984) - Les Vertébrés de la Formation Pisco (Pérou). Deuxième partie: Les Odontocètes (Cetacea, Mammalia) du Pliocène inférieur du Sud-Sacaco. *Tran. Inst. Fr. Etud. Andines*, 27: 1-188.
- Muizon C. de (1991) - A new Ziphiidae (Cetacea) from the Early Miocene of Washington State (USA) and phylogenetic analysis of the major groups of odontocetes. *Bull. Mus. Nation. Hist. Natur. Paris*, 12: 279-326.
- Oliver W.R.B. (1937) - *Tasmacetus shepherdi*: a new genus and species of beaked whale from New Zealand. *P. Roy. Soc.*

Lond. B. Bio., 107: 371-381.

Post K., Lambert O. & Bianucci G. (2008) - First record of *Tusciziphius crispus* (Cetacea, Ziphiidae) from the Neogene of the US east coast. *Deinsea*, 12: 1-10.

Sanchez J.A. & Berta A. (2010) - Comparative anatomy and evolution of the odontocete forelimb. *Mar. Mammal Sci.*, 26(1): 140-160.

THE SEDIMENTOLOGY OF THE LOWER PERMIAN DANDOT FORMATION: A COMPONENT OF THE GONDWANA DEGLACIATION SEQUENCE OF THE SALT RANGE, PAKISTAN

IRFAN U. JAN^{1*}, AZEEM SHAH², MICHAEL H. STEPHENSON³, SHAHID IQBAL^{4,5},
MUHAMMAD HANIF¹, MICHAEL WAGREICH⁵ & HAFIZ SHAHID HUSSAIN¹

¹National Centre of Excellence in Geology, University of Peshawar, Pakistan. *Corresponding author. E-mail: irfan_nceg@yahoo.com

²Department of Geology, University of Haripur, Pakistan.

³British Geological Survey, Keyworth, Nottingham, NG12 5GG, UK.

⁴Department of Earth Sciences, Quaid-i-Azam University Islamabad, Pakistan, 45320.

⁵Department of Geodynamics and Sedimentology, University of Vienna, Austria.

To cite this article: Jan Irfan U., Shah A., Stephenson M. H., Iqbal S., Hanif M., Wagreich M. & Hussain Shahid H. (2016) - The sedimentology of the Lower Permian Dandot Formation: a component of the Gondwana deglaciation sequence of the Salt Range, Pakistan. *Riv. It. Paleont. Strat.*, 122(1): 75-90.

Keywords: Lower Permian, Tobra Formation, Dandot Formation, Warchha Sandstone, Sardhai Formation, Nilawahan Group, Salt Range, Pakistan.

Abstract. The Dandot Formation is a part of the Lower Permian, dominantly continental, Gondwanan Nilawahan Group in the Salt Range, Pakistan. The formation conformably overlies the glacio-fluvial Tobra Formation and has a sharp conformable contact with the overlying fluvio-continental Warchha Sandstone. Sedimentary analyses show that the Dandot Formation consists of 1: bioturbated sandstone lithofacies (L1), 2: dark green mudstone/shale lithofacies (L2), 3: flaser bedded sandstone lithofacies (L3), 4: rippled sandstone lithofacies (L4), 5: cross-bedded sandstone lithofacies (L5), and 6: planar sandstone lithofacies (L6). These can be grouped into shoreface, inner shelf, and tidal flat and estuarine facies associations, deposited in shallow marine to intertidal environments. The upper part of the Tobra Formation at the Choa-Khewra road section, where it conformably underlies the Dandot Formation, contains palynomorphs assignable to the earliest Permian 2141B Biozone. In south Oman, the 2141B Biozone is closely associated with the Rahab Shale Member, a widespread shale unit which is considered to represent part of a Permian deglaciation sequence which culminates in the marine beds of the Lower Gharif Member, interpreted as due to post glacial marine transgression. Thus, the Tobra Formation and the overlying marine Dandot Formation may form part of a similar deglaciation sequence.

INTRODUCTION

The stratigraphic committee of Pakistan formalized the name Dandot Formation for the lithostratigraphic unit formerly known as the Dandot Group by Noetling (1901). The formation includes the former “Olive Series”, “Eurydesma Beds” and “Conularia Beds” of Wynne (1878), and the “Speckled Sandstone” of Waagen (1879). The maximum thickness of the formation is 50 m at the Makrach Nala in the eastern Salt Range (Fatmi 1973; Shah 2009; Fig. 1).

Striking variation in the lithology and thickness of the unit is observed in the eastern and central Salt Range. In the eastern Salt Range, the Dandot Formation is comprised of dark greenish and grey splintery shales and sandstone. Weathered surfaces of the sandstones are reddish and the fresh surfaces show green coloration. In the central Salt

Range, i.e. in the Nilawahan Gorge section, the formation comprises green and reddish sandstone alternating with shale and siltstone. The sandstone is fine-grained, micaceous, and thoroughly burrowed in the upper parts. Sedimentary structures include flaser bedding, lenticular bedding, ripple cross laminations and bioturbation. Abundant glaucony has been reported in some horizons at the Nilawahan Gorge and Pail-Khushab road sections (Shah 1977; Fig. 1).

Reed (1936) described *Eurydesma* and *Conularia* from the Dandot Formation and asserted that the fauna co-occurred between the Salt Range, Pakistan and Carboniferous-Permian of Australia. Reed (1939) described various non-marine lamellibranchs in the form of casts and impressions, and correlated them with age-equivalent lamellibranchs from Europe, Africa, China and Burma.

The stratigraphic position of the Dandot Formation is crucial to understand Permian deglaciation in Pakistan, as the formation overlies the

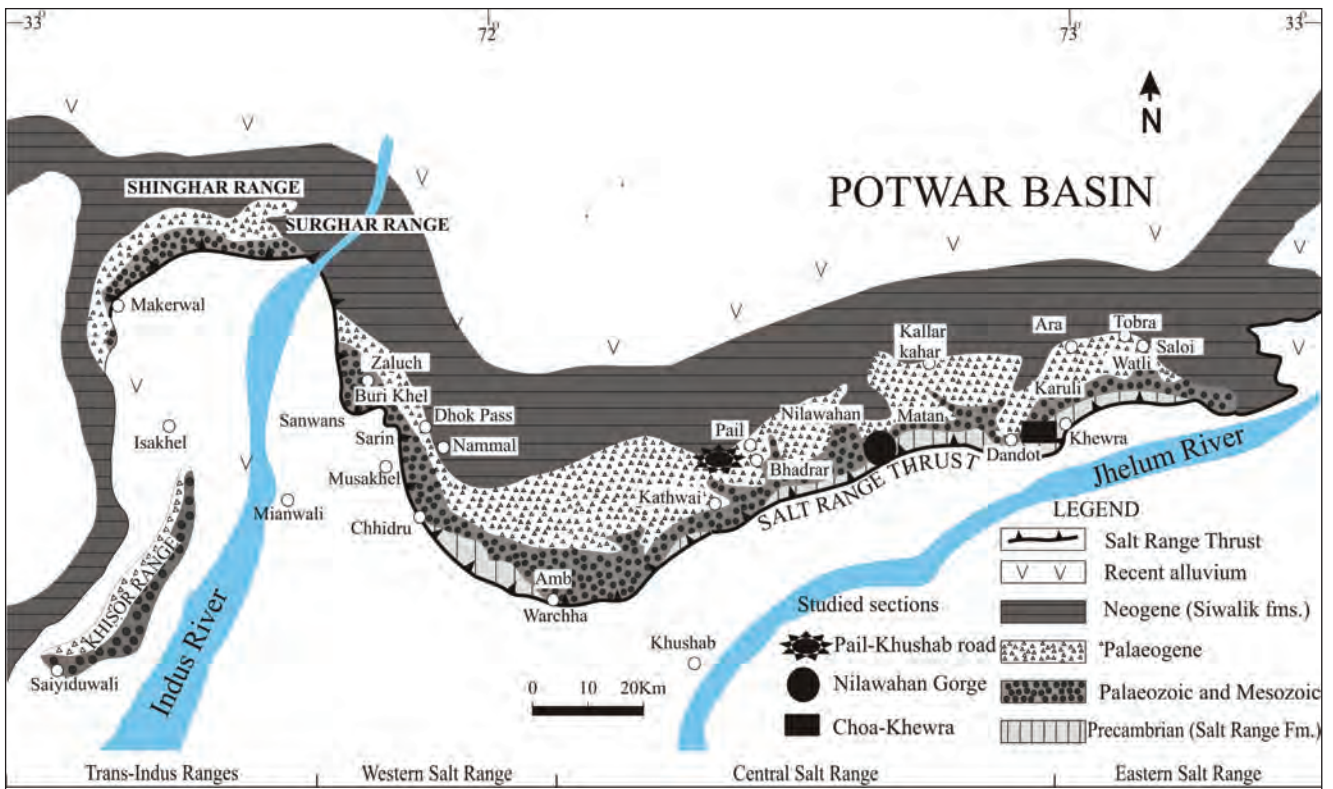


Fig. 1 - Location map of the Salt Range and Trans Indus ranges, showing Choa-Khewra road, Nilawahan Gorge and Pail-Khushab road sections, Pakistan (After Jan & Stephenson 2011).

glacio-fluvial Tobra Formation and underlies the fluvio-continental Warchha Sandstone (Fig. 2). The aim of this paper is to describe the sedimentology of the Dandot Formation in the context of deglaciation on the northwestern margin of the Indian Plate and correlate the Dandot Formation with other age-equivalent units of Gondwana basins (Fig. 3).

GEOLOGICAL SETTINGS

The Northern margin of the Indian Plate is occupied by an active fold and thrust belt of the Salt Range formed in response to the collision between Indian and Eurasian plates (Jaumé & Lillie, 1988; Fig. 4). This ongoing collision between the Indian and Eurasian plates started ~55 million years ago, as a result of northwards drift of the Indian Plate (Tahirikheli 1979; Yeats et al. 1984; Baker et al. 1988).

The Salt Range Thrust represents the southernmost fault and is considered the youngest compressional structure of the Himalayan foreland system (Grelaud et al. 2003). The syn-orogenic alluvium and fan material at the range front are over-ridden by the Precambrian evaporites and overlying

strata (Yeats et al. 1984). The Precambrian Salt Range Formation is thrust on top of the younger strata in the eastern Salt Range (Fig. 1), while the oldest rocks exposed in the western Salt Range are represented by the Carboniferous-Permian Nilawahan Group (Gee & Gee 1989).

The Salt Range represents rocks ranging from Pre-Cambrian to Tertiary (Shah 1977; Gee & Gee 1989). These rocks units are distributed in the eastern, central and western part of the Salt Range. The Carboniferous-Permian succession of the Salt Range Pakistan is subdivided into the dominantly continental Lower Permian Nilawahan Group of the Gondwanan realm and the overlying shallow marine Middle to Upper Permian Tethyan Zaluch Group (Wardlaw & Pogue 1995; Jan et al. 2009; Jan & Stephenson 2011; Stephenson et al. 2013; Fig. 2). The Upper Pennsylvanian-Asselian Tobra Formation represents the lowermost formation of the Nilawahan Group deposited periglacially (Shah et al. 2010; Fig. 2). It displays palaeontological and sedimentological similarities with the middle part of the Al Khilata Formation of Oman and Unayzah B member of Saudi Arabia and has been correlated with Al Khilata reservoir production units AK P5 to AK P1 of Petroleum Development Oman (PDO)

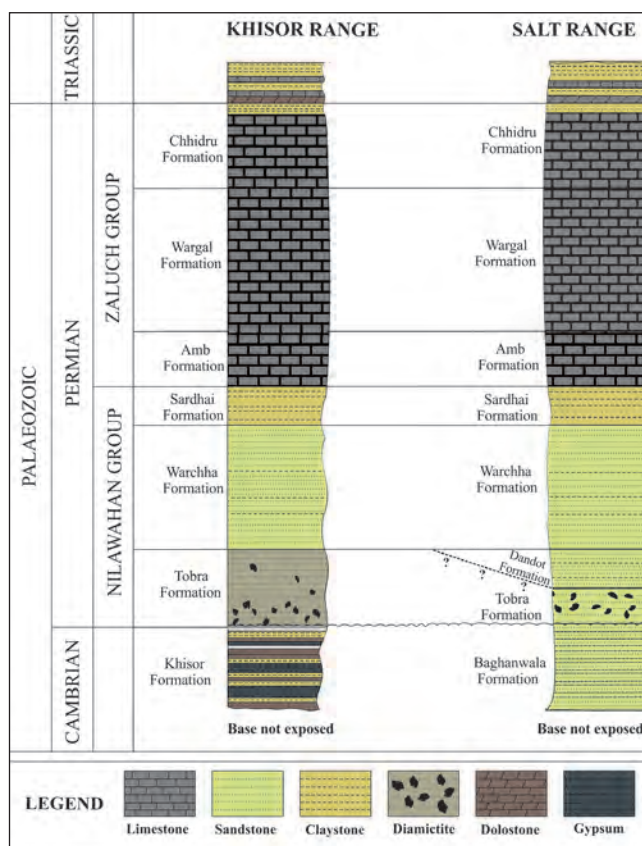


Fig. 2 - Carboniferous-Permian stratigraphy of the Salt Range and Trans Indus ranges, Pakistan. The Gondwana succession, i.e. Nilawahhan Group is represented by the Tobra, Dandot, Warchha and Sardhai formations. The Dandot Formation is not developed in the Trans Indus ranges. The overlying Zaluch Group is represented by Amb, Wargal and Chhidru formations (After Jan et al. 2009).

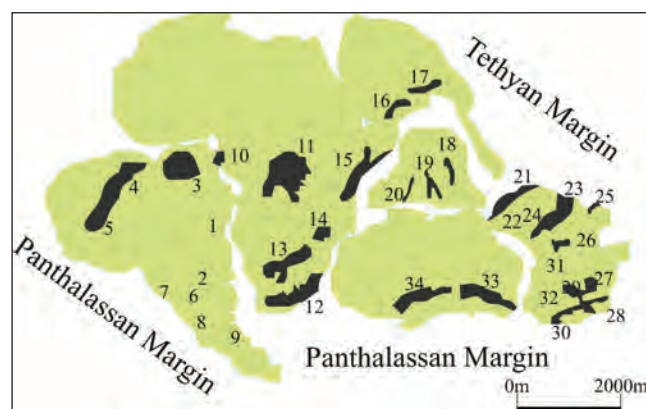


Fig. 3 - Chief Carboniferous-Permian basins of Gondwana, 1-9: South American basins, 10-15: South African basins, 16: Yemen, 17: Oman, 18: Himalayan zone, 19-20: Indian basins, 21- 32: Australian basins, 33- 34: Antarctic basins (After Stephenson 2008; Jan 2014).

and *Ottokaria* (Virkki 1939).

The overlying Sardhai Formation (Fig. 2) represents deposition in lacustrine to shallow-marine settings and has been correlated with the “Khuff transition section” of Oman and the “basal Khuff clastics” of Saudi Arabia within the Gharif Formation (Jan et al. 2009). The overlying Zaluch Group represents a dominantly carbonate succession (i.e. the Amb, Wargal and Chiddru formations), developed on a carbonate platform on the north-western Tethyan margin of the Indian Plate representing shallow marine to inter-tidal deposition (Mertmann 2003; Jan et al. 2009; Jan & Stephenson 2011).

METHODOLOGY

Sedimentological analyses of the Dandot Formation were carried out at the Choa-Khewra road section (eastern Salt Range; N 32° 39' 59.3" E 72° 59' 12.8"; Figs 1 and 5), the Pail-Khushab road section (central Salt Range; N 32° 35' 49.42" E 72° 27' 15.7"; Figs 1 and 6) and the Nilawahhan Gorge section (central Salt Range; N 32° 58' 32.0", E 72° 45' 56.5"; Figs 1 and 7). The locations are accessible and represent various intervals within the succession. Field observations, samples for petrography and grain size analysis from the formation were collected (Figs 5, 6 and 7). Proportions of the framework grains were counted using traditional methods. A Nikon polarizing LV 100ND microscope with DS-Fi2 Nikon digital camera was used for counting and photomicroscopy.

SEDIMENTOLOGICAL INVESTIGATION

The Dandot Formation (Fig. 1) shows lateral and vertical changes in the lithology with the following lithofacies and facies associations:

and south Oman 2165B Biozone (Jan & Stephenson 2011).

The Tobra Formation is overlain by the Dandot Formation in the eastern Salt Range; however it is absent in the western Salt Range and Khisor Range where the Warchha Sandstone directly overlies the Tobra Formation (Fig. 2). The lower contact of the Dandot Formation is gradational with the Tobra Formation (Ahmad 1970; Shah & Sastry 1973; Dickens 1996; Fig. 2). The upper contact is sharp with the Warchha Sandstone and is marked by an abrupt change in the lithology and sedimentary structures (Fig. 2). The Warchha Sandstone consists of medium- to coarse-grained, purple, arkosic sandstone, conglomeratic in places, with interbeds of reddish shale, and represents an arid paleoclimate (Ghazi & Mountney 2009; 2011). The unit is barren of palynomorphs (Jan 2012), however an Artinskian age has been assigned to it based on plant megafossils, including *Glossopteris*, *Gangamopteris*, *Samaropsis*

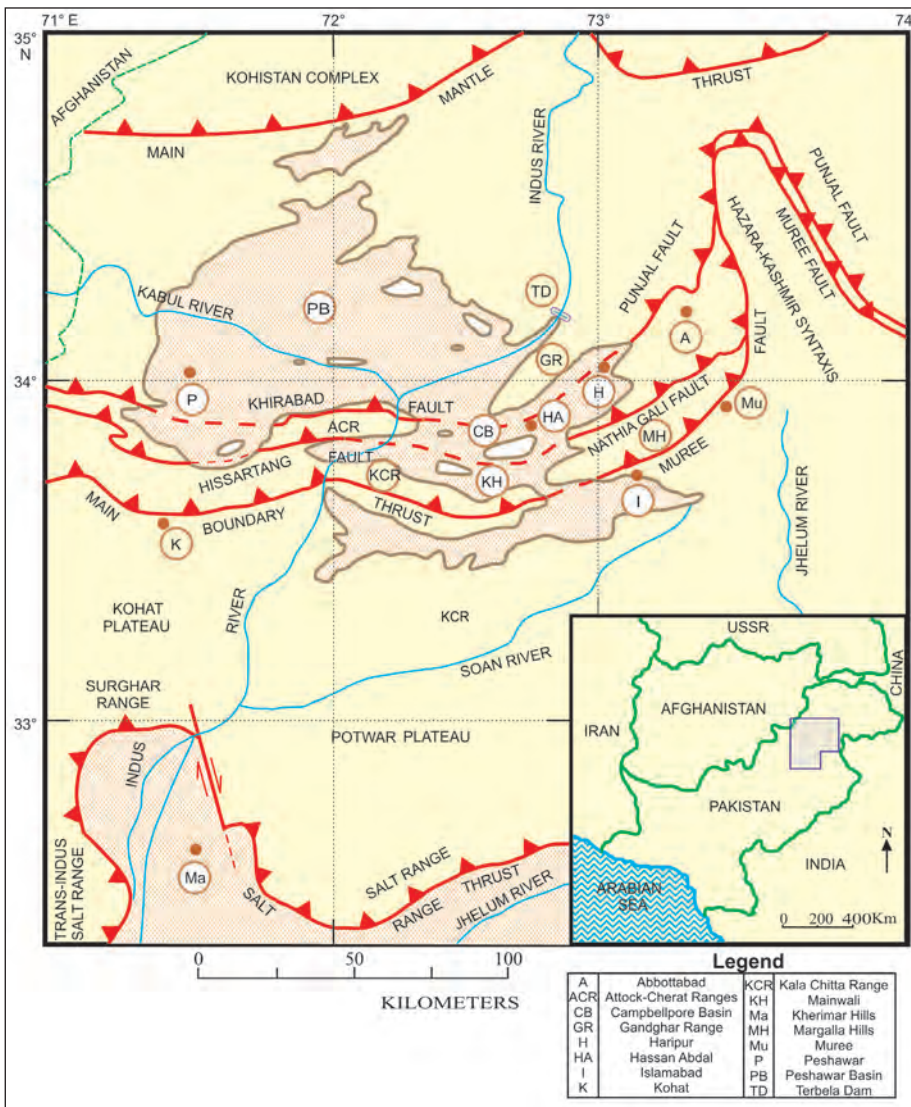


Fig. 4 - Tectonic Map of Northern Pakistan, showing major structural boundaries (After Hylland et al. 1988).

Bioturbated sandstone lithofacies (L1).

The bioturbated sandstone is present in the lowermost part of the Dandot Formation along with the contact of the underlying Tobra Formation and is comprised of fine to medium-grained sandstone (i.e. Figs 6 and 7). The lithofacies is 3.5 m-thick in the both stratigraphic sections, and is overlain by flaser bedded sandstone at the Pail-Khushab road section and planar sandstone at the Nilawahan Gorge section (Fig. 8A and B). The sandstone is thoroughly bioturbated and the intensity decreases upwards. Rootlets occur at the top of the bedding planes in the upper parts of the formation, associated with horizontally laminated sandstone. The sandstones are internally featureless, having erosive basal surfaces and having cross beds towards the top of the unit. The upper contact with the planar bedded sandstone lithofacies (L6) is sharp. Horizontal burrows and glaucony are common on the

bedding planes of the sandstone. The lithofacies displays tabular geometry in both sections.

The base of the formation is erosive and grades upwards into wave-rippled sandstone lithofacies, which contains hummocky cross stratification and represents shoreface sandstone (Reading 1996; Duke 1990; Cheel & Leckie 1993). The lithofacies represents deposition during flooding, resulting in the winnowing of the shoreface sandstones by waves or tides (Shukla & Singh 1990; Davies & Walker 1993; MacEachern et al. 1999; Al-Qayim et al. 2005). The cross-bedded sandstones were deposited in estuarine or tidal channels cutting across the lagoonal fill, where bioturbation also developed in protected areas (Singh & Shukla 1991). However, the absence of erosional surfaces and the tabular geometry of the lithofacies seldom support deposition in estuarine or tidal channels (Dalrymple et al. 1991). Glaucony present in the sandstone also supports deposition in a shallow marine environment.

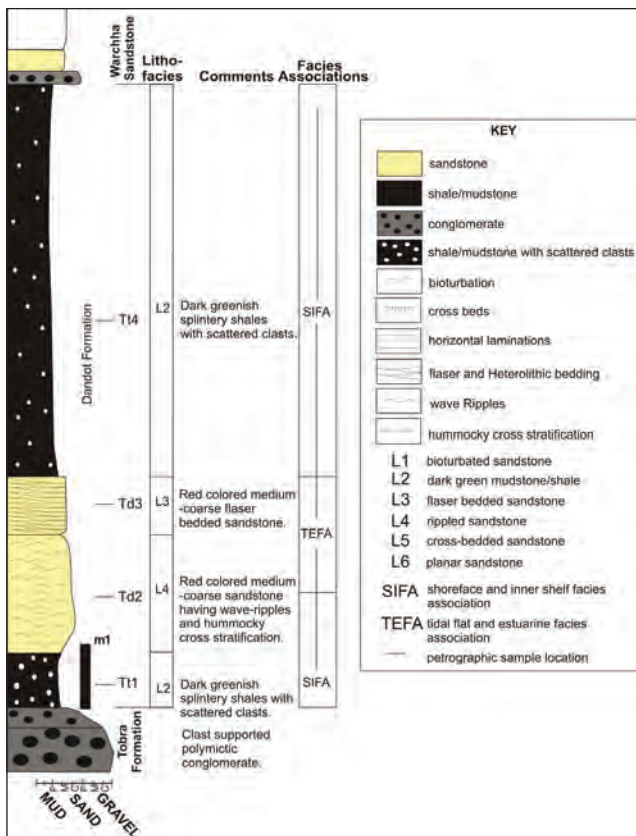


Fig. 5 - The distribution of lithofacies and facies associations of the Dandot Formation at the Choa-Khewra road section, eastern Salt Range. See the figure inset for key.

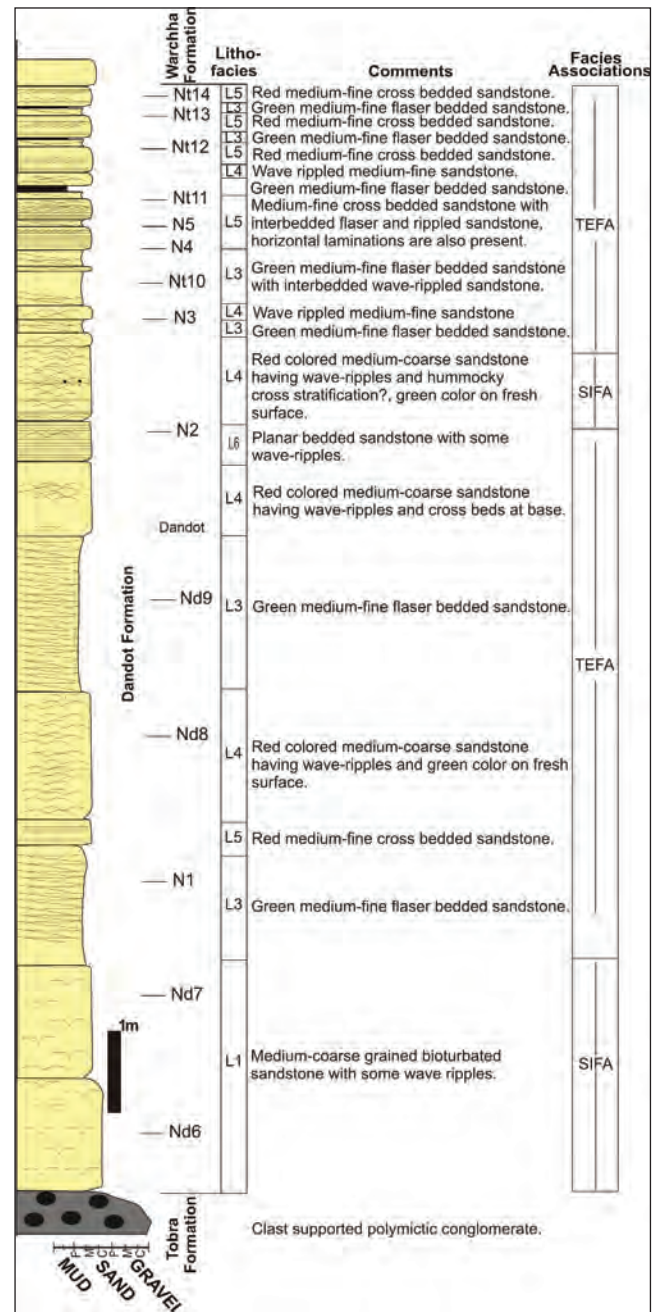


Fig. 6 - The distribution of lithofacies and facies associations of the Dandot Formation at the Pail-Khushab road section. See inset figure 5 for key.

Dark green mudstone/shale lithofacies (L2). Dark green splintery shales constitute the basal part of the Dandot Formation at the Choa-Khewra road section (Fig. 1) and are repeated in the uppermost part of the formation beneath the contact with the overlying Warchha Sandstone (Figs 4 and 8C). The thickness of L2 varies from 0.8 m in the basal part to 6 m in the uppermost part. The lower L2 unit contains scattered clasts of varying compositions including granite, volcanic, and sedimentary lithics derived from the underlying Tobra Formation. This unit grades into rippled sandstone, showing soft sediment deformation in the upper parts (Fig. 8C). The number of scattered clasts increases in the upper part of the formation. The lower contact of L2 is sharp with the underlying Tobra Formation, however it does not show erosive surfaces. L2 possesses a tabular geometry.

Fielding et al. (2006) attributed the presence of clasts to the melting of icebergs and the dropping of clasts in the marine environment. The absence of varves and other glacial features point

to a non-glacial origin. The dark green shale shows deposition in the nearshore environment (Genne-seaux 1962; Stanley & Swift 1967). The presence of soft sediment deformation also indicates deposition in a marine environment (Crowell 1956; Altermann 1986).

Flaser bedded sandstone lithofacies (L3). L3 is present at the Pail-Khushab road and Nilawahwan Gorge sections (Figs 6 and 7). The sandsto-

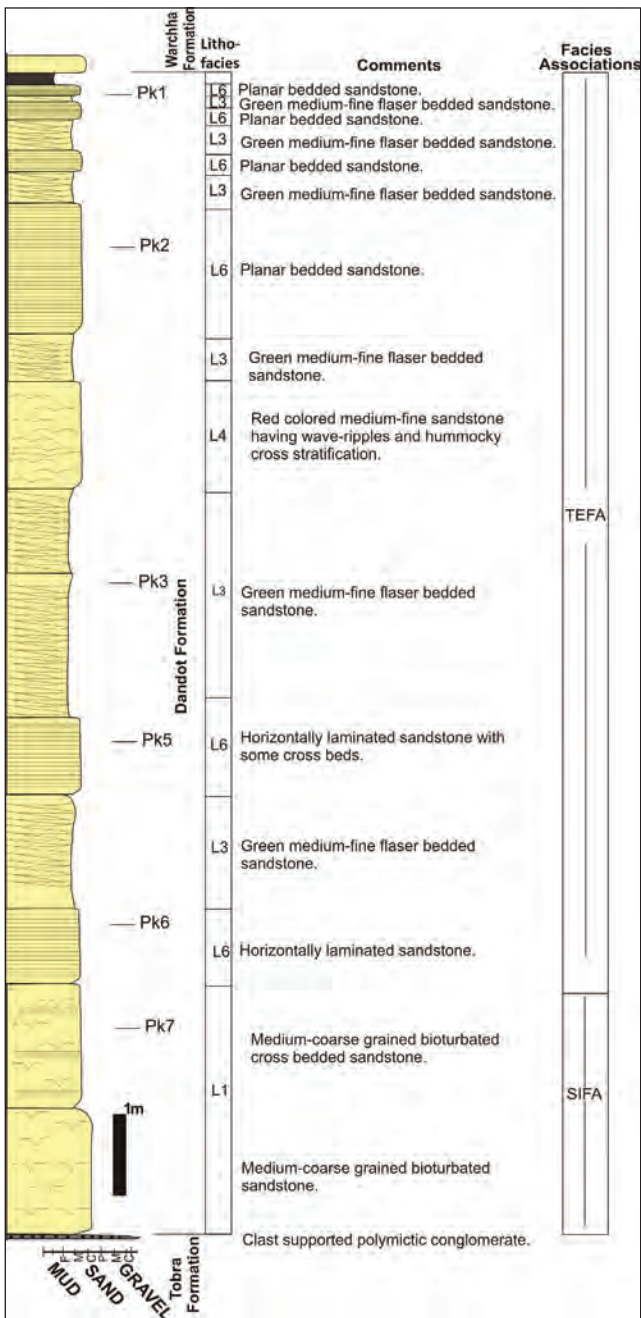


Fig. 7 - The distribution of lithofacies and facies associations of the Dandot Formation at the Nilawahen Gorge section. See inset figure 5 for key.

nes are fine- to medium grained, well sorted and green in color. The lithofacies is repeated several times at the Pail-Khushab road section (Fig. 6), having fining upward succession with thickness ranging from 0.2 to 3 m (Fig. 8D). Sand lenses are 1 to 2 cm in thickness with internal laminations, cross laminations and asymmetric ripples. In places these sand flasers sharply overlie cross-bedded sandstones. Similar fining upward successions are present at the Nilawahen Gorge section (Fig. 7) but with lesser

thicknesses than those present at the Pail-Khushab road section (Fig. 6). In places, flaser and lenticular bedding is replaced by tidal bedding, i.e. cyclic pattern of planar bedded sandstone and shale.

Flaser bedded sandstones are interpreted to represent deposition in a tidal setting, i.e., tidal flats and tidal channels (Terwindt 1971). The repeated fining upward cycles represent tidally-influenced estuarine channel fills (Fielding et al. 2006).

Rippled sandstone lithofacies (L4). This facies constitutes fine grained, well sorted sandstone with a red weathered surface and green fresh surface color. The sandstone is laminated with abundant wave ripples, combined flow ripples, and rare climbing ripples. Low angle hummocky cross stratification and herringbone cross stratification are common (Figs 5 to 7 and 8E). The upper surfaces of the ripples in places are marked by thin shale beds. The rippled sandstone grades into flaser bedded sandstones. This lithofacies is present in all the three stratigraphic sections and is repeated at the Pail-Khushab and Nilawahen Gorge sections with 0.2 m to 2 m variation in thickness (Figs 5 to 7). At the Nilawahen Gorge section, L4 displays thickening beds giving massive appearance and has fine- to medium grain size. Current-ripples predominate over asymmetrical ripples. These sandstones grade upward into flaser bedded units and overlie bioturbated sandstone lithofacies. Extensive horizontal burrows are present on the upper surfaces of these rippled beds in the upper parts of the formation. At the Choa-Khewra road section, this lithofacies is similar in appearance to that found at the Nilawahen Gorge section, with sandstone being much coarser, having red color with green shale on the rippled surfaces (Fig. 5).

An abundance of wave ripples and current ripples points towards deposition in a coastal environment (Reineck & Singh 1971; Wunderlich 1972). The association of this lithofacies with flaser bedded sandstone lithofacies upwards represents deposition in the intertidal environment (Reineck & Singh 1983). Thick sandstones with asymmetrical ripples of the Nilawahen Gorge and Choa-Khewra road sections represent deposition in relatively deeper waters of the shoreface (Newton 1968). The presence of hummocky cross stratification also supports this interpretation (Newton 1968; Reineck & Singh 1983). The comparatively large size of the

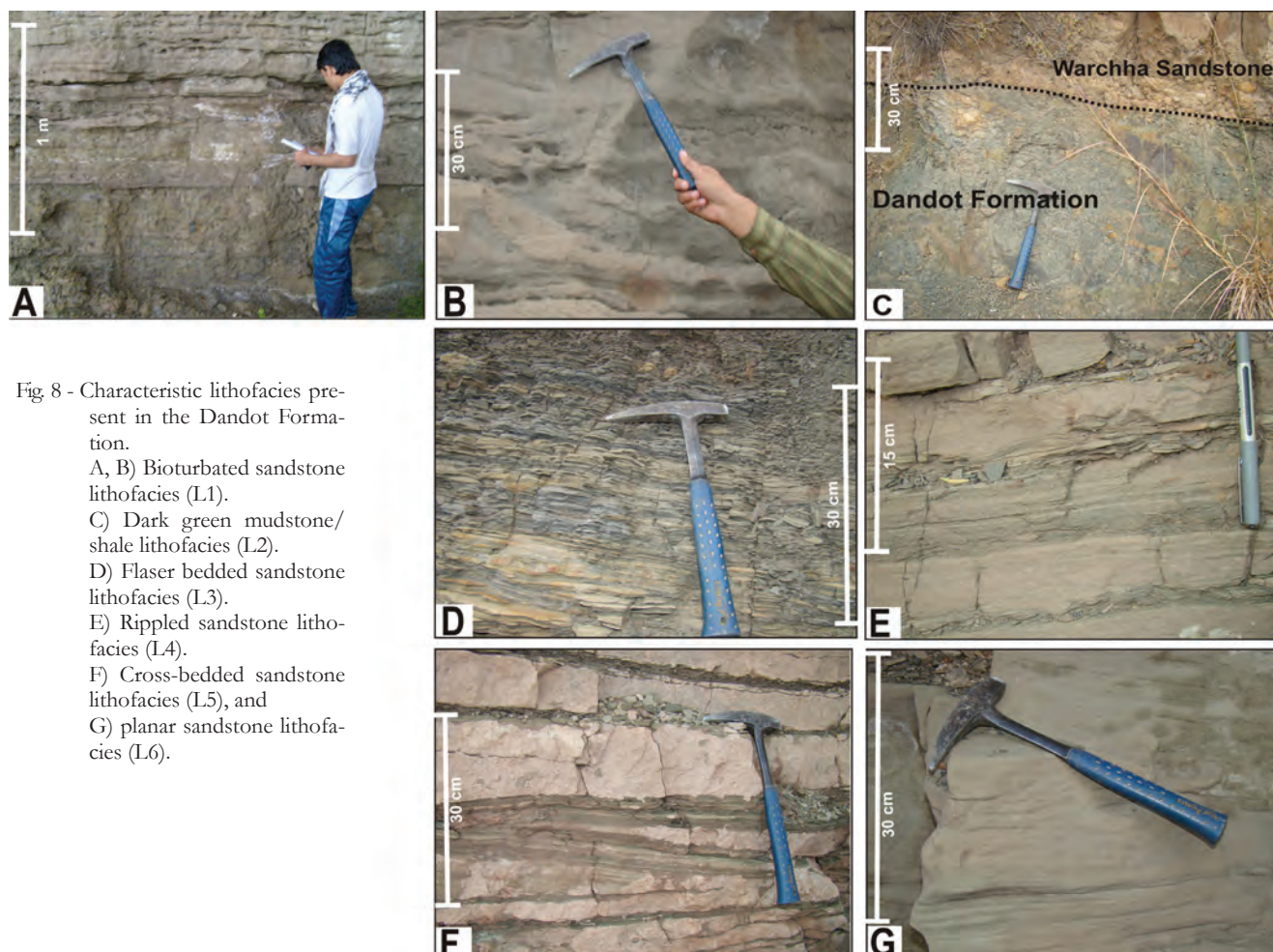


Fig 8 - Characteristic lithofacies present in the Dandot Formation.

A, B) Bioturbated sandstone lithofacies (L1).

C) Dark green mudstone/shale lithofacies (L2).

D) Flaser bedded sandstone lithofacies (L3).

E) Rippled sandstone lithofacies (L4).

F) Cross-bedded sandstone lithofacies (L5), and

G) planar sandstone lithofacies (L6).

ripples is also evidence of deposition in deeper waters (Reineck & Singh 1983).

Cross-bedded sandstone lithofacies (L5).

L5 is present at the Pail-Khushab road section in the central Salt Range and comprises coarse grained, occasionally friable reddish to whitish green sandstone (Figs 6 and 8F). This lithofacies is present in the middle and upper parts. Low angle planar cross bed sets are present within the sandstones, and are associated with the horizontally-laminated sandstone, and grade upwards into flaser bedded sandstone (Figs 6 and 8F). At some places, low angle planar cross bed sets also occur (Fig. 6).

The association of this lithofacies with the planar sandstones lithofacies and tidally influenced channel fills of estuarine environment suggest deposition on tidal flats in the tidal channels and estuarine fills (Davis 1983; Dalrymple et al. 1991).

Planar sandstone lithofacies (L6). L6 is present at the Pail-Khushab road and Nilawahan

Gorge sections only (Figs 5 to 7). This lithofacies is repeated vertically in the stratigraphic sections and is associated with the bioturbated sandstone below and flaser bedded sandstone above. It is also associated with the rippled sandstone lithofacies. The facies comprises medium to coarse-grained, well sorted, and friable sandstones and occurs in beds (thickness varies from 0.5 to 2 m) with planar/horizontal laminations. A fining upward trend is observed in L6 and grades into flaser bedded units (Figs 6 and 7). Low angle cross laminations also occur towards the top in the lithofacies (Fig. 6G). At Nilawahan Gorge section, horizontal burrows are found on the upper surfaces of the thin horizontal fine clayey beds interlaminated with sandstone (Fig. 7). These beds constitute fine grained well sorted and friable sandstones.

The stratigraphic position of L6 suggests an intertidal depositional setting. In the Nilawahan Gorge, the heterolithic bedding in L6 also represents cyclic change in the energy conditions due to the tidal activities.

FACIES ASSOCIATIONS

The lithofacies in the Dandot Formation can be grouped into two facies associations:

Shoreface and inner shelf facies associations (SIFA). SIFA is composed of L1 and L2. Part of the rippled sandstone lithofacies (i.e. L4) is also included in this association (Figs 5 to 7). The presence of sedimentary structures and textural trends and presence of wave ripples, hummocky cross stratification, bioturbation and mudstone/shale containing scattered pebbles indicate deposition in nearshore to slightly deep water settings (Reading 1996; Fielding et al. 2006). The shoreface and inner shelf facies association is present in all three stratigraphic sections (Figs 5, 6 and 7). The Dandot Formation at the Choa-Khewra road section (i.e. eastern Salt Range) contains pebbly mudstone/shale of this association in the lower and upper parts. In the central Salt Range (Fig. 1), lithologies representative of this facies association are restricted to the lowermost part of the Dandot Formation.

Tidal flat and estuarine facies association (TEFA). TEFA comprises L3, L4, L5 and L6 (Figs 5 to 7). The abundance of wave ripples, combined flow ripples, heterolithic bedding, tidal channel fill sequences and bioturbation indicate deposition of this facies association in tidal flats and an estuarine environment (Reineck & Singh 1983; Fielding et al. 2006). This facies association is present in all the three stratigraphic sections. At the Choa-Khewra road section, rippled sandstone and flaser bedded sandstone of this facies association are present in the middle part of the Dandot Formation while the other lithologies representing this facies association are present in the Nilawahan Gorge and Pail-Khushab road sections, where they represent the middle and upper parts of the formation.

VERTICAL AND LATERAL FACIES VARIATIONS

The Dandot Formation in the eastern part of the Salt Range (Fig. 1) shows relatively deeper facies of SIFA at the base which grade upwards into shoreface sandstone with development of ripples and hummocks subsequent to sea level rise possibly as a result of Carboniferous-Permian deglaciation (Di-

ckins 1996; Angiolini et al. 2003; Ghazi & Mountney 2011; Fig. 9). In the central part of the Salt Range, i.e., Pail-Khushab road and Nilawahan Gorge sections (Figs 1, 6, 7 and 9), transgressive bioturbated shoreface sandstones grade upwards into relatively shallow marine bioturbated sandstone. The progradation continues and the succession grades into tidal flat and estuarine sandstones and heteroliths. Several cycles of the fining upward successions indicate that the presence of estuarine/tidal channels is quite dominant in the upper and middle parts of the Dandot Formation at Nilawahan Gorge and Pail-Khushab road sections. Overall, a progradational sequence is recorded in the Dandot Formation which sharply truncates against the fluvial succession of the overlying Warchha Sandstone (Figs 2 to 7).

In the east, the Dandot Formation constitutes deeper facies of SIFA with presence of mudstone/shales with scattered pebbles. In the central part of the Salt Range, lithologies of shallow-marine settings predominate. Shoreface facies are present only at the basal part while the rest of the formation appears to have been deposited in a marginal marine setting, i.e., tidal flat and tide-dominated estuarine sequence. It is suggested that the eastern part of the Salt Range occupied a relatively distal position on the northwestern margin of the Indian Plate and as a result relatively deeper water facies were deposited in this part and the western part occupied a more proximal position and thus the central and western parts represent shallower facies.

Depositional system and regional setting. The distribution of the lithofacies at the three stratigraphic sections (i.e. Choa-Khewra road, Pail-Khushab road and Nilawahan Gorge sections; Figs 5, 6 and 7 respectively) shows interbedding with little cyclicity in the upper parts of the formation in two stratigraphic sections i.e. Pail-Khushab road and Nilawahan Gorge sections (Figs 6 and 7), and in the middle part of the formation at the Nilawahan Gorge section (Fig. 7). Major erosional surfaces like sequence boundaries were not identified within the vertical stacking patterns except the surface separating estuarine channel fills from the shoreface facies evident at the basal part of the Dandot Formation at Pail-Khushab road and Nilawahan Gorge section (Figs 6 and 7). This surface can be considered a sequence boundary because of an abrupt change in

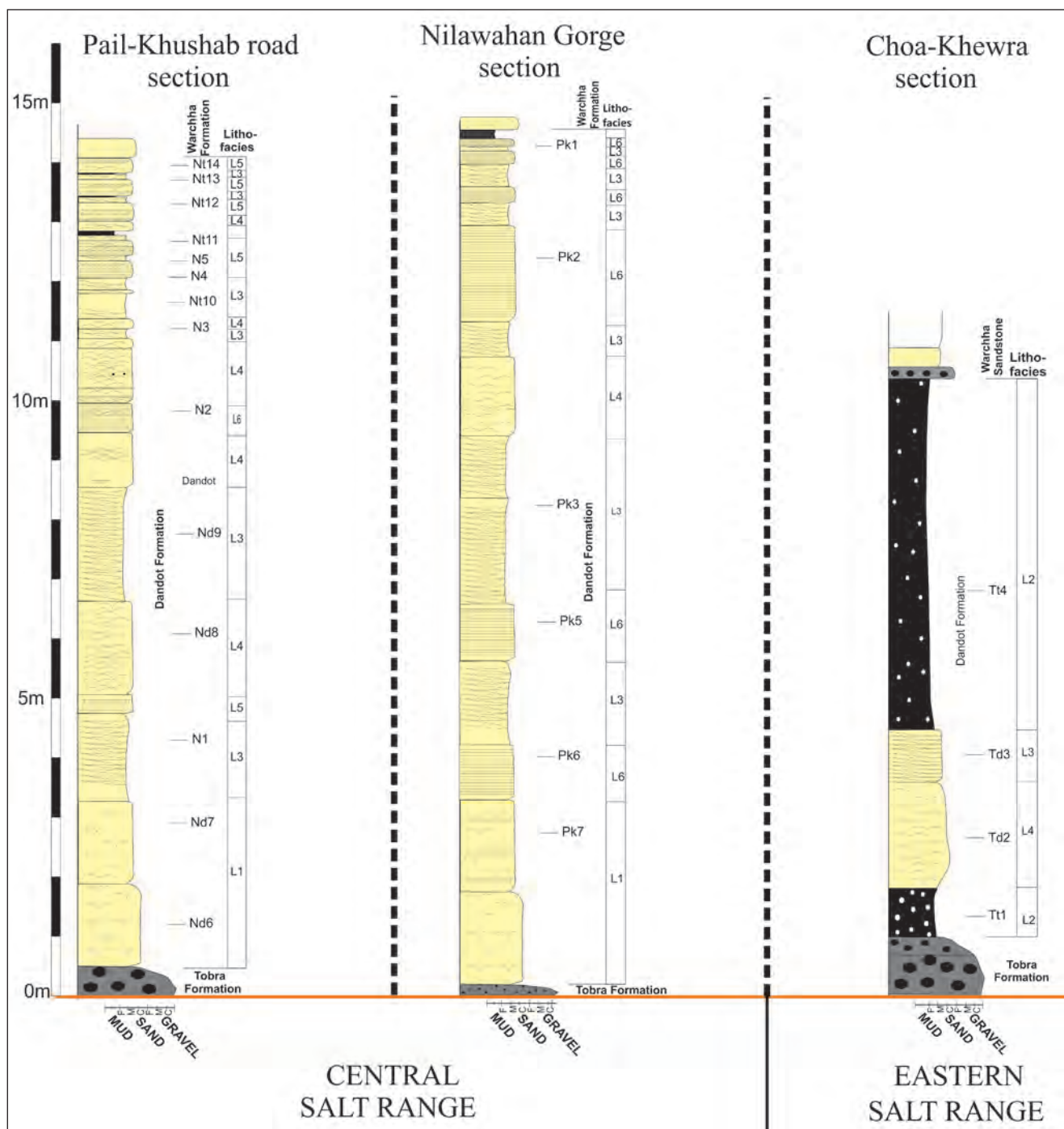


Fig. 9 - The Dandot Formation facies correlation in the eastern and central Salt Range. Refer to figure 1 for locations and inset figure 5 for key.

the facies and because the surface is traceable laterally for long distances. At the Choa-Khewra road section, an abrupt deepening is observed and lithofacies L3 is overlain by L2 of shoreface to inner shelf environment. Similar surfaces showing abrupt deepening are also present in the Nilawahen Gorge section (Fig. 5) in the middle and upper part where the cyclicity of upper shoreface sands and heterolithic bedding of the TEFA is observed. In the lo-

wer to middle part, the pattern in the sequence may be attributed to the short term cyclicity in sea level (Fig. 7), while in the upper part (Fig. 5), the presence of shoreface sandstone interbedded with the tidal flat and estuarine fill facies association represents abrupt deepening and thus a marine flooding surface. Overall, the vertical stacking pattern in the Dandot Formation represents a progradational sequence with shallow marine facies overlying the deep marine facies.

| Section | Sample# | Quartz | | | Feldspar | | | | Mica | Ca | Ioc | Qc | Lithic Fragments | | | Po | Op | Gl | Matrix |
|---------------------------|---------|--------|------|------|----------|-----|-----|-----|------|-----|-----|----|------------------|----|-----|----|-----|----|--------|
| | | Qm | Qp | Qt | Ch | Kf | Pl | Ft | | | | | Ls | Lv | Lm | | | | |
| Nilawahan Gorge section | N1 | 78 | 1 | 79 | 2 | 1 | 3 | 2 | 1 | 10 | 2 | | | | | 3 | | | |
| | N2 | 76 | | 76 | 2 | 1 | 3 | 5 | 1 | 10 | | | | | | | 4 | | |
| | N3 | 68 | 3 | 71 | 1 | 1 | 2 | 15 | | | 8 | | | | | | 3 | | |
| | N4 | 67 | | 67 | 3 | 2 | 5 | 10 | 5 | 9 | 1 | | | | | | 3 | | |
| | N5 | 69 | | 69 | 3 | 4 | 7 | 10 | 5 | 6 | 1 | | | | | | 2 | | |
| | Nd7 | 68 | 1 | 69 | 2 | 1 | 3 | 4 | 6 | 4 | | | | | | | 2 | 14 | |
| | Nd8 | 81 | | 81 | 3 | 2 | 5 | 1 | 1 | 9 | | | | | | 1 | 2 | | |
| | Nd9 | 65 | 2 | 67 | 4 | 3 | 7 | 14 | 1 | 8 | | | | | | | 3 | | |
| | Nd10 | 74 | 1 | 75 | 2 | 1 | 3 | 10 | | 7 | | | | | | | 1 | 4 | |
| | Nd11 | 78.5 | 1 | 79.5 | 2 | 0.5 | 2.5 | 3 | 8 | 6 | | | | | | | 1 | | |
| | Nd12 | 81 | 1 | 82 | 5 | 3 | 8 | 0.5 | 6 | 3 | | | | | | | 0.5 | | |
| | Nd13 | 77 | 1 | 78 | 5 | 3 | 8 | 1 | 5 | 4 | | | | | | | 1 | | |
| | Nd14 | 82 | 3 | 85 | 4 | 2 | 6 | 0.5 | 5 | 3 | | | | | | | 0.5 | | |
| | Nw15 | 65 | 3 | 68 | 8 | 4 | 12 | 1 | 1 | 3 | | 5 | | 2 | 1 | 1 | | 6 | |
| Pail-Khushab road section | Pk1 | 84 | | 84 | 1 | 4 | 3 | 7 | 1 | 3 | 3 | | 2 | | | 1 | | | |
| | Pk2 | 74.5 | 1 | 75.5 | 4 | 5 | 9 | 6 | 0.5 | 4 | 2 | 1 | | | | 1 | | | |
| | Pk3 | 80.5 | 1 | 81.5 | 2 | 1 | 3 | 4 | 0.5 | 5 | 2 | | | | 1 | 2 | | | |
| | Pk5 | 75 | 1 | 76 | 2 | 1 | 3 | 5 | 1 | 10 | 1 | | | | 3 | 2 | | | |
| | Pk6 | 83 | 1 | 84 | 1 | 1 | 2 | 1 | 1 | 8 | 1 | | | | 1 | 1 | 1 | | |
| Pk7 | 69 | 1 | 69.5 | 1 | 0.5 | 1.5 | | 2 | 6 | 0.5 | | | | | 0.5 | 20 | | | |
| Choa-Khewra road section | Td3 | 83.5 | 1 | 84.5 | 0.5 | 1 | 1.5 | 1 | 3 | 5 | 2 | | | | | 3 | | | |
| | Td1 | 70 | 5 | 75 | 2 | 3 | 5 | | 1 | 1 | | 3 | 5 | | | 1 | 10 | | |
| | Tw5 | 58 | 4 | 62 | 9 | 4 | 13 | | 8 | 4 | 1 | 5 | 3 | | 3 | 1 | | | |

Tab. 1 - Proportions of rock components of the sandstone of the Dandot Formation. Sample Tt1 belongs to underlying Tobra Formation and Tw5 and Nw15 belong to overlying Warchha Sandstone. For samples locations see figures 5, 6 and 7. Qm = Non undulose microcrystalline quartz, Qp = Polycrystalline quartz, Qt = Total quartz present (monocrystalline and polycrystalline including chert), Ch = Chert, Kf = Alkali feldspar (orthoclase and microcline), Pl = Plagioclase feldspar, Ft = Total feldspar (both K-feldspar and plagioclase), Ca = Calcite cement, Ioc = Iron oxide/hydroxide, Qc = Quartz cement, Ls = Sedimentary lithics, Lv = Volcanic lithics, Lm = Metamorphic lithics, Po = Porosity, Op = Opaque minerals, Gl = Glaucony.

SANDSTONE PETROGRAPHY

Sandstone constitutes about 85%, of the Dandot Formation; shale and mudstone is less common (Figs 5 to 7). The sandstones are homogeneous with fine- to medium-grain size, however occasional coarse-grained sandstones occur in the basal parts of the formation. Sandstones are moderately to well sorted and very well sorted in places. Texturally, the grains are rounded to sub-rounded, with occasional angular to sub-angular shapes and display loose packing; however in some places sandstone is compact and tightly packed. Contacts between the grains are mostly straight, with some concavo-convex, tangential and rare sutured contacts (Fig. 10C). Two sandstone samples collected from the base of the overlying Warchha Sandstone are moderately to poorly sorted and feldspatho-quartzose (Tab. 1).

Characteristics of the framework grains.

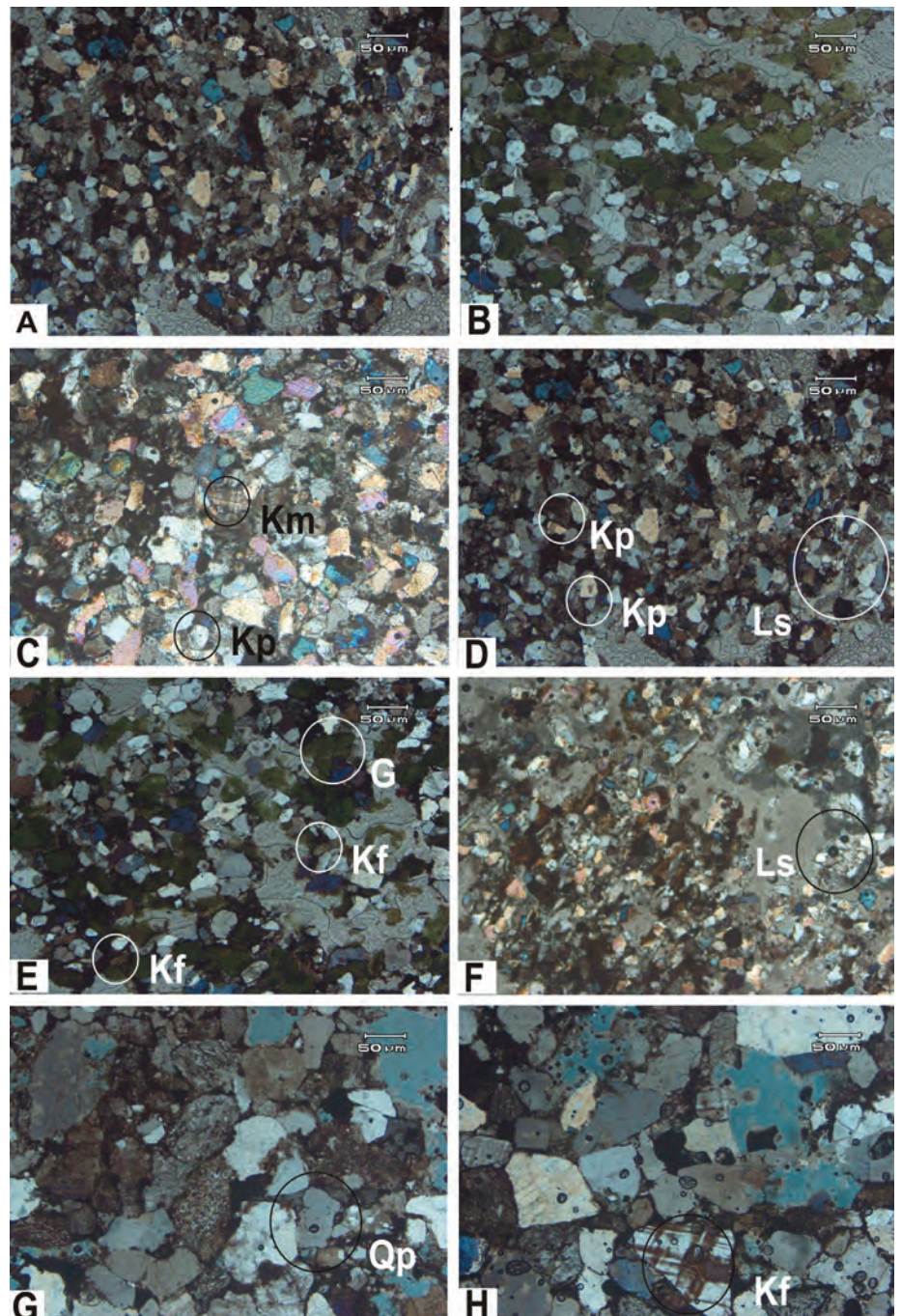
Clasts. Quartz crystals constitute 65-84% of the rock; 99% are monocrystalline, clear of inclusions, and mostly display unitary or slightly undulatory extinction (Figs 10A and B). Abraded overgrowths also occur. Mostly altered feldspar forms 1-9% of the rock, alkali feldspar prevails over plagioclase, and microcline is rare (Tab. 1). Sedimentary lithics (i.e. siltstone and rare chert) represent 0.2% on average and up to 2% of the rock (Fig. 10F). Igneous and metamorphic lithics seldom occur. Micas are aligned parallel to the bedding planes

and are most common in heterolithic and fine grained sandstone, decreasing in medium and coarse sandstone. Muscovite is more common than biotite and accounts for 4.6% on average of the total grains. Glaucony was observed only in bioturbated sandstone lithofacies at the base of the Dandot Formation (Figs 10B & E). Opaque magnetite and haematite comprise ~1.8% of the total rock grains (Tab. 1).

Cement. The color of the sandstone varies between red, reddish green, green, grey and white. This can be attributed to the types of cement and amount of the interstitial haematite in the matrix (Schluger 1976). Haematite is dominant with very rare siderite observed, and is found as filling in pore spaces, corroding the grain boundaries and coating and replacing grains and other types of cement. Calcite constitutes 2.8% of the rock grains. Percentages of calcite tend to increase upwards in the section with a decrease in ferruginous cementing material. The volumetric percentage of quartz overgrowths is 0.62%, and some of these overgrowths have a rounded periphery while others are recycled, precipitated around the grains in original sandstone.

Provenance. Twenty representative samples from three stratigraphic sections were selected for provenance studies. Sandstone compositions mainly depend on the type of the source rock, tectonic settings, climate conditions in the source area, nature, and chemical composition (in case of water) of the transporting agent and depositional settings (Weltje & Eynatten 2004). In general, com-

Fig. 10 - Representative photomicrographs of the lithofacies in the Dandot Formation. Km = Cross hatched twinning in microcline, Kp = Polysynthetic twinning in plagioclase, Ls = Sedimentary lithic fragment and Kf = Alkali Feldspar grains.



positions of the sandstones are not much affected by physical processes (Garzanti et al. 2015). Types of quartz grains could be used alone to determine the source rock type. Monocrystalline quartz having uniform to slightly undulose extinction is considered to be derived from plutonic rocks, e.g. granites (Basu et al. 1975; Pettijohn et al. 1987; Datta 2005). Polycrystalline and monocrystalline quartz grains having undulatory extinction are generally derived from a metamorphic source (Blatt et al. 1980; Asiedu et al. 2000), however these are seldom found in the studied samples. The K-feldspar is mainly derived from

crystalline rocks i.e., granites and gneisses (Ghose & Kumar 2000; Tucker 2001). Higher ratios of K-feldspar as compared to plagioclase indicate derivation from mixed plutonic and metamorphic source (Dickinson 1970; Tucker 2001). Further, the presence of rounded overgrowths of quartz in some quartz grains indicate recycled sedimentary sources (Basu et al. 1975; Tucker 2001; Jafarzadeh & Barzi 2008). Based on the petrographic evidence, e.g. presence of sedimentary lithics, abundance of monocrystalline quartz and presence of abraded overgrowths, a derivation from sedimentary source is interpreted (Fig. 7).

The deposition of the Dandot Formation took place in a cold climate. The sandstone represents derivation from crystalline rocks and enrichment of the quartz in the sandstone is because of the recycled sedimentary source rocks. Extensive reworking in the shallow marine environment was not responsible for the composition of the sandstone which is mainly affected by the source area.

STRATIGRAPHIC SETTING

The upper part of the Tobra Formation at the Choa-Khewra road section contains palynomorphs assignable to the earliest Permian 2141B Biozone (Stephenson et al. 2013). In Oman, the 2141B Biozone is closely associated with the Rahab Shale Member, a widespread shale unit in Oman, which is considered to represent part of a Permian deglaciation sequence which culminates in the marine beds of the Lower Gharif Member, interpreted as due to post glacial marine transgression (Stephenson et al. 2005).

Palynological sampling of the Dandot Formation conformably overlying the Tobra Formation yielded only barren samples, however the marine nature of the Dandot Formation and its stratigraphic position suggests that like the Lower Gharif Member it may represent post glacial marine transgression.

A similar transition is seen elsewhere across Gondwana (Angiolini et al. 2003; Stephenson et al. 2007) where deposition of marine strata occurred on the top of glacially-dominated facies.

For example in India, a transition at the top of the glaciogene Talchir Formation is observed, whereby the basin evolution is controlled by deglaciation as a result of climatic warming (Maejima et al. 2004). The Talchir Formation deposits are represented by mudstone with intercalations of sandstone and siltstone. The mudstone shows discrete beds of ripple cross- or climbing-ripple cross-laminated siltstone. The presence of a marine incursion at the top of the Talchir Formation in India is attributed to a eustatic sea level rise associated with the Carboniferous-Permian deglaciation (Maejima et al. 2004). This is then followed by the deposition of the fluvial succession of the Karharbari Formation (Maejima et al. 2004; Bhattacharya et al. 2005), which can be correlated with the Warchha Sandsto-

ne (Maejima et al. 2004).

The uppermost part of the Itarare group in Brazil, the Taciba Formation, also records the deglaciation sequence of the Early Permian and contains marine invertebrates including brachiopods overlying the Campo Muroa Formation (Vesely & Assine 2006).

A similar marine transgression has been observed in the Carboniferous-Permian deposits of Australia with the development of marine fauna (e.g. Foster & Waterhouse 1988). The marine fauna of the Dandot Formation e.g. *Fenestella fossula*, *Dielsma dadanense*, *Pterinea* cf. *lata*, *Nucula pidhensis*, *Cardiomorpha?* *pusilla*, *Maeonia* cf. *gracilis*, *Astartila* cf. *ovalis* and *Eurydesma cordatum*, reported by Reed (1936) has been correlated with the "Lower Marine Series" of New South Wales, Australia (Kummel & Teichert 1970). This fauna was attributed by Reed (1936) to the development of contemporaneous marine conditions in Australia and Salt Range, Pakistan.

The age-equivalent unit of the Dandot Formation in Australia, the Pebbly Beach Formation represents various stratigraphic surfaces and stacking pattern diagnostic of the sequences formed under icehouse conditions, showing cyclicity of the stacking pattern (Fielding et al. 2006). However, the Carboniferous-Permian paleogeographic reconstruction of Gondwana shows that Australian basins were exposed to open oceans whereas the Salt Range basin was located along a narrow depression where the effect of sea level rise was soon dominated by progradation due to the uplift of the basement (Valdiya 1997; Garzanti & Sciunnach 1997; Ghazi & Mountney 2011).

CONCLUSIONS

Overall the Dandot Formation represents deposition in a shallow marine to intertidal environment.

The sedimentological nature and the stratigraphic position of the Dandot Formation suggests that the Dandot Formation was deposited as a result of global sea level rise associated with the demise of Carboniferous-Permian glaciation, however robust biostratigraphy is required to place the Dandot Formation within a framework of deglaciation.

Petrographic investigations of the Dandot Formation indicate that the sandstones are compo-

sitionally quartzose; texturally, and mineralogically mature; and represent derivation from continental blocks with input from recycled sedimentary rocks. Based on petrographic studies, the Malani Range and Aravalli ranges may be the potential source areas for the Dandot Formation.

Acknowledgements. This study benefited from the Higher Education Commission of Pakistan's NRPU (National Research Program for Universities) grant to Dr. Irfan U. Jan as principal investigator via grant number 20-2706. M. H. Stephenson publishes with the permission of the Director of British Geological Survey, UK. The authors acknowledge the comments of Eduardo Garzanti, an anonymous reviewer and Associate Editor (Fabrizio Felletti).

REFERENCES

- Ahmad F. (1970) - Marine transgression in the Gondwana system of Peninsular India – A reappraisal. In: Haughton S.H. (Ed.) - Proceedings of Second Gondwana Symposium South Africa, Pretoria, Council for Scientific and Industrial Research: 179-188.
- Al-Qayim B., Al-Sanabani J. & Al-Subbary A. K. (2005) - Palaeoenvironmental implication of marine bioturbated horizons in the Majzir formation, Western Yemen. *Arabian J. Sci. Engin.*, 30(2): 165-180.
- Altermann W. (1986) - The upper Paleozoic pebbly mudstone facies of Thailand and Western Malaysia-Continental margin Deposits of Paleoeurasia. *Geol. Rund.* 75(2): 371-381.
- Angiolini L., Balini M., Garzanti E., Nicora A. & Tintori A. (2003) - Gondwanan deglaciation and opening of Neotethys: the Al Khlata and Saiwan Formations of Interior Oman. *Palaeogeogr., Palaeoclimatol., Palaeoecol.*, 196(1-2): 99-123.
- Asiedu D.K., Suzui S. & Shibata T. (2000) - Provenance of sandstones from the Lower Cretaceous Sasayama Group, inner zone of southwest Japan. *Sediment. Geol.*, 131: 9-24.
- Baker D.M., Lillie R.J., Yeats R.S., Johnson G.D., Yousuf M. & Zamin A.S.H. (1988) - Development of the Himalayan frontal thrust zone: Salt Range, Pakistan. *Geology*, 16: 3-7.
- Basu A., Young S.W., Lee J., Sutter W., Calvin J. & Mack G.H. (1975) - Re-evaluation of the use of undulatory extinction and polycrystallinity in detrital quartz for provenance interpretation. *J. Sedim. Petrol.*, 45: 873-882.
- Bhattacharya H.N., Chakraborty A. & Bhattacharya B. (2005) - Significance of transition between Talchir Formation and Karharbari Formation in Lower Gondwana basin evolution - A study in West Bokaro Coal basin, Jharkhand, India. *J. Earth. Syst. Sci.*, 114(3): 275-286.
- Blatt H., Middleton G. & Murray R. (1980) - Origin of Sedimentary Rocks. Prentice-Hall, New Jersey, 782 pp.
- Cheel R.J. and Leckie D.A. (2009) - Hummocky cross-stratification. *Sedim. Rev.*, 1: 31-103.
- Crowell J.C. (1956) - Origin of the pebbly mudstone. *J. Geol. Soc. Am.*, 68(8): 993-1009.
- Dalrymple R.W., Makino Y. & Zaitlin B.A. (1991) - Temporal and special pattern of rhythmic deposition on mud flats in macrotidal, Cobequid Bay Salmon River estuary, Bay of Fundy, Canada. In: Smith D.J., Reinson G.E., Zaitlin B.A. & Rehmani R.A. (Eds) - Clastic Tidal Sedimentology. *Can. Soc. Petrol. Geol.*, 16: 137-160.
- Datta B. (2005) - Provenance, tectonics and palaeoclimate of Proterozoic Chandarpur sandstones, Chattisgarh Basin: a petrographic view. *J. Earth Syst. Sci.*, 114: 227-245.
- Davies S.D. & Walker R.G. (1993) - Reservoir geometry influenced by high-frequency forced regressions within an overall transgression: caroline and garrington fields, Viking Formation (Lower Cretaceous), Alberta. *Bull. Can. Petrol. Geol.*, 41(4): 407-421.
- Davis R.A. (1983) - Depositional Systems. Prentice Hall, Englewood Cliffs, 254 pp.
- Dickins J.M. (1996) - Problems of Late Paleozoic glaciations in Australia and subsequent climate in Permian. *Palaeogeogr., Palaeoclimatol., Palaeoecol.*, 125: 185-197.
- Dickinson W.R. (1970) - Interpreting detrital modes of graywacke and arkose. *J. Sediment. Petrol.*, 40: 695-707.
- Duke W.L. (1990) - Geostrophic circulation or shallow marine turbidity currents? The dilemma of paleoflow patterns in storm-influenced prograding shoreline systems. *J. Sediment. Petrol.*, 60: 870-883.
- Fatmi A.N. (1973) - Lithostratigraphic units of Kohat-Potwar Province, Indus Basin. *Geol. Surv. Pakistan Memoir*, 10: 1-80.
- Fielding C.R., Bann K.L., Maceachern J.A., Tye S.C. & Jones B.G. (2006) - Cyclicity in the nearshore marine to coastal, Lower Permian, Pebbly Beach Formation, southern Sydney Basin, Australia: a record of relative sea-level fluctuations at the close of the Late Paleozoic Gondwanan ice age. *Sedimentology*, 53(2): 435-463.
- Foster C.B. & Waterhouse J. B. (1988) - The Granulatisporites confluens Opper-zone and Early Permian marine faunas from the Grant Formation on the Barbwire Terrace, Canning Basin, Western Australia. *J. Geol. Soc. Australia*, 35(2): 135-157.
- Garzanti E. & Sciunnach D. (1997) - Early Carboniferous onset of Gondwanian glaciations and Neo-tethyan rifting in South Tibet. *Earth Planet. Sci. Lett.*, 148: 359-365.
- Garzanti E., Resentini A., Ando S., Vezzoli G., Pereira A. & Vermeesch P. (2015) - Physical controls on sandstone composition and durability of detrital minerals during ultra-long distance littoral and Eolian transport (Namibia and southern Angola). *Sedimentology*, 62(4): 971-996.
- Gee E. R. & Gee D. G. (1989) - Overview of the geology and structure of the Salt Range, with observations on related areas of northern Pakistan. *Geol. Soc. America Spec. Pap.*, 232: 95-112.
- Genneseaux M. (1962) - Les canyons de la baie des Agnes leur remplissage sédimentaire et leur rôle dans la sédimentation profonde. In: Altermann W. (Ed.) - The upper Paleozoic pebbly mudstone facies of Thailand and Western Malaysia-Continental margin Deposits of Paleoeurasia. *Geol. Rund.*, 75(2): 371-381.

- Ghazi S. & Mountney N.P. (2009) - Facies and architectural element analysis of a meandering fluvial succession: the Permian Warchha Sandstone, Salt Range, Pakistan. *Sedim. Geol.*, 221: 99-126.
- Ghazi S. & Mountney N.P. (2011) - Petrography and provenance of Early Permian Fluvial Warchha Sandstone, Salt Range, Pakistan. *Sedim. Geol.*, 233: 88-110.
- Ghose S.K. & Kumar R. (2000) - Petrology of Neogene Siwalik Sandstone of the Himalayan foreland basin, Garhwal Himalaya: implication for source area tectonics and climate. *J. Geol. Soc. India*, 55: 1-15.
- Grelaud S., Sassi W., de Lamotte D. F., Jaswal T. & Roure F. (2002) - Kinematics of eastern Salt Range and South Potwar Basin (Pakistan): a new scenario. *J. Mar. Petrol. Geol.*, 19: 1127-1139.
- Hylland M.D., Riaz M. & Ahmad S. (1988) - Stratigraphy and structure of Southern Ghandghar Range, Pakistan. *Geol. Bull. Univ. Peshawar*, 21: 1-14.
- Jafarzadeh M. & Barzi M.H. (2008) - Petrography and Geochemistry of Ahwaz Sandstone member of Asmari Formation, Zagros, Iran. Implication for provenance and tectonic settings. *Rev. Mex. Cien. Geol.*, 25(2): 247-260.
- Jan I.U. & Stephenson M.H. (2011) - Palynology and correlation of the Upper Pennsylvanian Tobra Formation from Zaluch Nala, Salt Range, Pakistan. *Palynology*, 35: 212-225.
- Jan I.U. Stephenson M.H. & Khan F.R. (2009) - Palynostratigraphic correlation of the Sardhai Formation (Permian) of Pakistan. *Rev. Palaeobot. Palynol.*, 158(1): 72-82.
- Jan I.U. (2012) - Investigating the palynostratigraphy and palaeoenvironments of the southern Palaeotethyan Carboniferous-Permian succession of the Salt Range, Pakistan. Ph.D. Thesis, University of Leicester, UK.
- Jan I.U. (2014) - The development in the Carboniferous-Permian Nilawahan Group palynology and stratigraphic correlation: A brief review. *J. Earth Syst. Sci.*, 123(1): 21-32.
- Jaumé S.C. & Lillie R.J. (1988) - Mechanics of the Salt-Range Potwar-Plateau, Pakistan: A fold and thrust belt underlain by evaporites. *Tectonics*, 7: 57-71.
- Kummel B. & Teichert C. (1970) - Stratigraphy and paleontology of the Permian-Triassic Boundary Beds, Salt Range and Trans-Indus Ranges, West Pakistan. In: Kummel B. & Teichert C. (Eds) - Stratigraphic Boundary Problems: Permian and Triassic of West Pakistan. *Univ. Kansas Dept. Geol. Spec. Publ.*, 4: 2-110.
- Maceachern J.A., Zaitlin B.A. & Pemberton S.G. (1999) - A sharp-based sandstone of the Viking formation, Joffre field, Alberta, Canada: criteria for recognition of progressively incised shoreface complexes. *J. Sediment. Res.*, 69(4): 86-892.
- Maejima W., Das R., Pandya K.L. & Hayashi M. (2004) - Deglacial Control on Sedimentation and Basin Evolution of Permo-Carboniferous Talchir Formation, Talchir Gondwana Basin, Orissa, India. *Gondwana Res.*, 7(2): 339-352.
- Mertmann D. (2003) - Evolution of the marine Permian carbonate platform in the Salt Range (Pakistan). *Palaeogeogr., Palaeoclimatol., Palaeoecol.*, 191: 373-384.
- Newton R.S. (1968) - Internal structure of wave formed ripple marks in nearshore zone. *Sedimentology*, 11: 275-292.
- Noetling F. (1901) - Beitrage zur Geologie der Salt Range, insbesondere der Permian under Triasuecha Ablagerungen. *Venus Jabrb. Mineral Beil.*, 14: 369-471.
- Pettijohn F.J. (1975) - Sedimentary Rocks. 3rd ed. Harper & Tow, New York, 628 pp.
- Pettijohn F.J., Potter P.E. & Siever R. (1987) - Sand and Sandstones. Springer Verlag, 533 pp.
- Reading G.H. (Ed.) (1996) - Sedimentary Environments: Processes, Facies and Stratigraphy. Blackwell Scientific Publications Oxford, 245 pp.
- Reed F.R.C. (1939) - Non-Marine Lamellibranchs etc. from the 'Speckled Sandstone' Formation (Punjabian) of the Salt Range. *Rec. Geol. Surv. India*, 74(Pt 4): 474-491.
- Reed F.R.C. (1936) - Some fossils from the Eurydesma and Conularia beds (Punjabian) of the Salt Range: *Geol. Surv. India, Mem., Palaeontologia Indica*, ns 23, 361 pp.
- Reineck H.E. & Singh I.B. (1971) - Der Golf von Gaeta (Tyrrhenisches Meer) III. Die Gefuge von Vorstrand und Schelfsedimenten. *Senckenbergiana Marit.* 3: 185-201.
- Reineck H.E. & Singh I.B. (1983) - Depositional Sedimentary Environments, Springer-Verlag, 268 pp.
- Schluger P.R. (1976) - Petrology and origin of the red beds of the Perry Formation New Brunswick, Canada, and Maine, USA. *J. Sediment. Petrol.*, 46(1): 22-37.
- Shah A., Haneef M., Hanif M. & Jan I. U. (2010) - Lithofacies and palaeoenvironmental analysis of Carboniferous-Permian Nilawahan Group, Salt Range, Pakistan. *Pakistan J. Hydrocarbon Res.*, 20: 49-52.
- Shah S.C. & Sastry C.V. (1973) - Significance of Early Permian marine faunas of Peninsular India. In: Proceedings of 3rd Gondwanan Symposium: 391-395.
- Shah S.M.I. (1977) - Stratigraphy of Pakistan. *Geol. Surv. Pakistan, Memoir*, 12: 1-5.
- Shah S.M.I. (2009) - Stratigraphy of Pakistan. Government of Pakistan Ministry of Petroleum & Natural Resources, *Geol. Surv. Pakistan*.
- Shukla U.K. & Singh I.B. (1990) - Facies analysis of Bujh sandstone (Lower Cretaceous), Bujh area, Kuchchh. *J. Paleontol. Soc. India*, 35: 189-196.
- Singh I.B. & Shukla U.K. (1991) - Significance of trace fossils in the Bujh sandstone (Lower Cretaceous), Bhuj area, Kachchh. *J. Paleontol. Soc. India*, 36: 121-126.
- Stanley D.J. & Swift D.J.P. (1976) - The new concepts of continental margin sedimentation. Application to geological record. *Am. Geol. Inst. Washington*, p. 206.
- Stephenson M.H., Angiolini L. & Leng M.J. (2007) - The Early Permian fossil record of Gondwana and its relationship to deglaciation: a review. In: Williams M., Heywood A.M., Gregory F.J. & Schmidt D.N. (Eds) - Deep-Time perspective on Climate Change: Marrying the signal from Computer Models and Biological Proxies. *The Micropalaeontol. Soc. Spec. Publ. The Geological Society, London*. 169-189.
- Stephenson M.H., Jan I.U., Zeki S.A. & Al-Mashaikie K. (2013) - Palynology and correlation of Carboniferous-Permian glaciogene rocks of Oman, Yemen and Pakistan. *Gondwana Res.*, 24: 203-211.

- Stephenson M.H., Leng M.J., Vane C.H., Osterloff P.L. & Arrowsmith C. (2005) - Investigating the record of Permian climate change from argillaceous sedimentary rocks, Oman. *J. Geol. Soc. Lond.*, 162: 641-651.
- Tahirkheli R.A.K. (1979) - Geotectonic evolution of Kohistan. Geology of Kohistan, Karakoram, Himalayas, other Pakistan. *Geol. Bull. Peshawar Univ.*, 15: 1-15.
- Terwindt J.H.J. (1971) - Lithofacies of inshore estuarine and tidal inlet deposits. *Geologista Mijnbouws*, 50: 515-526.
- Tucker M.E. (2001) - Sedimentary Petrology. 3rd ed. Blackwell Publishing: 59.
- Valdiya K.S. (1997) - Himalaya, the northern frontier of East Gondwanaland. *Gondwana Res.* 1: 2-9.
- Vesely F.F. & Assine M.L. (2006) - Deglaciation sequences in the Permo-Carboniferous Itararé Group, Paraná Basin, Southern Brazil. *J. South Am. Earth Sci.*, 22(3-4): 156-168.
- Virkki C. (1939) - On the occurrence of winged spores in a Lower Gondwana glacial tillite from Australia and in Lower Gondwana shales in India. *Indian Acad. Sci.*, 9: 7-12.
- Waagen W. (1879) - Salt Range Fossils. *Geol. Surv. India Mem. Palaeontol. Indica*, 1: 1-7.
- Wardlaw B.R. & Pogue K.R. (1995) - The Permians of Pakistan. In: Scholle P.A., Peryt T.M. & Ulmer-Scholle P.M. (Eds) - The Permians of Northern Pangea. Palaeogeography, Palaeoclimates, Stratigraphy vol. 1: 215-224. Springer Verlag, New York.
- Weltje J.G. & Eynatten H.V. (2004) - Quantitative analysis of sandstones: review and outlook. *Sedim. Geol.* 171: 1-11.
- Wunderlich F. (1972) - Georgia Coastal region, Sapelo Island, U.S.A. Sedimentology and biology 3. Beach dynamics and beach development. *Senckenbergiana Marit.*, 4: 47-49.
- Wynne A.B. (1878) - On the geology of the Salt Range in the Punjab. *Geol. Surv. India Mem.*, 14: 313.
- Yeats R. S., Khan S. H. and Akthar, M., 1984. Late Quaternary deformation of the Salt Range of Pakistan. *Geol. Soc. America Bull.*, 95: 958-966.

